U.S. Department
of Transportation
**National Highway
Traffic Safety
Administration**

People Saving People
www.nhtsa.dot.gov

DOT HS 809 453 **May 2002**

Automotive Collision Avoidance System Field Operational Test

Phase I Interim Report

This document is available to the public from the National Technical Information Service, Springfield, Virginia 22161

This publication is distributed by the U.S. Department of Transportation, National Highway Traffic Safety Administration, in the interest of information exchange. The opinions, findings and conclusions expressed in this publication are those of the author(s) and not necessarily those of the Department of Transportation or the National Highway Traffic Safety Administration. The United States Government assumes no liability for its content or use thereof. If trade or manufacturer's names or products are mentioned, it is because they are considered essential to the object of the publication and should not be construed as an endorsement. The United States Government does not endorse products or manufacturers.

Technical Report Documentation Page

1. Report No.	2. Government Accession No.	3. Recipient's Catalog No.
DOT HS 809 454		

4. Title and Subtitle	5. Report Date
PHASE I INTERIM REPORT: Automotive Collision Avoidance System Field Operational Test	May 30, 2002
	6. Performing Organization Code
7. Author(s)	8. Performing Organization Report No.
9. Performing Organization Name and Address General Motors Corporation 30500 Mound Road Warren, MI 48090-9055 Delphi-Delco Electronic Systems One Corporate Center Kokomo, IN 46904	10. Work Unit No. (TRAIS)
	11. Contract or Grant No. DTNH22-99-H-07019
12. Sponsoring Agency Name and Address National Highway Traffic Safety Administration U.S. Department of Transportation 400 7th Street, S.W. Washington, D.C. 20590	13. Type of Report and Period Covered Phase I Interim Report June 2000 – December 2001
	14. Sponsoring Agency Code

15. Supplementary Notes

This project is being carried out by a team lead by General Motor Corporation, North American Operations. Other major team members include: Delphi-Delco Electronic Systems, Delphi Chassis, HRL Laboratories, HE Microwave and UMTRI.

16. Abstract

In June of 1999, the National Highway Traffic Safety Administration entered into a cooperative research agreement with General Motors to advance the state-of-the-art of rear-end collision warning technology and conduct a field operational test of a fleet of passenger vehicles outfitted with a prototype rear-end collision warning system and adaptive cruise control.

The goal of the research program was to demonstrate the state-of-the-art of rear-end collision warning systems and measure system performance and effectiveness using lay drivers driving on public roads in the United States.

The five-year program consists of a 2½ year development phase during which refinement of component technologies will continue and be integrated into a prototype test vehicle. In the three-year period of the second program phase, a fleet of ten vehicles will be constructed and outfitted with rear-end collision warning and adaptive cruise control systems and given to volunteer drivers to drive over a period of several weeks. Data collected from on-board vehicle instrumentation will be analyzed and used to estimate potential safety benefits, obtain information on the driving experiences of the volunteer drivers and their acceptance of this next-generation safety technology. The operational test will last approximately one year.

This document reports on the activities and results from the end of the first program year through the end of Phase I of this research project.

17. Key Words	18. Distribution Statement
Collision avoidance, crash avoidance, collision warning, rear-end collisions, forward collision warning, human factors, head-up display	This document is available to the public in printed and electronic form from the National Technical Information Service, Springfield, Virginia 22161, http://www.ntis.gov

19. Security Classif. (of this report)	20. Security Classif. (of this page)	20. No. of Pages	22. Price
None		303	

Form DOT F 1700.7 (8-72) Reproduction of completed page authorized

Automotive Collision Avoidance System Field Operational Test Program
Interim Report

TABLE OF CONTENTS

	Executive Summary	1
1	Introduction	1-1
2	System Integration (Task A)	2-1
3	Forward Radar Sensor (Task B1)	3-1
4	Forward Vision Sensor (Task B2)	4-1
5	Brake Control System (Task B3)	5-1
6	Throttle Control System (Task B4)	6-1
7	Driver-Vehicle Interface (Task B5)	7-1
8	Data Fusion (Task C1)	8-1
9	Tracking and Identification (Task C2)	9-1
10	CW Function (Task C3 And C5)	10-1
11	ACC Function (Task C4)	11-1
12	Fleet Vehicle Build (Task D)	12-1
13	Field Operational Test (Task E)	13-1
	Acronyms	

LIST OF FIGURES

	Executive Summary, FCW Visual Cues	3
1.1	Master Program Schedule, Page 1	1-7
1.2	Master Program Schedule, Page 2	1-8
1.3	Master Program Schedule, Page 3	1-9
1.4	Master Program Schedule, Page 4	1-10
1.5	Master Program Schedule, Page 5	1-11
2.1	ACC Vehicle Controls	2-3
2.2	Prototype Vehicle System Process Model	2-5
2.3	Prototype Vehicle System Block Diagram and Mechanization	2-8
2.4	Task A Schedule	2-15
3.1	MMIC Transceiver Hardware	3-2
3.2	Alumina Millimeter-Wave Substrate with VCO, Doubler and MPA MMICs Mounted	3-3
3.3	On-Wafer Measurements of New VCO Chips	3-4
3.4	On-Wafer Measurements of MPA Chips	3-4
3.5	Auto Alignment Geometry	3-6
3.6	Example Auto Alignment Convergence Time Results	3-8
3.7	Example Auto Alignment Response with Large Misalignment	3-8
3.8	Example Auto Alignment Steady State Response	3-9
3.9	Raw Alignment Estimates from Figure 3.7	3-10
3.10	Raw Alignment Estimates from Figure 3.7	3-11
3.11	Forward Radar Ground Clutter Spectrum with Fixed Frequency Waveform	3-14
3.12	Example Mainbeam Ground Clutter Return	3-19
3.13	Example Normalized Track Amplitude Data with 20 dB Attenuation Layer	3-20
3.14	Example Wideband FMCW Frequency Spectrum Using RADS Radar	3-21
3.15	Primary Detroit Freeway Test Loop	3-25
3.16	Secondary Detroit Freeway Test Loop	3-26
3.17	Indianapolis Freeway Test Loop	3-26
3.18	Probability of False Alarm on Bridges	3-28
3.19	Probability of Correct Classification of Stopped Vehicles	3-29
3.20	Task B1 Schedule	3-29
4.1	Vision System Role in the Overall ACC/FCW System	4-1
4.2	Vision System Block Diagram	4-3
4.3	Vision System Processing Unit	4-6
4.4	Processing Steps of the Auto Exposure Control Algorithm	4-7
4.5	Results of the Auto Exposure Control Approach	4-8
4.6	Typical Exit Lane Scenarios	4-10
4.7	Unresolved Vertical Curvature	4-10
4.8	Diverging Markers	4-11
4.9	Task B2 Schedule	4-13
5.1	Brake Subsystem Block Diagram	5-2
5.2	Vehicle Installation of the Electronic Control Unit / 12 Valve Brake	5-3

	Pressure Modulator	
5.3	"V" Cycle Design and Implementation Flow for Delphi Brake Systems	5-5
5.4	Task B3 Schedule	5-11
6.1	Task B4 Schedule	6-1
7.1	First Draft of the Multi-Stage Display; The CAMP (1999) Icon	7-4
7.2	Integrated Vehicle Display	7-5
7.3	The Rear-Perspective Imminent Icon	7-7
7.4	Displays as a Function of Alert Level (AL)	7-8
7.5	Gap/Warn setting display	7-10
7.6	Relative Size and Position of the HUD Images in the Delco Driving Simulator	7-12
7.7	Brake-Reaction-Time as a Function of Display Type	7-17
7.8	Required Deceleration at 50 Percent Braking Response as a Function of Display Type	7-18
7.9	Participant Rankings of Displays	7-21
7.10	Avoidance Rating as a Function of Number-of-False-Alarms for Each Age Group	7-24
7.11	Avoidance Rating as a Function of Display Type for Each Age Group	7-24
7.12	Annoyance Rating as a Function of Display Type for Each Age Group	7-26
7.13	Buy Rating as a Function of Display Type for Each Age Group	7-26
7.14	Headway Rating as a Function of Display Type for Each Age Group	7-27
7.15	Mean Rank as a Function of Display Type	7-28
7.16	Final Selection of the FCW Display	7-33
7.17	The Distinction Between ACC-Engaged and ACC-Not Engaged	7-35
7.18	Priorities for the Text Line Messages	7-37
7.19	Steering Wheel Button Layout	7-38
7.20	Task B5 Schedule	7-39
8.1	Data Fusion and Its Relationship to Other System Tasks	8-1
8.2	COF Algorithm Performance During Straightaway-to-Curve Transition	8-8
8.3	CNF Algorithm Performance During Straightaway-to-Curve Transition	8-9
8.4	Histogram (pseudo-pdf) Distributions of Forward Geometry Errors	8-11
8.5	Task C1 Schedule	8-13
9.1	Road Offsets and Road Categories	9-5
9.2	Target Selection Radar Collision Avoidance Processor	9-5
9.3	Collaborative Multi-Stage Prototype Integration, Testing and Validation	9-7
9.4	Subsystem Test, Validation, and Refinement Process	9-9
9.5	Delphi Diagnostic Tracking and Identification Display	9-10
9.6	Video from a Straight Road Stationary Object Collision Alert Test	9-12
9.7	Straight Road Stationary Object Collision Alert Test Result	9-13
9.8	Straight Road Moving Vehicle Collision Alert Test Result	9-14
9.9	Video from a 500m Curved Road Stationary Object Collision Alert Test	9-15
9.10	500m Curved Road Stationary Target Collision Alert Test Results	9-16
9.11	Video from a 300m Curved Road Moving Vehicle Collision Alert Test	9-18
9.12	300m Curved Road Moving Target Collision Alert Test Results	9-19
9.13	10-04-01 Sub-System Verification Short Test Route, held in Detroit Area	9-20
9.14	Typical Freeway Segment with Overhead Bridges	9-23

9.15	Typical Freeway Roadway Segment, Numerous Trucks and Cars	9-23
9.16	Valid CIPS Event on Host Lane Change Left into Adjacent Lane Stopped Vehicle	9-23
9.17	Valid CIPS Event on Intersection Approach	9-23
9.18	Straight Road False CIPS Event and Audible Alert Caused by Effect of Divergent Right Lane Marker on the Vision-Based Host Heading	9-24
9.19	Straight Road False CIPS Event and Audible Alert Caused by Effect of Vertical Road Curvature on the Vision-Based Host Heading	9-24
9.20	False CIPS Event Due to a Road Fork, No Audible Alert	9-24
9.21	False CIPS Event due to a T-Junction, No Audible Alert	9-24
9.22	False CIPS Event Due to a Right Turn Followed by a Left Turn, No Audible Alert	9-25
9.23	False CIPS Event Due to a Right Turn, No Audible Alert	9-25
9.24	False CIPS Event and Audible Alert Due to an S-Curve	9-25
9.25	False CIPS Event and Audible Alert Due to a Curve Entry	9-25
9.26	False CIPS Event and Audible Alert due to Triple Host Lane Change Right	9-26
9.27	Road Offsets from Various Prototype Subsystems, Test Segment 5 of the Open Road Validation Tests	9-27
9.28	Depiction of Error Measurement Scheme	9-31
9.29	Prediction Error at 80m for a Highway Scenario	9-32
9.30	Prediction Error at 80m For a Surface Street Scenario	9-33
9.31	Host's Post-Calculated Trajectory and Scene Tracker's Estimates of Upcoming Road	9-34
9.32	Estimated Host Heading Angle in Lane in the Vicinity of a Host Lane Change	9-35
9.33	Prediction Error at 80m in the Vicinity of a Host Lane Change	9-35
9.34	Overhead Snapshot Prior to Host Curve Entry	9-36
9.35	Prediction Error at 80m for Four Confidence Levels in a Highway Scenario	9-37
9.36	Overall Block Diagram of the GPS/Map Subsystem	9-39
9.37	GPS/Map Processor	9-40
9.38	Trimble AB132 Receiver and Antenna	9-41
9.39	In-Vehicle Data Logging Mechanism With Real-Time Data Display	9-44
9.40	Vtool Evaluation and Analysis of Logged Data	9-46
9.41	Video and Radar Overlay Display	9-47
9.42	Results From the GPS/Map Processor	9-47
9.43	Radar Data Screen	9-48
9.44	Sensor Data Display	9-48
9.45	Comparison of the HRL and GMR-Developed Ground Truth	9-49
9.46	Map Matching Over a Stretch of Freeway	9-53
9.47	Raw GPS Data Superimposed on a Section of Map	9-53
9.48	Map Matching Using GPS Data From Figure 9.46	9-54
9.49	Predicted Forward Geometry Superimposed on Map	9-54
9.50	Forward Geometry Prediction on a Straight Road	9-55
9.51	Forward Geometry Prediction on a Gently Curved Road	9-55

9.52	Forward Geometry Prediction on a Sharply Curved Road	9-56
9.53	Forward Geometry Prediction on a S-shaped Road	9-56
9.54	Forward Geometry on a Transition from Straight to a Gentle Curve	9-57
9.55	Forward Geometry on a Transition from Straight to a S-Shaped Curve	9-57
9.56	Upcoming T-Junction with Forward Geometry	9-58
9.57	Presence of Tunnel with Forward Geometry	9-58
9.58	Map with Intersections	9-59
9.59	Forward Road Preview for Map Section of Figure 9.58	9-60
9.60	Map Depiction of the Test Freeway Road Section	9-60
9.61	Road Offset at 80m with Road Classification	9-61
9.62	Road Offset at 80m for a Left-Hand Turn with Road Classification	9-61
9.63	Road Offset at 80m for a Right-Hand Turn with Road Classification	9-62
9.64	Road Offset at 80m in Curve Transitions with Road Classification	9-62
9.65	Road Offset at 80m During Lane Change with Road Classification	9-63
9.66	Evaluation of Confidence Assignment	9-64
9.67	Task C2 Schedule	9-65
10.1	The TASIM Tool	10-2
10.2	FCWS Functional Block Diagram	10-2
10.3	Accelerometer Model	10-6
10.4	Speed Sensor Model	10-6
10.5	Interfacing TASIM to CAN BUS Field Data	10-31
10.6	Descriptions of Low Pass Filter (LPF), Noise, and Limiter blocks	10-32
10.7	Definition of Threat Assessment Algorithm Terms	10-38
10.8	Determination of Output AL	10-40
10.9	Tasks C3 and C5 Schedule	10-49
11.1	Comparison of Two ACC/A Algorithms Using the ACC Simulator	11-3
11.2	Task C4 Schedule	11-4
12.1	Architecture of GM Engineering Development Vehicle	12-3
12.2	In-Vehicle Data Logger Components	12-5
12.3	Data Logger Screen	12-6
12.4	Brake Subsystem	12-11
12.5	Block Diagram of Prototype Vehicle	12-13
12.6	Task D Schedule	12-19
13.1	Opel Vectra Test Vehicle	13-2
13.2	Cruise Utilization Results, Comparing Opel ACC with Other Cases	13-4
13.3	Total Occurrence of Gradient Warning Displays in Manual Driving	13-5
13.4	Imminent Alert Rates from Driving the Blue Opel and GM EDV	13-6
13.5	Basic Elements of the FOT Data Acquisition System	13-9
13.6	The Data Model that Supports Data Collection & Analysis	13-12
13.7	Task E Schedule	13-15

LIST OF TABLES

1.1	Summary of Completed Phase I Milestones, by Date	1-5
1.2	Summary of Completed Phase I Deliverables	1-6
2.1	Adaptive Cruise Control Modes	2-4
2.2	System Modules and Their Primitive Functions	2-7
2.3	System-Level Verification-Test Scenario Descriptions	2-11
2.4	Safety Tasks	2-12
2.5	Sample Hazard List and Potential Accident Scenarios	2-13
3.1	Blockage Detection Components Implemented in the Forward Radar	3-13
3.2	Data Collection and Evaluation Test Conditions for Blockage Detection	3-16
3.3	Summary of Blockage Detection Test Results	3-17
3.4	Approaches Rejected by Initial Investigations	3-22
3.5	Components of Bridge Rejection and Stopped Object Classification	3-23
3.6	Summary of Tests Performed for Stopped Vehicles	3-27
4.1	Vision System Requirements Summary	4-4
5.1	Brake System Test Matrix	5-7
7.1	Responses to the Haptic Braking Stimulus Questionnaire	7-6
7.2	Responses to Absolute-Judgments Questionnaires as a Function of Display Types	7-19
7.3	Participants' Preference Ranks of the Four Displays	7-30
7.4	Selected Time-to-Contact and Time Headway Boundaries	7-35
9.1	Summary of the Short Route 10-04-01 Sub-System Tests vs. Road Type	9-21
9.2	Summary of 10-04-01 Open Road Sub-System Tests vs. Road Category	9-22
10.1	Radar Field of View Parameters	10-3
10.2	RCS for Objects of Interest	10-4
10.3	Radar Discrimination Parameters	10-4
10.4	Vision Model Parameters	10-8
10.5	Results of Test 1	10-11
10.6	Results of Test 2	10-11
10.7	Results of Test 3	10-12
10.8	Results of Test 4	10-13
10.9	Results of Test 5	10-13
10.10	Results of Test 6	10-14
10.11	Results of Test 7	10-14
10.12	Results of Test 8	10-15
10.13	Results of Test 9	10-15
10.14	Results of Test 10	10-16
10.15	Results of Test 11	10-17
10.16	Results of Test 12	10-17
10.17	Results of Test 13	10-18
10.18	Results of Test 14	10-18
10.19	Results of Test 15	10-19
10.20	Results of Test 16	10-19
10.21	Four Major Rear-End Pre-Crash Scenarios	10-20
10.22	Speed Distribution of SV for Test 1	10-21

10.23 Random Distributions T_R and A_F 10-22
10.24 Probability of Early and Late Alerts for Test 1 10-22
10.25 Speed Distribution of SV for Test 2 10-22
10.26 Probability of Early and Late Alerts for Test 2 10-23
10.27 Speed Distribution of SV for Test 3 10-23
10.28 Random Distribution A_L 10-24
10.29 Probability of Early and Late Alerts for Test 3 10-24
10.30 Speed Distribution of SV for Test 4 10-24
10.31 Probability of Early and Late Alerts for Test 4 10-25
10.32 Random Distributions R_0, T_R and A_F 10-26
10.33 Probability of False Alarms and Misses for Test 1 10-27
10.34 Probability of False Alarms and Misses for Test 2 10-27
10.35 Probability of False Alarms and Misses for Test 3 10-28
10.36 Probability of False Alarms and Misses for Test 4 10-29
10.37 ACC/FCW Alert Scheme 10-36
10.38 Target Selection and Radar Input Data 10-37
10.39 Other Threat Assessment Input Data 10-37
10.40 FCW Processor Output Data 10-37
10.41 Vehicle Verification Test Types 10-42
10.42 Tests Grouped by Test Facility 10-43
10.43 Quantitative Collision Alert and Qualitative ACC Test 10-45
10.44 Qualitative Nuisance Alert Test 10-46
10.45 Qualitative ACC Test 10-46

Executive Summary

Objectives

Forward Collision Warning (FCW) systems which aid drivers in avoiding collisions or mitigating their severity when they occur are now emerging. Adaptive Cruise Control (ACC) systems are also emerging as a convenience feature that enhances conventional cruise control by adjusting the vehicle's speed to match that of preceding vehicles. Adaptive Cruise Control and Forward Collision Warning systems rely upon similar sensors and, therefore, are likely to be offered as a package.

The goal of the Advanced Collision Avoidance System/Field Operational Test (ACAS/FOT) Program is to determine the practical suitability of the combined ACC/FCW function for widespread use by the driving public. Suitability for wide use will be determined by the extent to which the installed system (1) offers a marketable level of value, as perceived by its users, (2) yields significant safety and convenience benefits for most of them, and (3) poses minimal added risk to almost anyone. During the Field Operational Test a sampled pool of laypersons will be given vehicles equipped with ACAS for use as their personal car for four weeks each. A rich set of objective and subjective data will be collected before, during, and after the drivers use the system so that system performance, usage patterns, and changes to driving behavior may be analyzed.

Preparation for the Field Operational Test started in June 1999. Phase I finished in December 2001. Phase I included:

1. Development – The program improved technologies/components necessary for the FCW system, some of which were developed during the previous ACAS Program.
2. Integration – The refined FCW technologies/components were designed into the vehicle to form an integrated rear-end collision warning system,
3. Verification – The prototype vehicle was subjected to closed-course and in-traffic tests to verify that it functions as intended.

Phase II of the program started immediately after Phase I. It will include:

4. Deployment Fleet – The verified design will be used to build a deployment fleet of ten vehicles equipped with the system.
5. Field Operational Test – The field operational test plan will be implemented. The deployed vehicles will be used to collect valuable research data to assess/validate the technology, product maturity, and the response of the public to the technology.

Functional Overview

In ACAS the FCW and ACC functions are implemented using a combination of (a) a long-range forward radar-based sensor that is capable of detecting and tracking traffic, (b) a forward vision-based sensor that detects and tracks lanes and (c) a Global Positioning Satellite (GPS) receiver and a map database to help ascertain road geometry.

ACAS uses data fusion techniques to combine road-geometry estimates derived using multiple sensor and processing techniques. The radar tracks are then analyzed to select

the Closest In-Path Stationary object (CIPS) and the Closest In-Path Vehicle (CIPV) (i.e., one that is or has been seen to move). The Adaptive Cruise Control function uses the throttle and brakes to maintain the vehicle speed or to track the speed of a leading vehicle at a headway selected by the driver. The threat assessment function evaluates the dynamics of the CIPV and CIPS to generate an alert level. The driver can select the sensitivity of the threat assessment algorithm. The alert level is used to generate audio and visual warnings to the driver. The visual alerts, along with other status information, are displayed on a fully programmable, color, head-up display (HUD).

Development Approach

During Phase I, the various subsystems were refined on a number of Engineering Development Vehicles. The refined subsystems were integrated and tested in a single Prototype vehicle. The Prototype vehicle includes all the functionality required for the field operational test but the packaging is not the size required. During Phase II, two Pilot vehicles will be built that meet the functionality and packaging requirements. As the performance of the pilot vehicles is verified, ten deployment vehicles will be built.

Major Accomplishments in Phase I

The major accomplishments during Phase I included the following.

1. A Microwave Monolithic Integrated Circuit (MMIC) component that can be used to decrease the cost of future automotive radars was developed and tested.
2. Target detection, tracking, and identification algorithms were developed and enhanced, including improved bridge identification and radar blockage detection.
3. Three university-based teams developed vision-based lane sensing algorithms. The vision systems detect lane changes, estimate the road geometry (using a clothoid model), estimate lateral offset in the lane, and estimate host heading angle within a lane. One algorithm was chosen for further development and integration into ACAS.
4. A previously developed road geometry estimation function that uses GPS vehicle location measurements and a map database was enhanced to (a) increase the update rate to 10 Hz, (b) improve dead reckoning when GPS is missing, (c) improve shape estimates at transitions into and out of curves, (d) add confidence levels, and (e) add information about upcoming road features such as intersections.
5. A scene tracking function was developed that analyzes radar data from preceding vehicles to estimate forward road geometry and the host vehicle heading with respect to the road.
6. Two data fusion approaches (weighted combinations and consensus) were developed to combine multiple sources of road geometry and host state estimates.
7. Previously existing target selection algorithms were enhanced to (a) use the output from the data fusion function, (b) improve filtering to reduce errors in identifying in-path targets.
8. Four distinct threat-assessment algorithms were developed and tested: one based upon the recommendations of the Crash Avoidance Metrics Partnership (CAMP), one based upon concepts proposed by staff at the National Highway Transportation Safety

Administration (NHTSA) and two proposed by GM. One of the GM algorithms was selected for use in the FOT.

9. A driver-vehicle interface (DVI) was developed based upon extensive analysis of prior research, supplemented by new fixed base simulator tests, closed course tests, and evaluations on public roads. The final DVI includes (a) the standard Buick LeSabre cruise-control buttons on the steering wheel, (b) a new steering wheel button to control ACC headway and FCW sensitivity, (c) a head-up display showing vehicle speed, ACC/FCW settings, FCW visual alerts, and status information, (d) an audio output for FCW imminent alerts and to signal when status messages appear, and (e) the brake and accelerator pedals to disengage or override the cruise control respectively. The 3-stage multi-color looming display shown below was selected for the Prototype vehicle. A single-stage non-speech audio alert was also selected after evaluating several two-stage (cautionary and imminent) and one-stage (imminent only) audio alerts using several non-speech tones.

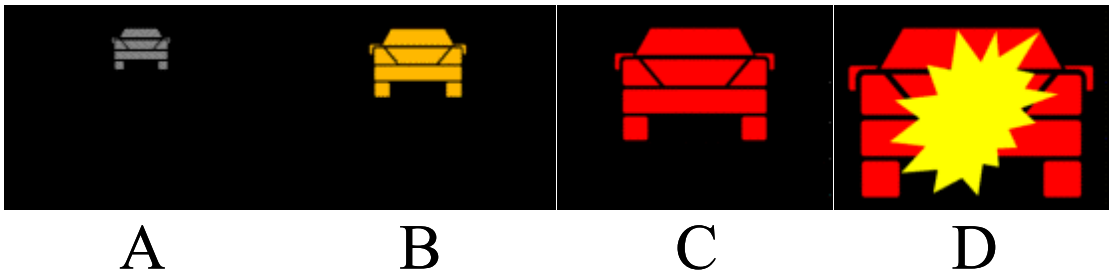

Figure 1: FCW Visual Cues (A) blue-green vehicle detected, (B) amber 1st stage alert, (C) red 2nd stage alert, and (D) red and yellow imminent alert.

10. A production brake system was enhanced to provide the auto-braking function used by the ACC. The production brake system also includes anti-lock braking, traction control, and vehicle stability enhancement features.

11. A production cruise controller was modified to provide the adaptive cruise control function. It was tuned to the Buick LeSabre and enhanced to provide greater driver comfort.

12. The entire ACAS system, as implemented on the prototype vehicle, was subjected to verification tests at the subsystem and system level. There were 30 system-level tests, including 29 on closed tracks and one on public roads. The system-level tests verified that FCW alerts occurred when intended, that there were few nuisance alerts, and that the ACC functioned properly.

13. A detailed Field Operational Test plan was developed and approved by the GM, University of Michigan, and Department of Transportation human use review panels.

Conclusion

Phase I of the ACAS/FOT program was completed successfully in December 2001. The FCW and ACC functions were developed and integrated into a prototype vehicle. The prototype vehicle passed the agreed upon verification tests. Completion of the verification tests and approval of the FOT plan led to approval to start Phase II.

1 INTRODUCTION

1.1 Program Overview

General Motors Corporation and Delphi-Delco Electronics Systems joined together to establish a program team in order to pursue the next logical progression in advancing the science of automotive safety in the field of Collision Warning (CW) systems. The integrated collision warning system incorporates the functionality of both Forward Collision Warning (FCW) and Adaptive Cruise Control (ACC). This report documents the activities and achievements of program Phase I (June 1999 – December 2001). In Phase II (January 2002 – March 2004), this program team will conduct an extensive Field Operational Test (FOT). The field operational test is aimed at bridging the gap between research-and-development and the deployment of new technology in the real world of driver-vehicle-highway systems. In this sense, the FOT is an opportunity to gain new knowledge concerning the influence of new technological capabilities on pertinent aspects of the driving process.

Through a series of formal verification tests during Phase I, the CW functionality was shown to be effective in detecting, assessing, and alerting the driver of potential hazard conditions associated with the threat of a rear-end collision ahead of the host vehicle. The ACC function provides active vehicle actuation (brake and throttle control) in response to maintaining a specified longitudinal headway control. During Phase II the program team will design and build ten passenger-style host vehicles, each equipped with a collision warning vehicle package and an unobtrusive data acquisition system, which will support the FOT.

1.2 Objectives

The main objective of the Automotive Collision Avoidance System Field Operational Test Program is to identify key enabling technologies that can accelerate the development of a collision warning system, which in turn can be used to assess the technological impact of a collision warning system through a comprehensive field operational test program. The performance of the cohesive collision warning vehicle package will be of sufficient fidelity, robustness, and maturity so that a meaningful field operational test program can be executed. To accomplish this the program is broken down into a number of defined tasks with the following objectives:

System Integration (Task A)

The ACAS team has been following the GM Vehicle Development Process to ensure that a robust, safe vehicle is provided for the field operational test. Systems Integration consists of preparing a system functional description, system architecture/mechanization, interface management documentation, a system verification plan and a risk management plan.

Forward Radar Sensor (Task B1)

The objective of the Forward Radar Sensor task was to make the sensor more robust by implementing:

1. An integrated Microwave Monolithic Integrated Circuit (MMIC) transceiver-antenna interface.
2. An Auto Alignment Algorithm that electronically adjusts the sensor for mechanical misalignment due to vehicle wear and tire alignment.
3. A Radome Blockage Algorithm that detects and warns the driver when the sensor is blocked by dirt, slush, or other material.
4. A Bridge Rejection Algorithm that classifies bridges as "safe" overhead obstacles so they do not cause unnecessary warnings.

Forward Vision Sensor (Task B2)

The overall goal of the Forward Vision Sensor task was to facilitate the development of a robust, real-time, forward-looking lane tracking system to enhance the overall forward Path Estimation and Target Selection algorithms.

Brake Control System (Task B3)

The key objective of this Task was the removal of the Original Equipment Manufacture's (OEM) brake components from the vehicle and replacement of them with the hardware and software for a new brake system. The new brake system supports automatic braking for Adaptive Cruise Control (ACC) while maintaining the electrical and diagnostic interfaces. Delphi Chassis and Energy Systems performed this Task.

Throttle Control System (Task B4)

The objective of this task was to provide a throttle control system for the ACAS vehicles. The basic approach to accomplishing this task was to use the existing throttle control system on the model year 2000 Buick LeSabre. This throttle control in the Buick LeSabre is a stepper motor cruise control (SMCC) designed and built by Delphi. It has been used successfully in other projects and the modifications required were known.

Driver-Vehicle Interface (Task B5)

The primary objective of the Driver-Vehicle Interface task was to convey information from the Adaptive Cruise Control and Forward Collision Warning systems to the vehicle operator in as unambiguous a fashion as possible. For the FCW system, warning cues and presentation methodology were selected and developed to direct the driver's attention immediately to the primary task of evaluating and reacting to the critical crash event, while allowing sufficient time to perform some corrective vehicle control action to either avoid the event or at a minimum to mitigate the crash energy. For the ACC system, sufficient information is presented to the driver so that he/she is constantly aware of the current status of the system (e.g., cruise control set speed, selected intervehicle separation distance, and whether or not a preceding vehicle has been detected by the system). For both systems, this information had to be presented in such a fashion as to be easily understandable at a glance by the operator and without imposing extra workload onto the driving task.

Data Fusion (Task C1)

The objective of the Data Fusion task was to develop algorithms for data fusion subsystem. The approach was to gather information on each sensor subsystem such as performance specifications, confidence measures, and interface requirements. This information was used to determine the fusion algorithms and set requirements on the data fusion architecture.

Tracking and Identification (Task C2)

The objective of the Tracking and Identification task was to refine the path estimation and target identification algorithms, incorporate vision and GPS/Map derived information and to integrate them into the vehicle system.

CW Function and NHTSA CW Algorithm (Tasks C3 and C5)

The objectives of the Collision Warning Task was to develop threat assessment algorithms. This was done by analysis, simulation, and test instrumented vehicle on test tracks and in real traffic. The Task included supporting the National Highway Transportation Safety Administration in their development of the "NHTSA Algorithm". The CW function was implement on GM Engineering Development Vehicle (EDV) and Prototype vehicles for verification.

Adaptive Cruise Control Function (Task C4)

The objectives of the Adaptive Cruise Control Function task were to provide an Adaptive Cruise Control (ACC) for the 2000 Buick LeSabre, determine the interface requirements to the other vehicle subsystems, and provide support to development and deployment groups.

Fleet Vehicle Build (Task D)

Engineering Development and Prototype vehicles were built in Phase I. In Phase II we will build the Pilot and Deployment vehicles. The purposes of the various vehicle builds are defined below:

1. EDVs were built to develop, design, implement and investigate the various subsystems that will be available on the Deployment vehicles.
2. The Prototype vehicle, which was also built in Phase I, contained all the developed subsystems, integrated into a single vehicle package. The Prototype is the precursor to the Pilot vehicles.
3. Two Pilot vehicles will be built in Phase II to verify the final Deployment vehicle design.
4. Finally, in Phase II, the Deployment vehicles having the full functionality as described in the proposal will be built for the FOT.

Field Operational Test (Task E)

The objectives of this Task center on the preparations and execution of the field operational test, itself. In Phase I of this project, the objectives included planning the pilot testing series, conducting Stage 1 and Stage 2 pilot tests, developing a Data Acquisition System, and developing procedures, software, and a plan for executing the FOT.

1.3 Approach

Due to the complexity and breadth of the system goals, the on-going design process has relied heavily on using the established principles of system engineering as a framework to guide this highly focused deployment design effort. As such, the technical activities of the program were grouped into two phases. Phase I started immediately after program inception, in June 1999, and lasted 30 months. Phase II started in January 2002.

The objective of Phase I was to refine the various subsystems on a number of Engineering Development Vehicles, and to integrate and test these subsystems in a single Prototype Vehicle. The objective of Phase II is the design and implementation of the Field Operational Test and to build the Deployment Vehicles. The deployment vehicle fleet will be used to collect valuable research data in order to assess/validate the technology, product maturity, and general public perception. The system engineering design process was highly effective in ensuring that design activity was preceded by defining requirements and on the timely identification of technical, performance trade-offs.

The primary goal of the Field Operational Test is to collect evidence that reveals the salient issues of FCW & ACC functionality interaction for lay drivers while they are otherwise engaged in virtually naturalistic usage of the host vehicles. The primary "salient" issues are those addressing real and perceived levels of safety and utility, or driver acceptance, which accrue during system usage. The approach to satisfying the goal is to capture the driving experience of a driver sample by means of electronic data collected via on-board instrumentation and through subjective feedback obtained via surveys and when de-briefing the participants. The University of Michigan Transportation Research Institute (UMTRI) has been sub-contracted to execute the day-to-day operations of the FOT.

1.4 Major Milestones and Deliverables

Table 1.1 below shows the major milestones that were accomplished during Phase I of the program.

Table 1.1 Summary of Completed Phase I Milestones, by Date

Milestone	Task	Phase I Milestone Description	Date
23	F	ACAS/FOT "Kick-Off" Program Team Meeting	Jul 99
4	B2	Lane Tracking "Kick-Off" Meeting	Aug 99
9	B5	DVI Technology Exchange "Kick-Off" Meeting	Aug 99
15	C3	Threat Assessment Technology Exchange "Kick-Off" Meeting	Aug 99
24	F	ACAS/FOT "Kick-Off" Meeting	Aug 99
12	C1	Data Fusion Architecture and Performance Requirements Definition	Sep 99
1	A	CW Architecture Definition	Dec 99
19	E	Submission Of FOT Pilot Test Plan	Jan 00
25	F	ACAS/FOT Program Review Briefing 1	Jan 00
7	B3	Brake System Design	Apr 00
26	F	ACAS/FOT Program Review Briefing 2	Jul 00
2	A	CW Verification Plan	Sep 00
5	B2	Lane Tracking Technology Down-Select Meeting	Sep 00
20	E	Completion Of FOT Professional Pilot, Testing & Data Processing	Nov 00
10	B5	DVI Warning Cue Set Selection	Nov 00
13	C1	Preliminary Data Fusion Algorithm Simulation Demonstration	Nov 00
27	F	ACAS/FOT Program Review Briefing 3	Jan 01
3	A	CW Interface Definition	Feb 01
8	B3	Brake System On Engineering-Phase Vehicle Demonstration	Feb 01
21	E	Completion Of FOT First HURP Approval Process	Feb 01
6	B2	Lane Detection/Tracking Vision System Selection	Mar 01
17	D	Engineering-Phase Vehicles Build Completion	Mar 01
14	C1	Data Fusion Algorithm Simulation Demonstration	Apr 01
11	B5	DVI/HUD System On Bench Demonstration	Jun 01
22	E	Submission Of FOT Operational Test Plan	Jun 01
16	C5	NHTSA Threat Assessment Algorithm on Prototype Phase Vehicle Demo	Nov 01
18	D	Prototype-Phase Vehicle Demonstration	Nov 01
28	F	ACAS/FOT Phase I Interim Program Review Briefing	Dec 01

Table 1.2 below shows the deliverables that were submitted to NHTSA during Phase I of the program.

Table 1.2 Summary of Completed Phase I Deliverables, by Date

Deliverable	Task	Phase I Deliverable Description	Date
9	B3	Brake Actuator System Design Summary Report	Jun 00
23	F	ACAS/FOT Program Review 2 Briefing & Program Plan Package	Aug 00
24	F	ACAS/FOT First Annual Report	Sep 00
3	A	System Verification Plan	Oct 00
4	A	Risk Management Plan	Nov 00
18	E	FOT First HURP Request	Nov 00
25	F	ACAS/FOT Program Review 3 Briefing & Program Plan Package	Feb 01
5	A	Interface Control Document	Mar 01
8	B2	Lane Tracking System Down-Select Summary Report	Apr 01
11	B5	Warning Cue Implementation Summary Report	Jun 01
14	C3	Threat Assessment Simulation Summary Report	Jun 01
15	C5	NHTSA Threat Assessment Simulation Summary Report	Jun 01
19	E	FOT Operational Test Plan	Jun 01
6	B1	FLR Interim Report	Jul 01
10	B3	Brake Actuator System Test Summary Report	Sep 01
16	D	Prototype Vehicle Verification Test Data and Report	Nov 01
26	F	ACAS/FOT Phase I Interim Report Briefing Package	Dec 01
12	C1	Data Fusion Algorithm Simulation Summary Report	Dec 01
13	C2	Path Prediction/Estimation Summary Report	Dec 01
27	F	ACAS/FOT Phase I Interim Report	Dec 01

1.5 Master Program Schedule for Phase I

Figures 1.1 through 1.5 are top level program schedules showing work completed in Phase I. More detailed schedules for each task are provided in the following Sections.

ID		Task Name
1		**A System Integration**
2	✓	**A1 Func Descr**
3	✓	***D1: Functional Description Document***
4	✓	*MS1: CW Architecture Definition*
5	✓	**A2 System Arch/Mech**
6	✓	***D2: System Architecture/ Mechanization Report***
7	✓	**A3 Interface Mgmt**
8	✓	***D5: Interface Control Document***
9	✓	*MS2: CW Verification Plan*
10	✓	*MS3: CW Interface Definition*
11		**A4 Syst Verification**
12	✓	***D3: System Verification Plan***
13		**A5 Risk Mgmt Plan**
14	✓	***D4: Risk Management Plan***
15		**B Subsystem Development**
16		**B1 Fwd Radar Sensor**
17	✓	**B1A Integ Xcvr/Ant**
18		**B1B Auto Align Algo Dev**
19		**B1C Radome Blkage Algo Dev**
20	✓	**B1D Bridge Rej Algo Dev**
21	✓	***D6: FLR Interim Report***
22		**B1E Syst Int/Dev Suppt Planning**
23		**B1E Syst Int/Dev Suppt**
24	✓	***D1: Functional Description Document***
25		**B2 Fwd Vision Sensor**
26	✓	**B2A Vision Syst Dev Plan**
27	✓	**B2B Baseline Lane Det/Trk Syst Demo**
28	✓	*MS4: Lane Tracking "Kick-Off" Meeting*
29	✓	***D8: Lane Tracking System Reqs Summary Rpt***
30	✓	**B2C Rqmts Def Lane Trk Syst**
31	✓	**B2D Syst Dev Lane Tracking**
32	✓	**B2E Tech Downselect Sessions**
33	✓	*MS5: Lane Tracking Technology Down Select Meeting*
34	✓	*MS6: Lane Detection/ Tracking Vision System Selection*
35	✓	***D7: Lane Tracking System Down-Select Summary Rpt***
36		**B2F Syst Int/Dev Suppt Planning**
37		**B2F Syst Int/Dev Suppt**

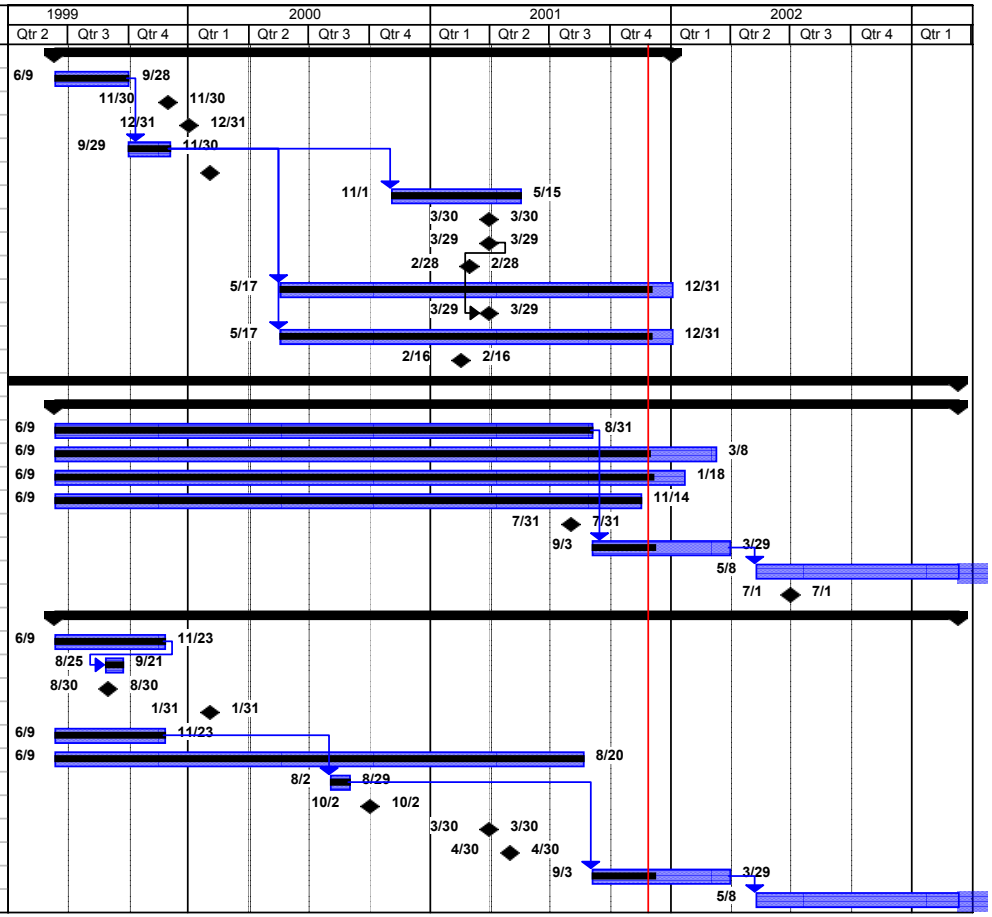

Figure 1.1 Master Program Schedule, Page 1

ID	Task Name
38	**B3 Brake Control System**
39	**B3A Brake Syst Design**
40	***D9: Brale Actuatpr System Design Summary Report***
41	*MS7: Brake System Design*
42	**B3B Brake Syst Verification Testing**
43	***D10: Brake Actuator System Test Summary Re[port***
44	**B3C Vehicle Builds**
45	*MS8: Brake Sys On Engineering Phase Veh Demo*
46	**B3D Syst Int/Dev Suppt Planning**
47	**B3D Syst Int/Dev Suppt Execution**
48	**B4 Throttle Control System**
49	**B4A System Development**
50	**B4B Syst Int/Dev Suppt Planning**
51	**B4B Syst Int/Dev Suppt**
52	**B5 Driver-Vehicle Interface**
53	*MS9: DVI Technology Exchange "Kick-Off" Meeting*
54	**B5A Warning Cue Suite Selection**
55	*MS10: DVI Warning Cue Set Selection*
56	***D11: Warning Cue Implementation Summary Report***
57	**B5B DVI Development**
58	**B5C Syst Int/Dev Suppt Planning**
59	*MS11: DVI/HUD System on Bench Demonstration*
60	**B5C Syst Int/Dev Suppt Execution**
61	**C Subsystem Processing Development**
62	**C1 Data Fusion**
63	**C1A Requirements & Architecture Definition**
64	*MS12: Data Fusion Arch and Performan Reqs Definition*
65	**C1B Initial Data Fusion Algorithm Dev**
66	*MS13: Preliminary Dat Dusion Algorithm Simulation Demo*
67	**C1C Real-time Data Fusion Algortihm Dev**
68	*MS14: Data Fusion Algorithm Simulation Demonstration*
69	***D12: Data Fusion Algorithm Simulation Summary Report***
70	**C1D Syst Int/Dev Suppt Planning**
71	**C1E Syst Int/Dev Suppt Execution**
72	***D29: Data Fusion Algorithm In-Vehicle Summary Report***

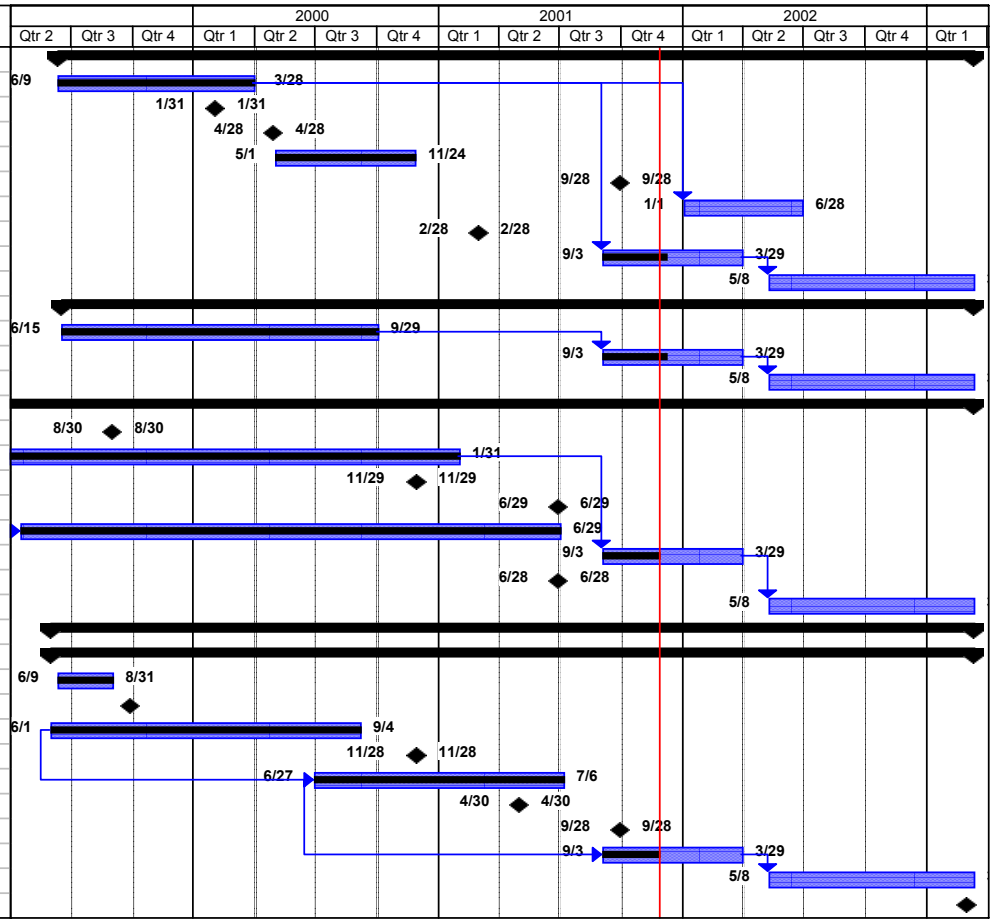

Figure 1.2 Master Program Schedule, Page 2

ID		Task Name
73		**C2 Tracking & Identification**
74	✓	**C2A Conventional Approach Development**
75	✓	**C2B Scene Tracking Approach Development**
76	✓	**C2C Enhanced GPS Approach Development**
77		**C2D Syst Int/Dev Suppt Planning**
78	✓	***D13: Path Prediction/Estimation Summary Report***
79		**C2D Syst Int/Dev Suppt Execution**
80		**C3 CW Function**
81	✓	*MS15: Threat Assessment "Kick-off" Meeting*
82	✓	**C3A Algorithm Development**
83	✓	**C3B Threat Assessment Simulation Dev**
84	✓	**C3C Threat Assessment In-Vehicle Dev**
85	✓	***D14: Threat Assessment Simulation Summary Report***
86		**C3D Syst Int/Dev Suppt Planning**
87		**C3E Syst Int/Dev Suppt Execution**
88	✓	***D30: Threat Assessment In-Veh Summary Report***
89		**C4 ACC Function**
90	✓	**C4A System Development**
91		**C4B Syst Int/Dev Suppt Planning**
92		**C4B Syst Int/Dev Suppt Execution**
93		**C5 NHTSA CW Algorithm**
94	✓	**C5A NHTSA Threat Assessment Sim Dev**
95		***D15: NHTSA TA Simulation Summary Report***
96		*MS16: NHTSA TA Algorithm on Prototype Veh Demo*
97		**C5B NHTSA Threat Assessment In-Veh Dev**
98		*MS29: NHTSA TA Algo on Pilot Phs Veh Demo*
99		*MS30: NHTSA TA Algo on Deploymnet Veh Demo*
100		***D30: NHTSA TA In-Vehicle Summary Report***

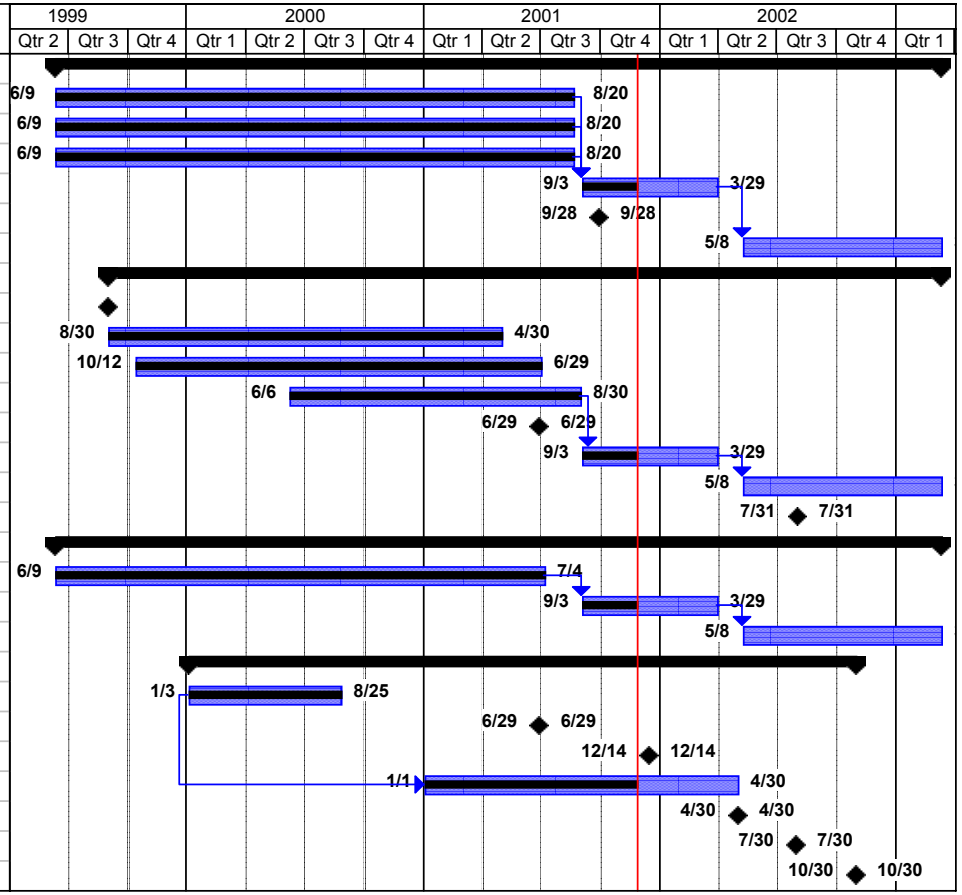

Figure 1.3 Master Program Schedule, Page 3

ID		Task Name
101		**D Fleet Vehicle Build**
102	✓	**Engineering-Phase Vehicles**
103		*MS17: EDV Vehicle Build Completion*
104	✓	**Prototype-Phase Vehicle Build & Test**
105	✓	**Prototype Vehicle Verification**
106		*MS18: Prototype Vehicle Demonstration*
107		**Order Phase II Material**
108		**Pilot-Phase Vehicle Build/Test**
109		**Pilot Vehicle Verification**
110		***D31: Pilot-Phase Vehicle Demonstration***
111		**Deployment Vehicle Build**
112		**Deployment Vehicle Verification**
113		***D32: Deployment-Phase Vehicle Demonstration***
114		***D33: Provide NHTSA Evaluation Vehicle***
115		**E Field Operational Test**
116	✓	**Preliminary Preparation**
117	✓	*MS19: Submission of FOT Pilot Test Plan*
118	✓	***D17: FOT Pilot Test Plan***
119	✓	*MS20: Completion of FOT Prof Pilot, Testing &n Data Acq*
120		***D18: FOT 1st HURP Request***
121		*MS21: Completion of FOT 1st HURP Approval Process*
122		***D19: FOT Operational Test Plan***
123		*MS22: Submission of FOT Operational Test Plan*
124		***D32: FOT 2nd HURP Request***
125		*MS34: Completion of FOT Pilot Test With Accompanied Lay Person*
126		*MS35: Completion of FOT Data Acquisition Package*
127		*MS36: Completion of FOT 2nd HURP Approval Process*
128		*MS37: Launch of FOT Operational Testing*
129		**Final Preparation**
130		**FOT Test**
131		***D33: FOT Data From All Test Subjects (Start)***
132		***D34: FOT Data From All Subjects (End)***
133		*MS38: Competion of FOT Operational Testing*
134		**Data Analysis**
135		*MS39: Submission of the FOT Report*
136		***D35: FOT Report***

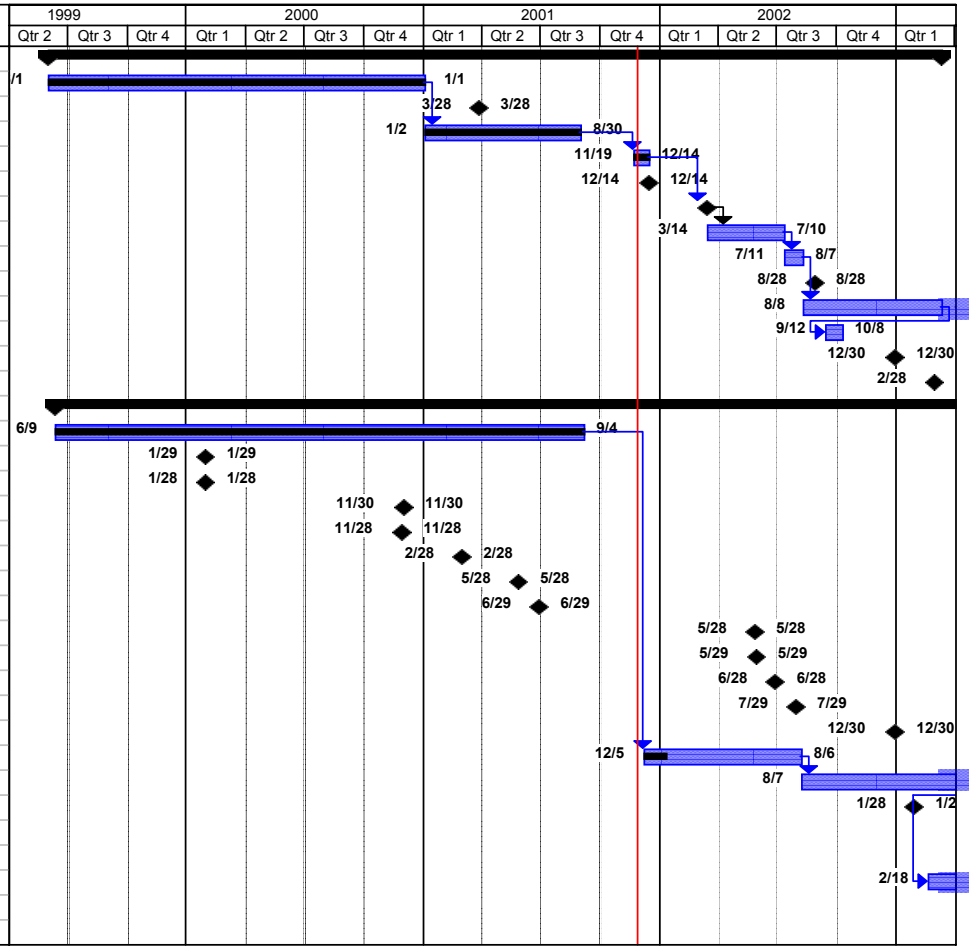

Figure 1.4 Master Program Schedule, Page 4

ID		Task Name
137		**F Program Management**
138		**Management**
139		**Start of Program**
140	✓	*MS23: ACAS/FOT "Kick-Off" Program Team Meeting*
141	✓	***D20: ACAS/FOT Program Schedule***
142	✓	*MS24: ACAS/FOT "Kick-Off" Meeting*
143	✓	***D21: ACAS/FOT "Kick-Off" Meeting Briefing Package***
144	✓	*MS25: Program Review Briefing 1*
145	✓	***D22: Program Review 1 Briefing & Program Package***
146	✓	*MS26: Program Review Briefing 2*
147	✓	***D23: Program Review 2 Briefing & Program Package***
148	✓	***D24: First Annual Report***
149	✓	*MS27: Program Review Briefing 3*
150	✓	***D25: Program Review 3 Briefing & Program Package***
151	✓	*MS40: Program Review Briefing 4*
152	✓	***D36: Program Review 4 Briefing & Program Package***
153		*MS28: Phase I Interim Program Review Briefing*
154		***D26: Phase I Intermi Report Briefing Package***
155		***D27: Phase I Interim Report***
156		*MS41: Program Review Briefing 5*
157		***D37: Program Review 5 Briefing & Program Package***
158		***D38: Third Annual Report***
159		*MS42: Program Review Briefing 6*
160		***D39: Program Review 6 Briefing & Program Package***
161		*MS43: Program Review Briefing 7*
162		***D40: Program Review 7 Briefing & Program Package***
163		*MS44: Final Program Review Briefing*
164		***D41: Final Program Review Briefing Package***
165		***D42: Final Program Report***

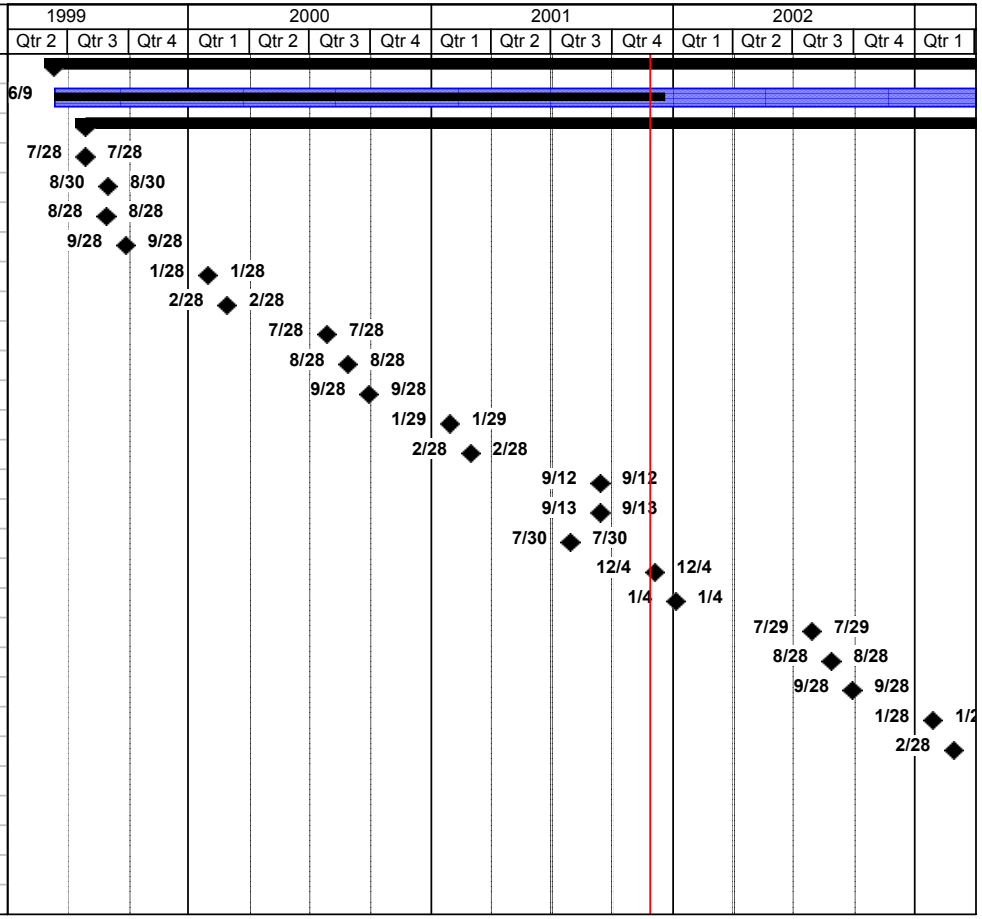

Figure 1.5 Master Program Schedule, Page 5

2 System Integration (Task A)

The ACAS team followed the GM Vehicle Development Process to ensure that a robust, safe vehicle is provided for the field operational test (FOT). Task A consists of the following subtasks, which are discussed in this section.

1. Functional Description (Task A1)
2. System Architecture/Mechanization (Task A2)
3. Interface Management (Task A3)
4. System Verification (Task A4)
5. Risk Management Plan (Task A5)

Deliverables for Task A are summarized below. The overall schedule for Task A is given at the end of this section.

Deliverable	Title	Delivery Date
1	Functional Description Document	1/00
2	System Architecture/Mechanization Report	12/99
3	System Verification Plan	3/01
4	Risk Management Plan	2/01
5	Interface Control Document	3/01

2.1 Functional Description (Task A1)

Goals, Purpose and Background

The purpose of this subtask was to:

1. Capture the system functional requirements
2. Allocate system functional requirements to subsystems and components

The approach for this task was based on the work of Hatley-Pirbhai [Strategies for Real-Time System Specification, 1988, Doerst House Publishing Co.]. System Requirement, Architecture and Specification models were developed using the Process Model (Data Context Diagram and Data Flow Diagram) and the Control Model (Control Context Diagram and Control Flow Diagram).

Intermediate and Final Results

Following is a description of the controls, displays, and operating modes that were defined for the Adaptive Cruise Control (ACC) and Forward Collision Warning (FCW) functions.

System Functional Description

The ACC provides operating modes similar to conventional cruise control with the following additional features:

1. For the purposes of the FOT, the cruise control may be commanded to operate like a conventional cruise control. The conventional cruise control mode will be maintained for the first week, and possibly the last week, that an FOT vehicle is in use by each subject.

2. When active, the ACC has two modes, maintaining the set speed and maintaining the selected headway.
3. When maintaining headway, the system is capable of slowing the vehicle to pace a moving lead vehicle that is traveling slower than the set speed.
4. Once the ACC subsystem slows the host vehicle below the minimum cruise speed, a message indicates that the driver should take full control of the vehicle. Once this message is displayed, the system will not command the host vehicle to accelerate until the driver manually accelerates above the minimum set speed and then initiates the resume function or the set speed function.

The primary driver interface to engage and operate the ACC function consists of the standard production cruise controls and a headway selection switch. Using this interface, the driver is provided with the following capabilities:

1. Turn the ACC on and off
2. Set the desired cruise speed (set speed)
3. Increase set speed by fixed steps
4. Decrease set speed by fixed steps
5. Accelerate to a new set speed
6. Coast (decelerate) to a new set speed
7. Resume a previously set speed
8. Set the desired headway (headway adjustment)

Additionally, the accelerator pedal may be used to over-throttle the ACC system. As in standard cruise control, manual braking causes the system to go to standby mode. When the ACC is first turned on, the initial headway setting is set to the maximum.

The primary ACC display is a head-up display that includes the following information:

1. ACC Engaged/Disengaged
2. Set Speed
3. Current Speed
4. Tracking/Not Tracking a Lead Vehicle while is ACC engaged
5. ACC headway setting
6. ACC Operational/Failed

While only conventional cruise control is available, only the current vehicle speed is displayed on the head-up display.

The vehicle provides an FCW capability that includes alerts and advisory displays to assist drivers in avoiding or reducing the severity of crashes involving the host vehicle striking the rear end of another motor vehicle. For the purposes of the FOT, the FCW will have enabled and disabled modes. The FCW will be disabled when only conventional cruise control is available in the vehicle. The driver will not be able to disable the FCW, but will be given a control to adjust the sensitivity of the FCW function. The sensitivity adjustment does not permit the FCW function to be disabled by the vehicle operator. The button to control the sensitivity of the FCW is the same button as that used to adjust headway when ACC is engaged.

The FCW crash warnings include visual and auditory cues to the driver. The visual and audio characteristics of the FCW crash warning were selected, based upon the results of human factors studies, to support timely return of an inattentive driver to active driving involvement under conditions in which the system determines that driver involvement may be lacking. The visual indicator also supports the driver in maintaining a safe distance when following behind other motor vehicles.

Cruise Control Modes-Adaptive Cruise Control Enabled

The cruise control behaves like a standard cruise control system until the adaptive features are enabled. Figure 2.1 shows the states and transitions for the cruise control when the adaptive features are enabled; Table 2.1 describes the various ACC modes.

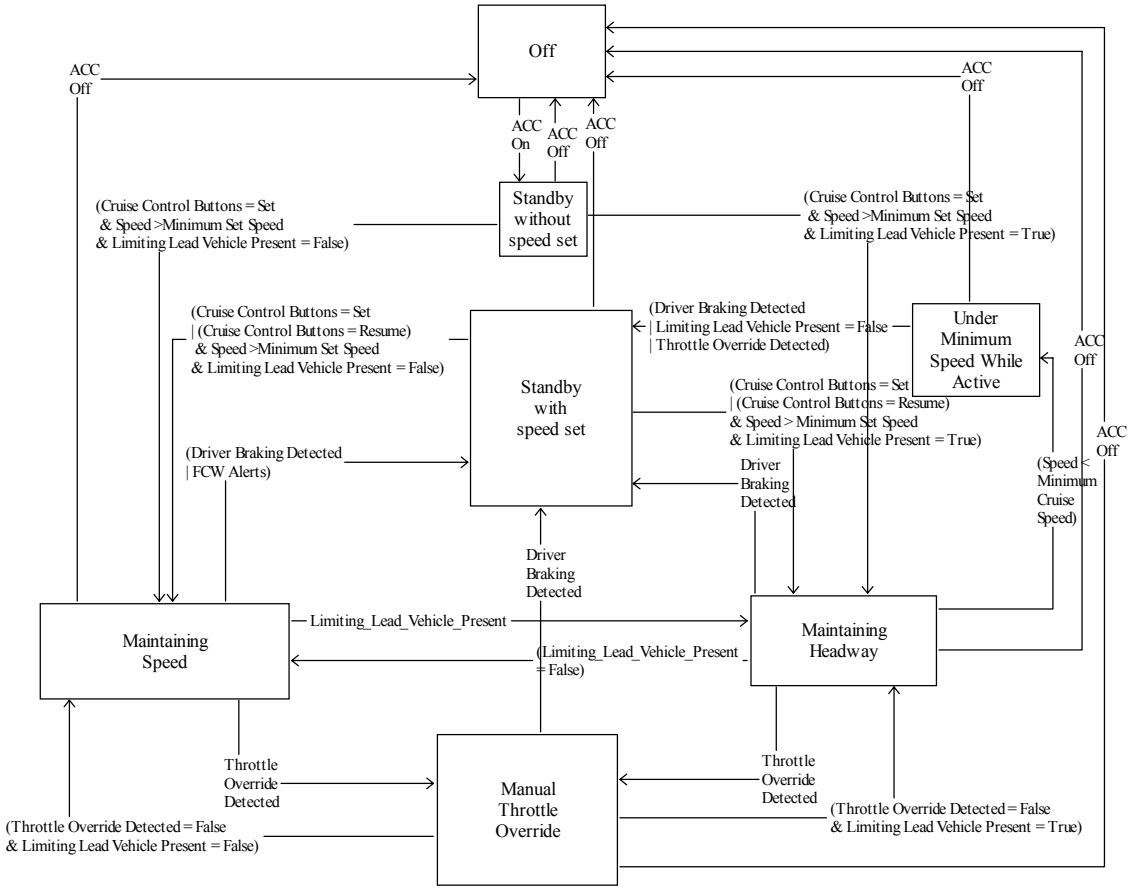

STD: ACC_Vehicle_Controls.c

Figure 2.1 ACC Vehicle Controls

Table 2.1 Adaptive Cruise Control Modes

ACC Off	The ACC system is not functional. This state is entered whenever the ignition is on and the ACC is turned off.
Standby without speed set	The system is waiting to take control of the throttle and brakes. This state is entered when the ignition is turned on and the ACC is turned on. From this state the system can be activated by pressing the set button after the vehicle has reached the minimum set speed.
Standby with speed set	The system is waiting to take control of the throttle and brakes. A set speed has been established previously.
Maintaining Speed	In this mode the ACC system attempts to reach and hold a specified speed. While in this mode the set speed can be increased or decreased by pushing or tapping on the resume/accel or set/coast buttons. Also, in this mode, the desired headway can be adjusted by tapping on the GAP/WARN button. Changes in headway impact ACC behavior once a lead vehicle is detected.
Maintaining Headway	In this mode the ACC system attempts to reach and hold a specified headway. While in this mode the set speed can be increased or decreased by pushing or tapping on the resume/accel or set/coast buttons. Also, in this mode, the desired headway can be adjusted by tapping on the GAP/WARN button.
Manual Throttle Override	In this mode the driver is pushing on the throttle to force the vehicle to go faster than the cruise control function would command.
Under Minimum Speed While Active	In this mode the ACC has reduced the vehicle speed below a minimum cruise speed because a slow vehicle is ahead. When this state is entered the driver is given a message to take control of the vehicle. Once this happens the ACC will not cause the vehicle to accelerate but it will continue to brake if the lead vehicle continues to decelerate.

System Process Model

System Requirement, Architecture and Specification models were developed using the Process Model (Data Context Diagram and Data Flow Diagram) and the Control Model (Control Context Diagram and Control Flow Diagram). Figure 2.2 summarizes the data flow model. The following paragraphs briefly describe the functional breakdown of the system.

The **Vehicle Sensor and Input/Output** functions include filters for the vehicle kinematics sensors to provide engineering units and to reduce noise in these measurements.

The **Radar Auto-Alignment and Blockage Detection** function evaluates the radar returns to detect when the signal seems to be attenuated by a blocked radome. It also looks at target tracks to produce electronic adjustments of the radar alignment. This function also produces control signals that indicate if the radome is blocked or if the alignment is beyond the range that can be corrected.

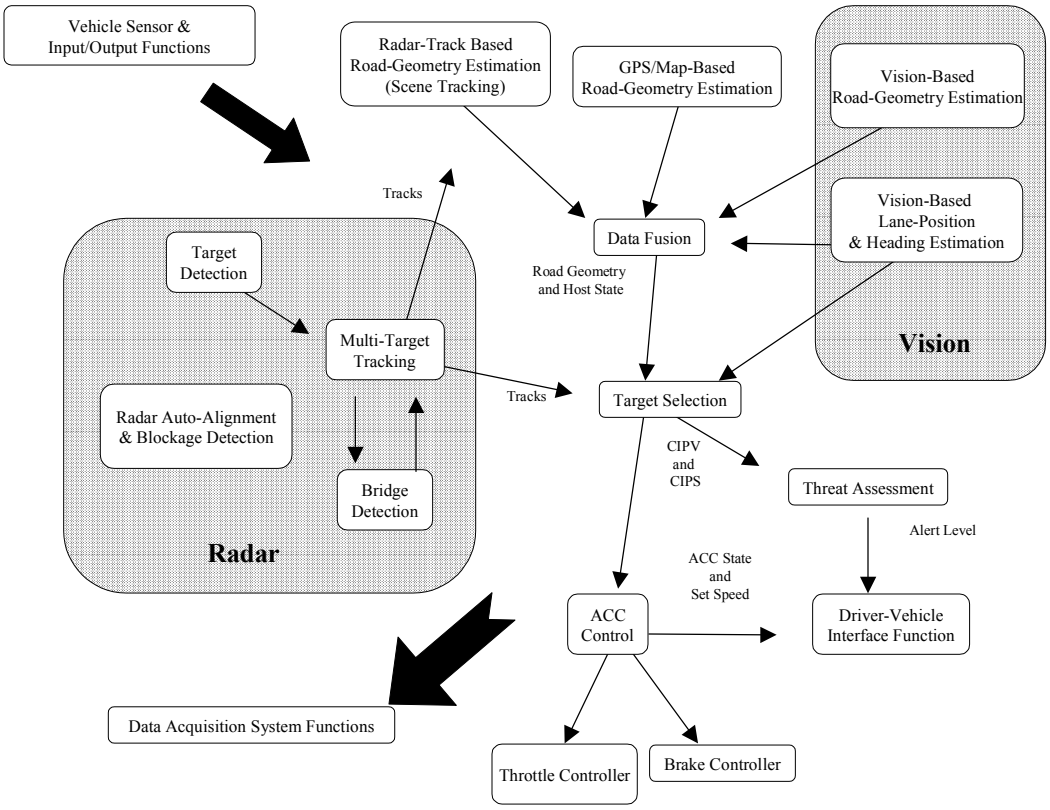

Figure 2.2 Prototype Vehicle System Process Model

The **Target Detection** function processes the radar signals to produce estimates of the range, range rate, relative acceleration, and extent of objects. It also reports the amplitude of the return from each detection.

The **Multi-Target Tracking** function associates detections in each new sample with previously observed tracks. It reports whether any currently stationary objects were ever observed to be moving, and can let a target "coast" if it disappears for a short period of time.

The **Bridge Detection** function looks at the target tracks to determine if any should be classified as bridge (this includes overhead signs). Objects classified as bridges will not be used to generate FCW alerts.

The **Radar-Based Road-Geometry Estimation** function (also called **Scene Tracking)** evaluates the target tracks to estimate the geometry of the road ahead of the vehicle and the vehicles relationship to the road.

The **Vision-Based Road-Geometry Estimation** function determines the geometry of the road ahead of the vehicle and the relationship between the road and the host vehicle. The road-geometry information includes the curvature of the road ahead of the vehicle. The relationship between the vehicle and the road includes the lateral position in the lane, the heading angle, and whether a lane change is occurring.

The **Map-Based Road Geometry Estimation** function uses a roadmap database, DGPS, and dead reckoning to determine the current map position of the vehicle. It then extracts information from the database indicating the geometry of the road ahead of the vehicle and the location of significant features along the road.

The **Yaw-Based Path Estimation** function predicts the host vehicles path using yaw-rate sensor input, vehicle speed, and acceleration measurements.

The **Data Fusion** Functions combine the evidence from the entire sensor suite to develop a higher confidence prediction of the host vehicle's path and to predict the driver/vehicle response in the event of an alert.

The **Target Selection** function evaluates the predicted path of the host vehicle and the objects to determine the threatening targets that will be used for ACC control and for FCW threat assessment. The FCW targets are those that are in the host vehicle's path or are predicted to cross the host vehicle's path. They may be moving or stationary.

The **Threat Assessment** function uses the host vehicle dynamics, the target dynamics, and the expected driver response to determine what level of warning should be generated. The warning algorithm also depends upon whether the ACC is active. When ACC is active a warning is produced if it is predicted that the maximum braking authority will not prevent a collision.

The **ACC Control** functions maintain the vehicle's speed or headway when the ACC is on and engaged. The controls are similar to those of a conventional cruise control system with the addition of a headway setting. The output includes throttle and brake actuator control signals. In headway maintenance mode the ACC gets range and range rate data for the primary target from the Target Selection function.

The **Driver-Vehicle Interface** functions control all of the devices that transmit information to the driver. These include audio, visual, and haptic outputs. The visual display includes a head-up display. The information displayed includes the status of the ACC (on, engaged, set speed, and target detected). The information also includes warnings that indicate maintenance is required or that the vehicle is being operated beyond the range of capability of the ACC/FCW.

2.2 System Architecture/Mechanization (Task A2)

Goals, Purpose and Background

The main objectives of this subtask were to:

1. Partition the system into subsystems and components
2. Allocate functional requirements to the subsystems and components
3. Designate interfaces among the subsystems and components

Following the structured method of Hatley and Pirbhai, the total vehicle, with all its embedded systems, was considered as one supersystem. The supersystem was partitioned into physical boxes that, in their totality, satisfy all the functional requirements. Processes in the requirement model were allocated to slots in the architecture model.

Intermediate and Final Results

Table 2.2 lists the system modules and their primitive functions.

Table 2.2 System Modules and Their Primitive Functions

Architecture Module	Function
Scene Tracking Subsystem	Radar-Track Based Road Geometry Estimation
Path Estimation & Target Selection Processor	Yaw-Based Path Estimation Bridge Detection Target Selection
Map-based Road Geometry Processor	Map-Based Road Geometry Estimation
FCW Processor	Vehicle Sensor and I/O Interfaces All of the Data Fusion Functions Threat Assessment
ACC Controller	ACC Vehicle Controls
Data Acquisition Subsystem (DAS)	All of the Data Acquisition Functions
Radar	Target Detection Multi-Target Tracking Auto-alignment and Blockage Detection
Vision System	Vision-Based Road Geometry Estimation Lane Position and Heading Estimation
Driver Vehicle Interface (DVI) Subsystem	Driver-Vehicle Interface function

Figure 2.3 shows the physical architecture, subsystems, and components of the system, with connections and buses between the processors. This drawing shows the top-level hardware used in the Prototype vehicle. More detailed drawings, including the flow and sources of information from and for each physical box (block) were provided in the System Architecture/Mechanization Report. That report describes the functional interaction between the blocks as well as the internal functions of each block. The main information artery is a high-speed CAN Bus (500kbaud) which transfers a large body of communication messages among the subsystems or the components. Additionally, a GM Class 2 Bus provides information linkage from the vehicle-based signals to all subsystems requesting such signals, either directly or indirectly via the CAN Bus. Other harnesses are direct wires.

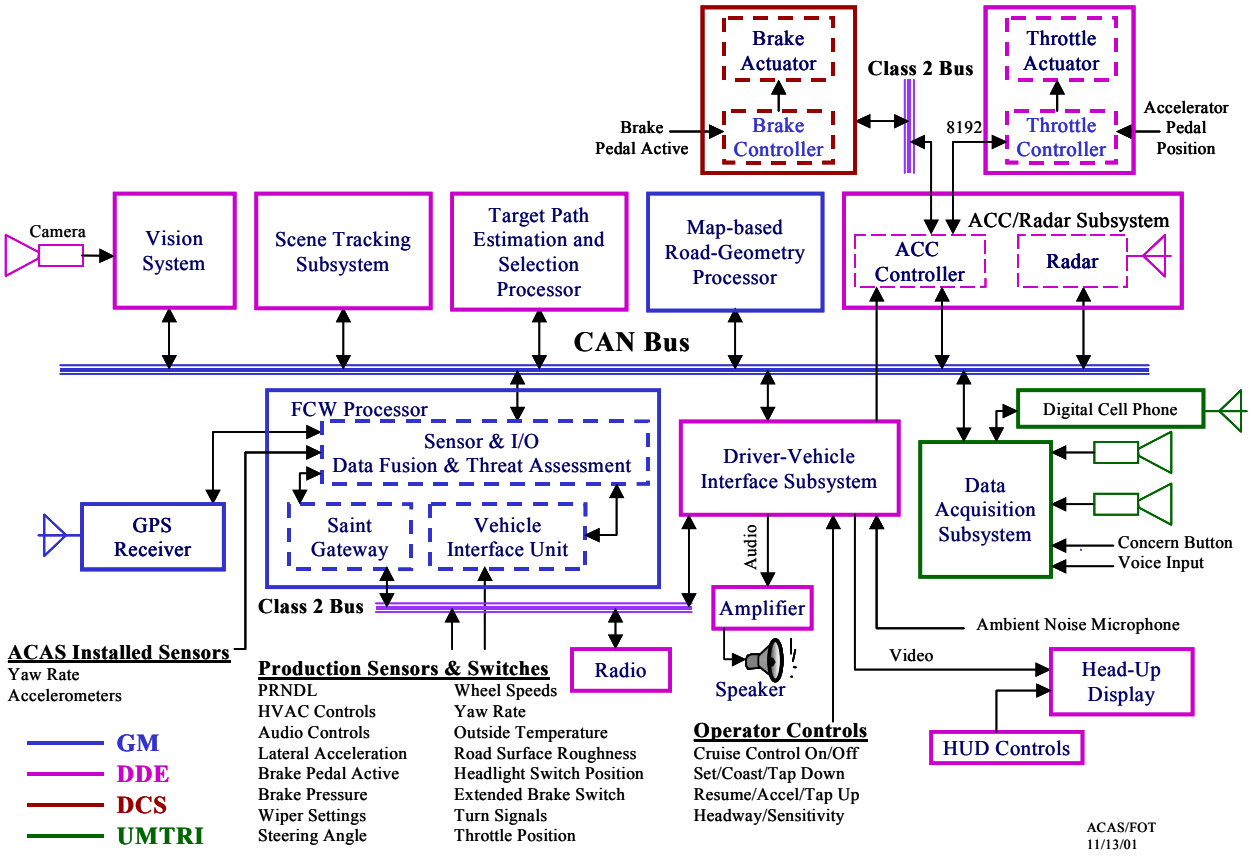

Figure 2.3 Prototype Vehicle System Block Diagram and Mechanization

2.3 Interface Management (Task A3)

Goals, Purpose and Background

The main objective of the Interface Management task is to ensure that independently developed subsystems or components satisfy the prescribed requirements and operate according to the specifications and in adherence with the communication protocol when connected as a system.

To ensure subsystem interface compatibility and traceability, a systematic approach was followed. First, the interface signals between each and every hardware block in the block diagram (Figure 2.3) were labeled. Then, every signal source, destination, bit structure, and other relevant information was tabulated. This approach allows:

1. Developing a complete record of all signals among different subsystems or components
2. Mapping a one-to-one correspondence between each input signal (to a block) and its source
3. Implementing changes with minimal effort

Intermediate and Final Results

The initial interface control document was generated in March 2000. The document includes four sections:

1. Introduction
2. Prototype Vehicle System Block Diagram and Mechanization Drawing
3. CAN Bus message definitions
4. Class 2 Bus message definitions

A total of 43 different eight-byte CAN Bus message types were defined. The definition of each message includes the number of bits for each variable contained in the message, the number format, its units, range, resolution, and accuracy.

The document has been updated regularly and distributed.

2.4 System Verification (Task A4)

Goals, Purpose and Background

The overall objective of the ACAS System Verification task is to make sure the system is ready for use by subjects in the FOT. This requires verification that the system satisfies certain minimum performance requirements at the component, subsystem, and system level. The System Verification Task includes:

1. Definition of the system verification process
2. Supervision of the definition and execution of verification tests at the component and subsystem level
3. Definition and execution of the verification plan at the system level.

Verification was done on the Engineering Development and Prototype vehicles at several levels: component, subsystem, and system. Component-level verification included the operation of the ACAS-specific on-board sensors. These included sensors for vehicle kinematics, environment sensors, and driver activity sensors. Subsystem-level verification included testing the operation of the interfaces between the subsystems and the functionality of each subsystem. System-level verification included subjecting the prototype vehicle to crash and nuisance alert scenarios on a test track and driving the vehicle on a prescribed route in traffic. The subsystem designers were responsible for definition of the test procedures at the component and subsystem level. The subsystem designers, under supervision of the systems engineers, executed these tests.

The systems engineers were responsible for definition of the test procedures at the system level. The systems engineers executed the system-level tests.

The dynamic scenarios shown in Table 2.3 were selected for use for system-level verification.

Table 2.3 System-Level Verification-Test Scenario Descriptions

Test	Scenario Description	Quantitative Collision Alert Test	Qualitative Nuisance Alert Test	Qualitative ACC Test
1	SV 60 mph to POV Stopped	X		X
2	SV 50 mph to POV 10 mph	X		X
3	SV 60 mph to POV Braking Unusually Hard from 60 mph	X		X
4	SV 60 mph to Motorcycle POV Braking Moderately Hard from 60 mph	X		X
5	SV 50 mph to POV Stopped on Curve	X		X
6	SV 50 mph to POV 25 mph in a Curve	X		X
7	SV 60 mph Cut-off by POV 40 mph	X		X
8	SV 45 mph Changes Lanes and Encounters POV Stopped	X		X
9	SV 60 mph Tailgating POV Braking from 60 mph	X		
10	SV 60 mph Approaches Motorcycle and Truck POVs 20 mph	X		X
11	SV 60 mph Approaches Motorcycle behind Truck POVs 20 mph	X		X
12	SV 50 mph on Curve to POV Braking Moderately Hard from 50 mph on Curve	X		X
13	SV 65 mph Following POV 60 mph	X		
14	SV 50 mph to POV Braking Unusually Hard from 50 mph	X		X
15	SV 40 mph to POV Stopping from 40 mph	X		X
16	SV 45 mph behind 45 mph POV Changing Lanes to Reveal Stopped POV	X		X
17	SV 50 mph Passing POVs 25 mph Around Curve		X	X
18	SV 60 mph Passing Truck POVs 20 mph in Adjacent Lanes		X	X
19	SV 60 mph following POV 60 mph		X	X
20	SV 50 mph POV 60 mph Cuts in Ahead of SV		X	X
21	SV on Simulated Open Road No Other Traffic		X	X
22	SV Daytime Public Road Test		X	
23	SV following POV on Simulated Open Road			X
24	SV 45 mph POV 45 mph Changes Lanes in front of Accelerating SV			X
25	SV 60 mph changing ACC Headway following POV 60 mph			X
26	SV 50 mph following POV Accelerating from 50 mph			X
27	SV 50 mph following POV 50 mph Changes Lanes to reveal POV 50 mph			X
28	SV 40 mph passes POV 40 mph			X
29	SV 50 mph Throttle Override during Automatic Braking			X
30	SV 50 mph ACC Test with Anti-lock Braking Activated			X

Briefings on the validation plan were prepared and presented during technical interchange meetings in Malibu, CA on November 16, 1999 and in Warren, MI on June 29, 2000. In addition, a briefing and discussion was held on system level testing scenarios with NHTSA, The Volpe Center, and other government representatives in Washington, DC on March 28, 2000. These technical interchange meetings led to the preparation and delivery of a testing scenarios report that was delivered to NHTSA in April 2000.

The System Verification Plan was submitted in July 2001. A review of the plan with NHTSA occurred in Washington, DC. This led to some modifications that were incorporated into a revised plan submitted in September 2001.

Intermediate and Final Results

The Subsystem Verification Tests were executed between August 2001 and September 2001. System Level Tests were performed during October 2001. Results of the system-level testing are reported in Section 10.2, Threat Assessment In-Vehicle Development.

2.5 Risk Management Plan (Task A5)

Goals, Purpose and Background

The overall objective of the Risk Management task is to define the hazard analysis and safety risk management program to be implemented by the team in the performance of the ACAS/FOT program. The Risk Management Plan was developed using guidelines from Mil Standard 882C and SAE J1789. Safety plan presentations were prepared and presented at meetings in November 1999 and June 2000. In addition, the Safety Engineering team met with the principal engineers working on each subsystem to gather the required information for the safety analysis and hazard mitigation plan. The Risk Management Plan was delivered to NHTSA in February 2001.

The ACAS/FOT program is committed to applying best-practice engineering methods to help insure the safety of the ACAS system. It is the intention that the safety risks of this research product will be no worse than the products that the driving public is used to. And, it will meet, or exceed, both the program requirements and the government regulations that pertain to research vehicles used on the public roads. The ACAS/FOT program is committed to the development and introduction of technologies that improve vehicle safety.

The safety tasks identified within the Risk Management Plan are listed in Table 2.7.

Table 2.4 Safety Tasks

Title	Participants
Preliminary safety assessment	
- Develop preliminary hazard list	ALL
- Perform preliminary hazard analysis	ALL
- Specify system-safety requirements	Program Manager, Safety lead
System hazard analysis	
- Fault tree analysis	ALL
Specify subsystem/component safety requirements	Individual suppliers
Specify diagnostics requirements	Program Manager, Safety lead
Human factors safety analysis	UMTRI (independent analysis)
Verify brake system safety related diagnostics and hardware	Delphi
Safety testing	ALL
Safety case	System Safety Consultant/ Facilitator

During the Preliminary Safety Assessment each responsible engineer provided information about the functions of the particular system, sub-system or component and identified the safety impact of those functions, i.e., what would the impact be if this high-level function disappeared or an unwanted situation occurred. That information has been synopsized and captured as a preliminary hazard list.

This has resulted in being able to identify which sub-systems, or components need to be considered as safety critical or safety related. In general, we categorized components by the ability of the vehicle occupants to take control of the vehicle should one or more of the components fail.

During this development program, testing of individual subsystems, integration of those systems into Engineering Development Vehicles (EDV), integration into a prototype vehicle, and finally a pilot FOT vehicle will be completed. At each stage of the process, engineers will be alerted to safety-critical or safety-related issues as they are observed. In particular, program management will be especially conscientious of issues identified in the Preliminary Hazard Analysis.

In addition, the University of Michigan Transportation Research Institute (UMTRI) will be involved in testing the EDV and the FOT vehicles for operator related functions. We expect that during the UMTRI testing, any observed deficiencies would be flagged. Again, this will be especially true of all safety-critical, or safety-related items identified in the preliminary hazard analysis.

Intermediate and Final Results

A list of 27 hazardous conditions that could develop as a result of a failure in the ACC or FCW systems was developed. Some examples of hazards and possible resulting accident scenarios are listed in Table 2.8

Table 2.5 Sample Hazard List and Potential Accident Scenarios

Hazard	Potential Consequences
Cannot disengage cruise manually	Driver is in either speed or distance mode and wishes to return to manual operation. Applying brake does not reset system. Turning off switch does not reset system.
ACC brake engages unexpectedly	Worst case brake application causes rear end collision and startles driver. Driver brake application (manual over-ride) in this situation is counter intuitive
ACC brake fails to engage when required	ACC applies brake in distance mode, nothing happens. Driver needs to be warned to take control
FCW does not identify in path target (missed detection)	Driver sees target vehicle, but FCW does not identify vehicle and/or change speed to avoid incident and/or warn driver to take control
Improper threat assessment logic triggers alarm that is not a threat or not perceived by driver to be a threat	Driver slams on brakes when not warranted or driver begins to discount future warnings

While a number of examples of risk mitigation strategies can be identified, our preliminary hazard analysis indicates that the ACC and the associated braking system are the areas of most concern. For these particular sub-systems, considerable evaluation has taken place at our team partners' facilities (also the suppliers), Delphi Delco Electronics (DDE) and Delphi Chassis Systems (DCS).

The auto-braking feature that is part of the ACC functionality is a capability that is added to the already existing functions of TCS (traction control), ABS (anti-lock braking) etc. Considerable testing and evaluation were performed by Delphi before the systems were released in the Prototype vehicle. Further winter testing will take place before production of the FOT vehicles.

From the preliminary hazard list that has already been made for the system, as shown in Table 2.5, the program has been able to identify unrequested braking as a primary concern. As part of the program, we have started to collect data and to analyze the events, and the associated subsystems that might lead to, or be used to mitigate this potential problem. In addition to assuring the reliability of the system and its diagnostics, one of the mitigation steps that has already been implemented was to limit the braking authority and the rate the brakes can be automatically applied (the jerk), providing time for a following vehicle to react or the driver to override the automatic braking.

Current Schedule and Progress for Task A

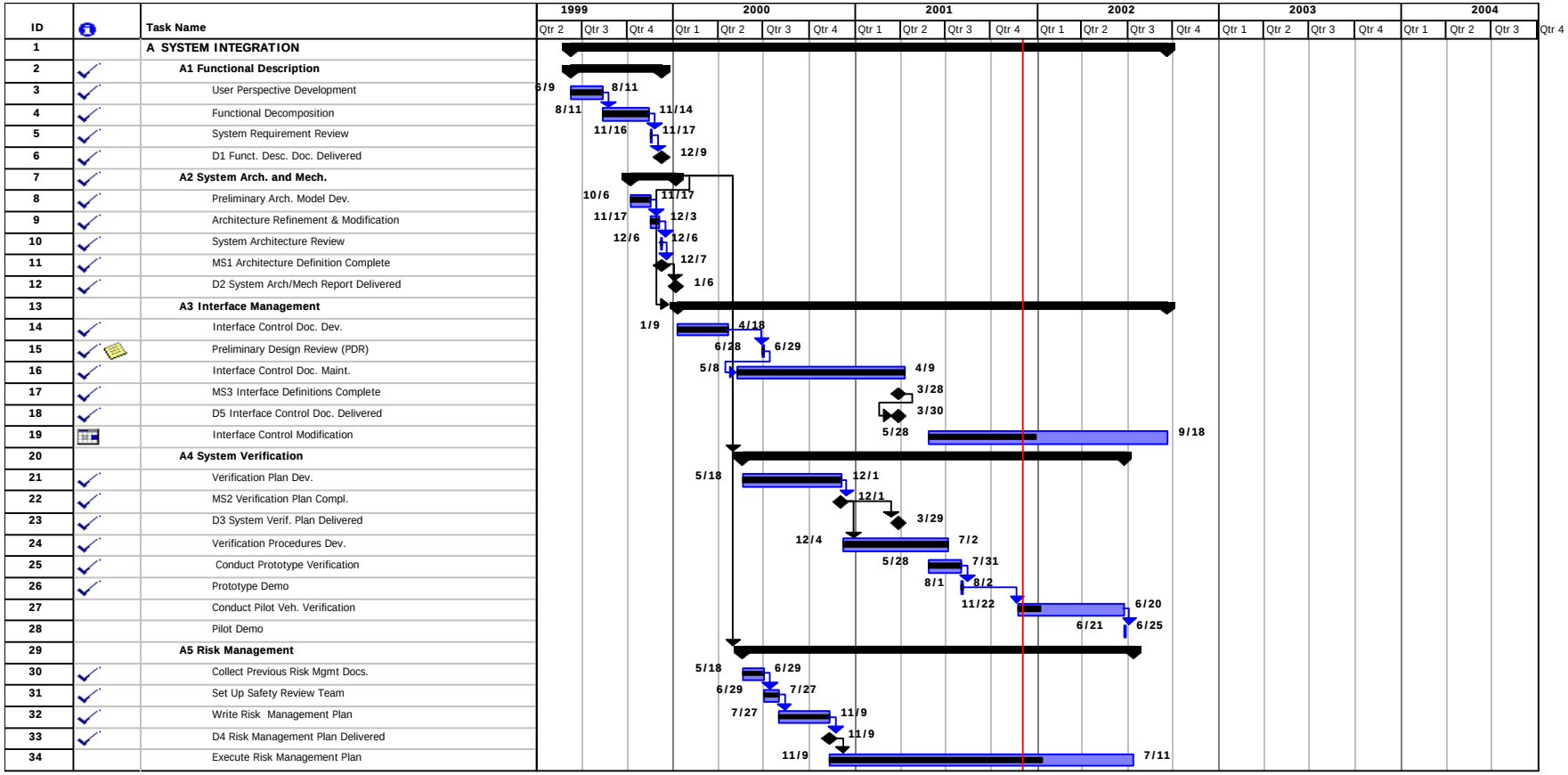

Figure 2.4 Task A Schedule

3 Forward Radar Sensor (Task B1)

3.1 Integrated Transceiver/Antenna (Task B1A)

Goals, Purpose and Background

Development of a microwave monolithic integrated circuit (MMIC) based transceiver with integrated antenna is essential to meet long-term cost and producibility requirements.

A MMIC-based transceiver has been designed to optimize reliability, cost and performance. Large sections of the Automotive Collision Avoidance System (ACAS) Program's Gunn-based transceiver have been replaced with MMIC components. The sensor housing and electronics have been modified to accommodate the new transceiver-antenna assembly and control electronics. The mechanically scanned, folded reflector, narrow beam antenna design is complete. Antenna performance objectives were met and the current design is robust and capable of meeting environmental requirements. Component cost is still an issue, because we are using components purchased as machined parts.

A high-performance MMIC chipset has been designed and fabricated by Infineon Technologies. The first wafers were completed in May 2000 with over-all good results. A second iteration was designed to improve the voltage controlled oscillator (VCO) temperature performance and doubler input voltage standing wave ratio (VSWR). On-wafer measurements were encouraging. Unfortunately, all wafers were lost due to a processing error in the Au/Sn bumping operation.

Design and testing of all MMIC transceiver functional blocks is complete. All components for the first iteration transceivers have been fabricated. The loss of the second generation wafers necessitates the use of the initial chipset. As a result, these first transceivers will have a limited operating temperature range. Assuming minor artwork upgrades as a result of these tests, second iteration transceivers capable of meeting the full temperature range should be available for prototype assembly in the first quarter of 2002.

Intermediate and Final Results

The MMIC transceiver hardware is shown in Figure 3.1. Final assembly and test are in progress. Figure 3.2 shows details of the millimeter-wave alumina substrate with MMICs mounted.

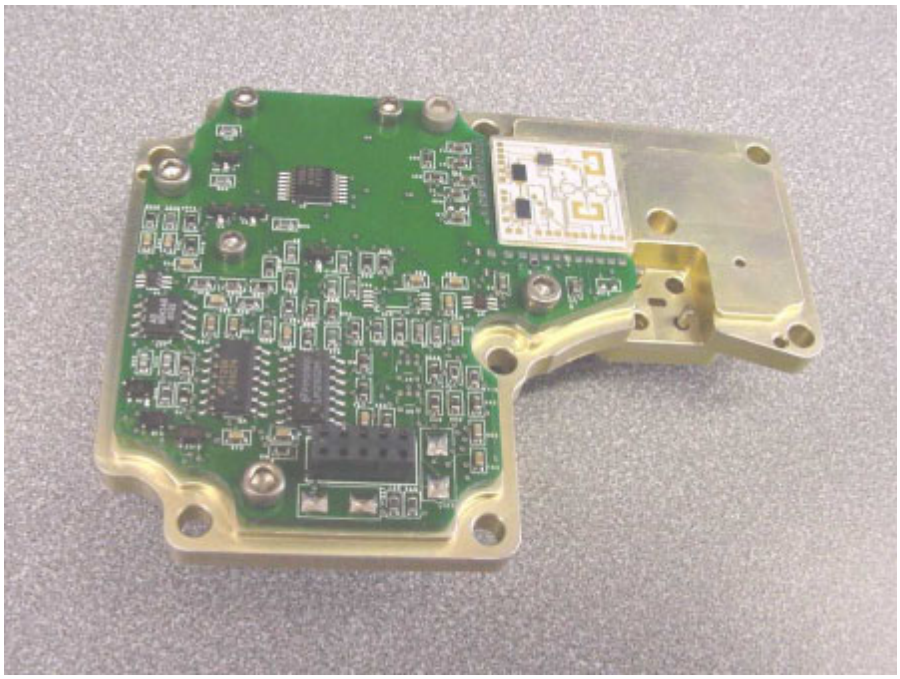

(a) Top view, showing linearizer circuit board, alumina substrate and antenna interface port

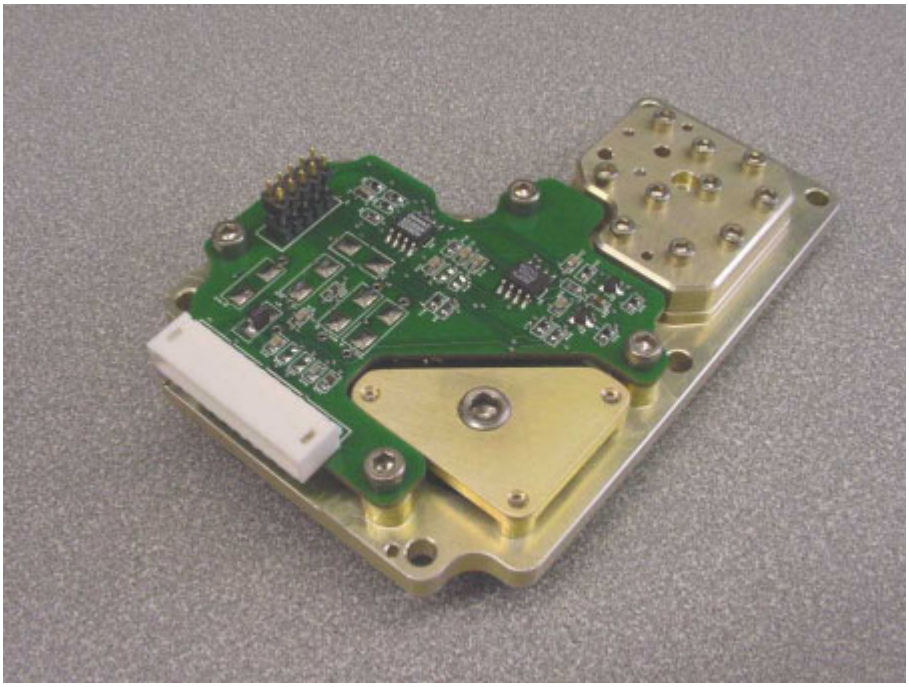

(b) Bottom view, showing power supply circuit board, circulator waveguide block and Dielectric Resonating Oscillator adjust tuning screw

Figure 3.1 MMIC Transceiver Hardware

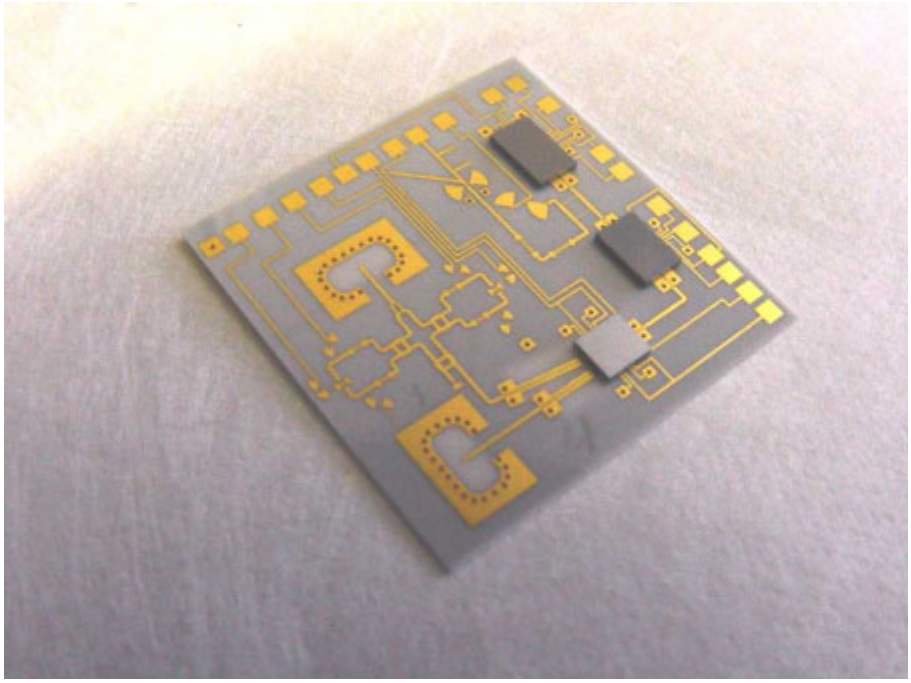

Figure 3.2 Alumina Millimeter-Wave Substrate with VCO, Doubler and Medium Power Amplifier MMICs Mounted

A new set of wafers to replace those lost due to processing error have been fabricated using Infineon's new 6-inch GaAs production line. On-wafer test results are excellent.

Measurements of the 38 GHz VCO are shown in Figure 3.3. Results are outstanding, with flat output power of greater than 8 dBm obtained over a tuning range of 1.3 GHz. Temperature drift is on the order of 4.5 MHz/C which will yield a full temperature range transceiver with comfortable margin. Figure 3.4 shows the W-band output characteristic of the MPA. Greater than 14dBm saturated output is seen, dropping to over 12 dBm at 105C.

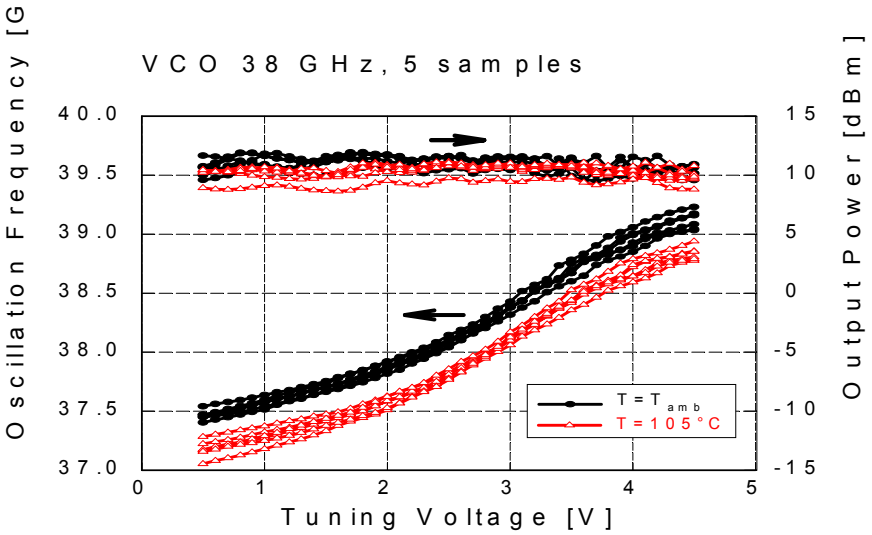

Figure 3-3 On-Wafer Measurements of New VCO Chips.

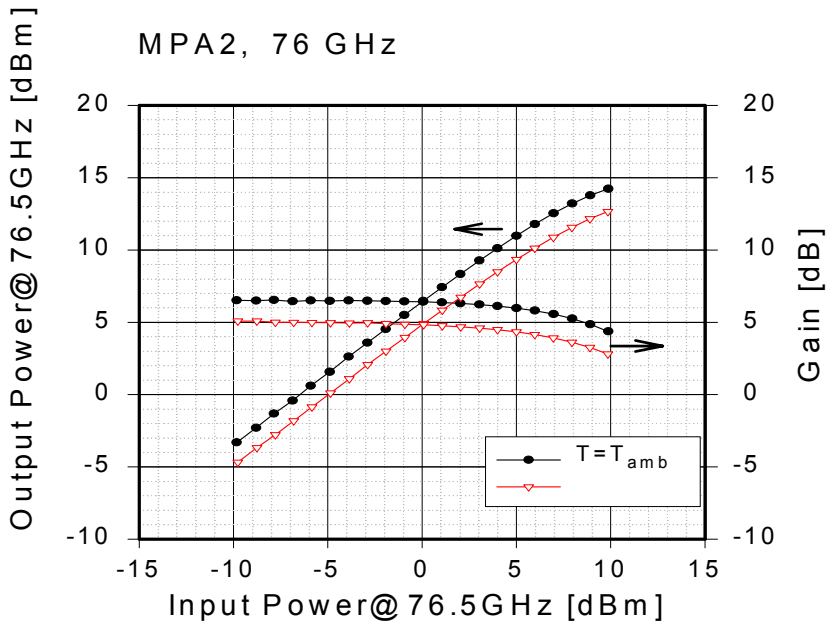

Figure 3.4 On-Wafer Measurements of MPA Chips

The primary technical problems are expected to be related to the transceiver assembly process. Attachment processes for both Au/Sn bumped MMICs and Schottky diodes are new procedures at Delphi. The attachment of the millimeter-wave alumina substrate to the baseplate also presents special challenges. Placement accuracy of less than 5 mils is required while limiting epoxy squeeze-out at the waveguide transitions. The epoxy thickness must also be fine-tuned to ensure proper circuit performance while maintaining enough elasticity to eliminate substrate cracking.

During the next reporting period, the primary activities will be:

1. Final preparation and delivery of prototype MMIC chips
2. Integration and test of the first MMIC transceivers
3. Update of the MMIC transceiver design
4. Pilot Vehicle transceiver parts fabrication and assembly.

3.2 Auto Alignment Algorithm Development (Task B1B)

Goals, Purpose and Background

Automotive Adaptive Cruise Control (ACC) and/or Collision Warning (CW) applications require detection and estimation of target parameters and estimation of the projected path of the host vehicle. Furthermore, target position must be accurately known relative to the vehicle direction of travel. Otherwise, false classifications and missed targets will occur with respect to the appropriate system response.

The radar sensor measures target location relative to the boresight of the radar antenna. For acceptable system performance, the antenna boresight must be accurately aligned to the vehicle direction of travel. Precise mechanical alignment is time consuming and expensive to implement in an automotive manufacturing environment and could change during vehicle operation due to, for example, misalignment of the vehicle suspension. Furthermore, precise alignment may not be practical at dealerships expected to perform service replacement of radar sensors.

The objective was to develop an automatic alignment algorithm in the radar software to continuously estimate the misalignment of the radar boresight relative to the vehicle direction of travel and to correct the radar angle data to compensate for the estimated misalignment. Based on error budget analyses and road testing, an auto alignment accuracy goal of ± 0.25° was established. Furthermore, the algorithm was to be sufficiently responsive to perform initial radar alignment in about 10 to 15 minutes (e.g., after service replacement of the radar sensor) and, thereafter, to track slow changes in alignment during vehicle operation. Note, the radar design also incorporates an electronic alignment algorithm by which the initial (or subsequent) alignment can be quickly performed given an alignment station with corner reflector placed on the vehicle centerline.

The auto alignment algorithm is a Delphi patented technique whereby the radar software processes detected targets of opportunity to estimate the misalignment angle. As shown in Figure 3.5 below, the trajectory of a target in radar x', y' coordinates is linear, assuming non-zero range rate and constant lateral offset (d). Furthermore, the angle of the trajectory relative to the y' axis, θ_a, corresponds to the misalignment angle of the radar boresight relative to the vehicle direction of travel.

In essence, the auto alignment algorithm performs a least squares fit to the target trajectory to solve for the misalignment angle. The implementation is limited to stopped objects since these objects cannot change their lateral offset. Host vehicle speed and yaw rate are used to compensate for lateral movement of the host vehicle. In effect, this compensation corrects for host vehicle motion on curves and during lane changes or lane wander to "linearize" the target trajectory. Otherwise, the auto alignment process would be limited to straight road sections and constant lane position for the host vehicle and would incur additional error for small deviations from these assumptions.

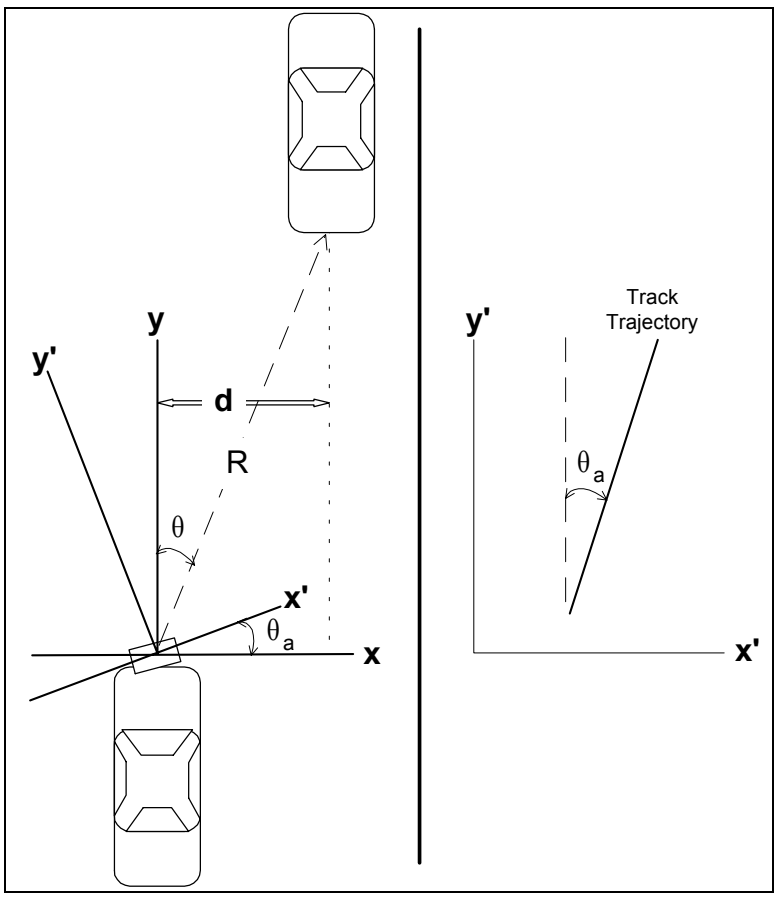

Figure 3.5 Auto Alignment Geometry

A set of criteria is used to screen stopped object tracks for input into the auto alignment function. The criteria include minimum thresholds on the host vehicle speed and stopped object track length, and a maximum threshold on the deviation of the track data points from the best fit straight line.

Auto alignment estimates from individual stopped-object tracks can exhibit significant error due to, for example, angle measurement errors, yaw rate measurement errors, and host vehicle slip angle on curves. To obtain sufficient accuracy, the individual (raw) estimates are smoothed via two filters, a single state Kalman filter, and an adaptive low pass filter. The filters are processed in parallel and their difference averaged to automatically detect convergence or loss of convergence of the alignment estimate, to adapt the filter parameters to speed convergence, and to provide heavier smoothing during steady state or slowly changing conditions. The more responsive convergence mode is used for initial alignment and also following loss of convergence due to a sudden or rapid change in the misalignment angle.

Convergence of the smoothed auto alignment estimate to within an error bound of the true value requires a fixed number of individual (raw) auto alignment estimates (i.e., valid stopped object tracks) for a given distribution of measurement error. The greater the measurement error, the greater the number of raw estimates required for convergence. Furthermore, since the time rate of valid stopped-object tracks depends on the roadside environment, the convergence time will vary even for a fixed measurement error.

The auto alignment algorithm was tested via extensive road testing in a variety of city, secondary road and freeway environments. To test convergence time, a series of tests was performed in which the radar sensor was intentionally misaligned by a known amount and was then operated in a variety of roadway environments. Many hours of road testing were also performed to establish the steady state performance of the algorithm. Furthermore, the algorithm has been implemented in a production ACC system for more than one year.

Intermediate and Final Results

The time required for initial convergence of the smoothed auto alignment estimate varied as a function of the roadway environment as expected. Adequate convergence time and transition to steady state was obtained by adjusting the algorithm to simply require 100 data points (valid stopped object tracks) for initial convergence. Under favorable conditions (i.e., favorable measurement errors), more rapid convergence could be obtained if desired by reverting to the adaptive scheme.

Figure 3.6 shows the initial convergence time for example test runs on three different routes; a freeway route, secondary road route and city route. The two different symbols represent results for two different sensors (on separate vehicles). As shown, the freeway results were consistently between 5 to 15 minutes for initial convergence. Results on secondary roads showed more variation with the longer convergence times caused by closely following a lead vehicle for a long period of time (this situation obscures long range coverage of road-side stopped objects). The city environment also showed a wider variation in convergence time. These results were obtained with the minimum speed constraint set to 40 mph which is difficult to maintain in city driving. The minimum speed threshold has since been lowered to 30 mph to improve convergence time in city environments.

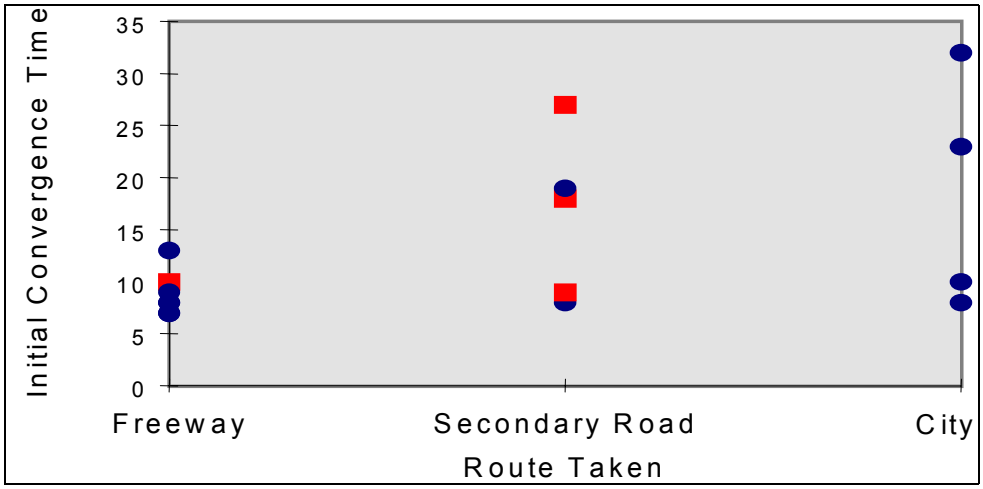

Figure 3.6 Example Auto Alignment Convergence Time Results

Figure 3.7 plots the auto alignment response for a selected test run with the sensor intentionally misaligned to –2.5°. Convergence based on 100 data points is achieved at about 18 minutes although, in this case, the smoothed estimate appears sufficiently stable after about 10 minutes.

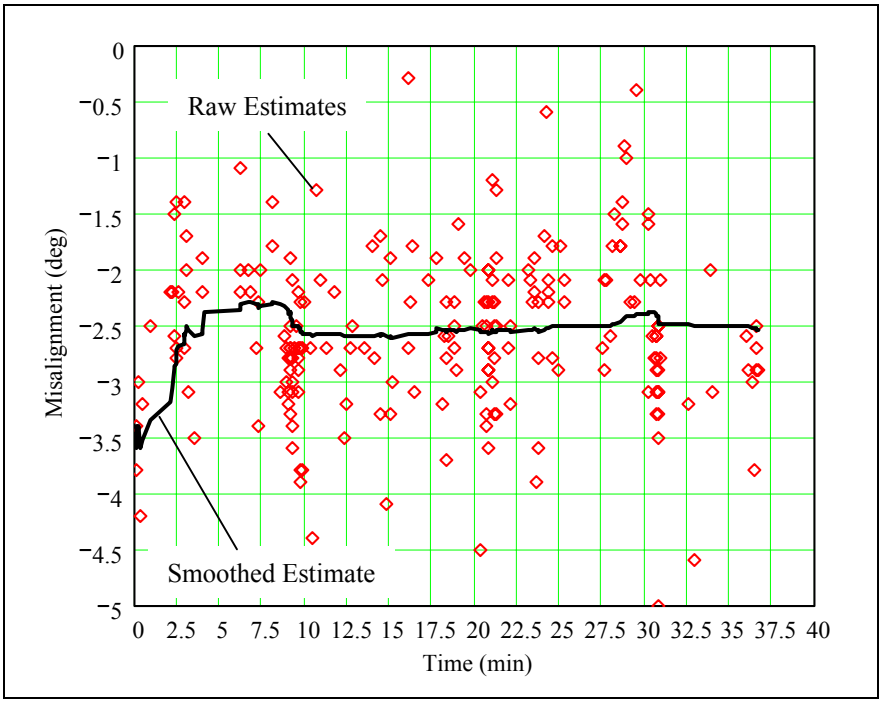

Figure 3.7 Example Auto Alignment Response with Large Misalignment
(True Misalignment = -2.5°)

Extensive drive testing was conducted to evaluate auto alignment performance and to tune the auto alignment filter parameters to achieve the desired accuracy (±0.25°). Analysis of the data indicated that the error deviation of the individual (raw) alignment estimates was greater than expected. Furthermore, the algorithm would at times transition to the unconverged state (flagging a system fault) when the actual alignment angle was stable. As a result, the responsiveness of the filter was reduced (i.e., heavier smoothing was implemented) and the logic to transition from converged to unconverged was disabled. Road testing and experience with an ACC production program indicates that performance of auto alignment with these adjustments is acceptable.

Analysis indicates that the peak auto alignment errors are due to the sideslip effect on curves. As mentioned, heavier smoothing was implemented to handle these errors. If improved responsiveness is required (i.e., to react more quickly to rapid changes in alignment), further development is required to compensate for sideslip effects.

Example steady state performance of the smoothed alignnment estimate is shown in Figure 3.8 for a test drive of about one hour with a true misalignment of 0.8°. As shown, the steady state error is less than the goal of ± 0.25°.

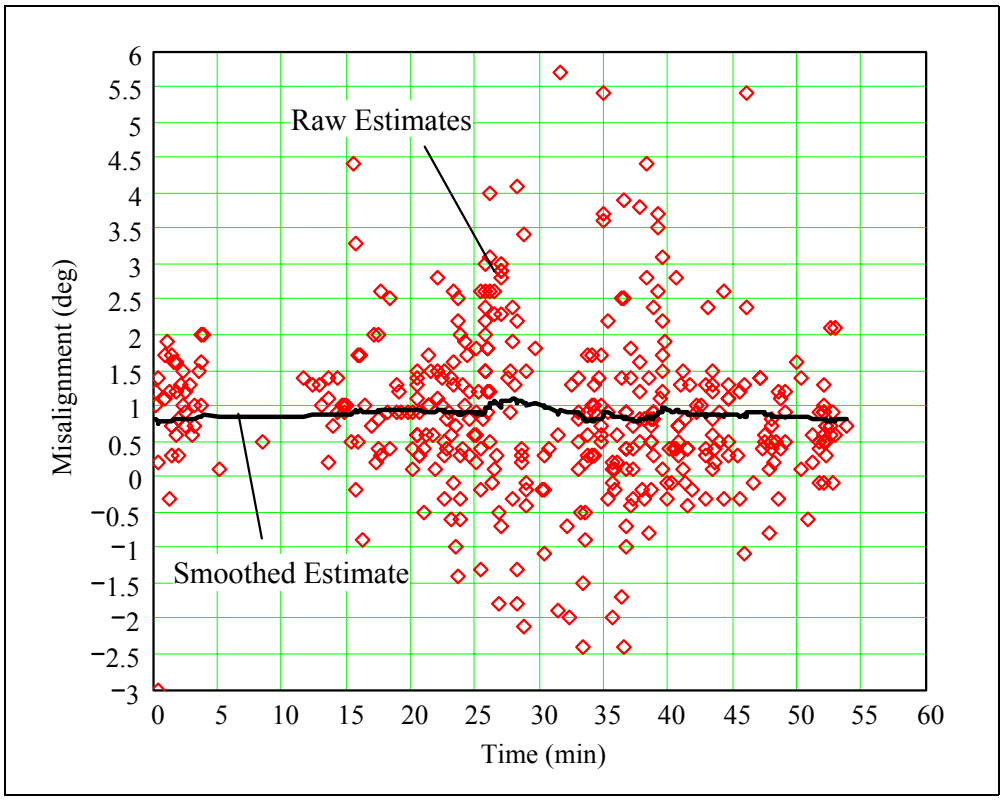

Figure 3.8 Example Auto Alignment Steady State Response
(True Misalignment = 0.8°)

Road test data collection and analysis indicates that the raw auto alignment estimates (i.e., from individual stopped object tracks) vary over a span of about ± 5.0° about the true alignment angle. Error sources include radar angle measurement error, yaw rate measurement error, and host vehicle sideslip on curves.

Vehicles naturally incur sideslip on curves and, as a result, the vehicle centerline does not line up with the vehicle direction of travel; that is, a true short term misalignment of the radar occurs relative to the projected path of the host vehicle. Since sideslip is short term and varies with lateral acceleration, correlated noise is introduced into the auto alignment process. The sideslip effect on curves was found to be a significant contributor to auto alignment error. That is, data analysis shows a strong correlation between auto alignment error and lateral acceleration. Furthermore, the angle error is consistent with the predicted sideslip angle as a function of lateral acceleration using representative physical parameters for the test vehicle.

Figure 3.9 plots the data of Figure 3.8 vs. road curvature categorized as straight, right curve and left curve. As shown, the straight road data shows a much tighter error distribution than the curved road data. Furthermore, bias is evident in the curve data with a positive bias for right curves and a negative bias for left curves. Figure 3.10 plots the data of Figure 3.8 vs. lateral acceleration and illustrates the strong correlation between alignment error and lateral acceleration.

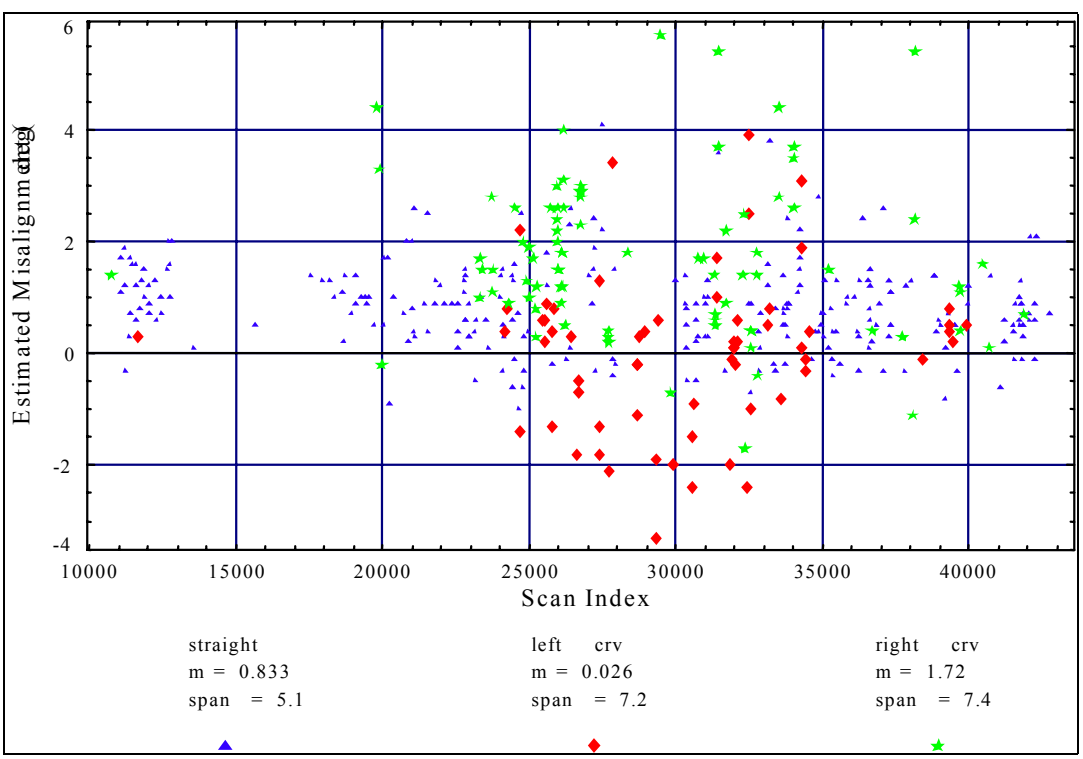

Figure 3.9 Raw Alignment Estimates from Figure 3.7
Categorized by Road Curvature

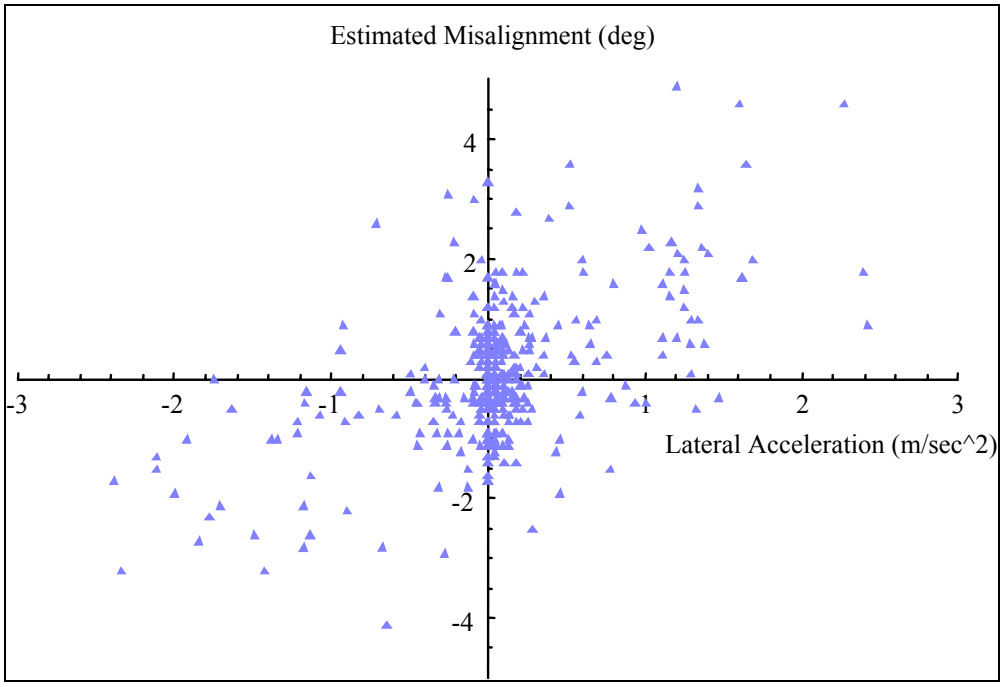

Figure 3.10 Raw Alignment Estimates from Figure 3.7
Plotted vs. Lateral Acceleration

The sideslip angle is the angle between the vehicle's centerline (x-axis) and its instantaneous velocity vector. It is dependent upon several vehicular parameters including vehicle weight per axle, cornering stiffness per wheel, lateral acceleration or radius of curvature of the roadway, and vehicle speed.

Application of "stiff" low pass filters, i.e., filters with long time constants, are currently utilized to minimize curve induced errors. As time constants become larger responsiveness is sacrificed. If a real incident were to occur that caused the sensor to become misaligned, then more time will be required to recognize such a condition. Assumptions regarding roadway symmetry must also be made for any low pass filter implementation with long time constant. Over a long period of time the number of left turns must approximate the number of right hand turns. Also, the number of tracks in left and right hand curves should average out to be nearly equal so biases are not introduced.

Although it is desirable to eliminate sideslip effects altogether, actual implementation of such an objective would likely involve the need for a high degree of processing complexity to be robust over all driving conditions. Mitigation is probably a more realistic expectation than elimination.

Minimizing sideslip effects can be approached from two directions. One approach would be based on a simple data editing strategy, using absolute yaw rate without trying to estimate the sideslip component. The limiting factor in this case would be the accuracy of processed yaw rate data. Another approach would solve for the sideslip component, either based on a-priori vehicle parameters or "on the fly" based on a linear regression fit of smoothed angle data vs. lateral acceleration. The solution could be verified onboard using available real time suspension data and/or known vehicular parameters. The sideslip angle solution would then be used to correct the auto alignment angle solution.

For an autonomous algorithm to conclude with confidence that a sideslip component is present requires sufficient sample size, adequate lateral acceleration, and some heuristic techniques that only can be learned once road test results can be analyzed and understood. Use of yaw rate sign may also become necessary to recognize when sampling intervals span more than one turn. This may be needed to address possibly nonsymmetrical host vehicle behavior in negotiating left and right hand turns.

Even if the sideslip component can be perfectly estimated, smoothing will still be required to reduce the effect of the other error sources (e.g., radar angle measurement noise and yaw rate measurement noise). However, the filters can then be tuned to be more responsive to rapid changes in the alignment angle.

3.3 Radome Blockage Algorithm Development (Task B1C)

Goals, Purpose and Background

The Forward Radar signal can be attenuated by buildup of a layer, such as wet snow, slush or mud, on the radome or secondary surface. Depending on the thickness and water content of the layer, radar detection can be degraded or completely blocked. The primary objective was to develop a technique within the forward radar design to automatically detect (within 20 seconds) blockage conditions that completely blind the radar. A secondary objective was to detect blockage which degrades detection sensitivity by 12 dB or more (i.e., detection range reduced by 50%). The latency goal for detection of partial blockage was 120 seconds.

Four techniques have been developed to detect blockage conditions. The first technique is based on processing Continuous-wave Radar (CWR) ground clutter data. The second and third techniques are based on processing normal Frequency Modulated Continuous Wave (FMCW) radar track data, and the fourth technique is based on a modified radar design using a special wideband waveform and processing to directly detect the presence of a blocking layer.

The radar blockage algorithm implemented in the Forward Radar is a patented Delphi approach that integrates the first three techniques into a single composite algorithm as listed in Table 3.1. Blockage is declared if any of the three components detect blockage. Blockage is cleared if none of the three components detect blockage. As a whole, the integrated components detect different levels of blockage under various conditions with rapid to medium response time.

Table 3.1 Blockage Detection Components Implemented in the Forward Radar

Blockage Detection Component	Approach	Performance
CWR Ground Clutter	Transmit fixed frequency waveform in the edge beams. Blockage detected if average ground clutter amplitude drops below a threshold.	Rapidly detects severe to complete blockage in the absence of radar track data.
Normalized Track Amplitude	Normalize amplitude of all tracks to a common range reference. Blockage detected if long term average track amplitude drops below a threshold.	Detects less severe blockage that degrades performance. Requires targets in track.
Sudden Track Drop	Evaluate sudden unexpected loss of track. Blockage detected if low sensitivity is the only plausible cause.	Rapidly detects moderate blockage which causes track drop at short to medium range. Requires targets in track.

The first component (continuous-wave radar ground clutter) transmits a fixed frequency waveform in the outer beams of each radar scan. The received radar samples are converted to the frequency domain via Fast Fourier Transform (FFT) processing to determine the distribution of Doppler shift frequencies. The amplitude of each of the ground clutter frequency bins is averaged over time via a low pass filter. Blockage is indicated if the integrated ground clutter amplitude drops below a specified threshold.

Figure 3.11 shows the ground clutter frequency spectrum for a fixed frequency waveform on a moving vehicle. The spectrum consists of ground returns (such as the road surface, roadside surface and roadside stationary objects) received through the radar mainlobe and sidelobes. The mainlobe clutter is typically strongest and appears at the doppler frequency corresponding to the component of the vehicle speed in the direction of the radar mainbeam.

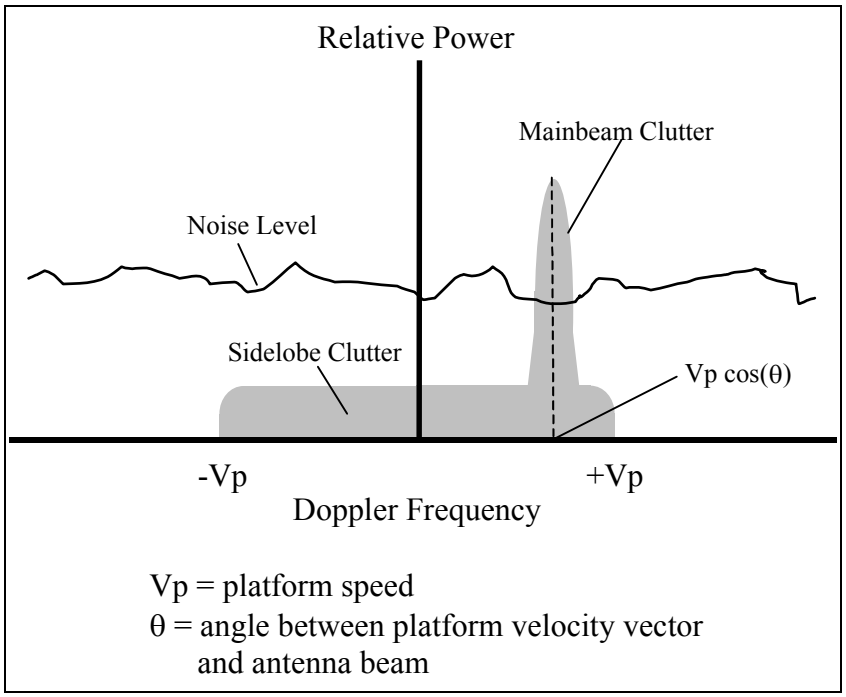

Figure 3.11 Forward Radar Ground Clutter Spectrum with Fixed Frequency Waveform

The standard FMCW waveform used for target detection spreads the mainbeam ground clutter returns over frequency according to the clutter range and frequency modulation rate of the waveform. Using a fixed frequency waveform concentrates the mainbeam ground clutter from all ranges into a narrow frequency region according to the speed of the host vehicle. In essence, the fixed frequency waveform provides an external target reference for blockage evaluation. If the ground clutter return is not detectable, then blockage is declared.

The amplitude of the mainbeam ground clutter varies significantly depending on the road surface characteristics and roadside environment. A low pass filter is used to average the ground clutter amplitude over time with a response time on the order of 20 seconds to rapidly detect a blockage condition in the absence of vehicle targets. Given the variation in the ground clutter amplitude, the rapid response time criteria and the need to minimize false alarms, this technique is limited to severe to complete blockage. Less severe blockage could be detected with additional averaging but the response time will degrade. Rapid response is critical to the ground clutter technique since this is the only component which can detect blockage in the absence of target tracks.

The second component (normalized track amplitude) computes the normalized amplitude for all moving targets and averages the amplitude over time via a low pass filter. Target amplitude is a function of the radar parameters, target range and the radar cross-section (RCS) or reflectivity of the target which depends on the physical characteristics of the target and the aspect or viewing angle. Range dependence is removed by normalizing the amplitude to 100 m range based on range to the fourth power scaling. Furthermore, only moving targets are processed, to somewhat limit the spread in RCS encountered. Significant variation in target amplitude remains in the automotive environment due to the difference in average RCS for vehicle targets and changes in the instantaneous RCS over time for a single target due to small changes in aspect angle.

Blockage is indicated if the average normalized amplitude drops below a given threshold. Response time of the low pass filter is tuned to be on the order of 120 seconds to minimize the variation in the average normalized amplitude, that is, to allow detection of less severe blockage, albeit with moderate latency. This strategy complements the continuous-wave radar ground clutter component which is set up to detect severe to complete blockage with minimum latency.

The third component (sudden track drop) has been developed to detect the unexpected loss of tracks at short to moderate range. The objective is to rapidly detect moderate blockage when blockage is clearly indicated by sudden loss of tracks. All dropped tracks are subjected to a series of tests to determine if reduced sensitivity (blockage) is the only plausible cause for loss of tracks. If so, blockage is declared. Blockage is cleared when targets are tracked with persistence at moderate to long range. Coding and bench testing have been completed for the track drop component and road testing is now in progress. The track drop component is not currently included in the radar code released for the ACAS/FOT vehicles.

Note, all three blockage detection components require host vehicle motion for several reasons. Fundamentally, the radar is required to radiate; this is not enabled until the host vehicle exceeds a minimum speed threshold. Furthermore, even if the radar is allowed to radiate when stationary, the continuous-wave radar ground clutter technique requires host vehicle motion to separate the mainbeam ground clutter from DC leakage and low frequency noise inherent in continuous-wave systems. Also, the track amplitude and track drop criteria implement a minimum host speed to help avoid false alarms.

To develop and tune the blockage detection algorithm, test data was collected over a variety of roadway and traffic conditions including surface street, freeway and test track environments as summarized in Table 3.2. Data collected was analyzed to establish the distribution in ground clutter and track amplitudes needed to develop and tune these components of the algorithm.

Performance of the blockage detection algorithm has been evaluated via road testing during blockage conditions of opportunity and also with controlled blockage conditions. Blockage conditions of opportunity included test drives in the Detroit and Indianapolis areas during snowstorms. Controlled blockage tests were conducted with a metal plate to simulate complete blockage and with layers of wet paper towels placed in a plastic bag to simulate partial blockage. The number of wet paper towels were varied to change the amount of radar signal attenuation. Signal attenuation was measured by collecting low level radar data with a corner reflector with and without the blockage layer. Besides blockage conditions, extensive drive testing was also performed in clear and rainy weather conditions to evaluate the blockage false alarm rate.

Table 3.2 Data Collection and Evaluation Test Conditions for Blockage Detection

Algorithm Development	Surface street roadside clutter Surface street paved median clutter Freeway roadside clutter Freeway cement barrier median clutter Asphalt and concrete road surfaces Surface street traffic conditions Freeway traffic conditions Controlled test track targets
Performance Evaluation	Blockage conditions of opportunity (snowstorms) Controlled blockage layers • Metal plate • Wet paper towels in plastic bag Clear and rainy conditions (test false alarm rate)

The fourth blockage detection technique envisions a modified radar design with a wideband waveform to detect objects at very close proximity to the radar; that is, to detect reflections from the blockage layer itself. The bandwidth of the standard FMCW waveform used for target detection is about 200 MHz which limits detection to a minimum range of about 1 m. The minimum range required to directly detect reflections from a blockage layer depends on the distance from the radar face to the secondary surface or fascia and the time delay or relative distance of the receive path within the radar. These factors depend on the radar design and mounting location. Other factors involve the DC leakage and low frequency noise inherent in FMCW systems; that is, adequate bandwidth is required to separate near range returns from these sources of low frequency noise. For the folded reflector antenna design used in the Forward Radar, bandwidth on the order of 1.5 GHz is likely to be required to directly detect blockage layers. In a manner similar to the approach used for the continuous-wave ground clutter beam, the wideband waveform could be transmitted in the edge beams of the radar scan.

The wideband technique would eliminate the need to evaluate returns from widely varying external targets and thereby has the potential to consistently and rapidly detect blockage regardless of the external environment. Furthermore, if permissible, the wideband approach could radiate and detect blockage with the host vehicle stationary; that is, before the vehicle is operated on the road. Issues include the potential for reflections from other near range objects to degrade performance; for example, reflections from the fascia itself or other structures within the bumper assembly. The reflectivity of blockage layers compared to these features is not known at this time.

The current Gunn diode transceiver design used in the Forward Radar is not capable of transmitting a waveform with sufficient bandwidth to directly detect blockage layers. Initial development and testing of the wideband blockage detection technique was performed with 76 GHz RADS radar modified to transmit a 17.7 microsecond FMCW ramp with 823 MHz bandwidth. Time domain data was collected and analyzed offline with a metal plate at various distances from the radar radome. Data was also collected with a flat sheet of Ultem to represent a level of reflection possible from the fascia itself.

The MMIC-based transceiver being developed under Task B1A will be capable of transmitting a wideband waveform with bandwidth up to 1.5 GHz. Further development and testing of the wideband blockage detection technique is planned to resume when the MMIC-based Forward Radar becomes available.

Intermediate and Final Results

Test results demonstrated the effectiveness of the blockage detection algorithm under a variety of conditions as summarized in Table 3.3.

Table 3.3 Summary of Blockage Detection Test Results

Test Condition	Performance
Blockage via a metal plate	• Blockage consistently detected within 20 seconds (detected by CW ground clutter component).
Controlled blockage with 40 dB attenuation	• Blockage consistently detected within 20 seconds (detected by CW ground clutter component).
Blockage events of opportunity (snowstorms)	• Blockage rapidly detected shortly after radar was blinded (test not set up to measure time delay). • Secondary surface covered by a thin layer of slush. • Attenuation measured to be 50 dB in one case.
Controlled blockage with 20 dB attenuation	• Blockage detected by track amplitude component. • Response time varies depending on target environment. • Addition of track drop component offers potential for improvement.
Controlled blockage with 12 dB attenuation	• Not able to consistently detect blockage. • 12 dB may not be practical or appropriate goal.
Clear and rainy weather without blockage	• Blockage false alarms can occur in rain (with low rate) due to attenuation by lead vehicle spray. • Attenuation by water spray can be 10 dB or greater.

Tests performed with a metal plate and controlled blockage layers demonstrated the ability of the CW ground clutter component to detect severe to complete blockage within the latency goal of 20 seconds. The CW ground clutter component was also effective using a controlled blockage layer with 40 dB attenuation. During blockage events of opportunity, blockage was rapidly detected shortly after the radar was blinded (as indicated by monitoring the radar track data in real time). After each event, the secondary surface was observed to be covered with a thin layer of wet slush. Subsequent measurements in one case indicated the attenuation was 50 dB.

The CW ground clutter component was not effective using a controlled blockage layer with 20 dB attenuation. In this situation, the track amplitude component is effective in detecting blockage with measured latency typically about 2 minutes. However, latency can vary significantly depending on the target environment and operating conditions.

During one test drive with the 20 dB attenuation layer, analysis of track data indicated that tracks were often dropped at moderate range well before the track amplitude criteria indicated blockage. Hence the motivation to develop the track drop criteria. As discussed, the new track drop software is currently being road tested and will be evaluated in the near future.

Drive testing in clear and rainy conditions without blockage indicates that blockage false alarms can occur in rain, albeit with low false alarm rate. Analysis of radar data shows that water spray from lead vehicles can attenuate the radar signal by 10 dB or more (much greater than predicted by theoretical models based on rain rate). In effect, the blockage algorithm is likely detecting a valid decrease in sensitivity even though it is not caused by a blockage layer.

Testing with controlled blockage layers indicates that the blockage detection algorithm is not able to consistently detect controlled blockage with 12 dB attenuation. Several issues now lead one to question if 12 dB is a practical or even appropriate goal. At first glance 12 dB appears to be a reasonable goal since this represents a 50 % reduction in detection range. However, adequate design margin exists to detect all but the smallest targets (e.g., motorcycles) to about 80 m even with 12 dB attenuation. Furthermore, to reliably detect this level of attenuation would require the blockage detection thresholds to be lowered and would increase the potential for blockage false alarms particularly in rain. Techniques would then be required to distinguish rain spray attenuation from blockage; otherwise setting a blockage diagnostic flag would lead to confusion. Even given a method to distinguish the two, setting diagnostics flag at a 12 dB level could be viewed by the driver as a nuisance alarm since, given the design margin, the system would likely appear to be functional. Finally, it is not known if a real world blockage condition such as wet snow or mud could lead to attenuation of only 12 dB. Further work is required to address these issues.

Figures 3.12 and 3.13 show example data from the CW ground clutter and track amplitude components. Figure 3.12 plots the frequency spectrum from a fixed frequency edge beam with a roadside vegetation environment to illustrate the mainbeam ground clutter target. Relatively smooth roadside vegetation provides about the weakest ground clutter return with relative amplitude of about 55 dB (about 20 dB above the average noise floor). The overall variation in roadside ground clutter amplitude was about 55 dB with concrete median barriers providing the strongest roadside clutter amplitude at about 110 dB.

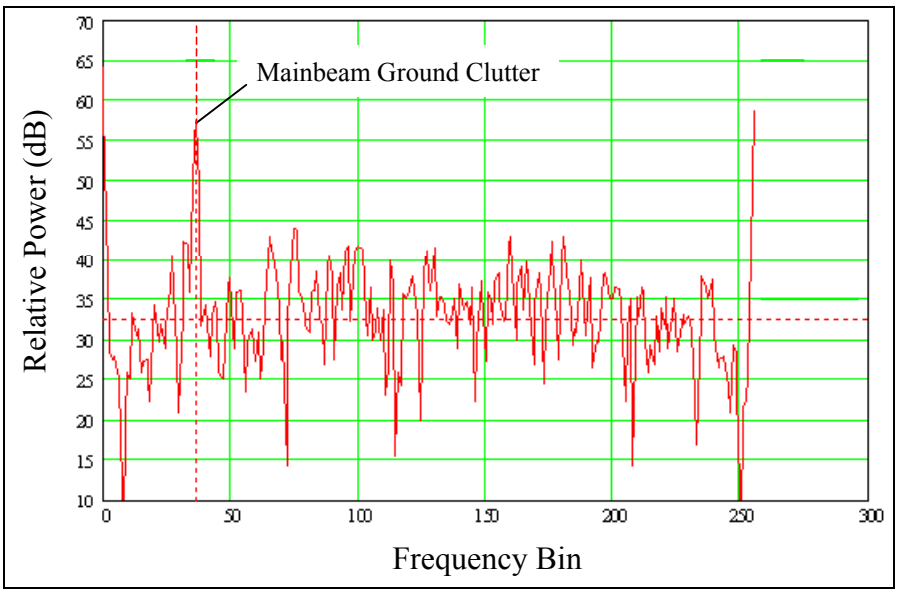

Figure 3.12 Example Mainbeam Ground Clutter Return
(Roadside Vegetation, Host Vehicle Speed = 80 mph, 500 Hz per Frequency Bin)

Figure 3.13 plots the normalized track amplitude with a controlled blockage layer of 20 dB attenuation. The test was conducted on a city street. Note, at each ignition cycle, the filtered amplitude is initialized at a level consistent with an unblocked condition. In the example shown, blockage was detected about 3 minutes after the beginning of the test (of which a total of 44 seconds was spent with the host vehicle stopped and not radiating). During the first 50 seconds of the test drive, traffic was light and the host vehicle followed an outgoing van with a persistent track to 100 m range and intermittent detections out to 150 m. Next, the host vehicle closed on a midsize passenger car and came to a stop for a duration of 34 seconds. Thereafter, the host vehicle followed the midsize passenger car at ranges between 30 to 50 m. Intermittent tracking was immediately observed with blockage detected about 80 seconds later.

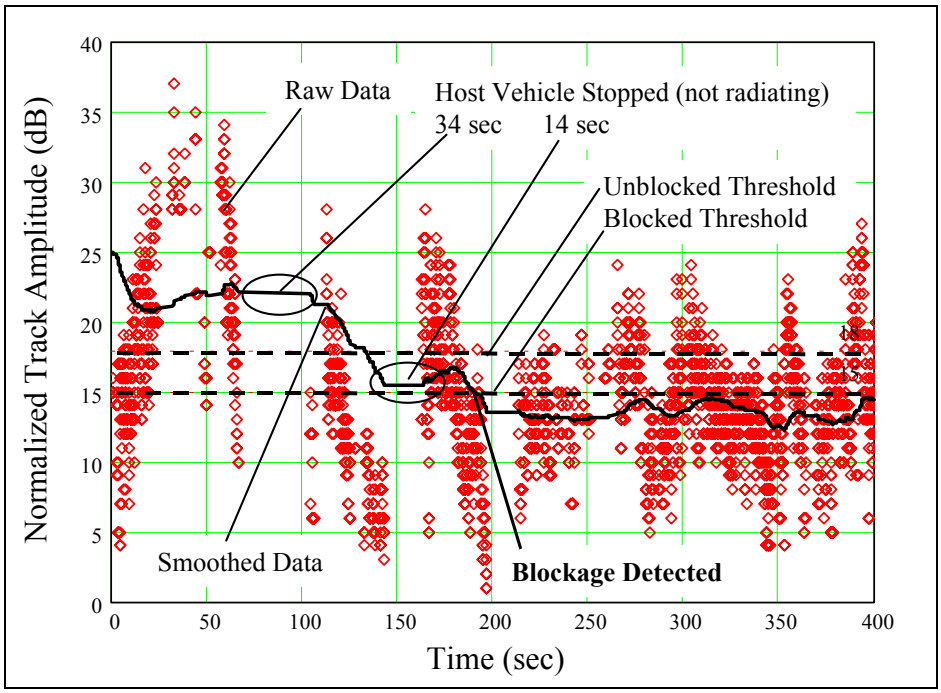

Figure 3.13 Example Normalized Track Amplitude Data with 20 dB Attenuation Layer (City Street Test Drive)

Testing performed using a Reconfigurable Advanced Development Sensor (RADS) radar demonstrated the ability of a wideband waveform to detect large reflections (i.e., a metal plate) at a distance of 44 cm. Scaling these results from 800 MHz and accounting for the receive path length within the Forward Radar folded reflector antenna, suggests the potential for a 1.5 GHz bandwidth waveform to detect objects at a distance representative of blockage layers. Further effort is required to establish the reflectivity of actual blockage layers compared to low frequency noise components and reflections from the fascia itself.

Figure 3.14 shows the frequency spectrum using an FMCW ramp with 800 MHz bandwidth with a flat sheet of Ultem at 44 cm range. Note, assuming zero range rate, the FMCW frequency spectrum is equivalent to the range response. As shown, the level of DC leakage and low frequency noise is significant in range bins 0, 1 and 2. The reflection from the Ultem sheet is evident in range bin 3. The range response using a metal plate in place of the Ultem sheet is similar except the amplitude of the metal plate is much greater than the Ultem sheet. Ultimately, the bandwidth required and performance of the wideband approach depends on the level of reflectivity of a fascia covered with a blockage layer (e.g., slush) compared to the DC leakage, low frequency noise, fascia and other nearby structures.

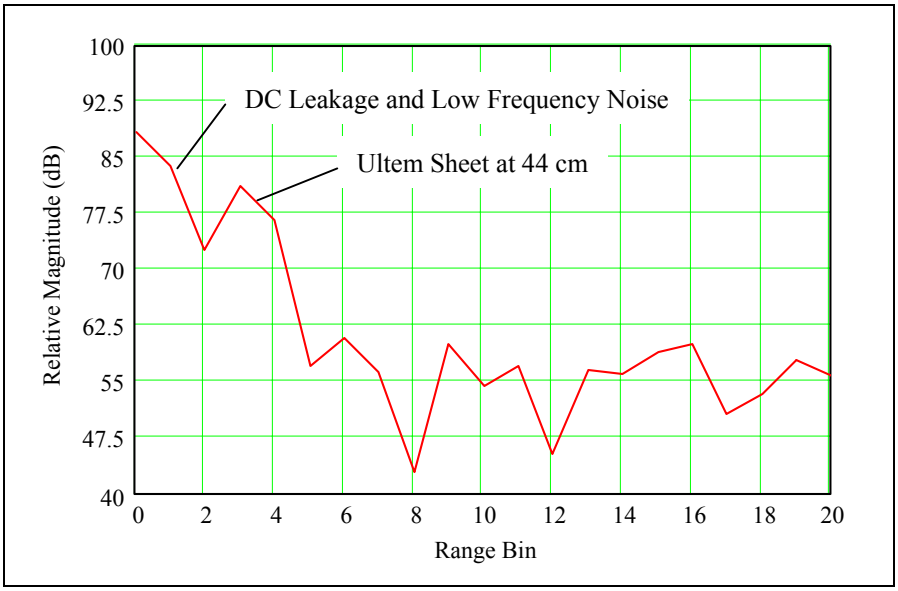

Figure 3.14 Example Wideband FMCW Frequency Spectrum Using RADS Radar
(Bandwidth = 823 MHz)

3.4 Bridge Rejection Algorithm Development (Task B1D)

Goals, Purpose and Background

The Forward Radar antenna beam intercepts roadside stopped objects, such as guardrails and sign posts, and overhead stopped objects such as bridges and overhead signs. For ACC applications, reaction to stopped objects is not required and the radar sensor can simply reject all stopped objects based on their calculated ground speed. However, for Collision Warning applications, system response to stopped objects is required and another means to reject off-roadway objects is needed. Roadside stopped objects can be rejected based on their lateral offset from the projected path of the host vehicle. Overhead stopped objects such as bridges will appear to be in the path of the host vehicle and will lead to false alarms unless rejected or properly classified by the radar sensor itself. The ultimate objective was to provide stopped object capability to 100 m range without excessive false alarms on overhead objects.

Initial investigations considered a variety of approaches which were ultimately rejected as summarized in Table 3.4.

Table 3.4 Approaches Rejected by Initial Investigations

Approach	Issues
Reject all overhead objects with narrow elevation beam.	• Requires multiple very narrow elevation beams. • Not practical given automotive constraints on radar frequency, antenna size, and cost.
Measure target height via elevation monopulse or multiple beams.	• Too expensive for automotive applications. • Elevation measurements corrupted by multipath.
Measure height via multipath lobing response.	• Works for point source targets. • Lobing structure corrupted by bridge reflections distributed in height and range.

One approach to the problem of overhead object detection is to design a radar with an elevation beam sufficiently narrow to reject all overhead bridges and signs. For a bridge height of 12 ft, the elevation angle at 100 m is 2° and the elevation beamwidth required to ensure rejection is then about 1° (since the null to null beamwidth is at least twice the 3 dB beamwidth). To ensure adequate roadway target detection would then require multiple elevation beams or beam steering to accommodate roadway grades, vehicle pitch and sensor misalignment. This approach is technically feasible from a radar standpoint but not within the automotive constraints of frequency allocation, antenna size and cost.

Given that overhead stopped objects will be detected along with valid in-path stopped objects, the objective was then to develop an algorithm to classify all detected stopped objects as either overhead or valid roadway stopped objects. A high rate of correct classification and low rate of incorrect classification is desired although a quantitative goal was not established.

The fundamental discriminant between overhead stopped objects and valid in-path stopped objects is, of course, height above the roadway. That is, bridges and other overhead objects can be correctly classified by directly or indirectly measuring target height. A radar design with elevation monopulse or multiple elevation beams can directly measure elevation angle; however, this approach is judged too expensive for automotive applications in the near future. Also, elevation measurements would be subject to multipath corruption unless the elevation beam was very narrow.

Radar propagation over a relatively smooth reflective surface results in a multipath lobing structure which depends on radar frequency, radar height, target height, and target range. Target height can be inferred by evaluation of the multipath lobing structure vs. range. That is, target height is inversely proportional to the range spacing between the peaks and nulls observed in the target amplitude. This approach works well for point source targets and has been implemented in airborne radar systems. However, given the operating range and automotive radar resolution, bridges present a target with multiple reflecting points distributed in height and range which corrupts the multipath lobing structure. Furthermore, given the scan rate of the Forward Radar, the multipath lobing structure is undersampled at high host vehicle speed. As a result, the height via multipath technique is not effective for the Forward Radar. Data collection on numerous bridges supports this conclusion.

The "bridge rejection" algorithm implemented in the Forward Radar is a Delphi patented technique consisting of a combination of geometric rejection and classification as summarized in Table 3.5.

Table 3.5 Components of Bridge Rejection and Stopped Object Classification

Algorithm Component	Rationale
Geometric Rejection (GR)	Narrow elevation beam rejects most overhead objects.
Amplitude Slope (AS)	Amplitude of roadway stopped objects increases as range decreases. Amplitude of overhead object decreases as range decreases (begins to exit the radar beam).
Short and Long Term Persistence (SLP)	Detection probability (track persistence) typically high for roadway stopped objects and often lower for overhead objects (due to radar beam and multipath effects).
Pass Through (PT)	A stopped object must be overhead if a moving object appears to "pass through" the stopped object.
Fail Safe (FS)	Elevation beam should reject all overhead objects at R<Rmin, therefore, must be a roadway object if R<Rmin.

Geometric rejection (GR) refers to the fact that many, but not all, overhead objects are rejected by the narrow elevation beam of the Forward Radar. For detected stopped objects, amplitude slope (AS) is the primary classification parameter and is implemented with clear choice and non-clear choice thresholds. Amplitude slope exploits the fact that as range decreases, the amplitude of overhead objects will follow a decreasing trend as the object begins to exit the elevation beam. This trend is reliable on a long term basis but is subject to variation due to several factors, including multipath, on a short term basis. To develop the amplitude slope trend, a fading memory recursive least squares filter is used.

In the non-clear choice regions, classification is then based on short and long term persistence (SLP) thresholds. These persistence parameters evaluate the detection probability (number of detections divided by the number of scans) for the last several scans and over the long term beginning at a specified range. Lower persistence is expected for overhead objects due to multipath and elevation beam effects while valid in-path stopped objects should have high persistence.

The pass through (PT) discriminant looks for moving tracks that appear to "pass through" the stopped object. If so, the stopped object must be overhead. Additional criteria are imposed to satisfy pass-through; for example the moving vehicle must not be decelerating at a high rate since this could indicate an evasive maneuver to avoid a valid stopped object. If successful, pass through overrides AS and SLP.

The fail-safe (FS) logic states that if a stopped object is still in track within the minimum range possible for overhead objects (based on the radar elevation beamwidth), the stopped object must be valid. Fail-safe overrides all other classification results.

Another suggested discriminant to classify bridges involves the width of detected stopped objects. That is, bridges are physically wide and vehicles are physically narrow. This approach was not pursued due to several issues. For example, multiple lanes of side by side stopped vehicles present a wide target and would likely be misclassified as a bridge. Conversely, overhead signs are similar in width to vehicles and would likely be misclassified as valid roadway stopped objects. Furthermore, data analysis on bridges indicates that, at the detection threshold level, many bridges appear as a strong localized reflection source in the lateral dimension located near the center of the bridge. Radar imaging would be required to observe the lower level reflections beyond the center region and is beyond the scope of the Forward Radar design at this time and in the near future.

Data collection and testing were performed in the Tucson, Detroit, and Indianapolis metropolitan areas to develop and evaluate bridge rejection and classification. Formal evaluation was performed on two Detroit freeway test loops shown in Figures 3.15 and 3.16 and one Indianapolis freeway test loop shown in Figure 3.17. The test loops contained about 65 different bridges or overhead signs and were driven multiple times for a total of about 190 overhead objects.

The primary Detroit test loop used for evaluation was I-75 South, I-94 West, Lodge Freeway North and Davison Freeway East. This test loop contains a total of about 40 bridges or overhead signs. Test data was collected and evaluated for three passes around the loop, for a total of about 120 overhead objects.

A secondary Detroit freeway test loop was also used to evaluate performance. The secondary test loop was the M53 freeway North and South between 19 Mile Road and 26 Mile Road. This loop contains a total of about 10 overhead bridges or signs for each direction. The loop was driven two times for a total of about 40 overhead objects.

The Indianapolis test loop consisted of the southeast portion of the I-465 loop between, and including, the intersections with I-70 and I-65. It contains a total of about 15 bridges or overhead signs. Data was collected and evaluated for an "out and back" drive for a total of about 30 overhead objects.

Performance was also evaluated with 14 different stopped vehicles in test track and on-road situations of opportunity as summarized in Table 3.6.

Figure 3.15 Primary Detroit Freeway Test Loop
(I-75 South, I-94 West, Lodge North, Davison East)

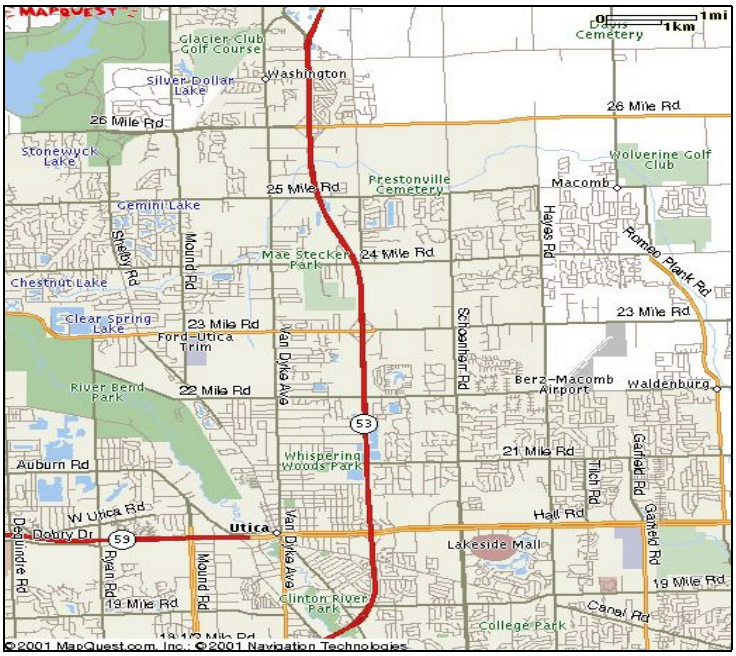

Figure 3.16 Secondary Detroit Freeway Test Loop
(M53 Between 19 Mile Road and 26 Mile Road)

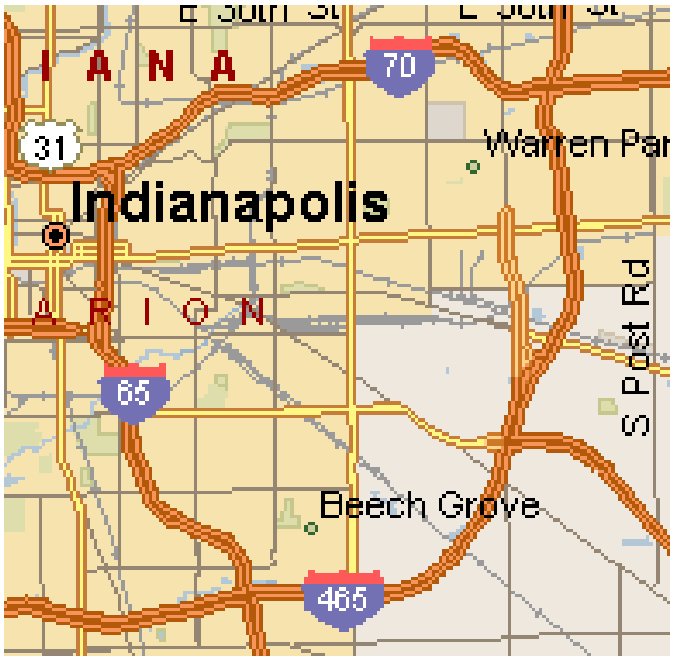

Figure 3.17 Indianapolis Freeway Test Loop
(Southeast Corner of I-465 Loop)

Table 3.6 Summary of Tests Performed for Stopped Vehicles

Location		Vehicle	Speed (m/s)
Detroit	MPG	Chevy Cavalier	13, 26
Tucson	Hughes	Toyota Corolla	13, 20, 25
Detroit	MPG	Pontiac Sunfire	12
Detroit	MPG	GMC Yukon	12, 24
Detroit	On-Road	Dodge Shadow	18
Detroit	On-Road	Van	13
Detroit	On-Road	Unknown	15
Detroit	On-Road	Mail Truck	17
Detroit	On-Road	Chevy Silverado	14, 12, 14
Detroit	On-Road	Chevy Astro Van	13, 13
Detroit	On-Road	Dodge Van	16, 17
Detroit	On-Road	Cadillac DeVille	19
Detroit	On-Road	Ford Explorer	20
Detroit	On-Road	Chrysler Concorde	14
Detroit	On-Road	Toyota Corolla	18

Intermediate and Final Results

Performance of bridge rejection and classification indicates, as expected, that stopped object range involves a tradeoff between false alarms and late valid alarms. At 80 m range, false classification rate is about 5% with late classification rate of about 20% on valid roadway stopped objects. At 100 m range the false classification rate is much higher and is likely unacceptable. Hence, to limit false alarms, the algorithm was adjusted to classify all stopped objects as overhead until range decreases to less than 80 m. Algorithm upgrades and tuning are possible to reduce the false alarm rate on bridges but at the expense of increased rate of late alarms on valid roadway stopped objects. It is believed that a fundamental hardware design change would be required to significantly reduce the false alarm rate on bridges and simultaneously maintain range performance on valid roadway stopped objects (e.g., direct elevation measurement via elevation monopulse).

Bridge rejection and classification performance is highly scenario dependent and, as expected, the false alarm rate on particular bridges is much higher than the ensemble average (e.g., false alarm rate as high as 25% was encountered on several bridges). The minimum false alarm range on bridges is about 50 m and, as a result, the “fail-safe” range limit is set to 50 m.

Figures 3.18 and 3.19 plot the probability of false classification on bridges/overhead signs and the probability of valid classification on stopped vehicles, respectively, as a function of range for the formal tests previously described. The plots labeled "geometric rejection only" shows performance while only depending on the elevation beam for rejection of overhead objects (i.e., classification of detected stopped objects is not performed). For this situation, since classification of detected stopped objects is not attempted, the probability of valid alarm on detected vehicles is unity. Furthermore, the probability of false classification is simply the probability of detecting overhead objects which is about 25% at 100 m range, dropping to about 10% at 80 m range.

The plots labeled "classification added" shows performance of the composite algorithm, that is, geometric rejection with classification of detected stopped objects. As shown, classification improves the false classification rate on overhead objects to 12% at 100 m and to about 2% at 80 m. The tradeoff involves late alarms on valid stopped vehicles. For example, the probability of valid alarm now drops from 100% to just over 40% at 100 m range and just over 80% at 80 m range. Note, these are actually late valid alarms; that is, as range to the stopped vehicle decreases, the probability of valid alarm increases to near unity at 60 m range.

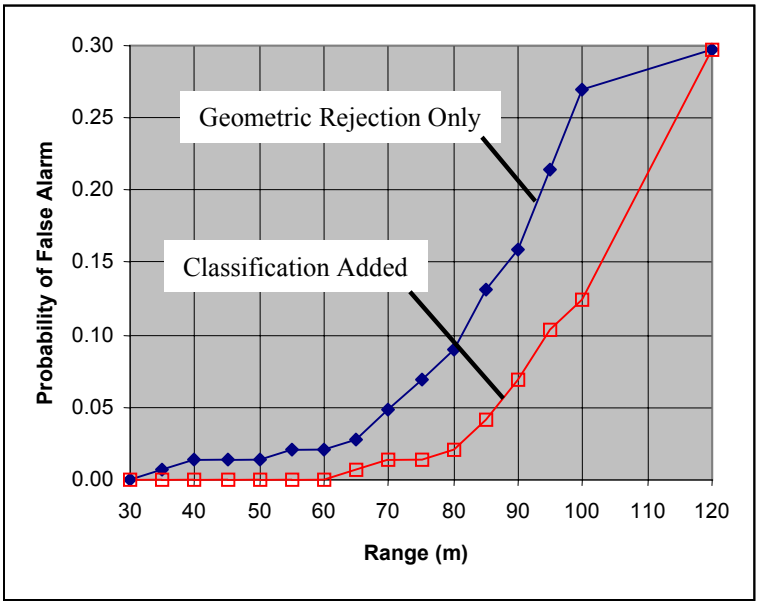

Figure 3.18 Probability of False Classification on Bridges

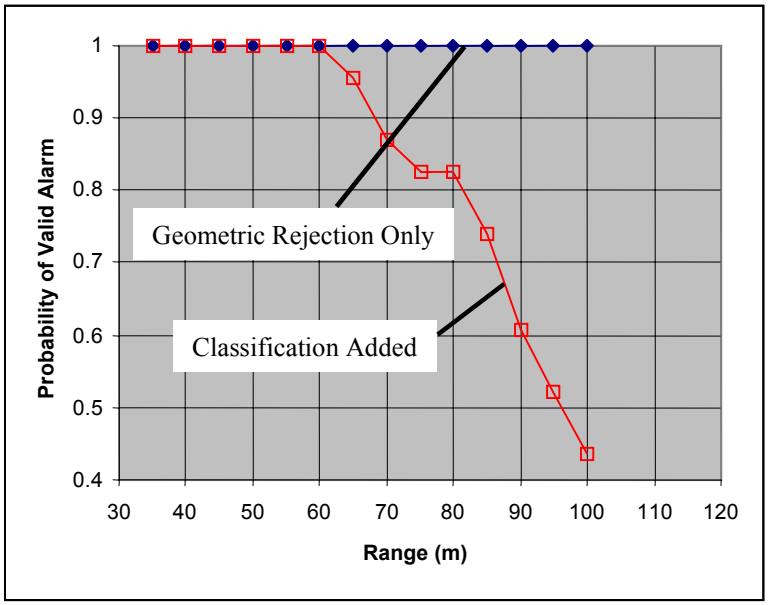

Figure 3.19 Probability of Correct Classification of Stopped Vehicles

Current Schedule and Progress for Task B1

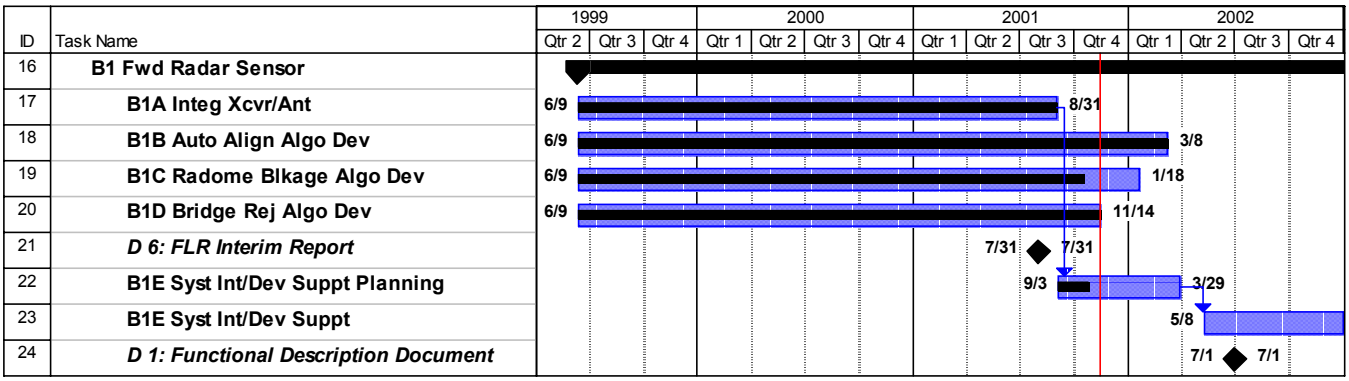

Figure 3.20 Task B1 Schedule

4 Forward Vision Sensor (Task B2)

Goals and Purpose

The objective of the Forward Vision Sensor task is to develop and implement a vision system that provides a description of the lane geometry in the region ahead of the host vehicle. Additionally, it should give a robust estimate of the host vehicle's lateral position and heading in the lane. This road shape and host state information is needed by the Adaptive Cruise Control (ACC)/Forward Collision Warning (FCW) system to reduce the incidence of false alarms on roadside stationary objects during curve entry/exit and host-vehicle lane change maneuvers. To this end, the goal of the vision system, which consists of a forward looking camera mounted near the rear-view mirror and a remotely located image processing unit, is to detect and track the lane markers on the road to about 75 meters ahead of the host.

The block diagram in Figure 4.1 shows this task in relation to others in the overall ACC/FCW system. The primary consumer of the vision system output is Data Fusion (Task C1), which will fuse the vision system's road predictions with those from the GPS Map Matching and Scene Tracking systems and, ultimately, supply the road shape and host state information to Target Tracking and Identification (Task C2).

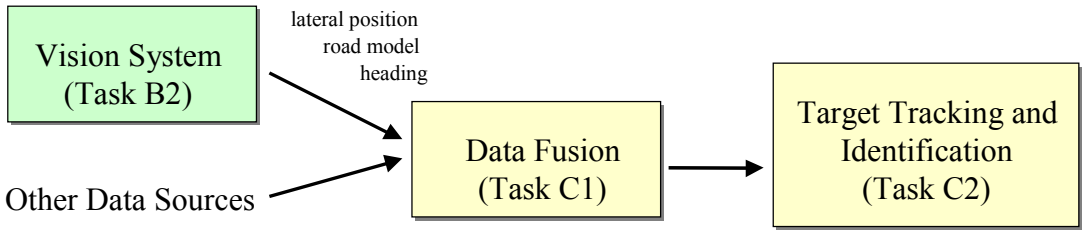

Figure 4.1 Vision System Role in the Overall ACC/FCW System

Background

Key to the success of the ACC/FCW system is the correct selection of in-path targets, i.e., those that are in the expected future path of the host vehicle. Typically, yaw rate and speed measurements are used to estimate the instantaneous road curvature, which is then projected to predict the vehicle path and select in-path targets from the sensor field of view. Under constant curvature conditions, this results in a very accurate prediction of the road ahead (given sufficient speed). Thus, yaw rate-based curvature is an excellent source of local road shape through the vast majority of the driving experience. It is, however, a very poor predictor of *changing* road shape, for example, in curve entry and exit scenarios. Yaw rate-based curvature can also be completely wrong during a host lane change, and it degrades significantly at low host vehicle speed.

Vision-based lane tracking is a good candidate to fill these gaps because it can directly measure not only road curvature, but also host state. In practice, however, the extraction of lane markers from an image, and determination of the related roadway and host vehicle parameters is a significant challenge. The wide variation in marker types and quality, non standardized horizontal and vertical curvature layout of the roads, old (supposedly obliterated) lane markers, tar seams that look like bright markers in reflected sunlight, pavement texture and contrast variations, and obscuring traffic and weather are just some of the oddities easily filtered out by the amazing capacity of the human mind, but difficult to deal with in a digital system and with cameras of limited dynamic range. Vision-based lane tracking is therefore only one of four, often complementary, subsystems used in the Automotive Collision Avoidance System (ACAS) system to predict road shape and/or determine host state.

Because of its potential value to applications such as collision warning, lane departure warning, and autonomous vehicles, lane tracking has been the focus of research for many years by a number of universities and laboratories. Prior to the start of this program, Delphi conducted a survey of existing lane tracking systems and technologies. Although we found a diverse set of approaches to the problems of short-range lane tracking, little existed in the way of a robust long-range system ready for use in even a small vehicle deployment. Based on the results of this survey, teams from Ohio State University, University of Michigan at Dearborn, and the University of Pennsylvania were asked to participate in Phase I of this Program. Delphi contracted with each of the university teams to refine and extend their existing short-range lane tracking systems in an attempt to meet the ACAS Field Operational Test (FOT) program's vision system performance requirements. The results of these efforts were documented in the "Lane Tracking System Down-Select Summary Report" and will be summarized below.

Technical Approach

Detailed descriptions of each of the university team algorithms are included in the appendices of the "Lane Tracking System Down-Select Summary Report." Despite their diverse approaches, the fundamental mechanization of each can be described by the three main processes summarized below. The diagram in Figure 4.2 shows the main functional blocks of the final, long-range lane tracking system.

The first step in the lane tracking function is a low-level feature extraction process used to identify candidate lane markers. This process employs classical image processing techniques such as edge detection, matching filters, convolution, correlation, thresholding, thinning, or chaining. Control of the camera exposure is performed in order to maximize feature contrast.

The second, or mid-level, process centers on grouping the extracted features, and on the subsequent detection and tracking of lane or road boundaries, either separately (left and right) or together. The mid-level process employs a variety of methodologies for outlier rejection, curve fitting, optimization, and model-based tracking of the lane boundaries. Key to the mid-level processing stage is the (inverse) perspective transformation used to convert from the image to camera/vehicle coordinate frame, where real-world constraints are applied to enforce temporal continuity of the solution.

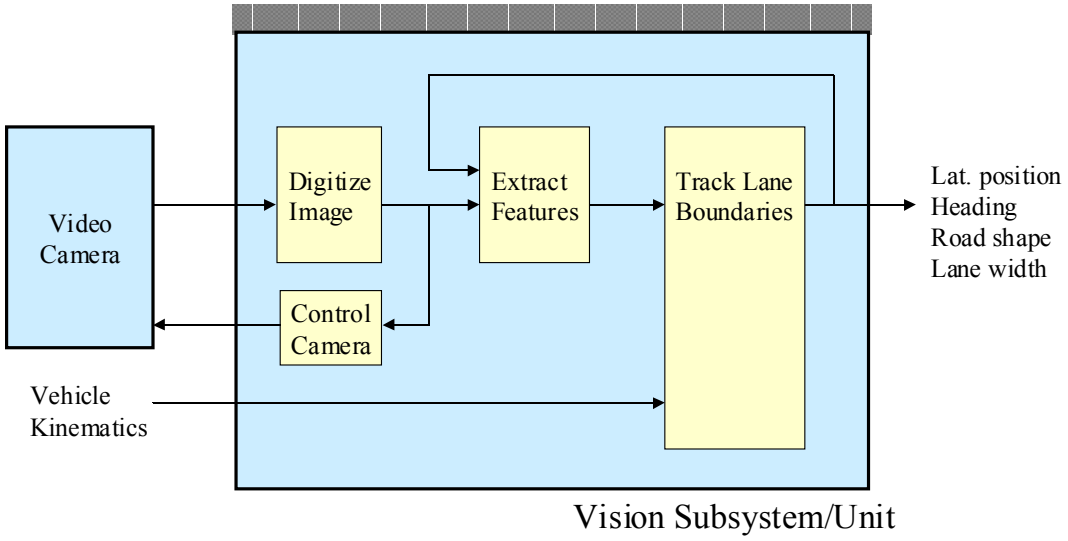

Figure 4.2 Vision System Block Diagram

The final, high-level stage of processing acts as the system executive, controlling program flow, and implementing procedures to identify and deal with special situations such as lane changes, lane bifurcation/merging, and missing markers. Here, the system manages one or more hypothesized solutions and implements rules to select or reject each. Finally, it compiles internal measures of confidence from the various algorithm components, and reports the system's overall confidence in the results passed to Data Fusion.

Relevant Activities

Specifications and Requirements

Work on Task B2 began with the specification of functional and performance requirements for the system. These were derived from a combination of geometrical considerations and application of experience with current ACC and FCW systems and their limitations. Table 4.1 summarizes some of the key accuracy and operational requirements for the system. Full text of the functional and performance requirements can be found in Appendix D of the "Lane Tracking System Down-Select Summary Report." As the requirements were being completed, the three university teams set out to extend their respective short-range lane tracking systems to meet these new long-range goals.

Table 4.1 Vision System Requirements Summary

Max Data Latency	100 ms (e.g. min 10 frames/sec)
Lateral Lane Position Accuracy	$\sigma \leq 0.2$ m
Lane Width Accuracy	$\sigma \leq 0.2$ m
Heading Accuracy	$\sigma \leq 0.2$ deg
Road Model Accuracy	$\sigma \leq 0.75$m (error relative to true road shape) Min range of validity 15-75m
Road Types	Limited access highways and their transitions
Min Radius of Curvature	300 m
Marker Types	Solid, striped/dashed, dots, road/shoulder transition, missing
Additional Features	Self-calibration/alignment Immune to highway entrance/exits Confidence measures reflect quality of data

Development and Analysis Tools

In order to aid algorithm development and to evaluate and compare the performance of each vision system, a hardware-in-the-loop development environment was created. The main features of this system are hardware and software developed to collect and replay video-taped sequences consisting of road imagery and correlated vehicle kinematic and time stamp data. The collected data sequences could then be replayed repeatedly through the lane tracking system hardware allowing algorithm iteration and tuning under controlled circumstances and in real-time.

While the university lane tracking systems were being developed, Vision and Data Fusion task members worked together to determine methods to evaluate each system's performance relative to the system requirements. These efforts to use post-processed GPS, yaw rate and short-range vision data to determine ground truth are discussed in the Data Fusion section of this report.

Data analysis was performed through extensive use of custom Matlab functions. These functions allow loading, plotting, and analyzing the data for a particular run, and for each University system. Functions were also created to generate ground truth data from both yaw and GPS data. Of particular use is the capacity to simultaneously analyze the performance of all three lane tracking systems along with GPS and yaw rate, even when the data was generated at different times and differing update rates. This is accomplished through use of the video/data collection system along with Matlab functions used to synchronize the data.

Engineering Development Vehicles
To facilitate collection of data and testing of the lane tracking systems, two Engineering Development Vehicles (EDVs) were equipped with a video camera and recorder, digital yaw rate sensor, vehicle interface processor, and the data acquisition system described above. One of these EDVs was shared among the three universities, and used for data collection and algorithm development. The second vehicle was equipped with an OMNISTAR Digital Global Positioning System (DGPS), and hardware to correlate the GPS data with the vehicle data from the hardware-in-the-loop data acquisition system. This second EDV was used to collect data for system evaluation and comparison.

Technology Downselect
The performance of the university systems was evaluated by analyzing the results of running each system on a master tape. This tape was generated using the Video/Data collection system developed for the program. The tape contained sets of typical roadway conditions, including curve entries, exits, lane changes, and distracting roadway features. The university systems were evaluated using mean and standard deviation statistics, curve entry and exit prediction, and quality of state variables, i.e. road model parameters c0 and c1 (discussed later). The systems were evaluated relative to each other as well as against three ground truth systems, post-processed yaw, post-processed high resolution GPS, and Delphi's short-range vision system. The post processed yaw and GPS gave an indication of each system's curve entry preview, and the short-range vision system was used to evaluate each system's host state estimation. This evaluation process effectively demonstrated the strengths and weaknesses of each system. For example, the Ohio State University system provided the best curve entry preview, yet provided no useable host state information, while the University of Pennsylvania system provided good host state information with only some curve entry preview. The goal of the ACAS/FOT vision effort is to take advantage of the strengths of these systems and the knowledge gained in their development. For full details on the university systems and the downselect process, see the "Lane Tracking System Down-Select Summary Report".

Hardware Implementation
The lane tracking system requires a significant amount of data processing capability. Some of the other ACAS/FOT subsystems use PC104 form factor hardware. Unfortunately, performance of this very compact, special purpose PC generally significantly lags the desktop PC state-of-the-art, and the fastest processor currently available is only marginally acceptable for the final system. To achieve the lane tracking goals, a single board computer utilizing a 500MHz Pentium III processor was selected. Though somewhat larger than the PC104 system, a compact 7"x8"x3" enclosure houses the motherboard and the two PC104 expansion cards (CAN interface and frame grabber) required for the system. The lane tracking algorithms were implemented in an Embedded NT operating system booted from a compact flash card, eliminating any need for a hard disk. Three prototype systems were constructed for the ACAS program. One was installed in the FOT Prototype vehicle, where the communications interface was validated.

The camera selected for the ACAS/FOT is a small off-the-shelf "lipstick" Charge-Coupled Device (CCD) camera. The small size of this camera will simplify vehicle installation and insure no obscuration of the driver's vision. The camera also allows external adjustment of exposure which will greatly enhance the performance of the lane tracking system over varying lighting conditions. Delphi has developed a region-based adaptive exposure control algorithm to use in conjunction with this camera. By adapting the camera exposure to fit the region of interest in the image, more robust feature extraction is possible, particularly under varying lighting conditions.

Figure 4.3 Vision System Processing Unit

Adaptive Exposure Control

A major problem of electronic imaging systems relates to the tradeoff between the enormous dynamic range of luminance intensities, which can vary up to 180 dB depending on the time of the day, and the low dynamic range of the reflectance of objects. Typically, the reflectance of objects is less than 80 % and more than 4 % of the incident light, corresponding to less than 8 bit resolution (48 dB). Since a CCD-based camera system only offers a dynamic range that closely corresponds to the dynamic range of object's reflectance, the goal of an adaptive exposure control is to adjust the imager's exposure settings to account for changing illumination levels of the scene (due to entering shadows, etc.). This allows the limited instantaneous dynamic range of the imager to be more effectively used in distinguishing reflectivity differences rather than covering illumination changes.

The selection of an appropriate exposure time is based on an a priori chosen region of interest. This region can be defined as a full frame, one or multiple sub-frames, or a sub-sampled image. A dynamic adaptation of the region of interest dependent on previously identified objects is also possible, e.g. a dynamic windowed region of interest around lane markers. The idea behind the auto exposure algorithm is to identify under- or over-exposure by evaluating the gray-level distribution of the pixels defined by the area of interest and to determine the optimum exposure time from the gray-level distribution while maintaining a minimum latency in adapting to illumination changes.

The algorithm has been implemented in Matlab for evaluation purposes and in C++ in order to demonstrate its real-time capability in an embedded system. In order to emphasize the benefits of the presented auto exposure control against a fixed exposure control, sequences acquired with a high dynamic range imager (LARS II) have been used. These images show a dynamic range of up to 120 dB. Therefore, they are ideally suited for a closed loop simulation, since pixel data acquired by a CCD imager can be considered as an 8 bit subset of the 20 bit pixel data provided by the LARS imager. Shifting of the 8 bits through the 20 bit pixel data field enables the simulation of externally controlled exposure time changes, without the need of an actual camera. This allows exact repetition of the same image sequence for algorithm development and adjustment. The result of this approach is shown in Figure 4.5. By including the lane markers in the region of interest, it is possible to improve the exposure control to aid in lane marker extraction.

The auto exposure control algorithm is being implemented to control an actual off-the-shelf CCD camera (JAI CV-M536) that allows an external shutter adjustment via a parallel Transistor-Transistor Logic (TTL) interface.

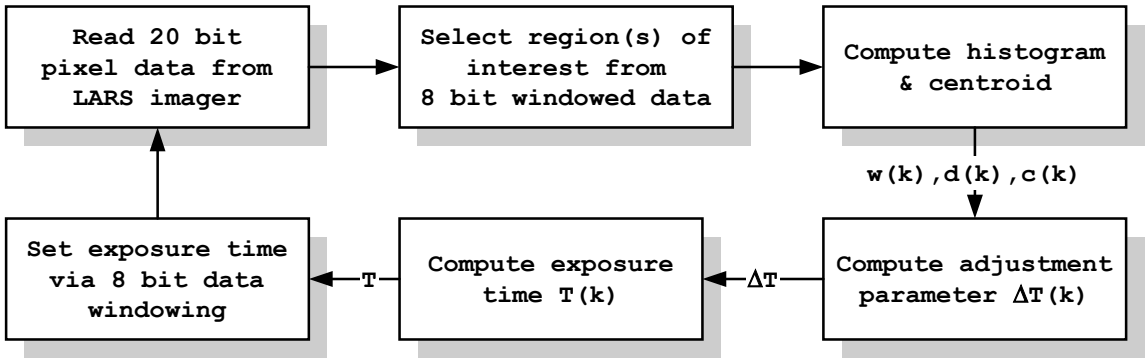

Figure 4.4 Processing Steps of the Auto Exposure Control Algorithm

Figure 4.5 Results of the Auto Exposure Control Approach. Left: Exposure controlled image. Right: Image without exposure control (i.e., fixed exposure time).

Intermediate and Final Results

All three university approaches resulted in functioning lane tracking systems that predicted road curvature at least some of the time. At the time of the downselect, each of these systems still required a significant amount of work to make this prediction reliable and robust, and to handle the myriad special situations that arise on the open road. Schedules for the Prototype development and testing, and for data fusion efforts, required that we have a stable vision system in place before the long-range system was ready. To bridge this gap, we turned to an in-house, short-range vision system that could be quickly modified to meet the Prototype system interface requirements, and to provide Data Fusion with preliminary road and host state information. Though this system would have no curve preview, it would provide valuable assistance during lane change maneuvers and periods of significant driver hunting (i.e., weaving, etc.).

The short-range system was ported to the hardware system described in the sections described above, and was used during the validation tests of the Prototype. Although use of this system has proven valuable, and could be made more valuable with just a few enhancements, we believe that the long-range vision system will provide important added value to the overall system. In addition, the results of related tasks, such as the camera exposure control discussed above, should further increase the value of vision system.

Because a great deal of testing is required to validate the performance and robustness of the vision subsystem, we are currently installing vision systems on three non-FOT Delphi vehicles that will be operated frequently and on a diverse set of roads around the country. A fourth system may also be installed on the GM EDV to support testing and system integration, and to gain experience on a wider variety of road conditions.

Verification Testing

Performance of the short range vision subsystem during on-road tests of the Prototype vehicle, performed both in California and Michigan, has been reviewed and analyzed in relation to sources of ground truth and the results of other subsystems.

Generally, the system performed as expected, providing valuable information about driver maneuvers such as lane changes. Reporting of the host vehicle position was accurate and timely, and nearly all lane changes were detected. The level of noise on the heading and curvature data, however, was higher than expected, and generally higher than that experienced in earlier evaluations. Post-processing of selected images in the problem regions has resulted in enhancements to the outlier rejection scheme that should significantly improve this performance.

Prior to the validation tests, the long and short-range algorithms had been tested primarily on limited-access highways and in well-marked urban environments. In contrast, much of the validation testing of the complete system has been performed on rural and residential roads, where lane boundary markings are not as tightly regulated. Consequently, the system performance was significantly better on highway segments of the tests. Since the FOT will not be restricted to well marked roads, these tests have indicated some areas that need more attention in both the long and short-range approaches. In some cases, lane markers were very poor or non-existent. Clearly, it will be important for the success of the subsystem to better identify these areas and report low or zero confidence in the results.

The rest of this section reviews examples of problem scenarios that were encountered frequently during the validation tests. Many hours of the tests were recorded on videotape suitable for post-processing by the vision subsystem. This data will be used to refine system operation in these regions, and to measure performance improvements.

The images in Figure 4.6 are typical of scenes on the rural roads near the Milford Proving Grounds in Michigan. The single lane highway has numerous intersections fed by right-hand-turn lanes, such as that shown on the left, and passing lanes such as that shown in the image on the right. Both circumstances present a similar problem for the vision system. The markings on the left side consist of a straight, low-contrast yellow, dashed line. On the right, a very high-contrast solid line bends sharply into the exit. As the host approaches these features, the vision system, attempting to react quickly to changes in road shape, will report the beginning of a curve ahead. Because there is little data on the left side of the vehicle to refute this hypothesis, incorrect road shape is reported for more than a few cycles before the system recognizes the error. For the scenario on the left, there may not be a solution to this problem. In the example on the right, however, the dashed demarcation of the pull-out lane provides potential for a solution. Additional high-level processing should prevent the vision system from taking exits of this type.

Figure 4.6 Typical Exit Lane Scenarios

The image in Figure 4.7 depicts a scene in which the host vehicle has just crested a hill on a road with significant vertical curvature. Though the road was actually very straight, the center marker in the image appears to bend to the right, straight toward the parked car. Without a matching lane boundary on the right hand side, its not possible to resolve this vertical curvature. In situations with only one lane boundary, vision data may need to be severely discounted in the Fusion system.

In Figure 4.8, the left and right lane markers diverge to two different roads. The "average" solution often taken by the vision system directs us right to the roadside signs ahead. To solve this type of problem, we are looking at insisting on agreement between the left and right markers, and reducing the confidence accordingly. This may, however, continue to be a scenario which produces false alarms in the overall system.

Figure 4.7 Unresolved Vertical Curvature

Figure 4.8 Diverging Markers

Technical Problems

One of the most difficult problems in the lane tracking system is to sufficiently constrain the road model and host state parameters such that the resulting lane representation, as well as the individual parameter values, are correct. For example, in order to define the position of a lane marker at some distance, say 75m, ahead of the host vehicle, it is necessary to combine host lateral position, host heading, curvature parameter c0, and curvature parameter c1. The resulting polynomial completely describes the forward lane position. It is possible to combine completely nonsensical values for the individual parameters and still get the correct answer because a nonsensical value for one parameter can be compensated for by another nonsensical parameter in another. We have termed this possibility "sloshing," as water might slosh from one container to another while maintaining the same sum total volume. In attempting to draw lines through lane markers, there are frequently situations where numerous, slightly different lines, might be drawn through the extracted features. This is particularly true when there is no marker data present in a particular region of the image, as with a dashed line. In such a situation, the derived host heading might be significantly wrong, along with host lateral position, yet these two compensate for each other and still create a good line through the lane markers in the regions where they exit. This sloshing remains a major contributor to lane tracking uncertainty and noise.

A key link in the lane marker tracking process is the initial feature extraction. This process is strongly affected by several uncontrollable variables, including shadows cast across portions of the road (by vehicles for example), low contrast lane markers (poor markings, yellow markings), or light colored pavement. In addition, lane markers can vary in width, and in quantity (double or triple stripe). The current lane extraction technique employs a matched filter to attempt to maximize the signal to noise ratio of the extracted features. The quality of this method suffers when lane markers are of a width different than the calibrated width. Also, adjacent lane markers affect the performance of the matched filter if the template kernel size encompasses part of the second lane marker

during extraction of the first. The matched filter process utilizes normalized correlation, which is very good at finding any feature, regardless of contrast, that looks like an intensity step of lane marker width. This results in outliers, especially at longer range where a lane marker width is close to the MTF (modulation transfer function, or resolution) of the system. The effect is that many marks on the road are a good match to the filter. All of these effects create noise in the data that requires heavier filtering and slower system response. The ultimate result is that of reducing the amount of curve entry preview that is possible from the system.

To improve the performance of the system, a new feature extraction technique is under development. The goal of this new marker extraction procedure is to produce a more accurate segmentation of lane markers in the image that will be far less sensitive to correlation score thresholds, contrast issues in the image, and variations in lane marker width and shape. The approach has two stages. The first stage is an adaptive thresholding step that is based on a careful analysis of local gray level histograms. The goal of this analysis is to choose threshold values that automatically adapt to changes in lighting, changes in roadway reflectance and variations in glare along the roadway. This technique is also insensitive to changes in lane marker width and shape; double and single lane markings can be handled in the same framework. In the second phase of the technique, a simple segmentation procedure is applied that will group the pixels that pass the adaptive thresholding step into ribbons. The goal of this stage is to identify connected groups of pixels with the right shape and orientation to correspond to lane markers. This has two beneficial effects: first, it allows rejection of outliers that have no chance to correspond to actual lanes based on their shape, and second, the curve fitter now can operate on pixel groupings instead of on individual slices of lane markers. Since the fitting procedure operates on more and better data, the numerical conditioning of the fitter is improved.

Significant Research Findings

We had the opportunity to investigate how the results of a short-range lane tracking system could aid the target selection process. As expected, accurate estimates of host lateral position and heading in the lane were beneficial in removing the effects of driver hunting, and in reducing false alarms during lane changes. We did not expect, however, that this same behavior might have a negative effect on the curve entry performance of the system.

Drivers frequently hug the inside of a curve, and often anticipate the curve by as much as one second. Thus, even before the host vehicle enters the curve, we see changes in yaw rate foretelling the beginning of that curve and providing some preview of the road shape ahead. Because a short-range system (such as that designed for lane departure warning applications) does not look out very far, it has little preview of the road curvature ahead and interprets the driver's move toward the inside marker as driver hunting, effectively erasing the bonus preview we received from the yaw rate.

Even with a long-range vision system, distant markers will not always be visible (at night, for instance), and the system will provide a road geometry based only on nearer range data. In this case, it will likely be important to not extrapolate the system results beyond their region of validity before combining the results with other sources of road shape in data fusion. A change in lateral position under conditions of limited visibility might be used to support the validity of a curve predicted by the GPS or scene tracking system.

Current Schedule and Progress for Task B2

The vision system schedule continues to be somewhat out of sync with other areas of the program. A significant portion of the development effort was originally slated to be performed in Phase II, though completion of the Data Fusion task (which requires a complete characterization of the vision system) was scheduled to be completed much earlier. Supporting development of the Prototype in 2001 diluted some of the resources on this task, and staffing issues at the university this summer delayed progress on long-range algorithm enhancements. These issues are being resolved. Still, the task schedule and technical need will require that vision system upgrades be performed well into next year.

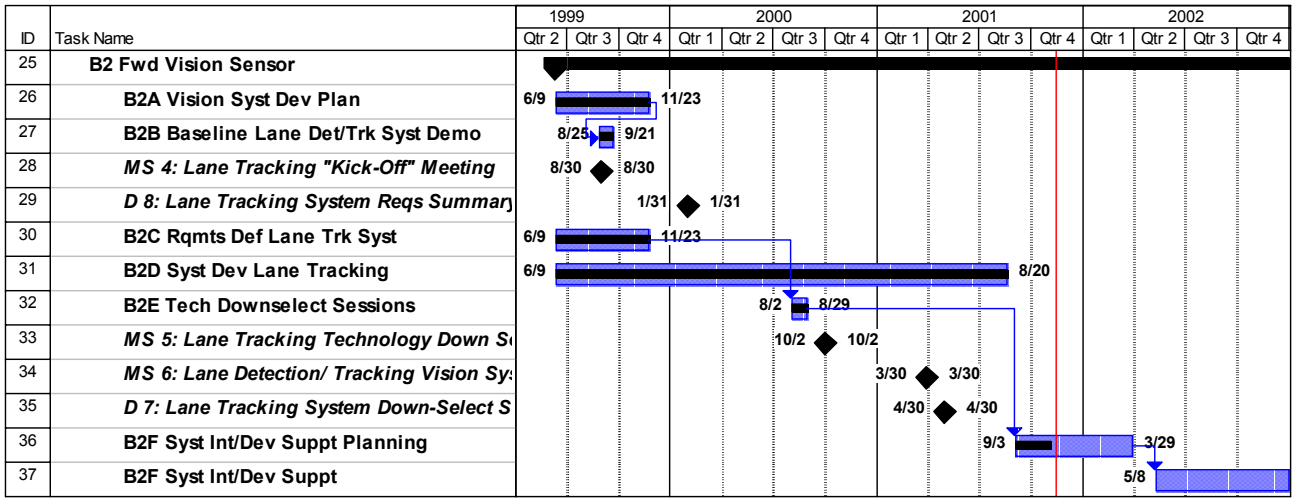

Figure 4.9 Task B2 Schedule

5 Brake System (Task B3)

Goals, Purpose and Background

The goal of Task B3 is to develop and implement a computer-initiated braking function that is performed without the driver in the loop. This computer-initiated braking will be referred to as "autobraking" for Adaptive Cruise Control (ACC) applications. The production vehicle is equipped with a standard braking system, incorporating the base braking system, the antilock braking system, the traction control system, and the vehicle stability enhancement (VSE). The autobraking feature was developed, calibrated, tested, and verified as a stand-alone part of this project prior to integration into the prototype vehicle. The engineering activities required removing production hardware from the test vehicle and replacing it with Delphi Brake Controls 7.2 (DBC 7.2) hardware and software.

The new autobraking feature provides vehicle deceleration without driver input via the brake pedal. The anti-lock brake system (ABS) controller signals the motor in the modulator to pump brake fluid from the master cylinder into the wheel brake lines through hydraulic valves, which are opened by energizing their coils. Key features of this new brake technology are to match the deceleration control requirements for smooth, quiet, and uniform autobraking during ACC scenarios.

Figure 5.1 shows the brake subsystem block diagram, which shows the interconnections to vehicle sensors, the Class 2 communications bus, telltales, and the powertrain controller. The vehicle sensors provide information regarding vehicle performance for processing by the brake controls algorithm. The warning lamps provide fault information, and status of ABS, traction control (TCS), and park brake features. The wheel speed sensor components produce a sine wave that is related to the wheel speed. The Powertrain Control Module (PCM) sends a message back to the Electronic Control Unit (ECU) indicating what percentage of the front or rear wheel torque was reduced. Other functions performed by the PCM include spark retardation, air/fuel ratio mixtures, and transmission shift control. Figure 5.2 shows the brake modulator installed on the ACAS/FOT prototype vehicle. Specifications of the program vehicle tested include:

2000 Buick LaSabre Limited Sedan
VIN Number: 1G4HR54K4YU263295
Options: Grand Touring Package and Prestige Option Package (SE)
Software: B17FOTVA.t00
Powertrain Software: Production
Brake Control System: DBC 7.2

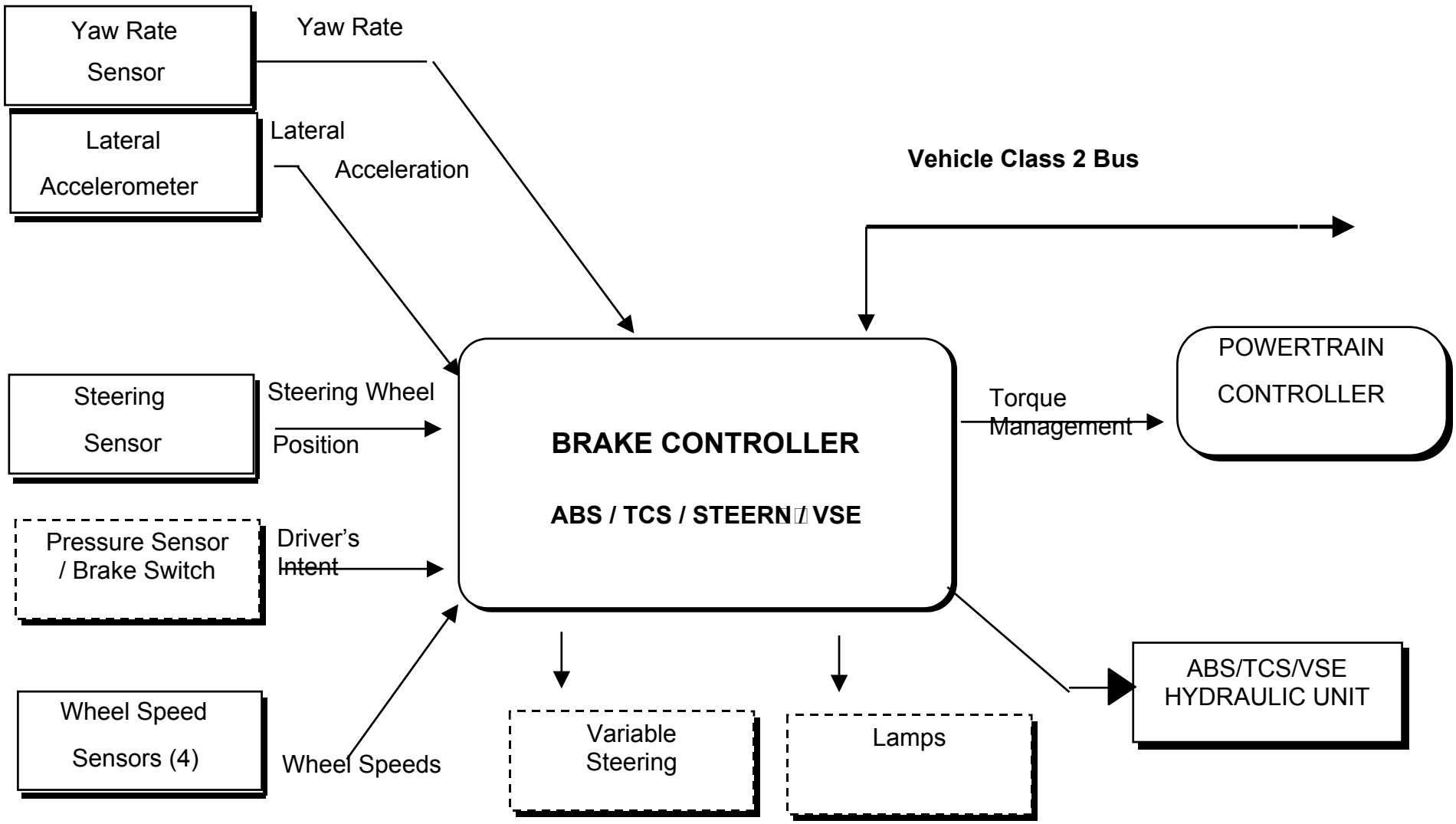

Figure 5.1 Brake Subsystem Block Diagram

The brake control system is an integral unit that includes the ECU that incorporates the algorithm and the Brake Pressure Modulator Valve (BPMV). The vehicle wire harness connector, hydraulic brake lines, and pressure switch are also visible in Figure 5.2. The Brake Pressure Modulator (BPM) unit has the capability to modulate hydraulic line pressure independently to all four wheels in order to maintain vehicle control during ABS, TCS, VSE, or ACC autobraking.

The ECU performs the following functions:

- Process input signals and convert to digital form.
- Execute the control algorithm stored in non-volatile memory to achieve the vehicle performance requirements.
- Convert control commands to physical outputs.
- Perform diagnostic checks on internal and external system hardware and store fault codes in non-volatile memory when a fault is detected.

The class 2 communications interface is compliant with SAE J-1850 and has the following options: 10.4 Kbaud variable pulse width modulation, cyclic redundancy error detection, and single wire transmission media.

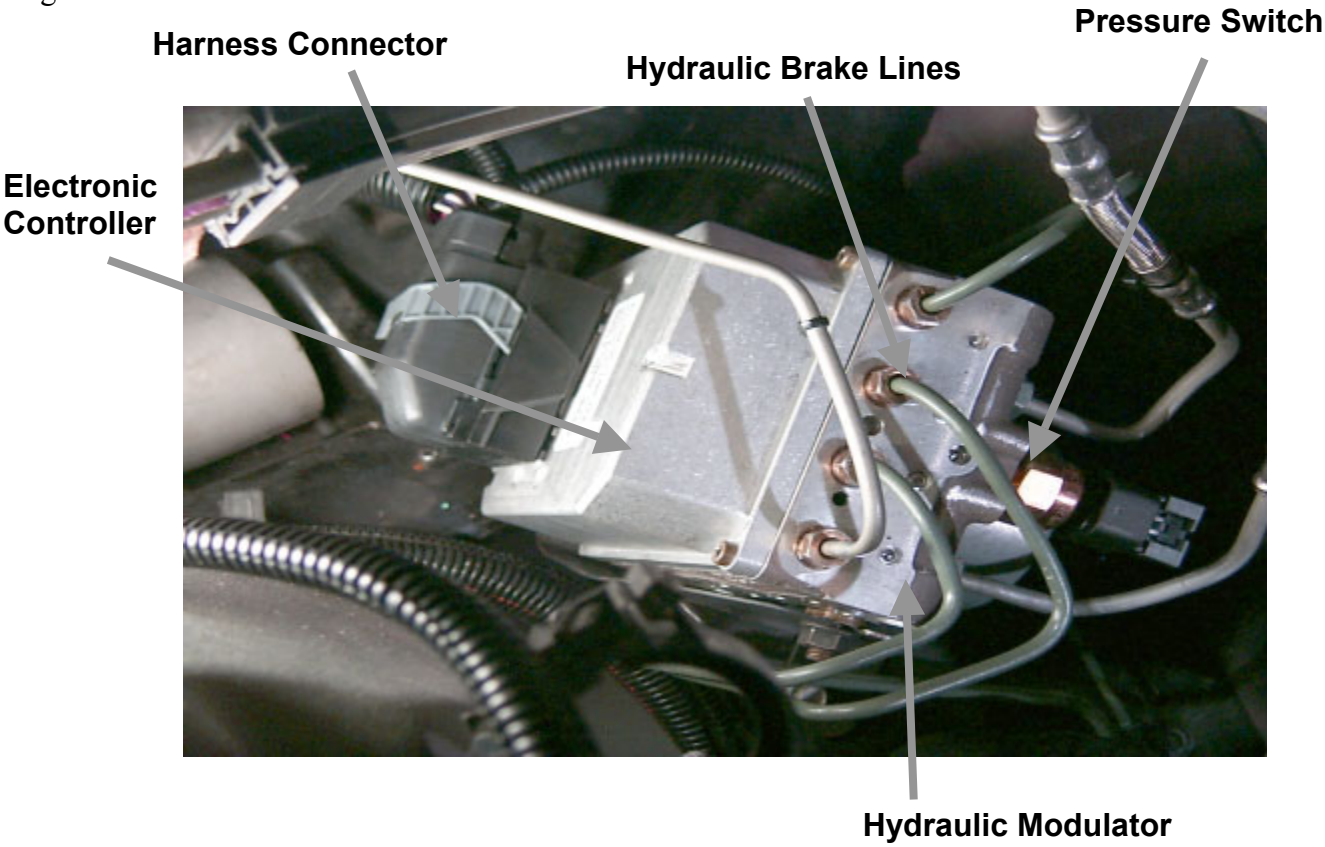

Figure 5.2 Vehicle Installation of the Electronic Control Unit / 12 Valve Brake Pressure Modulator

Technical Approach

Requirements Development

Typically Delphi receives a request for quote from a customer where the requirements are stated. In the case of this ACAS/FOT Program the requirements are established by the systems team for each subsystem including the brake system. The requirements are established as:

- Perform autobraking at levels of 0.3g and below
- Braking should be smooth and quiet (benchmark production vehicle)
- Activate the brake tail lamps during autonomous braking
- Incorporate the diagnostics as appropriate for the new autobraking feature
- Maintain production brake features of ABS, TCS, Vehicle Stability Enhancement and Dynamic Rear Proportioning (DRP)

Professional drivers conducted performance level and benchmarking brake tests on the production Buick LaSabre prior to removing any Original Equipment Manufacturer's (OEM brake hardware. The benchmark testing established the pedal feel, pedal force versus displacement, and stopping distance parameters so as not to radically change the vehicle's braking performance when Delphi DBC 7.2 brake hardware was install and calibrated. The above parameters were measured, recorded, and tracked during the brake system integration and testing process.

A Federal Motor Vehicle Safety Standard is the guide that mandates the braking system be 4 corner diagonal split brake system or a front axle independent / rear axle independent brake system. The Buick is configured as a diagonal split system where a failure in one diagonal will reduce the braking to a degraded (power) mode. The base braking capability remains intact and unaffected. The system is configured such that at least two independent lines leave the master cylinder circuits. The system tested and installed on the ACAS/FOT vehicle provides redundancy and a single point failure may result in a degraded mode of operation but it will not result in the loss of all braking. Braking is accomplished by generating a frictional force on a part that is rigidly attached to the wheel. As a result of the pressure exerted by DBC 7.2 hardware and embedded controls, fluid presses a brake pad against an area on the disc, creating a force resisting the rotation of the disc and therefore the wheel.

Design and Implementation

The Delphi/Bosch 5.3 production brake system, on the prototype Buick LaSabre, was changed to a total Delphi Brake Solution (Delphi DBC 7.2). The DBC 7.2 ABS/TCS/Vehicle Stability Enhancement (VSE) System for passenger cars provides state-of-the-art full-performance wheel-lock control to optimize stopping distance, steerability, and vehicle stability along with acceleration slip control to optimize vehicle launch (i.e., acceleration from stop) and traction capabilities. Figure 5.1 shows vehicle system mechanization. In this ACAS/FOT application, on the prototype Buick LaSabre, the end product is not a production equivalent, but rather development hardware and software.

The DBC 7.2 solution consists of the algorithm/software, electronic controller, and hydraulic modulator. Calibration changes were made to compensate for hardware differences between the OEM brake system and Delphi brake system in addition to satisfying the brake system requirements.

A major emphasis of the brake system development was centered on building the software package for the Buick LaSabre. Based on production programs and practices, along with the benchmarking data, the software package was designed to meet the vehicle communications protocols, diagnostic message reporting, and moding of autobraking with ABS, VSE and DRP.

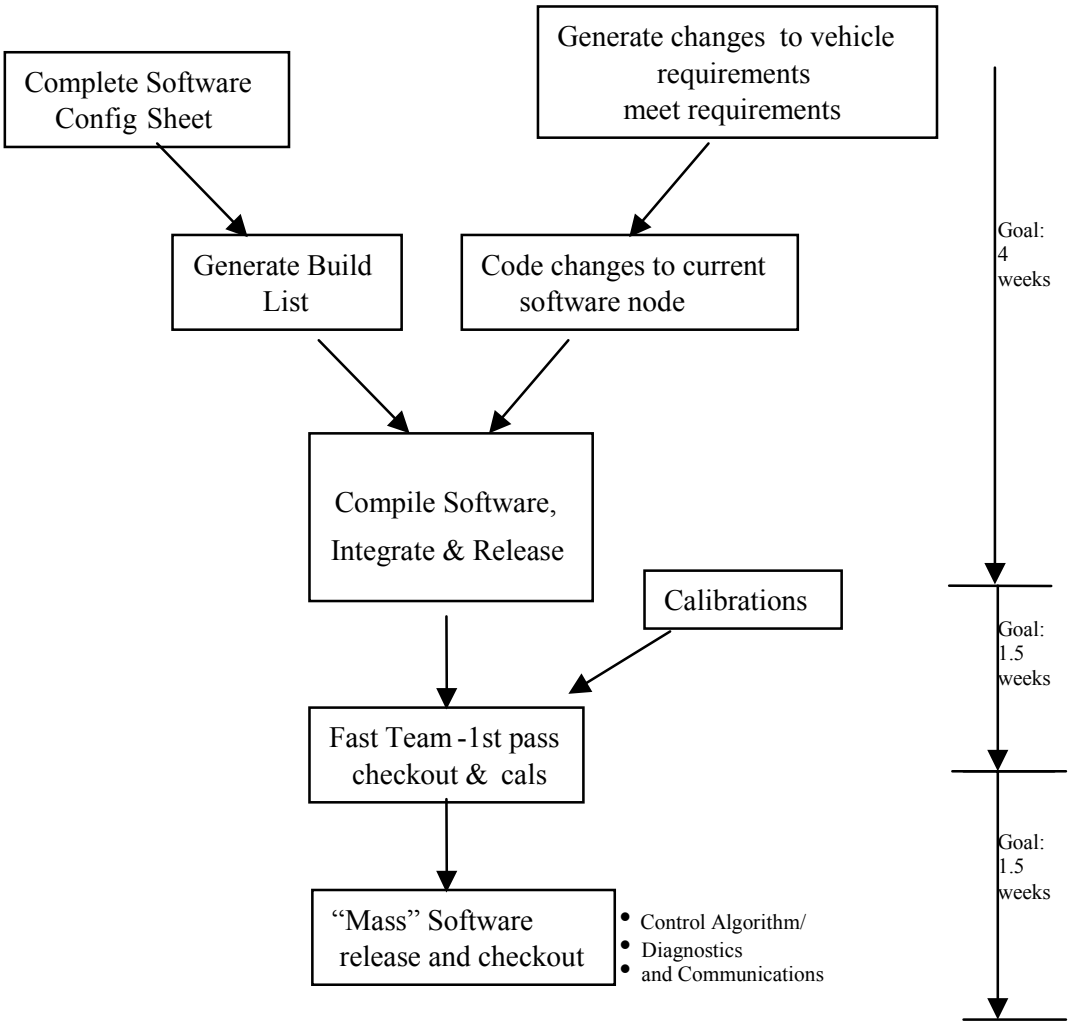

Figure 5.3 "V" Cycle Design and Implementation Flow for Delphi Brake Systems

The brake system software release process for this program maps to the "Traditional 'V' Cycle shown in Figure 5.3". We follow the production process where the design and coding of the brake control algorithm, software, and vehicle calibrations are specified for the Buick LaSabre. The software package was verified on a laboratory bench where vehicle inputs were simulated through hardware-in-the-loop methodologies. Vehicle calibration and verification were performed using the specified software package. The next section describes the vehicle verification process for the brake controls subsystem.

Vehicle Verification

Verification included testing the vehicle provided by the ACAS/FOT program to verify that the ride, braking, and handling performance are unchanged relative to the vehicle's benchmark data. Typically during production programs, the OEM has the responsibility of validating the subsystems and full vehicle functionality and performance. The OEM validates the vehicle as a product to be ultimately sold to customers. As a supplier, Delphi Chassis verifies the requirements of the brake subsystem relative to the vehicle performance as a completion step in satisfying the contractual obligations of a statement of work (SOW). We also note that the customer validates new features and functions on a fleet of production-intent vehicles whereas Delphi verifies the specified performance using a representative vehicle and laboratory resources.

The test sites for brake system verification testing were Delphi's Marquette Winter Test Site and GM's Milford Proving Grounds (MPG). Delphi Chassis conducted the brake subsystem verification testing. This was followed by vehicle-level verification tests conducted by GM per the ACAS/FOT Verification Test Plan.

Vehicle level testing of the ABS/TCS/VSE system was conducted for the LaSabre. All testing was conducted using the standard production interfaces to the powertrain, steering, and other related vehicle systems along with production-sized tires. Before testing the vehicle configurations were set as they would be for production with the DBC 7.2 brake system

Level 1 tests are formalized tests performed by professional drivers. These tests are performed after the control algorithm changes are completed and the calibrations have been fine-tuned for a specific vehicle model. The intent of Level 1 is to verify performance vs. quantified targets. The Level 1 Configuration Matrix explicitly labels which maneuvers are performed on the vehicles and the test surfaces on which the maneuvers will be performed. The test results are compared to data in the Level 1 Target and Tolerance Matrix. The data is based on World-Class performance targets. The number and frequency of tests were dependent upon the status and performance of the specific test. Problem Corrective Action Reports (PCARS) are written for any test where the median of five runs does not meet the target or an individual run does not meet the tolerance.

Prototype Buick LaSabre Brake Verification Test Results

Level 1 testing are defined as verifying the brake system performance against quantified targets. The prototype vehicle tests are run to a Delphi performance specification. The brake system performance targets and tolerances are defined based on world-class benchmarks. A verification test matrix was defined to test the brake system during various cold and mild weather conditions and on surfaces with varying coefficients of friction (i.e. snow, packed snow, ice, and rain); it was populated with the vehicle-specific ABS, TCS, and VSE targets and tolerances. A non-confidential version of the Level 1 Test Matrix is provided in Table 5.1 and it represents the formal engineering testing practices for production applications of Delphi Brake Systems.

Table 5.1 Brake System Test Matrix

						Performance Criteria																	
Test Procedures: ACC Vehicle Test						*Deceleration*								*Yaw Rate (deg/sec)*						*Response Time (sec)*			
Maneuver				*Speed*	*Steer*									#		#		#		#		#	
Surface Options						#		#		#		#		#		#		#		#		#	
						Trgt	Tol	Trgt	Tol	Trgt	Tol	Trgt	Tol	Trgt	Tol	Trgt	Tol	Trgt	Tol	Trgt	Tol	Trgt	Tol
Asphalt	or	Concrete	S/L	#	#	#	#					#	#	#	#	#	#						
				#	#	#	#					#	#										
Asphalt	or	Concrete	S/L	#	#	#	#	#	#			#	#	#	#	#	#						
				#	#	#	#	#	#			#	#										
Asphalt	or	Concrete	S/L	#	#	#	#	#	#	#	#	#	#	#	#	#	#						
				#	#	#	#	#	#	#	#	#	#										
Ice			S/L	#	#	#	#																
Ice			S/L	#	#	#	#																
Gravel			S/L	#	#	#	#	#	#	#	#												
Asph/Ice	or	Conc/Ice	Split	#	#	#	#	#	#														
Asph/Ice	or	Conc/Ice	Split	#	#													#	#				
Ice to Asph	or	Ice to Conc	Trans	#	#																	#	#
Asph to Ice	or	Conc to Ice	Trans	#	#															#	#		

*Listed Speeds May Need Modification For Some Applications
'data' Refers To Reported Data Without A Specific Target/Tolerance

Level 1 testing was performed at various program milestones using a Buick LaSabre identical to the prototype vehicle and dedicated explicitly to brake controls development. Tests were conducted using the latest version of autobraking software, which may not necessarily be the final version of the ACAS/FOT software release. The intent was to capture and evaluate vehicle performance at significant development stages within the development and application process.

Level 1 Testing — Anti-Lock Brake System
Performance testing of the ABS system was conducted per the Delphi Level 1 Test Matrix. The vehicle passed the target and tolerance goals for world class performance. When the Electronic Brake Control Module senses one or more wheels approach lockup, ABS is activated to optimize brake pressure to the affected wheels. ABS winter verification tests were conducted using the 2000 Buick LaSabre vehicle. The ABS calibrations are verified and no further changes are recommended. ABS performance tests conducted include:

- 40kph straight line snow
- 70kph straight line snow
- 50kph straight line concrete
- 100kph straight line concrete
- Transition - Concrete to Ice (70kph)

ABS summer and mild weather verification tests were conducted using the 2000 Buick LaSabre. The vehicle passed all target and tolerance goals for world class performance. ABS summer and mild weather verification tests conducted include:

- Transition - Asphalt to Jennite (70kph)
- Transition, low to high - Basalt
- Straight line - Jennite
- Steer right - Jennite
- Steer left - Jennite

Autobraking and ABS moding tests were conducted. The autobraking/ABS results indicate that noise, product operation, and performance targets meet ACAS/FOT system requirements. The ABS Level 1 test procedures and data from the various ABS tests are on file as part of the project archive and are Delphi Confidential.

Level 1 Testing — Traction Control System
Performance Testing of the TCS was conducted per the Delphi Level 1 Test Matrix. The vehicle passed the target and tolerance goals for world class performance. When the Electronic Brake Control Module senses positive slip, TCS is activated. The speed of the drive wheels is compared to that of the non-drive wheels and the Electronic Brake Control Module uses engine torque management and applies the brakes. The drive wheel brakes are applied to reduce positive slip and allow the tires to maximize traction. TCS winter verification tests were conducted using the 2000 Buick LaSabre. The TCS calibrations were verified and no further changes are recommended. TCS tests conducted include:

- Straight line concrete
- Straight line ice

- Corner right - ice
- Corner left - ice
- Steer left - ice
- Steer right - ice
- Transition, Low to High - Ice

The TCS results indicate that noise, product operation, and performance targets meet ACAS/FOT system requirements. The TCS Level 1 Test Matrix and data from the various TCS tests are on file and are Delphi Confidential.

Level 1 Testing — Vehicle Stability Enhancement
Performance Testing of the VSE system was conducted per the Delphi Level 1 Test Matrix during the winter of 2001. Testing of VSE requires winter surfaces. The VSE Level 1 Test Matrix and data from the various VSE tests conducted to date are Delphi Confidential and are available for review upon request. The vehicle passed VSE/autobraking moding tests conducted during Phase I.

Full scale VSE and ABS moding will be conducted during the winter 2002 using the Buick Chassis mule vehicle. The chassis mule is identical in OEM content and functionality to the ACAS/FOT prototype vehicle and FOT Program vehicles. The VSE/Autobraking feature should indicate that noise, product operation, and performance targets will meet ACAS/FOT system requirements.

Although the ACAS/FOT Buick brake system will be used for a limited number of vehicles builds, it is based upon a production implementation of the DBC 7.2. control algorithm and hardware. The deceleration, stopping distance, braking efficiency, pedal feel, and system response have been verified to be safe and operational as required in a production vehicle.

Prototype Buick LaSabre Brake Verification Test Results - Summary
During Phase I, there were several "lessons learned" relative to the development of an autobraking feature. The current level of software tested in the vehicle is version B17. During the verification testing several updates will be incorporated as a result of brake systems development to meet systems requirements. Updates shall be incorporated and verified in software release 23B.

An update to brake system software (ver. 23B) corrects a low speed entry criteria for Vehicle Stability Enhancement. At low speeds, while making cornering maneuvers, the yaw input would cause VSE braking. The solution was to increase the VSE low speed threshold as part of this ACC brake controls' software release.

A second update will be incorporated to address thermal conditions for brake hardware overheating. The scope of the modifications will be to provide diagnostics when brake hardware overheating conditions are imminent. Autonomous braking for ACC applications will increase the number of braking cycles. A thermal model incorporates the calibrations and profiles to prohibit autobraking conditions if the brake lining temperatures become excessive. The testing and data collection for calibration of a thermal model for the ACAS/FOT vehicle have been conducted, and the thermal model will be incorporated in software release 23B. Release 23B contains updates from Production ACC programs and the thermal model.

Brake system software release 23B will also include zero decel control capability. Zero decel — the vehicle ability to maintain a constant speed — will be necessary in downhill following scenarios in order to minimize jerk. The vehicle processor will initiate a zero decel command to the brake controller for this purpose.

Current Schedule and Progress

The schedule for supporting the prototype vehicle level testing, updating the software to version 23B and supporting the Field Operational Test during Phase II is provided below.

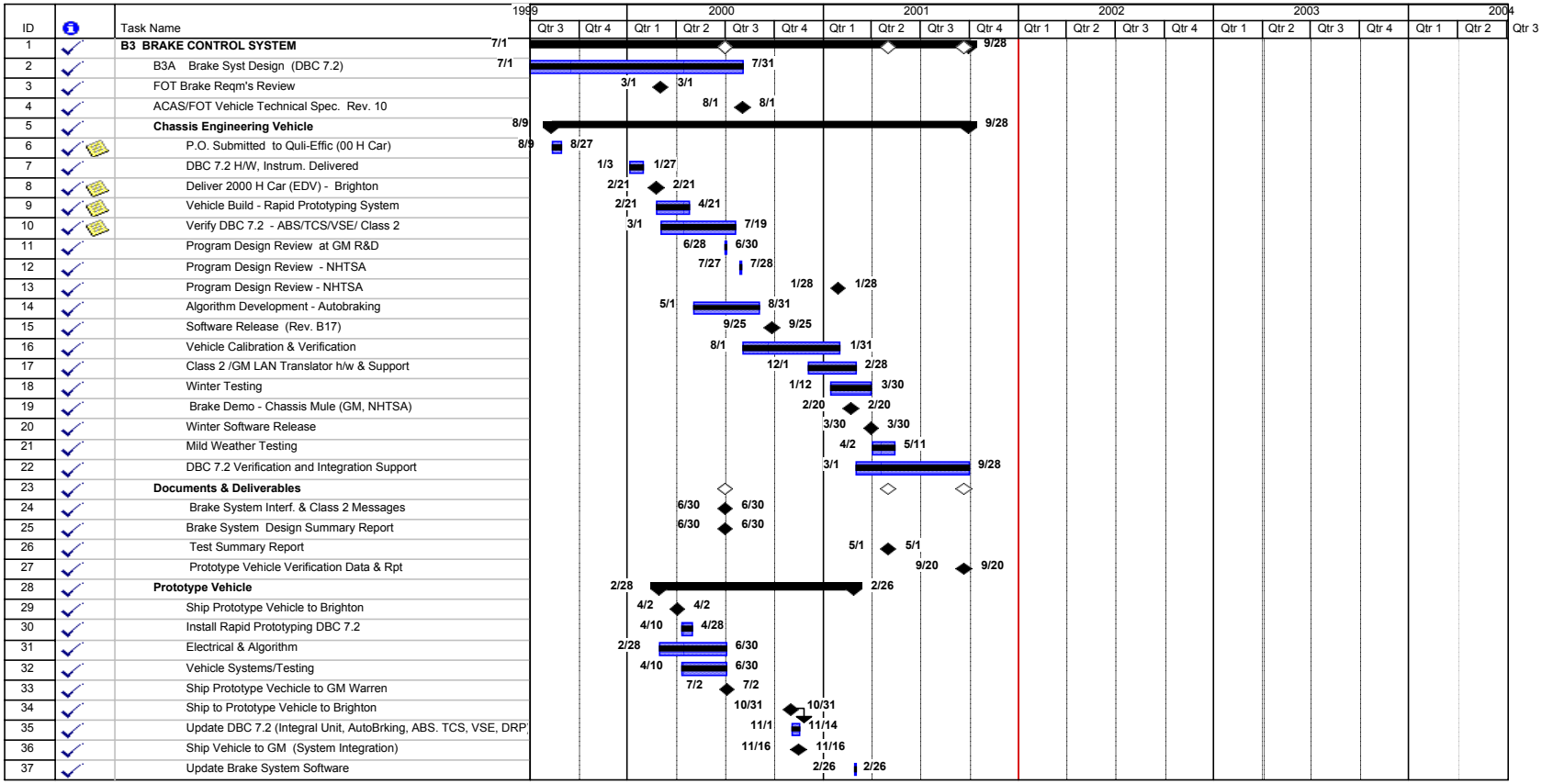

Figure 5.4 Task B3 Schedule

6 Throttle Control System (Task B4)

Goals, Purpose and Background

The purpose of this task is to modify the vehicle's cruise control to accept commands from the ACC/A radar subsystem, to provide vehicle speed control. The final outcome is a cruise system that can be controlled externally by the ACC/A radar. This is necessary to adjust the vehicle speed when following a lead vehicle which is moving more slowly than the initial cruise set speed.

The vehicle's stepper motor cruise control (SMCC) is a standard module and has been used in other vehicles that have been modified to provide adaptive cruise control (ACC) capability.

The vehicle's SMCC controller board was replaced with a modified board that contains an 8192 serial interface. The control software was modified to accept the commands from the ACC/A subsystem and report the control functions back to the ACC/A subsystem.

Analysis of the issues associated with supporting the throttle control system during the deployment period has begun. Issues that have been raised, and will be addressed, include

1. How to isolate an ACC failure to the throttle control system
2. How to repair failed throttle control subsystems
3. How to perform a field upgrade to the subsystem

It is expected that further issues will be identified as the planning effort continues.

Results

The SMCC is operating as expected. Vehicle control by the ACC/A radar subsystem was successful.

Current Schedule and Progress for Task B4

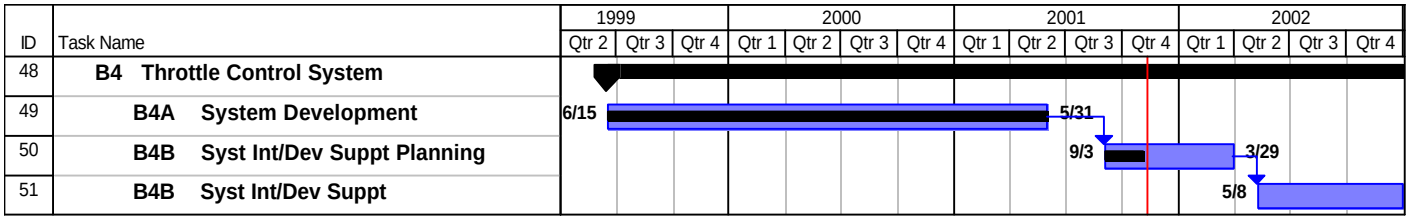

Figure 6.1 Task B4 Schedule

7 Driver-Vehicle Interface (Task B5)

Goals, Purpose and Background

The goal of Task B5 was to design and build a driver vehicle interface (DVI) that presents information regarding vehicle speed, Forward Collision Warning (FCW) states, and Adaptive Cruise Control (ACC) states in such a way that the driver receives maximal safety benefit from the collision avoidance systems, but is minimally annoyed, minimally distracted. The collision warning should be conspicuous and interpretable, to support the timely return of an inattentive driver to active driving involvement when the system determines that the vehicle is approaching a collision situation.

The literature review was completed on schedule. A summary of insights resulting from this review was presented to NHTSA as "Comments on NHTSA-Furnished Research Reports," Robert Hogan, October 20, 1999. After extensive internal review, copies of the document, "Human Attentive Processes and the Choice of Warning Cues for Rear End Collision Warning Systems," by Robert Hogan, were submitted to NHTSA on November 30, 2000. The surveyed literature included reaction time for warning alerts, benefits of preview for serially organized behavior, driver-in-the-loop experiments with FCW, dual-task performance, automotive alerts, analog vs. discrete alerts, driver situation awareness, mode confusion, proliferation of modes and warnings, and operator vigilance.

Hogan reached the following conclusions:

1. The degree of driver inattention has not been well controlled in FCW experimentation. Surprise and distraction techniques have been used in some studies. These techniques manipulate two qualitatively different attentive states; it would be desirable to measure and control degree of inattention on a continuum.
2. The frequency of nuisance alerts and false alarms is generally believed to be a critical metric for evaluation but the extent to which an alert might contribute to disruption/distraction/ nuisance has not been studied as a function of the type of DVI or situational context.
3. (Crash Avoidance Metrics Partnership 1999) provides insight into the coupling between braking response and the kinematics of the car-following situation.
4. The operator-out-of-the-loop problem, which has been studied in cockpits and complex process control, may be equally important in FCW/ACC systems. According to the vigilance literature, a driver's ability to intervene is expected to decline with the reduction of circumstances calling for intervention.
5. Mode confusion may occur due to the integration of ACC and FCW in the same vehicle. Mode confusion results when the driver is uncertain of the current state of the automation, potentially causing inappropriate behavior by the driver. Although these modes are not complex, the requirement for sudden intervention makes the potential for mode confusion problematic.
6. Multi-level alerts should enhance driver vigilance, promote traffic situation awareness, assist in appropriate allocation of resources, and reduce the startling character of a sudden alert. These benefits have been documented in other systems but have not been directly demonstrated for FCW on closed course or public roads.

The program initially adopted many of the CAMP (1999) Program DVI recommendations, such as:

1. The crash alert timing may be adjustable by the driver
2. The highest level of the alert should be presented across at least two modalities (visual icon on a head-up display (HUD) and non-speech tone)
3. The audio component of the warning should be presented so that the sound is perceived to emanate from the forward direction of travel
4. The intensity of the audio warning should be automatically set at an appropriate level relative to the ambient noise and other sources should be muted during the warning presentation
5. The flash rate of the imminent visual alert should be 4 Hz
6. A daytime and nighttime display luminance should be provided

CAMP developed a single stage alert comprising visual and auditory components. The emphasis of the ACAS concept design was to develop a multi-stage warning system and to evaluate this against a corresponding single-stage design. COMSIS (1996b) recommend that a multi-stage warning, compared to a single-stage warning, allows the warning system to provide an appropriate degree of intrusiveness at differing levels of urgency. In the maximally urgent situation of an impending collision, the alert must be sufficiently intrusive to immediately elicit an appropriate response from the driver. Because of the inherent correlation between intrusiveness and driver annoyance, the high degree of intrusiveness required by an imminent warning would render it inappropriate for less imminent situations. In ACAS the appropriate level of intrusiveness is obtained by providing a single-stage (highly intrusive) auditory alert similar to that provided by CAMP, and in addition a (much less intrusive) multi-stage visual alert. The earlier visual alert advises the driver to caution as headway decreases. The advantage of a multi-stage display is that it provides the opportunity for advanced warning while the highly intrusive auditory warning provides an imminent alert. As COMSIS (1996b) articulate:

> *As a general approach to minimizing the conflict between broader protection and greater annoyance/degradation, these Guidelines recommend multiple levels of warning for a particular warning device. The highest level of warning, termed an "imminent crash avoidance warning," uses a more urgent and intrusive signal. Cautionary warnings provide the driver with greater advanced warning, in a less disturbing form. (p. 2-5).*

The philosophy guiding the development of multi-stage concepts was to address unresolved issues in collision-avoidance (i.e., driver situation awareness, vigilance, and vulnerability to disruption) and completely integrate FCW and ACC sub-systems into one coherent and intuitive interface. Consistent with Dingus, et al.'s (1997) observation that an FCW display may be able to increase headway, the display was designed with the goal not only of alerting the driver in imminent situations, but of actively promoting safer driving. Initial guidelines were developed by Delco and GM representatives:

1. The visual icons can be used to provide an association between the display stimulus and the meaning of the warning, however, they cannot be used in isolation because the visual stimulus fails if the driver is not oriented toward the visual display. To achieve a successful alert, regardless of driver orientation, the warning must be presented across a second modality that is independent of driver orientation. Visual and haptic displays have the potential to fulfill this criterion.
2. The visual display will employ redundant coding, simultaneously using both color (green, amber and red) and shape to communicate increasing urgency. At the highest level of urgency, the visual icon will flash on and off at 4 Hz.
3. A head-up display (HUD) was selected for the prototype vehicle, rather than a high head-down display (HHDD), because CAMP (1999) participants preferred the HUD to the HHDD. A HUD is also considered to be a desirable component of an FCW interface because of its proximity to the forward visual scene, allowing it to be noticed by a driver who is oriented toward the outside environment. For the same reason, a HUD is likely to attract driver visual attention away from the forward scene to a lessor extent. An FCW display that attracts driver attention away from the forward scene at a critical moment would be highly undesirable. Because the HUD is located in close proximity to the forward visual scene and renders an image located several meters in front of the driver, it has the potential of offering drivers the opportunity to attend to the forward scene and the HUD content simultaneously.
4. A single display will integrate ACC and FCW information for the sake of simplicity and will be designed to reduce the likelihood of mode confusion.
5. Haptic stimuli (brake pulse and seat-vibration) are promising but immature candidates for FCW systems
6. The frequency of false alarms and nuisance alerts is critical to driver acceptance of an FCW system. If the number of false alarms and nuisance alerts is high, the system may be required to be less intrusive, in order to reduce driver annoyance.

After the human factors personnel reviewed the vehicle technical specifications, more specific DVI guidelines were established:

7. The problem of automatic braking for some stopped objects but not for others was flagged as a potential source of danger for drivers using the ACC system. This may be especially critical given that more rear-end accidents occur with stationary lead vehicles than with moving lead vehicles (Mortimer, 1988).
8. An ACC generated deceleration alert should be activated before the maximum deceleration requested condition is met.

The first candidate multi-stage display was based on a nine-bar trapezoidal display that Dingus et al. (1997) had demonstrated could increase headway in open road experiments. To reduce complexity, the display was scaled down to a six-bar trapezoid display and a vehicle icon was added to indicate “vehicle detected” and to increase display saliency. In addition to this change, the display was altered to display a single color at a given time for all trapezoids in contrast to the Dingus et al. display, which could display bars of different colors at a single instant in time. The resulting display is shown in Figure 7.1.

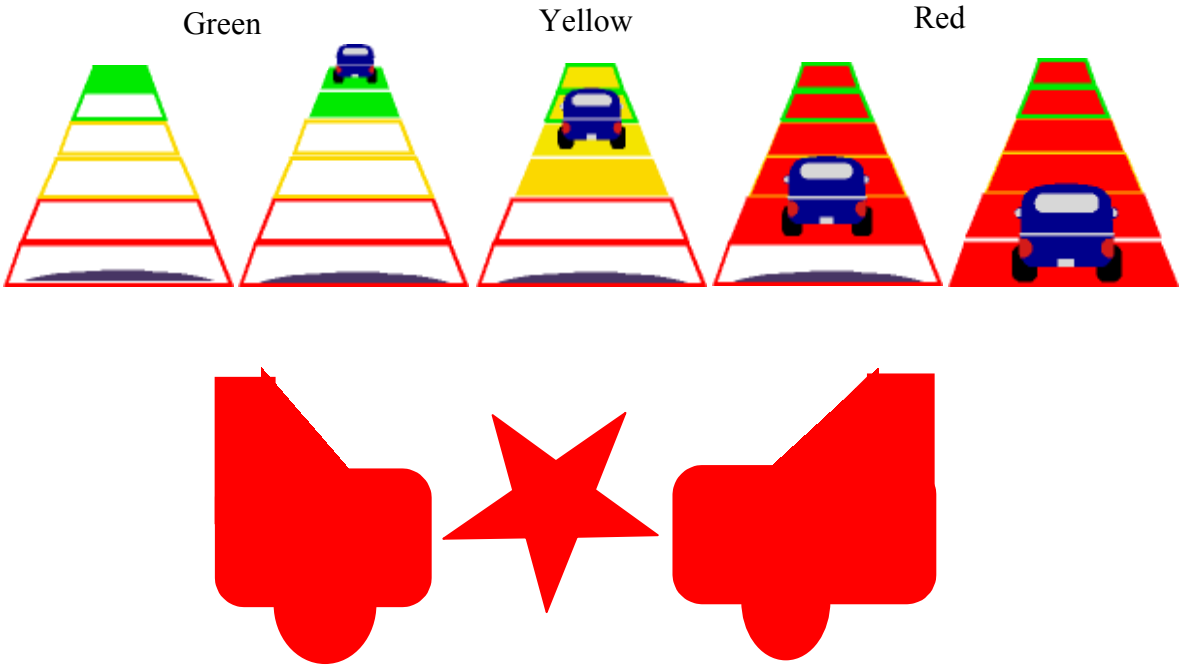

Figure 7.1 [Top] First Draft of the Multi-Stage Display
[Bottom] The CAMP (1999) Icon

Initial commitments in the design of the DVI were reported in the Program Review 2 of July, 2000. The following items were specified:

1. DVI Inputs and Outputs
2. Hardware Deliverables
3. DVI/Vehicle Layout
4. HUD Design Approach
5. HUD Mechanical Configuration
6. HUD Performance and Mechanical Specifications
7. Integrated Gradient Warning Display including speedometer, ACC Message Line, and Warning Gap/Interval Display (see Figure 7.2).
8. Steering wheel controls
9. HUD Controls

During this period, several candidate sounds were created. Some were based on the Patterson Guidelines for the Design of Auditory Warning Sounds, while others were recommended by CAMP (1999).

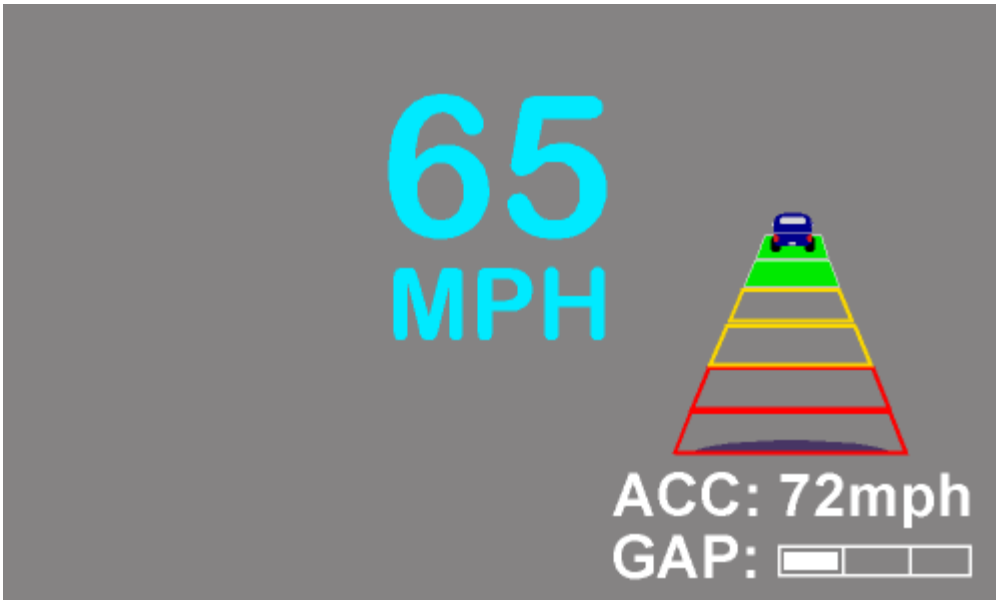

Figure 7.2 Integrated Vehicle Display. Shows FCW alert level, speedometer, ACC message line, and Gap/Warn Interval display

During the latter half of 2000, Delphi Brake and Chassis developed a haptic braking prototype. In September of that year, several GM and Delphi members of the ACAS FOT team met at the Milford Proving Grounds to evaluate haptic braking as a potential warning stimulus. The group (consisting of four human factors and three systems engineers) rode in the prototype vehicle and were given the opportunity to drive the vehicle, while they were provided with their requested combinations of brake pulse frequency (3, 5, 8, and 12 Hz) and brake pulse intensity (0.1, 0.2, 0.3 g). Following exposure to these stimulus variables, participants responded to a questionnaire (generated by the Delphi Brake and Chassis group). The responses to the questionnaire items are summarized in Table 7.1. It can be observed in the table that the responses to the haptic braking stimulus were highly favorable.

Despite the positive feedback for the haptic braking stimulus, at the Program Steering Committee meeting of December 4, 2000, it was decided that the brake pulse work would be discontinued. This decision was based on the excessive complications to the vehicle architecture and safety implications involved with modifying the brake system. Haptic braking required an increase in research and design that was not feasible given the deadlines facing the Delphi Brake and Chassis group.

Table 7.1 Responses to the Haptic Braking Stimulus Questionnaire

	Overall Impression	Noise and Vibration Acceptable	Effective alert?	Level and Duration Acceptable?	Compare with Visual and Auditory?	Other
1	Low Freq- not effective, 5 Hz best.	Acceptable	Effective, needs tuning.	Level okay, Duration too long.	More effective	
2	Don't like 8 & 12 Hz, If 3 or 5 Hz is selected duration should be < 4 s at > .2 g.	Higher freq too much like rumble strips.	Onset effective but repeated are lost.	< 4 s and > .2 g	More intuitive as it draws attention forward.	Preferred CAMP monopulse
3	Above 5 Hz becomes almost like DC braking that seems like regular decel. Attention getting.	Subtle. Single stronger pulse preferred, peak. Decel felt too low.	Yes, but lower freq and higher amplitude.	If like rumble strips, it would feel better. Vehicle big damper so single stronger pulse does a better job.	They complement each other. Dash lights are the least effective.	Haptic braking is a very clear message to the drvier. Needs tuning-- Loss of traction.
4	5 Hz very salient and effective.	Yes	Effective	Yes	Good for attention-getting	
5	Good	Yes	Yes	Consider speed dependent pulse rep rate.	Very good	Preferred .2 g at 8 Hz for 4 s. 3 Hz like boat over waves. 5 Hz like thumping tire. 8 Hz like warped disk brake. 12 Hz like gravel road.
6	Useful	Yes	Pulses even at .1 g would tend to alert the driver.	Brake controller seems acceptable but the pulse definition needs TBD.	Not sure it will bring eyes-front faster than audible but maybe it will.	If it can be implemented safely with integration to ABS & VSE then it's a sound brake pulse.
7	Like it-- good indicator	Yes	Yes with audio and vis.	Liked the lower frequencies better. 0.1 g seemed okay.	Need to combine.	Need work to select the best candidate. Safety issues?
	5 Positive impression 2 Not specified	7 acceptable	7 Affirmative			

In September of 2000, there was a transition in leadership of the DVI task within Delphi Delco Electronics. The transition of leadership resulted in a new round of developments to the DVI system. The new task lead observed the following weaknesses with the current display candidates.

1. The most prominent transformation in the vehicle icon as a function of alert level was a downward translation. Vehicle icon expansion was less prominent than this downward translation. Even though a visual image may be expanding due to increasing proximity, downward translation specifies a shrinking (and therefore less threatening) object.
2. The change in display shape as a function of alert level was masked by an ever-present global trapezoid shape. All icon changes occurred within the confines of the global trapezoid shape, possibly making state-changes less salient to an inattentive driver.
3. The display appeared to be overly complex, with seven different colors displayed at any given time, and the vehicle detection icon was too small to meet minimum HUD size specifications.
4. The message text line and the gap/warn setting display interfered with one another. The two displays presented separate information and should appear to be separate displays.

5. The most imminent level of the display was insufficiently distinct from the rest of the display sequence. In addition to this, the single-stage candidate (the CAMP icon depicted in Figure 7.1) was not directly comparable to the multi-stage display because the displays differed across more than one dimension (appearance of imminent icon and number of stages). The human factors group had discussed making the imminent stage of the multi-stage warning equivalent to the CAMP icon; however, this would have resulted in a perspective change from rear-end to side-on at the final stage.

The observation that the side-on perspective of the CAMP icon would conflict with the front-on perspective of the gradient display led to the development of a similar front-on imminent icon. After several design iterations, Ray Kiefer (General Motors) evaluated a selection of one- and two-stage visual alerts using two paper and pencil questionnaire studies. The first study examined the preferences of a one-stage icon. Nineteen GM participants selected their top three one-stage icons from ten alternatives (which included the CAMP icon). The icon displayed in Figure 7.3 was the most preferred, receiving the most first place votes (12) and the most "top three" votes (17). Based on the results of this study, a set of two-stage sequences was developed, and a second paper and pencil study was conducted to evaluate the two-stage alternatives. Fifteen GM participants selected their top three candidates from nine alternatives. A sequence with a smaller yellow rear-end view of the car followed by the icon displayed in Figure 7.3 was preferred, receiving the most first place votes (6) and most "top three" votes (11). Although the Figure 7.3 icon was preferred in these subjective studies, it should be noted that it is not as friendly as the CAMP icon for industry-wide production implementation (because current industry practice is to use single color visual telltale indicators).

Figure 7.3 The Rear-Perspective Imminent Icon

Because the new imminent icon was of the same perspective as the gradient display, it could be placed at the end of the gradient display sequence. This permitted a more rigorous experimental approach, with displays of a different number of stages all ending with a common icon (see Figure 7.4). The effectiveness of the imminent icon was no longer confounded with number of stages, allowing the observed differences to be more readily attributed to the number of display stages.

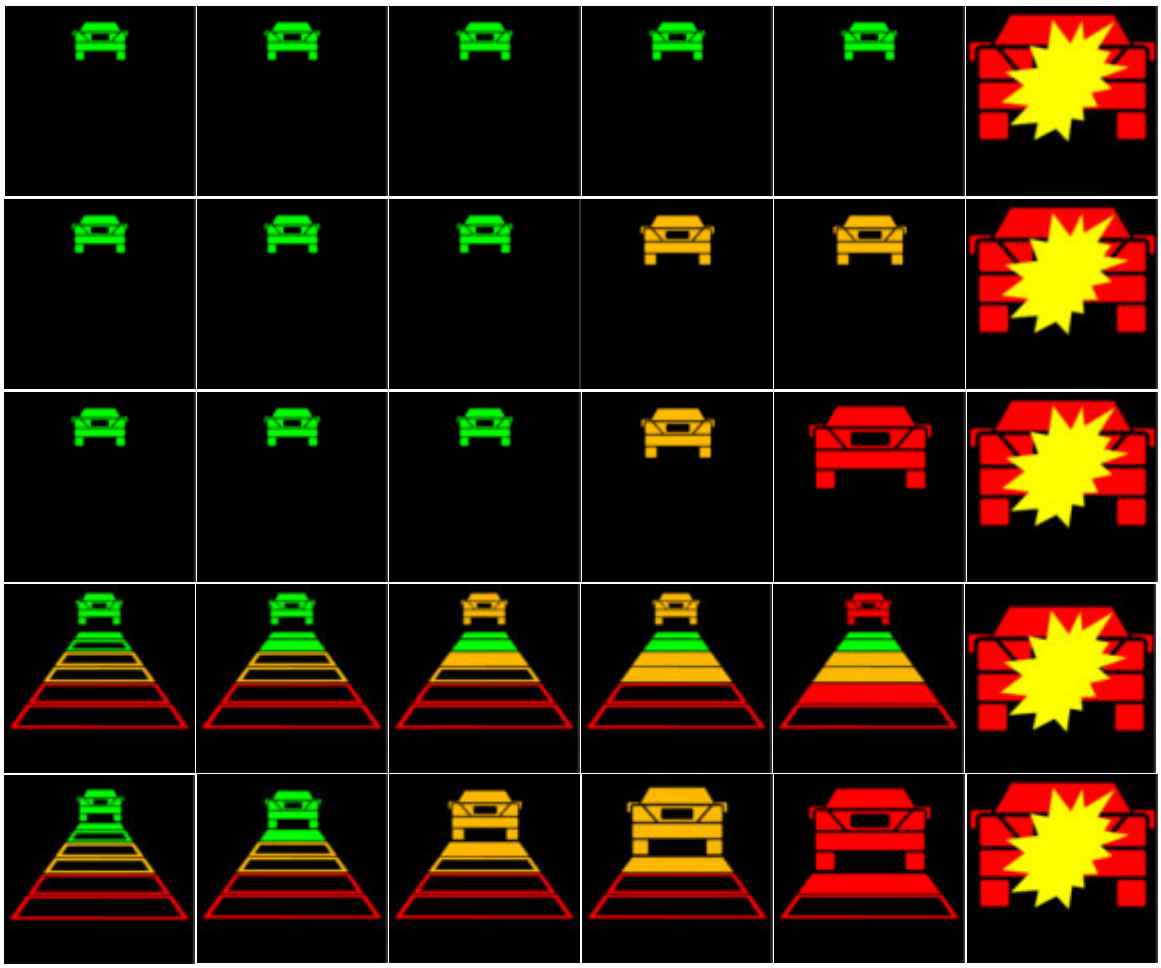

Figure 7.4 Displays as a Function of Alert Level (AL). From the top, the one-stage (1), two-stage (2), three-stage or looming (L), scale (S), and looming-plus-scale (LS) displays used in Experiment 1. The term "looming" is used to refer to the pattern of optical expansion. Note that the looming display was reduced to three warning levels after it was observed that the shape change was insufficient for providing finer distinctions that were discriminable.

The scale display with the expanding vehicle icon (in Figure 7.4) was redesigned to enhance the expansion. Whereas the most salient transformation of the vehicle icon in the original gradient display (Figure 7.1) was downward translation, the new display was designed so that the vehicle icon did not appear to translate downward but rather to expand. This change better approximates the natural pattern of optic flow that a driver would observe when approaching an external object. It has been demonstrated that a wide range of animals, including human infants, display an avoidance response to a quickly expanding pattern of optic flow (Schiff, 1965). This pattern of optical expansion, referred to as "looming" has been demonstrated to play an important role in collision control behavior and is a powerful source of information to specify impending collision (see Smith, Flach, Dittman, & Stanard, 2001). Looming was identified as a promising source of information through which the FCW system could communicate proximity and the new displays (depicted in Figure 7.4) reflect this shift in focus. The term "looming" was used in this application to describe any display with an expanding vehicle with three or more warning stages.

It can be observed that the changes made to the gradient display enhance the looming effects of the display; however, Robert Hogan argued that this was achieved to the detriment of the scale presentation. The earlier version of the gradient display had maintained a persisting backdrop of the six trapezoids, allowing the driver to observe the current state in relation to other less urgent states. In the newer version, the expanding vehicle occludes the trapezoids of the less urgent states. Hogan was concerned that this occlusion could incur a cost in driver response and the question arose: *which is more important, looming or the scale?*

In the Dingus et al. (1997) study, a nine-level bars display (without a vehicle icon), a four-level car icon display (with bars and a vehicle icon—similar to the original gradient display) and a three-level blocks display (with amber and red blocks) were compared on the open road. In their first experiment, Dingus et al. observed that during their braking event both the car icon and bars displays increased headway, however during the coupled headway events only the car icon display produced significantly longer headway. Despite the hint that there could be a potential benefit associated with the vehicle icon, Dingus et al. carried only the bars display forward to the next round of experiments.

In theory, a scale display is more effective than the looming display for precisely communicating a specific value of a dimension, relative to other potential values. The presentation of a scale permits the system to communicate more finely-grained information, allowing a greater number of discriminable display states. A purely looming display, on the other hand, because it lacks a point of reference, cannot communicate a specific value as precisely, and when used in isolation for this particular application, appears to limit the system to displaying four or five discrete system states. However, in the looming display the vehicle expansion is more salient and could potentially yield a benefit in recapturing the attention of a distracted driver. Looming is also expected to be more easily understandable because of its natural association with impending collision. It might be argued, to use an aviation metaphor, that because a driver operates in VFR (visual flight rules) rather than IFR (instrument flight rules), more salient but less precise information may be of more value than the less salient presentation of a precise value. The primary purpose of the FCW display is to draw the driver's attention to a critical event rather than to provide a complete surrogate for the natural optic flow. COMSIS (1996b) advised against presenting graphical information for warning displays because of the limited time for the driver to respond in an urgent situation.

In order to compare the effects of looming with the effects of scale information, new displays were developed for the first experiment. Looming-only and scale-only displays were developed to accompany the looming-plus-scale display (previously referred to as the gradient display). These displays permitted the investigation of the effects of looming, independent of scale, scale independent of looming, and the interaction between scale and looming. The looming-only, scale-only, and looming-plus-scale displays are illustrated in Figure 7.4.

In addition to the alert level icon development, new icons were developed to represent gap and warn settings (see Figure 7.5). These icons were designed to provide more discriminable "ACC-engaged" versus "ACC-disengaged" modes and by removing the text, the gap/warn setting line became more distinct from the set-speed text line. Blocks versus radar-waves were chosen to represent the tighter coupling between vehicles in the "ACC-engaged" versus the "ACC-disengaged" state. The blocks communicate a stronger link between the vehicles (as if they are connected) compared with the purely informational coupling represented by the radar waves. This distinction is redundantly displayed in both shape (blocks vs. radar-waves) and color (cyan vs. light gray) to reduce the likelihood of mode confusion. The absence of the set speed indicator can also be used to communicate the "ACC-disengaged" state.

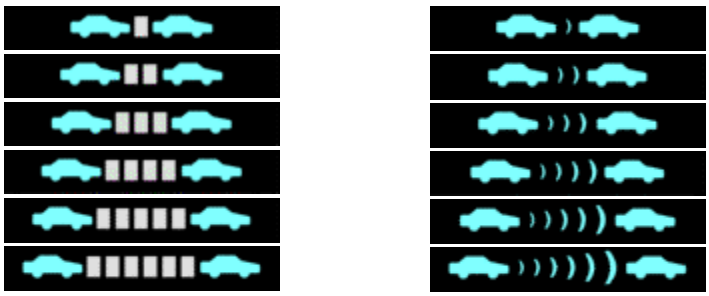

Figure 7.5 Gap/Warn Setting Display. Vehicles closer together represent a closer headway for ACC or a later warning for FCW. Note that the background is black, which appears as transparent on a HUD.

Technical Approach

The first human factors experiment investigated the relative effectiveness of looming versus scale and the potential benefits of an increased number of display stages. A simulator scenario was developed wherein participants followed a speed-varying lead vehicle for 12 min, during which they could interact with the FCW display and would have a tendency of becoming increasingly inattentive due to the constancy of the situation. The lead vehicle would begin from a stop and accelerate at a rate of 0.15 g to reach 50 mph. During the 12-min period that followed, the lead vehicle would intermittently change speed according to an algorithm that was designed to simulate natural traffic flow:

1. If speed is greater than 43 mph, select a random target speed between 41 and 43 mph, else select a random target speed between 42 and 45 mph. Select a random time it takes to reach target speed between 7 and 11 s.
2. When vehicle reaches target speed, select a random dwell time for which to stay at target speed between 1 and 3 s. Repeat the cycle.

The participant would follow the lead vehicle along a mostly-straight two-lane road with no intersections. Most of the road was rural, with a speed limit of 55 mph; however, to prevent excessive repetition of scenery, a short section of industrial scenery (speed limit 45 mph) was included in the middle of the course. As the car-following phase of the trial drew to a close, participants approached a police vehicle that was parked on the left side of the road, facing into the roadway. The police vehicle was used as a decoy, for distracting participant's from the lead vehicle. Timed so as to maximize the visual distraction caused by the police vehicle, the lead vehicle suddenly decelerated at 0.5 g to a complete stop. The car-following scenario provided a measure of time-headway magnitude and variability whereas the sudden braking scenario provided a measure of brake reaction time.

Eighty participants, between the ages of 21 and 64 (M=39.6, SD=9.6), were recruited from Delphi Delco Electronics. In attempt to balance these demographics within each group Participants were assigned to groups as they arrived based on their gender and age. The average age within groups ranged from 36.1 to 41.8. The sixteen female participants were divided evenly into eight groups, resulting in two females and eight males per group. All participants were licensed drivers and had normal or corrected-to-normal vision. The experiment was advertised on the local Delco website and in newsgroups and participants were compensated with a $10 gift certificate to a local restaurant. None of the participants were associated in any other way with the ACAS FOT project, nor had they participated in a collision avoidance study before.

For the purposes of this program, a fixed-base Hyperion simulator was installed at Delphi Delco Electronics in Kokomo. The simulator projected a 1024x768-pixel 50-deg-vertical forward field-of-view image located at the front bumper of the vehicle cab. The vehicle handling system was configured to represent a mid-size front wheel drive sedan, such as a Ford Taurus. Steering feedback was presented with a force-feedback torque motor, to reproduce the feel of the road at the steering wheel, as well as the forces on the front tires during evasive maneuvers. The vehicle cab consists of the front half of a 1995 Pontiac Bonneville exterior (with doors and roof removed), with a 1996 Buick Park Avenue instrument cluster and dashboard. The cab was equipped with a previous generation full-color reconfigurable 2.5x3-deg of visual angle HUD, driven by 230x263-pixel 1.3-inch-diagonal Seiko-Epson cell, which was used for this experiment to display speed and alert-level. The smaller field of view offered by the previous-generation HUD forced the speedometer and alert-level displays to be both slightly smaller and closer together, resulting in a display that appeared similar to that depicted in Figure 7.6. The HUD image was projected at the front bumper of the vehicle, displaying graphics that were generated using Altia software, and the supporting PC platform was linked to the simulator through a local ethernet network. The alert-level display was driven by the GMR2 algorithm, using the current intermediate sensitivity settings of tau = 4 s and Tg = 1.5 s The HUD brightness was preset to an appropriate level for the lighting conditions of the simulator room, and was not adjustable by the participant. A seat-vibration system was added to the cab, to produce pulses of vibration on the seat surface at a rate of 4-Hz using a pair of 3-V DC motors with offset counterbalances. Speakers were placed in the engine compartment of the cab directly in front of the driver and the volume was set to play the alert tone at 72 dBA.

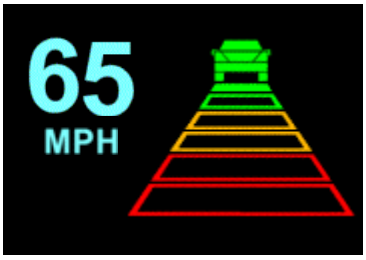

Figure 7.6 Relative Size and Position of the HUD Images in the Delco Driving Simulator. The alert-level indicator subtended a visual angle of approximately 1.5 x 2-deg of visual angle.

A single-factor between-subjects experimental design was developed to examine the effects of the FCW display on headway maintenance (mean and variability) during the car-following phase and brake reaction time during the sudden braking event. Ten participants were assigned to each of the following eight levels of FCW display type:

C-- Control (No display)
1--One-stage (no audio)
2--Two-stage (no audio)
L-- Looming (no audio)
S-- Scale (no audio)
LS-- Looming-plus-scale (no audio)
LA-- Looming and Audio (CAMP #8 tone at the imminent stage)
LAV-- Looming, Audio, and Seat Vibration (CAMP #8 tone and seat-vibration at the imminent stage)

The eight levels permitted the evaluation of several effects: number of stages (C, 1, 2, L, and LS), looming (L vs. C), scale (S vs. C), the interaction of looming with scale (C, L, S, and LS), audio (LA vs. L), and seat-vibration (LAV vs. LA).
During the steady-state car-following phase of the experiment, time-headway and time-headway-variance were measured as dependent variables. Whereas time-headway-mean provided a measure of how close the driver was willing to travel to the lead vehicle, time-headway-variance provided a measure of how accurately participants could maintain constant time-headway during the trial.

After the onset of the 0.5-g lead-vehicle deceleration maneuver, brake reaction time (BRT) and required deceleration were measured as dependent variables. To ensure that it was the driver's response to the sudden braking event being measured, rather than routine speed or headway maintenance, BRT and required deceleration measured the driver response at the moment the brake was depressed by at least 50 percent. BRT was measured as the time between the deceleration maneuver and the 50-percent braking response. Whereas drivers routinely elicited small brake depressions throughout the car-following period, they only depressed the brake by 50 percent in response to the severe lead-vehicle deceleration event. Furthermore, five participants were already depressing the brake pedal by a small amount before the lead vehicle began the 0.5-g maneuver.

Using a conventional BRT measure would have resulted in five missing values. The average control-group participant released the accelerator pedal 1.94 s after the 0.5-g maneuver began, contacted the brake pedal 0.41 s later, and 0.87 s later had depressed the brake pedal by 50 percent.

After completing an informed consent form, participants were (falsely) informed that "the purpose of this exercise is to collect some driving data in order to calibrate various aspects of the simulator, and to get Delco employees to evaluate its realism." This ruse was similar to that used by John Lee (personal communication, 2001). Participants were subsequently briefed on how to operate the vehicle, and how to adjust the seat and HUD position. After participants were shown the HUD, they were instructed:

> *The head-up display will be used to present speedometer information to you as you drive. To the right of this, and still on the head-up display, it is possible that you may see some car-following information. This comes from an old experiment before we had the simulator upgraded. It presents the driver with information regarding proximity to the lead vehicle. If this information appears and you find it helpful, feel free to use it.*

These instructions were designed to prevent participants from paying an unrealistic amount of attention to the FCW display and anticipating a lead-vehicle collision event. By informing participants that the display was peripheral to the purposes of the experiment, it was expected that participants would better approximate someone accustomed to driving with an FCW display. Participants who considered the display to be peripheral would be more likely to pay attention to the extent that it was useful, and ignore it to the extent that it was not. On the other hand, if participants had been informed that the purpose of the study was to evaluate the FCW display, they would likely apply a disproportionate amount of attention toward the display and might expect the lead vehicle to suddenly brake at any moment. To provide an alternative explanation for the purpose of the study and to maximally distract the driver with the surrounding scenery, the following passage was read to participants:

> *You will begin parked behind a stationary car. In order to evaluate the realism as you drive, pay attention to the feel of your vehicle and oncoming traffic, and in particular, pay attention to see if there are any anomalies in the surrounding scenery (like trees and houses etc). I will ask you some questions about this when you complete your driving. When I put you in drive, the car in front of you will begin to move. Do not overtake but make sure you keep up with traffic. Drive as you normally would if you were trying to get somewhere in a reasonable time. Try to travel at least as fast as the speed limit wherever you can, so keep an eye out for speed-limit signs along the roadside. After you have been driving for about 15 minutes I will come back to get you.*

The emphasis on keeping up and trying to travel at the speed limit was added after it was observed in pilot testing that several participants failed to keep up with the lead vehicle and reached time headway in excess of 10 s. Driving in the simulator differs from driving in the real world in that there is no intrinsic desire to reach a destination. The instructions to "keep up", "travel at least as fast as the speed limit", and "drive as you normally would if you were trying to get somewhere in a reasonable time" were designed to provide a surrogate for the natural desire to reach a destination in a timely fashion. Upon completion of the trial, participants were debriefed on the true purpose of the experiment asked not to discuss the details of the experiment with others until the end of May. Participants then answered a series of questions that they viewed through a Powerpoint presentation. The questionnaire queried participants on which aspects of the display they noticed and what did the imminent icon mean. It also asked participants to rate the display that they had experienced according to how much they agreed that they display was:

1. "A good method for presenting car-following and collision-warning information"
2. Detectable
3. Understandable
4. Startling
5. Interfering
6. Attention-getting
7. Annoying

Because participants only experienced a single display, these responses were absolute judgments because they had no explicit basis of comparison. To examine relative comparisons between displays, participants were exposed to a range of different visual displays, iterating through the different stages of the displays in a Powerpoint presentation so that they could experience them dynamically. The displays included 1, 2, L, S, LS, and an expanding line display (Li) that was similar to the looming display except that rather than using a vehicle icon, the display was an expanding horizontal line. This display was added in response to a NHTSA suggestion to include a display that could mimic a set of expanding brake lights. Displays were ranked from most to least according to the extent that they were:

1. Preferred
2. Discriminable
3. Understandable
4. Startling
5. Interfering
6. Attention-getting
7. Annoying

In the first human factors experiment, the scale display provided no evidence for any benefit to the driver and made the display overly annoying. The objective and subjective results of the first experiment combined to provide sufficient basis for rejecting the scale display. Due to poor subjective rankings, the line display was also removed from consideration. The one-stage display failed to provide evidence for any performance benefit, however, because of its simplicity and because the CAMP (1999) program has invested so much towards a one-stage display (and did reveal a BRT benefit), the one-stage display was included in the second experiment.

After the first experiment, the looming display appeared to be the most effective candidate, balancing good performance with high driver acceptance. The purpose of the second human factors experiment was to better evaluate driver acceptance of the remaining displays (one-stage, two-stage, looming, and looming-plus-scale), therefore focusing on questionnaire responses rather than performance data. Unlike the first human factors experiment, in the second experiment participants drove through the simulator scenario with each level of display type, so they were able to more accurately evaluate the different display alternatives. Participants were instructed that their task was to evaluate the different display types. The simulated scenario was similar to that of first human factors experiment except that each trial lasted for only 4 min, and drivers were instructed to drive so as to evaluate the display. In addition to this, the lead vehicle's behavior was programmed to be more erratic, following a similar algorithm to the lead vehicle of first human factors experiment, except that the speed varied between 35 and 55 mph.

This experiment was also designed to evaluate the effect of the number of false alarms on driver acceptance of the different displays and to examine whether the displays differed in their resistance to the annoyance or reduced trust caused by false alarms. False alarms will be defined here as an imminent alert level activation that is unrelated to the presence of a relevant vehicle. In the real FCW system, false alarms could be caused by radar returns from bridges or signs, however, in this experiment false alarms were generated as randomly occurring 0.5-s activations of the imminent alert.
Twelve participants, between the ages of 24 and 60 ($\underline{M}$=40.75, $\underline{SD}$=12.33), were recruited from the same subject pool that was used in the first human factors experiment. The apparatus was the same as that used in the first human factors experiment.

A 3 (Number-of-false-alarms) x 4 (Display type) repeated-measures factorial design was developed. Participants experienced each of the following displays:

1— One-stage (audio and seat-vibration)
2— Two-stage (audio and seat-vibration)
L— Looming (audio and seat-vibration)
LS— Looming-plus-scale (audio and seat-vibration)

The combination of number-of-false-alarms and display type created twelve unique trials. Participants completed three trials of each display type with zero, one, and two false alarms (in that order) and the order of display type was counterbalanced using a Latin Square. No performance variables were measured because participants were instructed in the following way:

> *Drive as you normally would, however, make sure that you interact with the different displays that you are experiencing to a sufficient extent that you can make informed comparisons between them. As you drive, try to evaluate the display in terms of how annoying or distracting it is, how reliable it is, and how much you like the display.*

Because the emphasis of the instructions was on evaluating the display rather than driving normally, the driving performance may have been somewhat abnormal, rendering performance measures less reliable. The dependent measures consisted of the participants' responses to questionnaire items, which were administered after each trial (absolute judgments) and responses to a questionnaire that was administered after participants had completed all twelve trials (relative comparisons).

After experiencing the CAMP auditory tone in the GM Engineering Development Vehicle and in the Delco Driving Simulator, it was agreed upon by the human factors group that the CAMP tone was overly annoying and that a less annoying alternative should be used. A half-second tone using a double sequence of 2500-Hz and 2650-Hz pulses was created and substituted for the CAMP tone. The imminent level icon was accompanied by the new tone at 72 dBA and seat-vibration for all display types.

Intermediate and Final Results

The following is a discussion of the results from the first human factors experiment. Time-headway and time-headway-variance were recorded during the period of time between 2 min after the participant began the trial until the onset of the 0.5-g deceleration maneuver. The average time-headway-mean across all participants was 1.61 s with a standard deviation of 0.49 s. A single-factor between-group analysis of covariance (ANOVA) was conducted using time-headway as the dependent measure. The effect of display on time-headway failed to reach statistical significance, $F(7, 72) = 0.533$, $p = 0.807$. The average time-headway-variance across all participants was 545 ms^2 with a standard deviation of 345 ms^2. Like time-headway, time-headway-variance also failed to reach statistical significance, $F(7, 72) = 1.209$, $p = 0.309$. No measurable displays effects were observed during the steady-state car-following phase of this experiment. Although there were no observable effects of display type on car-following performance, a large amount of variation in time-headway was present at the onset of the lead-vehicle deceleration maneuver ($\underline{M} = 1.648$ s, $\underline{SD} = 0.794$ s). This time-headway variance presented serious implications for the severity of the event to which drivers reacted. If the driver had a large time-headway at the deceleration onset (e.g., greater than 3 s) then the 0.5-g maneuver was not particularly threatening, and the driver could safely wait several seconds before reacting to the situation. On the other hand, a driver with a small time-headway (e.g., less than half a second) at the deceleration event would be required to respond almost immediately in order to avoid collision. As expected, time-headway at the deceleration event was highly correlated with BRT ($r = 0.847$), implying that over 68 percent of the variance in BRT could be accounted for by the time-headway at the deceleration event. If an ANOVA did not take into account the influence of time-headway, the amount of error variance introduced by the time-headway would make it exceedingly difficult to detect differences between displays.

In order to attribute the variance to the appropriate source (time-headway) rather than to error, an ANCOVA was performed on each of the dependent measures. Given that time-headway at the event onset (THEO) was unrelated to display type; $F(7,79) = 1.97$, $p = 0.316$, THEO could be included in the model as a random covariate.

Display type significantly affected BRT, $F(7,79) = 4.675$, $p < 0.0005$, and required deceleration, $F(7,79) = 2.797$, $p < 0.05$. LSD pairwise comparisons revealed that, compared with the control condition, all displays resulted in a statistically significant benefit across both performance measures, except for the one-stage and scale displays. BRT values and required decelerations (evaluated at the THEO mean value) are plotted as a function of display type in Figures 7.7 and 7.8 respectively.

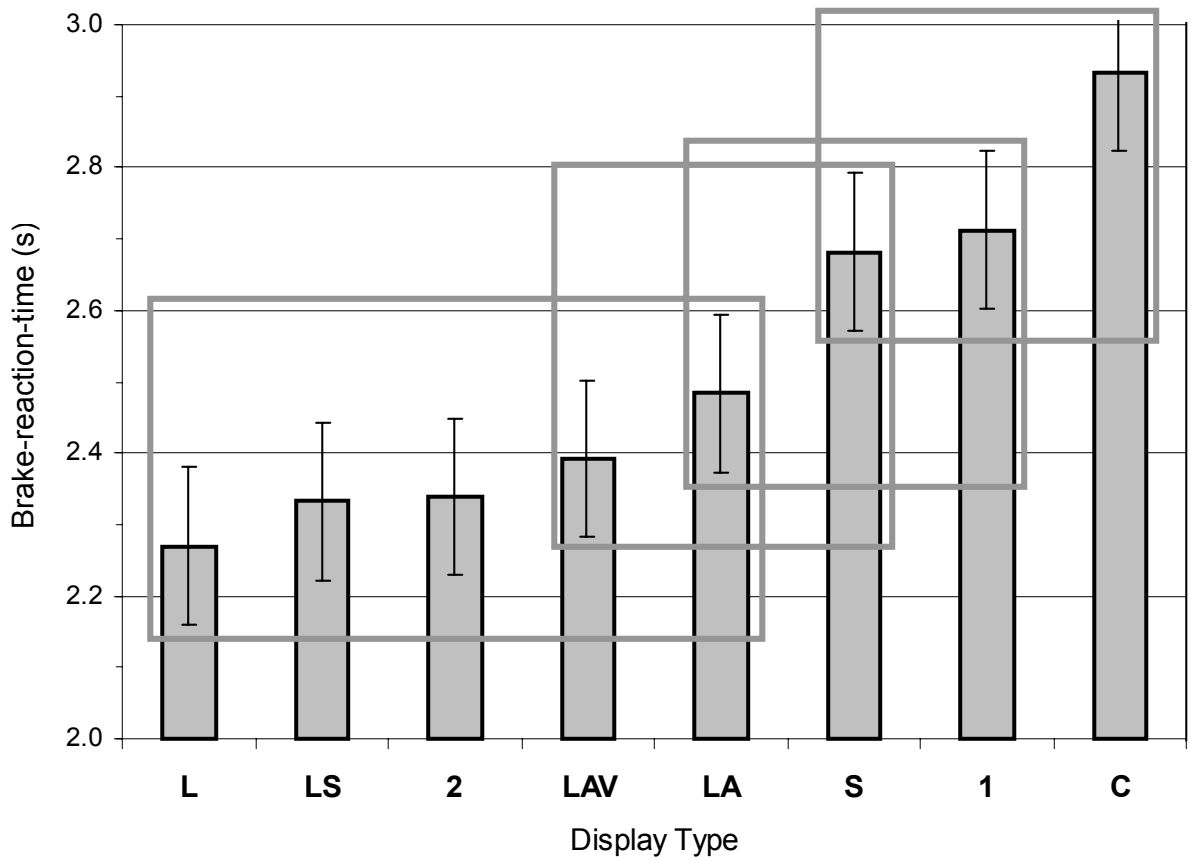

Figure 7.7 Brake Reaction Time as a Function of Display Type. The error bars represent plus or minus one standard error of the mean. The gray boxes represent groups of displays that are not statistically different, according to LSD pairwise comparisons using an alpha level of 0.05. If one display does not co-occur with another display in any of the boxes, then the two displays are statistically distinct. For example, L, LS, and 2 are statistically different from S, 1, and C, however 2 is not statistically different from LAV because they co-occur in the first box.

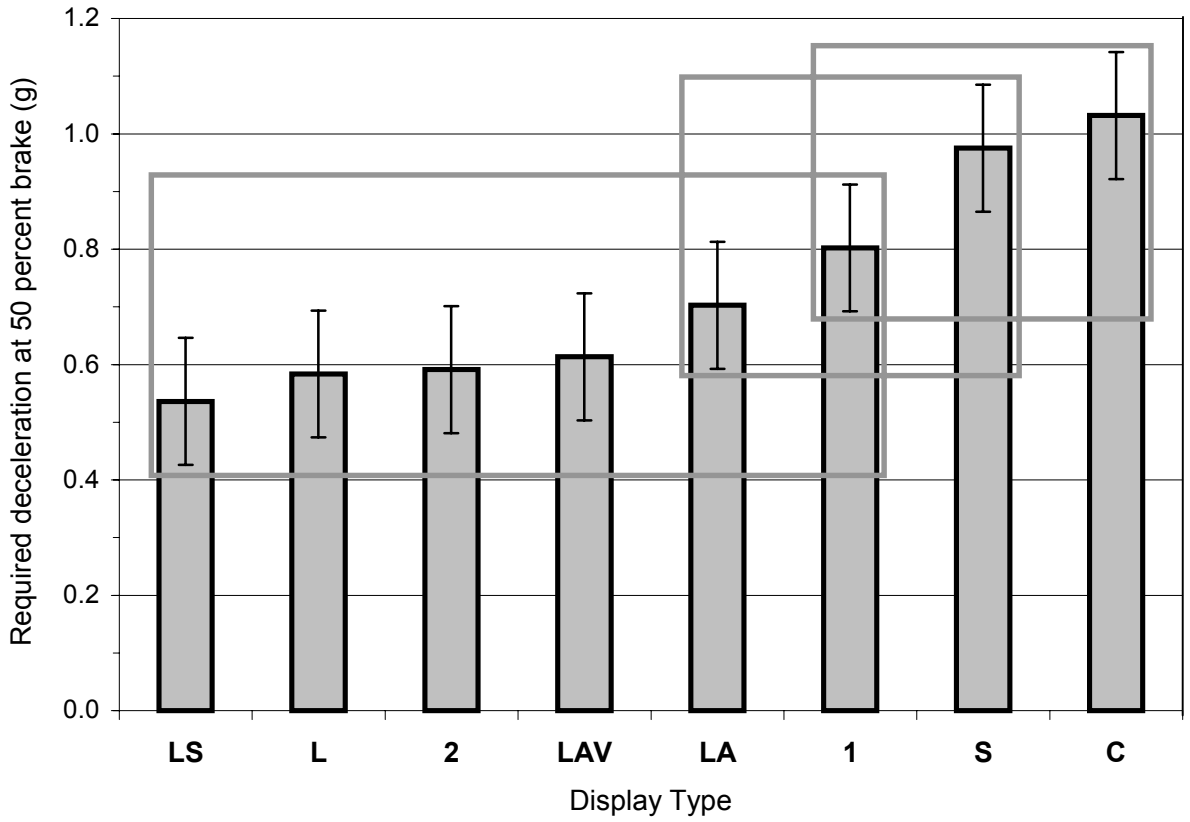

Figure 7.8 Required Deceleration at 50 Percent Braking Response as a Function of Display Type. The error bars represent plus or minus one standard error of the mean. The gray boxes represent groups of displays that are not statistically different, according to LSD pairwise comparisons using an alpha level of 0.05. If one display does not co-occur with another display in any of the boxes, then the two displays are statistically distinct.

A single-factor between-subjects ANOVA was conducted on the responses to questionnaire items that asked participants to rate the displays that they had experienced in the simulator. Table 7.2 presents the responses to the items as a function of display type. There were significant display-type effects for the items corresponding with **understandability** [*This method could clearly tell me that I am in danger and need to react immediately,* $F(6,63) = 4.722$, $p < 0.0001$] and **attention-getting** [*This method would get my attention effectively if I was distracted and not concentrating on the driving task*, $F(6,63) = 3.96$, p M 0.005]. LSD post-hoc comparisons, with an alpha level of 0.05, revealed that the scale display was less understandable than all but the one-stage and the looming-plus-scale displays, and that the looming-plus-scale was less understandable than all but the scale display. Post-hoc comparisons also revealed that the two displays with audio (LA and LAV) were more attention-getting than the looming, scale, and looming-plus-scale displays, and that the one- and two-stage displays were more attention-getting than the scale display.

Table 7.2 Responses to Absolute-Judgments Questionnaires as a Function of Display Types. Participants rated the extent to which they agreed with the above statements on a scale from 1 to 6, corresponding to strongly disagree, moderately disagree, perhaps disagree, perhaps agree, moderately agree, and strongly agree.

Questionnaire Item	1	2	L	S	LS	LA	LAV	M	SD
This is a good method for presenting car-following and collision-warning information to drivers.	4.56	5.00	4.90	4.00	4.40	5.10	5.00	**4.71**	*1.16*
Using this method, changes of display-state would be clearly detectable.	4.33	4.50	5.00	3.70	4.10	4.80	4.90	**4.48**	*1.28*
This method could clearly tell me that I am in danger and need to react immediately.	4.56	5.30	5.20	3.70	3.60	5.20	5.00	**4.65**	*1.21*
This method would NOT startle me, that is, cause me to blink, jump, or make a rapid reflex-like movement.	4.22	4.30	4.80	4.60	4.80	4.30	5.00	**4.57**	*1.43*
This method would NOT interfere with my ability to make a quick and accurate decision about the safest driving action to take (brake, steer, brake and steer, do nothing).	4.56	4.70	4.90	5.10	4.60	4.90	5.20	**4.85**	*1.07*
This method would get my attention effectively if I was distracted and not concentrating on the driving task.	4.44	4.20	4.00	3.00	3.70	5.30	5.20	**4.26**	*1.45*
This method would be annoying.	2.78	1.80	2.00	2.80	2.20	2.30	2.30	**2.31**	*1.16*

Out of the twenty participants who experienced the auditory tone with the alert, 70 percent indicated that they noticed it, compared with 8 percent who indicated that they noticed a tone when no tone was actually present (out of 50 participants). The seat-vibration was detected less frequently-- only 20 percent of the ten participants in the seat-vibration condition indicated that they detected its presence, compared with 6.67 percent of the 60 participants who did not experience the seat-vibration.

Friedman χ^2 tests were conducted on the ranking data for each of the subjective measures. There were significant main effects of display type for each measure: preference [$\chi^2(5) = 216.67$, $p < 0.0001$], discriminability [$\chi^2(5) = 192.79$, $p < 0.0001$], understandability [$\chi^2(5) = 216.96$, $p < 0.0001$], startle [$\chi^2(5) = 121.21$, $p < 0.0001$], interference [$\chi^2(5) = 48.39$, $p < 0.0001$], attention-getting [$\chi^2(5) = 181.73$, $p < 0.0001$], and annoyance [$\chi^2(5) = 80.54$, $p < 0.0001$]. The relative rank scores for each measure (except startle) are displayed in Figure 7.9. The results for the startle measure are not displayed because the only observed difference was that the Line display was ranked as being less startling than the other displays. The Line display was consistently ranked last on every measure, whether desirable or undesirable.

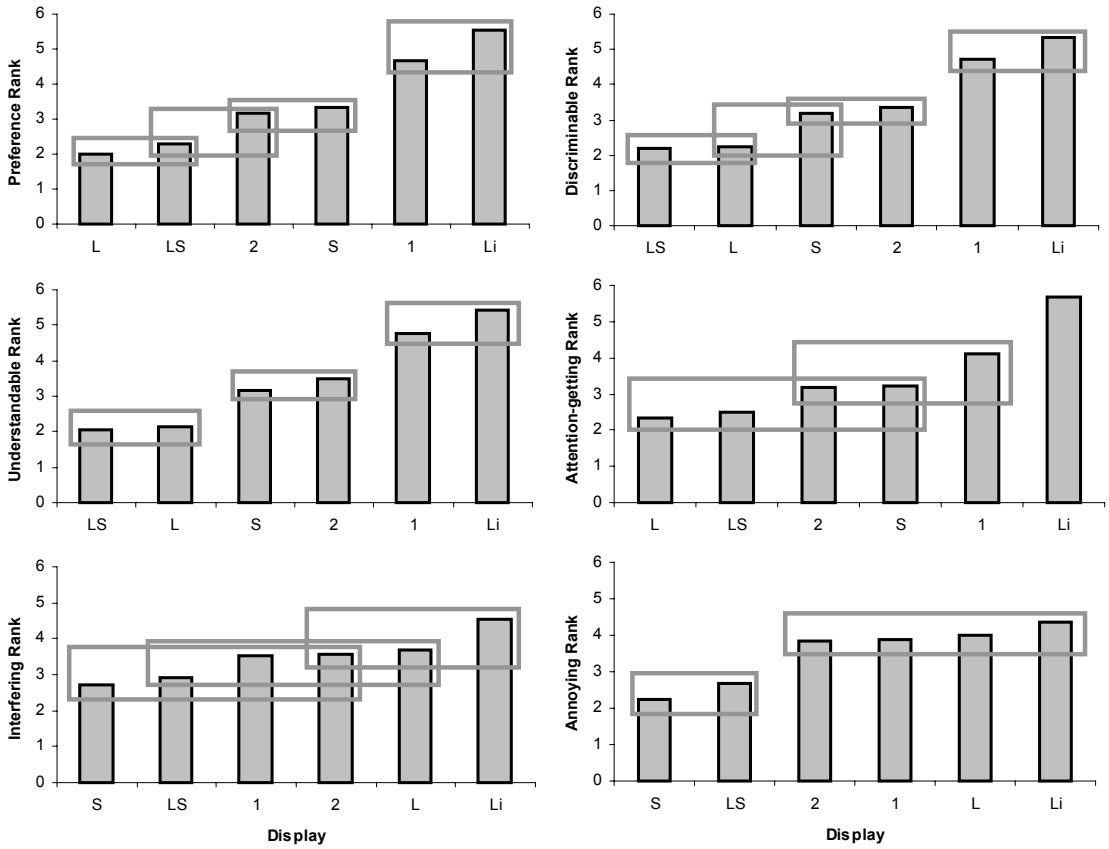

Figure 7.9 Participant Rankings of Displays. Participants ranked the displays for preference, discriminability, understandability, attention-getting, interference, and annoyance, in order from most to least, so that lower numbers indicate that participants consider the display to be more representative of the given measure. The gray boxes represent groups of displays that are not statistically different, according to Nemenyi'a procedure for post-hoc comparisons (using an alpha level of 0.05.) If one display does not co-occur with another display in any of the boxes, then the two displays are statistically distinct.

The variables of looming and scale can be considered as separate factors, allowing the independent manipulation of each factor into the four factorial combinations: C (without looming or scale), S (scale without looming), L (looming without scale), and LS (looming plus scale). In terms of brake reaction performance, L and LS are statistically equivalent, but different from C and S, which are also statistically equivalent. This implies that adding scale to either no display or a looming display yields no performance benefit. There were no observable performance effects of scale, nor was there an interaction between scale and looming. The differences between these four conditions can be entirely accounted for by the effects of looming. In short, the looming display reduced BRTs and required-deceleration, whether it was accompanied by the scale or not.

However, there is some evidence of a driver-acceptance cost of the scale. In the absolute judgments, the two displays with the scale were rated as less understandable than the looming display. Strangely, this effect was not reiterated in the relative rankings, where the looming display and the looming-plus-scale displays were similarly ranked. This may have occurred because participants in the scale conditions (LS and S), faced with

graphics of higher complexity, may have felt like there was more information being communicated to them than the other participants, and thus more room for confusion. However, when participants had viewed all of the displays, they may have believed that the displays were communicating the same basic concepts, and the additional complexity of the scale may have helped to clarify the meaning of the display. In addition to this, by the time participants began answering the relative rankings questions, they had more opportunity to learn the meaning of the displays through the preceding questions. The learning process may have clarified the meaning of the graphics to a greater extent for the more complex displays.

The looming and looming-plus-scale displays were consistently ranked as being more with respect to the desirable dimensions (where more of the variable implies better). They were preferred to the scale, one-stage, and line displays, considered to be more discriminable than the one-stage, two-stage and line displays, more understandable than the scale, one-stage, two-stage, and line displays, and more attention-getting than the one-stage and line displays. The inclusion of a scale, however, appeared to have a negative effect on the undesirable dimensions (where more implies worse). The scale display was considered to be more interfering than the looming and line displays, and more annoying than the one-stage, two-stage, looming and line displays. The looming-plus-scale display was also considered to be more annoying than the one-stage, two-stage, looming and line displays.

There is little evidence that the consistent scale provides any added benefit to either performance or driver-acceptance; however, there is evidence to suggest that the addition of a scale increases driver annoyance.

The experimental design included displays of one, two, and three stages (C, 1, 2, and L). Note that the "vehicle detected" icon was not considered to be a stage because it does not represent a warning per se. Performance data revealed little additional benefit after the display contains at least two stages. There was no statistical basis to differentiate the displays with two or three stages, but both displays decreased BRT more than the one-stage and control conditions. The subjective data mirror this, with similar ratings for the displays with two and three stages. The looming display, however, was ranked as being more preferred, more discriminable, and more understandable than the two-stage display. Both the looming and two-stage were ranked as being more preferred, more discriminable, and more understandable than the one-stage display and the looming display was ranked as being more attention-getting than the one-stage display. There were no observed benefits of having a one-stage display over a two-stage or looming display. Although there may be no brake reaction benefit of increasing the number of display stages beyond two, there may be some subjective benefits of having a greater number of stages. Increasing the number of stages beyond three appears to require a display that is more graphical in nature, such as the scale or looming-plus-scale display, and therefore three may be the upper limit for a simplistic display that uses only size change and color coding.

There was no evidence that the auditory tone or the seat-vibration decreased driver reaction time. Numerically, the reaction times with the inclusion of auditory tone or seat-vibration were actually larger, although the difference was not statistically significant. This result may have occurred because of limitations of the simulator. Because the field of view of the simulator was only 50 degrees and there were no visual distractions outside of this area, it is likely that all participants were able to detect the change occurring on the HUD. If this is correct and all participants were sufficiently oriented toward the primary visual display, the auditory tone and seat-vibration were redundant. Without any requirement for their presence, the auditory tone and seat-vibration could have even slightly increased reaction time by startling the driver and providing additional unnecessary stimulation. Although the HUD is an effective means of alerting the driver, in reality there are likely to be many instances where the driver's attention is oriented too far away from the HUD eye-box for the driver to detect a warning, requiring an additional means of alerting the driver. Both the auditory tone and seat-vibration fulfill these criteria because they do not require that the driver be oriented in any direction (COMSIS, 1996b). For this reason, these additional sensory modes cannot be eliminated. Although only fourteen of the twenty participants who experienced the auditory tone during the imminent stages indicated that they detected the tone, the tone did significantly increase attention-getting ratings.

Surprisingly, only two out of the ten participants experiencing seat-vibration indicated that they detected its presence. This rate of detection is especially low given that four participants (of 60) who did not experience the seat-vibration also indicated that they detected it. This was not expected because the seat-vibration had previously seemed to be detectable to the engineers who were involved in its creation. One explanation for the low rate of detection may be that the visual (flashing imminent icon and braking vehicle) and auditory stimuli perceptually masked the vibrating seat, especially because participants were not expecting it and were unaware that the seat was capable of vibrating. If the auditory stimuli had been removed and participants were aware that the vehicle was equipped with a seat-vibration system, it is likely that detection rates may have been far greater. However, the fact that it was difficult to detect may indicate that seat-vibration is not an effective means of alerting a driver.

The following is a discussion of the results from the second human factors experiment. After the second experiment data were collected, it was observed that the age of participants was an important factor in determining their responses. Post hoc, participants were divided into three age groups: younger (24, 25, and 28 years old), middle (34, 38, 38, 38, 45, and 46 years old), and older (56, 57, and 60 years old). Age group, number-of-false-alarms, and display-type were entered as independent variables into a general linear model (GLM) analysis, and the responses to the absolute-judgments questionnaire were entered as the dependent measures.

For the responses to the item "*This display would assist me in avoiding collisions with the lead vehicle*" (Avoidance rating), there was a significant interaction between number-of-false-alarms and age group, $F(2,20) = 4.088$, $p < 0.05$. The interaction is plotted in Figure 7.10. It appears that although younger participants were more approving of the displays in general, they appeared to be less tolerant of false alarms, because their responses to the avoidance item declined as number-of-false-alarms increased.

Surprisingly, this was the only statistically significant effect of number-of-false-alarms for any dependent measure that emerged from the analysis. There were no main effects of number-of-false-alarms.

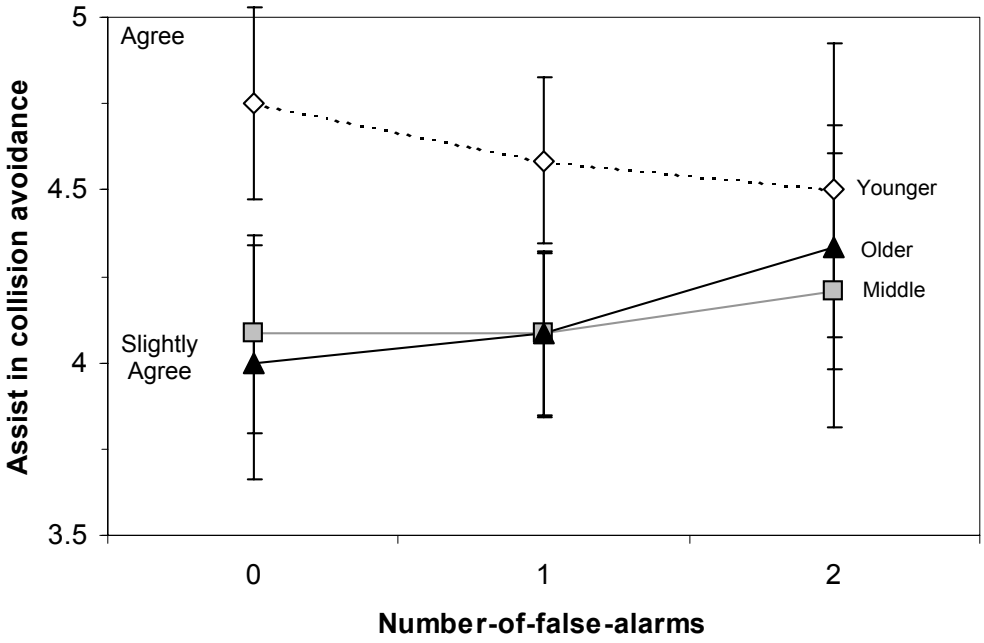

Figure 7.10 Avoidance Rating as a Function of Number-of-False-Alarms for Each Age Group. Error bars represent plus or minus one standard error of the mean.

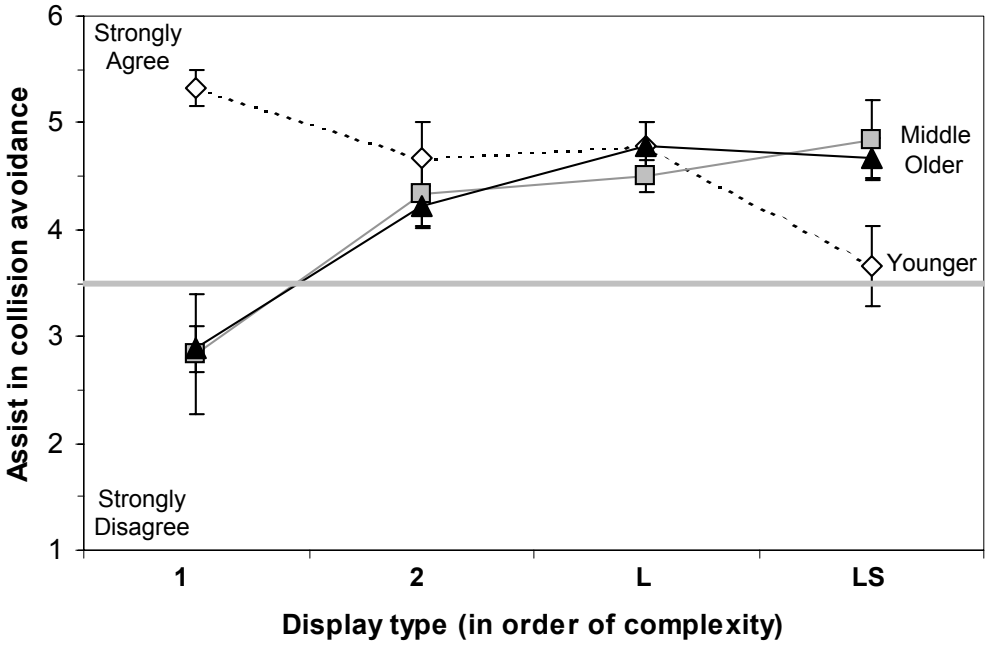

Figure 7.11 Avoidance Rating as a Function of Display Type for Each Age Group. Error bars represent plus or minus one standard error of the mean. The horizontal gray line represents the boundary between agreement and disagreement for the questionnaire item.

The significant interaction between age group and display type for the Avoidance rating dependent variable, $F(3,30) = 2.968$, $p < 0.05$, is displayed in Figure 7.11. Whereas Middle and Older group Avoidance ratings tended to increase as a function of display complexity, this trend was reversed for the Younger group. There was no main effect of display type for the Avoidance rating.

Figure 7.12 displays the significant interaction between age group and display type for the responses to the item "*This display is overly annoying*" (Annoyance rating), $F(3,30) = 3.390$, $p < 0.05$. Younger and middle age groups indicated that the displays became increasingly annoying as the display complexity increased, whereas the older group appeared to be less affected by the increase in display complexity. The main effect of display type was also significant for Annoyance rating, $F(3,30) = 7.414$, $p < 0.001$. Posthoc LSD tests revealed that the looming-plus-scale display was rated as more annoying than the one-stage, two-stage, and looming displays and that the looming display was rated as more annoying than the one-stage display.

Figure 7.13 displays the significant interaction between age group and display type for the responses to item "*I would buy this warning system for my vehicle if it were reasonably priced*" (Buy rating), $F(3,30) = 4.472$, $p < 0.05$. Unlike the younger group, the middle and older groups appeared to be resistant to buying a system with the one-stage display. Unlike the older group, the younger and middle groups appeared to be resistant to buying a system with the looming-plus-scale display. The main effect of display type was also significant for Buy rating, $F(3,30) = 4.650$, $p < 0.01$. Posthoc LSD tests revealed that participants would be more likely to buy a system with the looming display than the one-stage or looming-plus-scale displays.

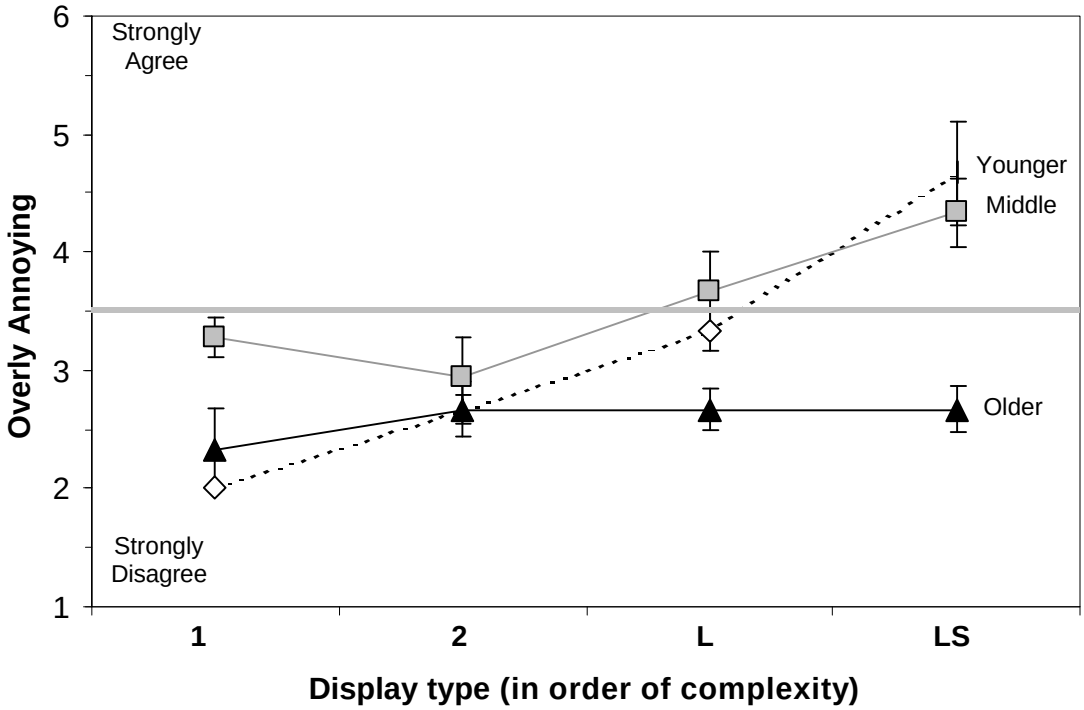

Figure 7.12 Annoyance Rating as a Function of Display Type for Each Age Group. Error bars represent plus or minus one standard error of the mean. The horizontal gray line represents the boundary between agreement and disagreement for the item.

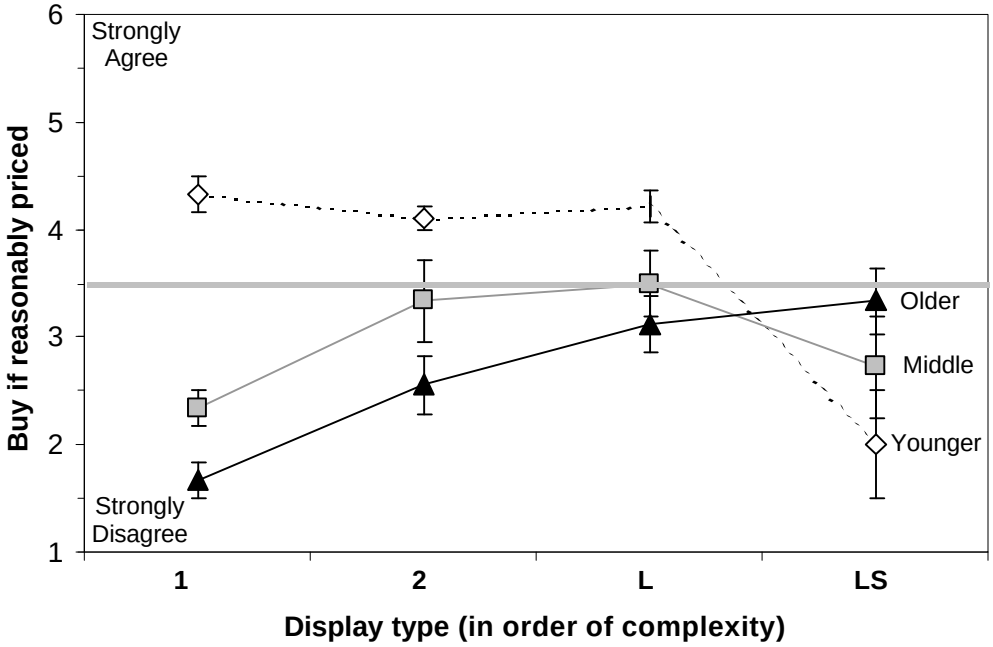

Figure 7.13 Buy Rating as a Function of Display Type for Each Age Group. Error bars represent plus or minus one standard error of the mean. The horizontal gray line represents the boundary between agreement and disagreement for the questionnaire item.

Figure 7.14 displays the significant interaction between age group and display type for the responses to item "*This display would assist me in the task of maintaining safe headway*" (Headway rating), $F(3,30) = 3.568$, $p < 0.05$. Whereas Middle and Older group Headway ratings tended to increase as a function of display complexity, this trend was reversed for the Younger group. There was no main effect of display type for Headway rating.

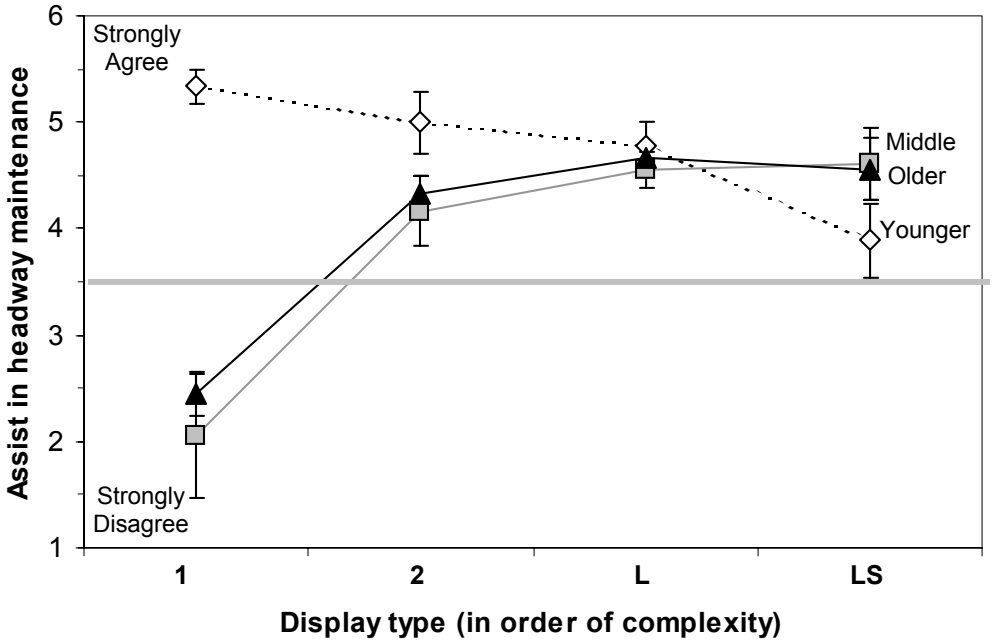

Figure 7.14 Headway Rating as a Function of Display Type for Each Age Group. Error bars represent plus or minus one standard error of the mean. The horizontal gray line represents the boundary between agreement and disagreement for the questionnaire item.

Although the interaction between age group and display type for the response to the item "*This system would distract me from the driving task*" (Distraction rating) was not significant, a significant main effect of display type was observed for Distraction rating, $F(3,30) = 4.648$, $p < 0.01$. Posthoc LSD tests revealed that participants rated the looming-plus-scale display ($\underline{M} = 3.667$, $\underline{SD} = 0.629$) as more distracting than the one-stage ($\underline{M} = 2.611$, $\underline{SD} = 0.465$), two-stage ($\underline{M} = 2.889$, $\underline{SD} = 0.474$), and looming displays ($\underline{M} = 3.028$, $\underline{SD} = 0.448$).

Friedman χ^2 tests were conducted on the rank data for each of the subjective measures. There were significant main effects of display type for annoyance [$\chi^2(3) = 10.90$, $p < 0.02$], distraction [$\chi^2(3) = 20.70$, $p < 0.0005$], attention-getting [$\chi^2(3) = 11.10$, $p < 0.02$], and understandability [$\chi^2(3) = 9.90$, $p < 0.02$]. The effect of preference approached significance [$\chi^2(3) = 7.00$, $p < 0.1$]. The rank scores for each measure are displayed in Figure 7.15. Nemenyi's post-hoc procedure revealed the following significant comparisons:

1. The looming-plus-scale display was more annoying than the one- and two-stage displays
2. The looming-plus-scale display was more distracting than one- and two-stage displays
3. The looming display was more distracting than the one-stage display
4. The looming display was more attention-getting than the one- and two-stage displays.
5. The looming and looming-plus-scale displays were more understandable than one-stage display.
6. The looming display was more preferred than the one-stage display

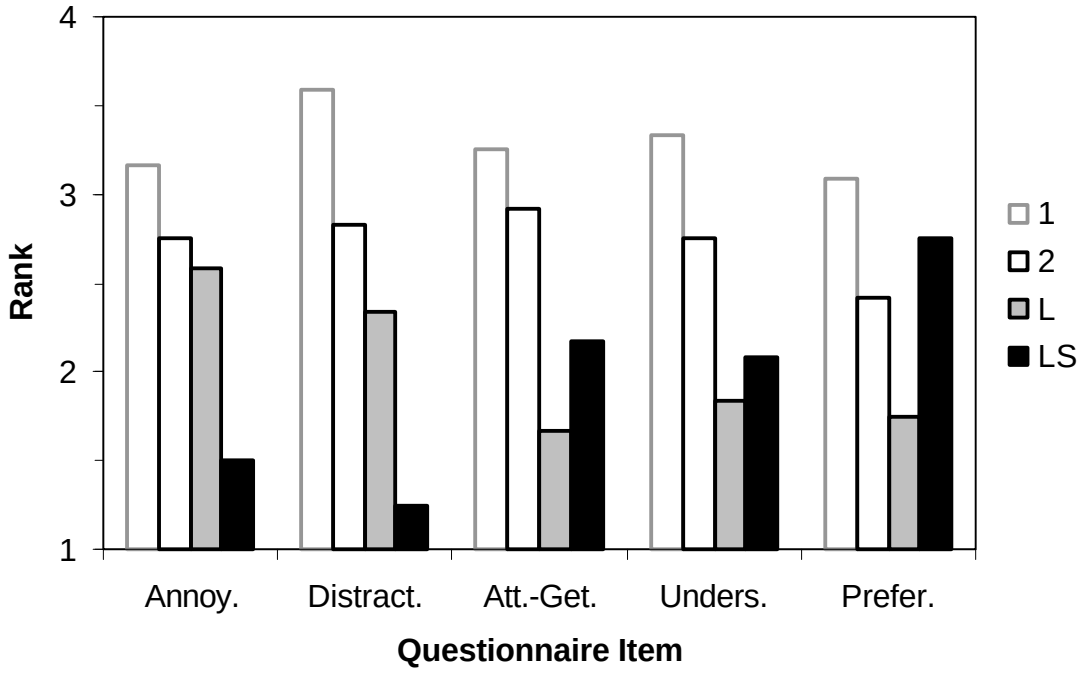

Figure 7.15 Mean Rank as a Function of Display Type. The four displays were ranked from most (1) to least (4) for the items annoyance, distraction, attention-getting, understandability, and preference. A lower score indicates that participants rated the display as being more representative of the given dimension, whether desirable or undesirable.

When participants were asked to rate the urgency of the display tone from 1 (far too urgent) to 6 (not nearly urgent enough) the mean response was 3.58 (SD = 0.67), where a score of 3.5 would have indicated no bias towards too urgent or not urgent enough. Participants were also asked to rate the timing of the transition between display levels from 1 (far too early) to 6 (far too late). The mean response was 3.42 (SD = 0.90), compared with a score of 3.5 that would have indicated no bias.

Participants were asked to respond to a series of questionnaire items addressing the effectiveness of the seat-vibration as an alerting stimulus. When asked whether they noticed the seat-vibration associated with the alert, 92 percent responded affirmatively, compared with only 20 percent in the first experiment. They indicated the extent to which they agreed on a scale from 1 [strongly disagree] to 6 [strongly agree] with the following statements:

1. *The seat-vibration enhanced the display*, M = 4.33, SD = 1.72 (9 of 12 agreed to some extent)
2. *The seat-vibration made the display more annoying*, M = 2.17 SD = 0.94 (11 of 12 disagreed to some extent)

3. *If I had this display in my vehicle, I would want S-V to accompany the alert*, M = 4.33 SD = 1.97 (8 of 12 agreed to some extent)
4. *I would turn off the sound if this alert system was in my vehicle*, M = 3.58 SD = 1.73 (7 of 12 agreed to some extent)

Surprisingly, there appeared to be little effect on the number-of-false-alarms. The younger drivers were the only participants who demonstrated any downward trend in display acceptance as a function of number-of-false alarms and this only occurred for a single dependent measure (avoidance rating). The absence of this effect might be attributed to the number-of-false-alarms being confounded with trial order. Participants experienced each display with zero false alarms, one false alarms and two false alarms. If participants became increasingly accepting of the display over the course of the three trials, this effect could work directly against a number-of-false-alarms effect. The absence of a number-of-false-alarms effect might also be attributed to the short exposure duration (4-min trials). Perhaps, false alarms do not become annoying until the driver experiences the system for several hours under normal driving conditions. Alternatively the result could be valid, indicating that with this given display (including a 0.5-s 72 dBA tone), high false alarm rates are tolerable to a large number of drivers. COMSIS (1996a) revealed a wide range of annoyance sensitivity to false alarms exists and found that tonal (as opposed to voice) alarms were generally more tolerable.

The age of participants appeared to have a large impact on how they rated the different display alternatives. Younger drivers rate more complex displays (especially the looming-plus-scale display) as less effective (in terms of headway maintenance and collision avoidance), more annoying, and less desirable. Buy rating dropped dramatically for younger drivers when the scale was added to the looming-display (Figure 7.13). Middle and older drivers, on the other hand, rated the more complex displays as being more effective; however, there is little difference between the looming and looming-plus-scale displays of the headway and avoidance ratings. Middle drivers indicated a general increase in annoyance associated with more complex displays, whereas, older drivers indicated little increase in annoyance as a function of display complexity. Middle drivers indicated that they would be more likely to buy the two-stage and looming displays than the one-stage and looming-plus-scale displays, whereas, the older drivers revealed a buy rating that monotonically increased with display complexity. Averaged across all groups, the looming-plus-scale display was rated as being the most distracting display candidate.

Because these conclusions are based on such a small sample of participants, the effect of age must be observed cautiously. The younger and older groups included only three participants each. Because the age trends appeared to be internally consistent and reliable, age was included as a variable in the statistical analysis. This data is strongly suggestive that there are meaningful differences between age groups in the preference of forward collision warning displays, however, these results should not be considered conclusive until further research replicates these trends.

Overall the looming-plus-scale display was ranked as being more annoying and distracting than the simpler displays. The only positive attribute of the looming-plus-scale display was that it was ranked as being significantly more understandable than the one-stage display. The looming display was ranked as being more understandable and more attention-getting than the one- and two-stage displays, and more preferable than the one-stage display. The only negative attribute of the looming display was that it was ranked as being more distracting than the one-stage display. This analysis shows a clear driver-acceptance advantage of the looming display over the looming-plus-scale display.

Table 7.3 displays the preference ranks from all twelve participants as a function of display type. It can be observed that five participants ranked the looming display as their first choice, compared with three for the one-stage, two for the two-stage, and four for the looming-plus-scale display. The looming display was the second choice of five participants. Therefore the looming display was the first or second choice of ten out of twelve participants. The remaining two participants (who ranked the looming display as their third choice) preferred simpler displays and therefore selected the one-stage display as their first choice.

Table 7.3 Participants' Preference Ranks of the Four Displays.
The second column contains the mean rank scores for each display. Participants who responded similarly have been grouped together.

1	**3.08**	1	1	1	4	4	4	4	4	4	2	4	4
2	**2.42**	2	2	3	1	1	3	3	3	2	3	3	3
L	**1.75**	3	3	2	2	2	1	1	1	1	1	2	2
LS	**2.75**	4	4	4	3	3	2	2	2	3	4	1	1

The responses to the auditory item on the questionnaire revealed that participants were generally comfortable with the urgency conveyed by the auditory tone that was used, indicating that it was neither too urgent nor not urgent enough. This tone used the same frequency peaks (2500 and 2650 Hz) as the CAMP #8 sound so may share many similar positive features. Despite positive urgency ratings, many participants (seven of twelve) also indicated that they would want to turn the sound off. Ratings of the extent to which participants agreed that they would want to turn the sound off were highly correlated ($r = 0.64$) with ratings of the extent to which they agreed that the seat-vibration enhanced the display. This suggests that many might want to substitute seat-vibration for the auditory warning tone.

The seat-vibration stimulus received low annoyance ratings with only one participant (slightly) agreeing that the seat vibration was annoying. One advantage of the seat-vibration warning is that the stimulus would not impinge on other passengers. This feature would be similar to the vibration function on a cellular phone where the user is alerted without impinging on other people. It might be especially important if there were large numbers of false alarms. Unlike visual stimuli, seat-vibration and the auditory stimuli both share the common feature that they do not require the driver to be oriented in a particular direction. This may imply that the seat-vibration is a suitable candidate for replacing the auditory stimulus. However, until further research validates that seat-vibration is as beneficial to driver reaction performance as an auditory stimulus, an auditory stimulus must accompany the imminent alert. The fact that only two out of ten participants detected the seat-vibration in the first experiment suggests a potential weakness of this stimulus. Efforts are currently underway at Delco to create a seat-vibration system of greater intensity.

Given that nine of twelve participants agreed that the seat-vibration enhanced the display and eight of twelve participants agreed that they would want the seat-vibration to accompany the alert if it were in their own vehicle, a seat-vibration system will be included in the prototype vehicle. Seat vibration, like haptic braking, appeared to have potential for future FCW applications, however, due to the lack of research addressing the impact of seat vibration on the driver, the Human Use Review Panel (HURP) advised against the inclusion of seat-vibration in the FOT.

The two experiments provided little evidence that the scale addition provided any benefit to the looming display. Participants in the looming-plus-scale display condition showed no brake reaction time benefit over participants with the looming display. The scale in isolation also failed to provide any benefit when compared with no display. These results suggest that the scale is an ineffective means of presenting forward collision warning information. One explanation for the failure of the scale component may be that it is overly graphical and complex in nature, requiring too much attention from a driver who must react immediately. Whereas the two-stage and looming displays present a global change in color and size between each stage, the change in a scale display is more local, occurring in only a small portion of the display. The fine-grained distinction provided by the scale may be unnecessary given that the driver controls the position of the vehicle using the external visual scene rather than the internal instruments. Given that the driver is able to use the external visual scene to make fine tuning speed adjustments, salience is more important than precision in a forward collision warning display.

Although no display effects were observed on headway maintenance, based on Dingus et al.'s (1997) it is expected that the looming display can be as effective as the looming-plus-scale display for increasing headway. In Dingus et al.'s first experiment only their display with a car icon significantly increased temporal headway during coupled headway events, suggesting that the car icon may have been the most active component of the display. Despite this result, Dingus et al. discarded the car icon display in the next two experiments, choosing to focus instead on the bar display.

The scale addition to the looming display appears to provide little advantage, however, there is evidence for a driver-acceptance cost. The looming-plus-scale display was rated as being more annoying than the looming display in both experiments and for the absolute judgments of the second experiment, it was rated as being more distracting than the looming display. Participants rated themselves as being significantly less likely to buy a system that used the looming-plus-scale display than the looming display and preferred the looming display over the looming-plus-scale display.

The decreased driver acceptance of the scale display may relate to the fact that the scale display violates the "display by exception" axiom of display design, suggesting that displays should only present information when the message is important and relevant. Even when no vehicle is detected, the scale and looming-plus-scale display presents an empty scale on the HUD. The ever-present scale provides little additional information and may to some extent mask the arrival of a more urgent state when such a state is detected. COMSIS (1996b) claim that it is easier for drivers to detect a change from nothing to something than it is to detect a change from something to something else. For all of the above reasons, the looming-plus-scale display is rejected.

The two-stage and the looming displays differ only in that the looming display provides a distinction between an amber and static red cautionary stage (see Figure 7.4). These displays performed very similarly in most regards throughout the two experiments, however, the looming display showed a significant advantage over the two-stage display in participant ratings of preference (Experiment 1), discriminability (Experiment 1), understandability (Experiment 1), and attention-getting (Experiment 2). Given that the displays are so similar in nature, implying that there can be little benefit of one display over the other, selecting the looming display over the two-stage display appears to be a safe option. Therefore, although the two-stage display also appeared to be an effective candidate, it is rejected in favor of the looming (three-stage) display.

The one-stage display exhibited significantly more resistance to annoyance and distraction than the looming display. Younger participants rated the one-stage display as being more effective for collision avoidance and indicated that they would be more likely to buy a one-stage display. However, in the second experiment the one-stage display failed to demonstrate any performance benefit over no display (inconsistent with the 1999 CAMP work). The looming display led to significantly shorter brake reaction times than the one-stage display and was significantly more preferred in both experiments. Although there may be a group of drivers who prefer the one-stage display and there may be times when the looming display provides too much distraction, based on the overall pattern of data in the two experiments, the looming display appears to be the most effective candidate. However, there appears to be a means of utilizing the benefits of both displays.

The sensitivity setting in the GMR2 algorithm adjusts the timing of the pre-imminent phases of the alert level, while leaving the imminent phase fixed. When the driver selects a more aggressive sensitivity setting with the looming display, the cautionary phases are pushed later in time (closer to the imminent phase). More aggressive settings allow less time for the cautionary phases to be presented. The sensitivity settings are mapped into the algorithm in units of time (either time headway or time to the imminent margin). If drivers were permitted to select a sensitivity setting that corresponded to zero seconds, they would be able to select a one-stage display as the most aggressive sensitivity setting.

Because the zero value represents the logical aggressive extreme of the sensitivity spectrum, it is likely that providing drivers with the option of a zero setting will make intuitive sense to the driver. They can think of the sensitivity settings as the amount of pre-warning before the imminent phase and they can select no pre-warning as the most aggressive setting. This implementation (a looming display allowing a zero sensitivity setting) extends the capability of the sensitivity setting, allowing the driver to select a one-stage display wherever appropriate. For this reason, this display was selected for the ACAS FOT.

During a meeting on May 15, 2001, the human factors group decided to change the color of the green "vehicle detected" indicator to a gray of lesser intensity. It was agreed that because of the association between green and safety, it would be beneficial to avoid the potential liability implications of informing the driver that they are "safe." In the scale display, green was used because the scale represented a continuum of the amount of threat from the forward vehicle. One extreme clearly communicates danger, therefore the opposite extreme must imply safety. However, because the looming display is not necessarily a continuum and can be thought of as five discreet states (no vehicle detected, vehicle detected, caution, approaching imminent, and imminent), the "vehicle detected" icon should communicate that a vehicle is detected rather than the fact that the driver is safe.

The reduced intensity was selected to conform more closely with the design axiom of "display by exception." Given that "vehicle detected" is not an inherently urgent state, the representing icon should be less salient to the driver, so that it can be ignored (when desired). As a direct result, the change in intensity from dark-gray to amber will be more salient. Figure 7.16 displays the final selection of the FCW icons.

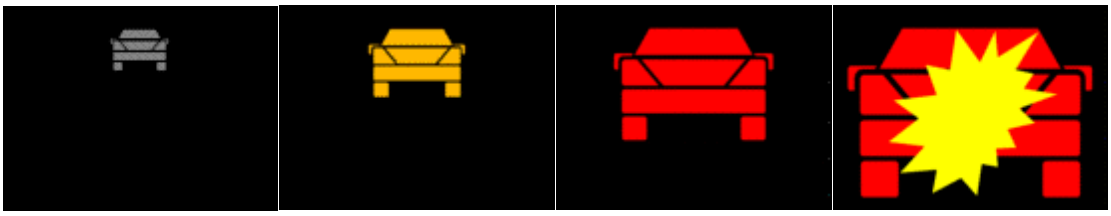

Figure 7.16 Final Selection of the FCW Display. From left to right the icons mean "vehicle-detected," "caution," "approaching imminent," and "imminent." When no vehicle is detected, this display is blank. The imminent icon will flash at 4 Hz.

On May 16th 2001, GM and Delphi jointly selected values for the sensitivity settings, using the GM Engineering Development Vehicle (EDV) at the Milford Proving Ground. The sensitivity settings specify the time at which the display transitions from the gray icon to the amber icon. This transition can occur either as a result of the time headway (THW) sub-algorithm, when the driver crosses a time headway boundary, or as a result of the time-to-contact (TTC) sub-algorithm, when the driver is given a time away from imminent alert. Because a given sensitivity settings maps onto both of these sub-algorithms, values for both the THW and the TTC boundaries were selected. Values were selected though a subjective evaluation of perceived urgency.

The first procedure was designed for selecting TTC boundaries. The driver of the EDV approached the lead vehicle according to the following specifications:

1. Lead vehicle travels 35 mph and host vehicle travels at 50 mph
2. Lead vehicle travels 35 mph and host vehicle travels at 65 mph
3. Lead vehicle travels 50 mph and host vehicle travels at 65 mph
4. Lead vehicle travels 50 mph and host vehicle travels at 80 mph

Several approaches to the lead vehicle were conducted combining the above vehicle speed conditions and different values of the TTC boundary. After appropriate values for the two extreme TTC boundaries were selected, these values were evaluated using a lead vehicle deceleration maneuver. The host vehicle followed the lead vehicle at 60 mph at a time headway of 2 s before the lead vehicle decelerated at either 0.2 or 0.3 g. The deceleration maneuvers revealed that a slightly higher value should be used for the most conservative setting. This was because the deceleration operated to contract the range between the different display states (caution, warning, imminent), as the threat level increases at an increasing rate. This contraction of the range made the pre-imminent levels appear more aggressive, so the conservative value was adjusted to compensate for this possibility.

The final procedure for selecting the TTC boundaries involved approaching a stationary vehicle at 30, 40 and 50 mph. Because of the limited range of the radar (approximately 120 m), approaches at the higher speeds resulted in the immediate activation of later alert stages, without passing through the earlier stages.

Once the TTC boundaries had been selected, the TTC sub-algorithm was disabled and the THW sub-algorithm was evaluated by following the lead vehicle at 40, 50, 60 and 70 mph, while systematically varying time headway. After getting a subjective impression of how the different headways felt (in relation to the literature), the THW boundaries were selected.

On the 45-minute drive through rush-hour traffic from the Milford Proving Ground back to the GM Technical Center, he combinations of TTC and THW boundaries were evaluated as they were systematically changed in the GM EDV. The selected values appeared to be appropriate and it was revealed that TTC boundaries should be the equivalent to double the THW boundaries for a given sensitivity setting. The selected values are displayed in Table 7.4. For sensitivity setting 3, the values specify that the amber icon will be presented when the host vehicle is at a time headway of less than 1 s or when the host vehicle is less than 2-s before reaching the imminent margin, whichever

occurs first. For a constant velocity the red icon appears half way between the amber icon and the imminent icon.

Table 7.4 Selected Time-to-Contact and Time Headway Boundaries

Sens. Setting	Boundaries TTC	Boundaries THW
0	0	0
1	1	0.5
2	1.5	0.75
3	2	1
4	3	1.5
5	5	2.5

The drivers' selections of the sensitivity settings during the FOT should indicate whether the values in Table 7.4 are appropriate. However, it is expected that the range of these values will be wide enough to accommodate the most aggressive and the most conservative drivers.

Decisions on display moding were based on the combined reasoning of the human factors group rather than on paper-and-pencil studies involving multiple participants. It was thought that because of the inherent engineering complexity, it was not expected that participants could gain a sufficiently complete understanding of the FCW and ACC systems on which to base their decisions. Instead the design criterion was unanimous human factors agreement between the group participating in the human factors decision making.

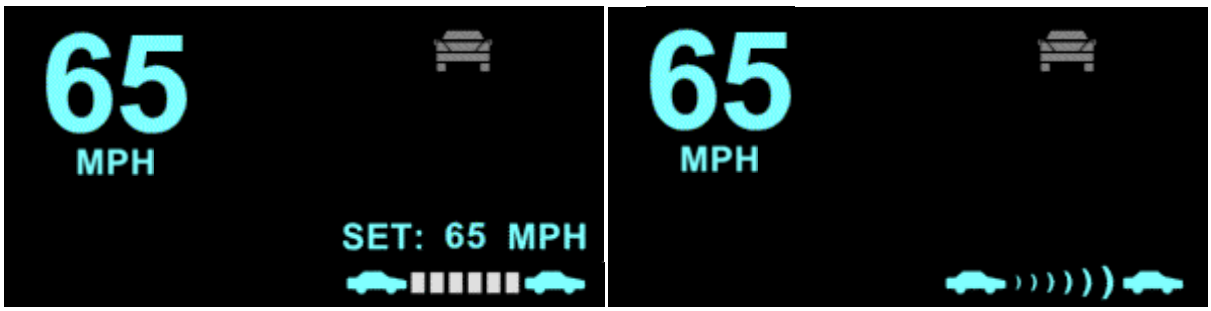

Figure 7.17. The Distinction Between ACC-Engaged (left) and ACC-Not Engaged (right). The right half of each display contains three elements: the alert-level icon at the top, the message line in the middle, and the gap/warn setting line at the bottom. When ACC is engaged, the set speed text will display by default and the gap (as opposed to warn) setting is displayed at the bottom.

The DVI layout is displayed in Figure 7.17 for the ACC-engaged and ACC-not engaged conditions. In addition to observing the natural vehicle throttle control cues during the ACC-engaged state, the driver can observe that ACC is engaged by noticing the set speed text and the solid gray blocks between the gap/warn display vehicles, as opposed to the radar waves. The set speed text is the only cyan text that can appear on the text line, so the presence of the set speed text should be salient to the driver.

The other messages (and their associated meanings) that can appear on the set speed line are "Dirty Radar" (the radar is obstructed, reducing the reliability of the ACC/FCW system, and needs to be cleaned), "Heavy Rain" (heavy rain is reducing the reliability of the ACC/FCW system), "Slippery" (the cool temperature suggests that the roads may be slippery and so the FCW algorithm will assume a more cautious friction coefficient), "Sharp Curve" (the radar is unable to detect what is around the curve, so use caution), and "Speed too fast" (the vehicle is traveling beyond the range of the radar). The messages "Driver Control Required" (the ACC-system has automatically been disengaged, so driver control of the vehicle is now required), and "Malfunction" (ACC/FCW system failure) will simultaneously occupy both the text and gap/warn setting lines.

Because a single line is being used to provide several different possible messages, the messages were prioritized according to the order displayed in Figure 7.18. A single type of message can assume more than one priority, assuming a higher priority if it has just been detected, or a lower priority if it is older information. To avoid driver annoyance, only some of the messages are accompanied with an audible tone (a pair of 50-ms 3000-Hz tones, separated by 20 ms of silence). The entire right side of the HUD will be blanked when a "FCW Inactive" message is broadcast over the CAN interface and during the first week of the FOT (when only conventional cruise control is available). "FCW Inactive" occurs when the vehicle speed is less than 25 mph and when the driver applies the brake. The text and gap/warn setting lines will be blanked when the imminent alert level is reached.

Malfunction	When present (+audio)
Driver Control Required	-When ACC is automatically disengaged until brake or gas pedal (+audio)
	-When FCW Inactive, Malfunction, or imminent alert present
SET: MPH	-When or set speed changed (or ACC is engaged) in last 2 s
Seat Vibration	-When armed in last 2 s (+audio when armed or disarmed)
Sharp Curve	-When present
Speed Too Fast	-When detected in the last 10 s
Dirty Radar	-When detected in last 10 s and not active in past 15 min (+audio)
Heavy Rain	-When detected in last 10 s
Slippery	-When det. in last 10 s and not yet activated (retry until >= 2 s activation)
Dirty Radar	-When present
SET: MPH	-When ACC engaged
Speed Too Fast	-When present
Heavy Rain	-When present

Figure 7.18 Priorities for the Text Line Messages. Visual display of messages will be accompanied with audio, where indicated.

When the driver is in park the text line will cycle through "Dirty Radar" (plus audio) and "Slippery" when these messages are present. Each message will display for 2 s and loop continuously. The audio accompanying "Dirty Radar" will play only once in this sequence. The gap/warn setting will also be displayed and adjustable when the vehicle is in park.

To avoid the delays associated with communicating with the radio over the Class 2 bus, an additional speaker and amplifier were added to the vehicle to play the ACC/FCW system sounds. The 4-ohm 3-inch mid-range speaker was placed in front of the driver seat so that the sound would appear to emanate from a frontal direction. The DVI will mute the radio during the imminent alert level and play the imminent alert tone through the added amplifier and speaker, keeping the Class 2 communication to a minimum. Half a second after the imminent tone has played, the DVI system will un-mute the radio. To avoid unnecessary annoyance, the radio will not be muted during the message audio. Because an automatic volume adjusting system required excessive hardware additions to the vehicle (ambient noise measuring apparatus), with relatively little benefit, and given that the radio would be muted, it was decided that a constant level of 75 dB would be sufficient for the ACC/FCW sounds.

The steering wheel button arrangement was finalized at a human factors meeting in Warren on February 15, 2001. Figure 7.19 displays the configuration of the steering wheel buttons in the prototype vehicle. To make room for the gap/warn addition to the steering wheel, the temperature button (inner right) was removed. Given that the outer buttons are easier to manipulate than the inner buttons, the seek button (outer left) was moved to the position that the temperature button had previously occupied (inner right), to allow the gap/warn button to occupy the outer left position. This mapping groups the ACC functionality in the lower left quadrant. Because the volume control is the most frequently used function, its location was preserved on the outer right location. As required by the ACC system, the "ACC on/off" and the "SET/RESUME" buttons remained in the same position. Buttons in the prototype vehicle are labeled according to the new arrangement.

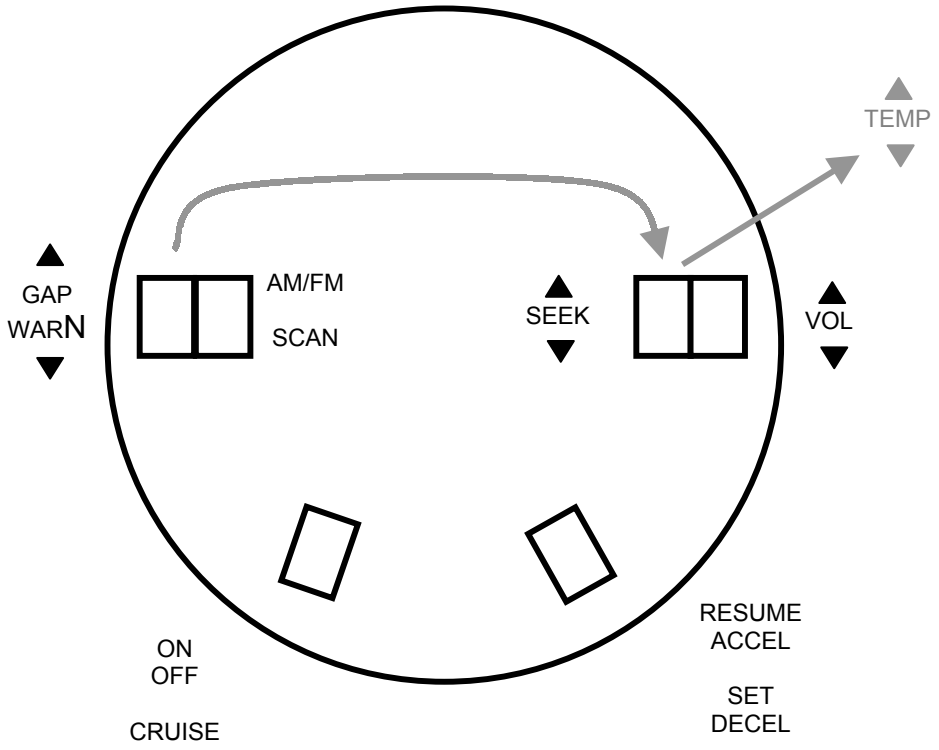

Figure 7.19 Steering Wheel Button Layout. The rectangles represent where the buttons are located on the steering wheel. The temperature button was removed and the seek button replaced it. The gap/warn setting button was placed where the seek button had been.

Current Schedule and Progress

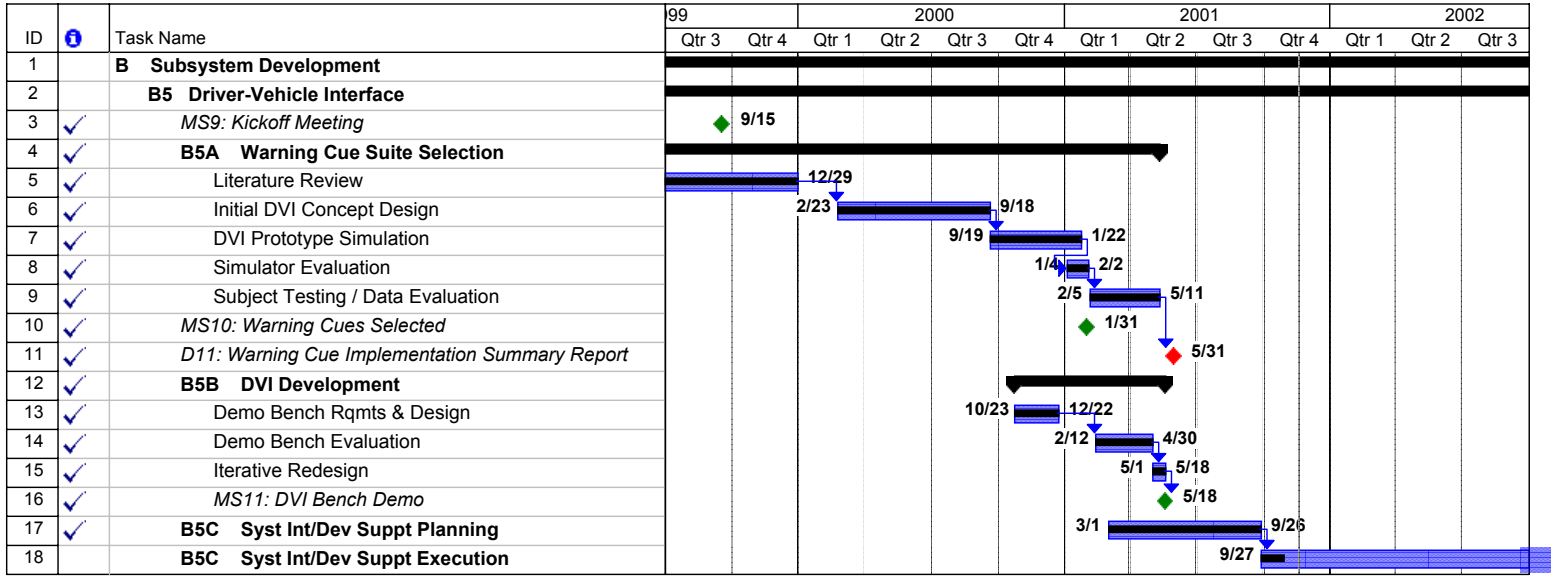

Figure 7.20 Task B5 Schedule

References

Crash Avoidance Metrics Partnership (1999). *Development and validation of functional definitions and evaluation procedures for collision warning/avoidance systems*, Report under contract DTNH22-95-H-07301. Washington, DC: National Highway Traffic Safety Administration.

COMSIS (1996a). *Inappropriate alarm rates and driver annoyance*, Report under contract DTNH22-91-07004. Washington, DC: National Highway Traffic Safety Administration.

COMSIS (1996b). *Preliminary human factors guidelines for crash avoidance warning devices*, Report under contract DTNH22-91-07004. Washington, DC: National Highway Traffic Safety Administration.

Dingus, T. A., McGehee, D. V., Manakkal, N., Jahns, S. K., Carney, C., & Hankey, J. M. (1997). Human factors field evaluation of automotive headway maintenance/collision warning devices, *Human Factors, 39*(2), 216-229.

Mortimer, R. G. (1988). Rear-end crashes. In G. A. Peters & B. J Peters (Eds.), *Automotive Engineering and Litigation*, Vol. 2 (pp. 275-306). New York: Garland Law Publishing.

Schiff, W. (1965). Perception of impending collision: A study of visually directed avoidance behavior. *Psychology Monographs: General and Applied, 79* (Whole No. 604).

Smith, M. R. H., Flach, J. M., Dittman, S. M., & Stanard, T. (2001). Monocular optical constraints on collision control, *Journal of Psychology: Human Perception and Performance, 27*, 395-410.

8 Data Fusion (Task C1)

Goal and Purpose

The Data Fusion (DF) task has 3 main subtasks:

- Task C1A: Requirements Definition and Architecture Development
  The goal of subtask C1A is to develop requirements (performance, interface) and architecture for the data fusion system.
- Task C1B: Initial Algorithm Development
  The goal of subtask C1B is to develop fusion algorithms to fuse radar, lane tracking, GPS/Map, and host vehicle sensors to produce a robust estimate of the host lane geometry, host state, driver distraction level, and environment state.
- Task C1C: Real-time Algorithm Development
  The goal of subtask C1C is to develop real-time versions of the algorithms developed in Task C1B for integration into pilot and deployment vehicles.

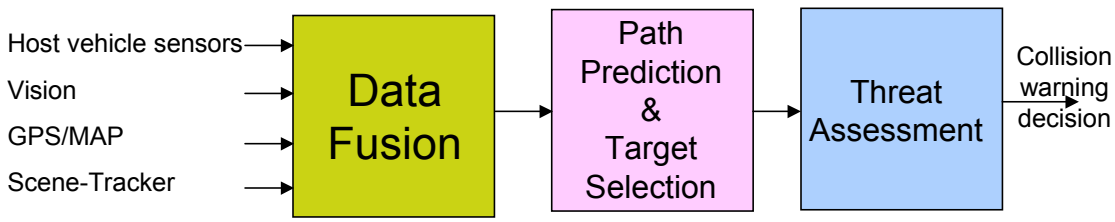

Figure 8.1 Data Fusion and Its Relationship to Other System Tasks

Figure 8.1 shows the relationship of the data fusion task to other subsystems and the overall project. As shown in Figure 8.1, DF receives its inputs from a variety of subsystems (host vehicle sensors, vision, GPS/Map and Scene Tracker). The DF function evaluates multiple sources of potentially conflicting information to produce improved estimates of the road-geometry, vehicle state, driver distraction and environmental conditions. These DF outputs are to be used by the path prediction and target selection system to identify in-path targets. The Threat Assessment system then makes a collision warning decision on these in-path targets. The final expected outcome of the task is real-time data fusion software that is fully interfaced and integrated into the pilot vehicle and providing all the output estimates described above.

Background

The DF function can be divided into four main functional subunits.

Host Lane Geometry Estimation

DF provides an estimate of the host lane geometry of the current host vehicle lane for a distance of up to 100 m ahead of the host vehicle by fusing host lane geometry estimates from the vision subsystem, the map-based subsystem, the scene-tracking subsystem, and the curvature estimates based upon vehicle dynamics sensors. The host lane geometry is described as the parametric geometry and range limits of two segments in front of the host vehicle: near-range and far-range. The geometry of each segment is described in terms of coefficients of a polynomial that relate the lateral offset (from a fixed coordinate system on the vehicle) of the current lane as a function of distance ahead of the vehicle.

For each segment, the system also provides a confidence measure of the estimated host lane geometry which indicates whether it is unable to determine geometry from the available inputs and/or under current conditions. Since vehicle motion along the road makes forward road geometry a quantity that varies dynamically with time, we need to use a dynamic recursive estimation approach such as the Kalman filter. Kalman filters perform recursive estimation using both a model-based update of state variables and update of the state estimates using a weighted version of the new measurements.

Host State Estimation
The DF function provides a "fused" host state estimate by fusing information from vision and scene-tracking subsystems. Host state primarily consists of heading angle and lateral offset. It fuses heading angle estimates from the forward vision sensor subsystem and the scene-tracking subsystem and provides a fused estimate of heading angle of the host vehicle (angle between host vehicle centerline and lane tangent). It also produces a confidence measure of the estimated heading angle and provides an estimate of the host lateral offset in lane (from the lane centerline), based on vision subsystem estimates and a confidence measure.

Driver Distraction Estimation
The DF function estimates driver distraction by monitoring if the driver is performing a secondary task.

Environment State Estimation
When used to interpret environment state, the DF function detects and reports conditions indicative of slippery road surfaces. Data on conditions is used to modify the expected braking intensity the driver will achieve when responding to an alert. In turn, the expected intensity has an impact on the timing of the alerts.

Technical Approach

In this work, fusion for host lane geometry estimation and host state estimation is done using Kalman filters. This method provides a natural framework of fusing incomplete and inaccurate information from multiple sources and can provide more accuracy and improved robustness to stochastic errors (e.g., sensor noise), as it acts as a sort of "low-pass" filter. A fundamental issue in fusing different forms of information about forward lane geometry in a Kalman filter framework is the choice of a good road model. We investigated several different road models (parabolic, single-clothoid, spline) and chose a "higher-order" road model after extensive testing on simulated and some real data. We have also developed an adaptive Kalman filter approach for road geometry and host state estimation which is superior to a conventional Kalman filter. The adaptive Kalman filter performs better during sharp transitions in road geometry compared to a conventional Kalman filter. Performance evaluation using real data is in progress.

The overall fusion architecture was initially based on the idea of fusing the subsystem estimates based on their confidence measures. However, ground-truth analysis of the subsystem outputs on available real data suggested that, in general, their confidence measures were not adequate for fusion. As a result, the data fusion architecture and software was modified.

We have developed and tested several different fusion methods on real driving data. The confidence-based fusion (COF) algorithm uses the subsystem confidence measurements for fusion. The disadvantage of this approach is that since confidences are not always correct/reliable, fusing subsystems based on confidence "as is" may make things worse.

The consensus-based fusion (CNF) algorithm uses agreement between subsystems to detect "incorrect subsystems(s)" and ignore them. However, it requires at least two subsystems to be in good agreement for the method to work. The disadvantage of this approach is that good "lone" performers will not be fused. For example, the Map subsystem provides the best information about upcoming transitions amongst all subsystems, many of which do not provide any preview. As a result, when Map correctly indicates an upcoming curve, while all other subsystems incorrectly indicate an upcoming curve, fusing based on consensus may actually loose preview information from Map at transitions.
An alternate algorithm fuses based on both rules and confidences. This approach relies on modifying confidences based on heuristic rules prior to fusion. An example would be to ignore scene-tracker outputs when it is operating in zero or low confidence modes and artificially bump up its confidence otherwise. The disadvantage of this approach is that if a rule is violated, it can make "good" confidences "bad," which may make the fused output worse.

The DF function provides an estimate of driver distraction by monitoring if the driver is performing a secondary task. In our working model, there are two major categories of secondary tasks that may affect driver situation awareness. The first category is a simple task that requires just one glance to gather the necessary visual information. The second is complex and requires many short sampling glances away from the forward view. For the first category, once the control is activated, the amount of distraction left to predict is insignificant. In other words, the activation of the control essentially follows the single-glance distraction time. In complex secondary tasks, the driver's vision is time-shared with the primary driving task. The driver cyclically samples the task, activates the control and returns to the forward view for as many glancing cycles as are needed to complete the task (adjusting the radio, perhaps, or turning on the air conditioning). The domain knowledge assumes that the first activation of any of the controls for such tasks follows the first glance time and predicts a high degree of distraction for the next 8-10 seconds. In fact, the elapsed time from the first activation is used to predict the coming level of driver distraction for a given complex task such as radio knob adjustments. To predict driver distraction level, we have developed a set of fuzzy rules based on the strength of elapsed time from the first activation and duration (of the activation).

When used to interpret the environment state, the DF function detects and reports conditions indicative of slippery road surfaces. Data on conditions is used to modify the expected braking intensity the driver will achieve when responding to an alert. In turn, the expected intensity has an impact on the timing of the alerts. We define road conditions as dry, dry-icy, wet, or icy. They are provided at a confidence level specified as none, low, medium or high. Both the road conditions and their associated confidence levels are derived based first upon windshield wiper activity; then further refined through use of outside temperature measurements.

Relevant Activities

Task C1A (Requirements Definition and Architecture Development)
Hughes Research Laboratories (HRL) has developed and completed performance and interface requirements for the DF subsystem. Milestone MS12 (Architecture and Performance Requirements Definition) was completed with a meeting held at HRL on 9/16/99 in which HRL presented performance and architecture requirements of the data fusion subsystem. In addition, HRL presented a preliminary architecture for the data fusion subsystem.

Task C1B (Initial Algorithm Development)
The initial fusion algorithms have been completed and tested on simulated data. Milestone MS13 (Preliminary Data Fusion Algorithm Demonstration) was completed with a presentation to the National Highway Traffic Safety Administration (NHTSA), General Motors (GM) and AED on Dec 4, 2000. This milestone demonstrated non real-time performance of all four parts of the data fusion subsystem: host lane geometry estimation, host-state estimation, driver distraction level estimation, and environment state estimation. Although not part of the official list of program deliverables, a preliminary version of the data fusion software was delivered to GM for insertion into the Engineering Development Vehicle (GM EDV) in September 2000. Also, a model of the data fusion subsystem was provided to PATH for use in the PATH simulator.

We have developed and implemented initial versions of algorithms for host lane geometry, host state, driver distraction and environment state estimation. These algorithms were chosen and developed after extensive literature survey and testing of several competitive and promising approaches. For example, we tested several different commonly used road models and compared errors in estimating road geometry in both a recursive (Kalman) and a non-recursive (least-squares) framework. This performance evaluation demonstrated that conventional "single-clothoid" road models have estimation errors that would not meet the system performance requirements. This motivated us to develop a higher-order road model that was amenable to a state-space representation in a Kalman filter framework.

We have completed development and implementation of this novel road model and evaluated its performance. Results show that this model is superior to a conventional "single clothoid" road model as it has smaller road geometry estimation errors, especially during sharp transitions in road curvature. We have also developed an adaptive Kalman filter approach for road geometry and host state estimation which is superior to a conventional Kalman filter. The adaptive Kalman filter performs better during sharp transitions in road geometry compared to a conventional Kalman filter. However, due to issues related to accuracy of subsystem confidences, the latest fusion software uses a conventional Kalman filter. We also performed comparisons between instantaneous and Kalman filter based fusion approaches. As expected, instantaneous fusion tends to be more noisy, but has less lag at transition in comparison to a Kalman filter based fusion method. Trade-off studies were carried with different road geometry scenarios to assess the magnitude of lag vs. noise. The conclusion was that a recursive filtering method is not only a natural choice but also a more accurate one for host lane geometry estimation.

In order to validate the basic functionality and effectiveness of data fusion algorithms and software, we developed a simulation tool that allows us to simulate the various subsystem outputs on different types of road geometry and host state behavior. These outputs are then fed to different versions of the data fusion algorithm which run in real-time in the tool. Performance metrics related to performance of the fusion algorithms are also readily available (since ground truth is known in the simulations) and displayed in the user interface. The interface also allows us to change the performance of the subsystems in real time by modifying the confidence estimates and visualize its effects on the performance of the data fusion algorithm. This tool was used to demonstrate preliminary DF algorithms in MS13.

Task C1C (Real-Time Algorithm Development)
Real-time data fusion software has been ported and integrated into the prototype vehicle. We have verified, tested and resolved all data fusion input/output interface issues in the prototype as well as performed statistical analysis of the data. Milestone MS14 (demonstration of real-time data fusion algorithm) was completed on May 1, 2001 with a demonstration to GM and AED at HRL.

To develop real-time versions of the algorithms developed in Task C1B, our approach was to first port the algorithms onto the real-time hardware platform specified by GM for the data fusion subsystem. After porting the algorithms, we evaluated algorithm real-time performance to determine if there are portions of the fusion algorithm that must be tuned or modified to meet real-time processing requirements. In addition, several different versions of the algorithm were developed and tested for both accuracy and speed comparisons. We evaluated the performance of various subsystems on driving data collected under different scenarios. Results of the analysis were used to tune and modify heuristic rules.

Real Data Playback/Analysis Tool

We also developed a tool that allows us to view, playback, and analyze real data recorded from the prototype vehicle. The main advantage of this tool is that it allows us to quickly access sections of interest in the data set and view the various subsystem and Data Fusion outputs/confidences for debugging and troubleshooting. This tool is optionally linked (off-line) to the actual data fusion software which allows us to plug in different versions of the fusion software and relog fusion outputs without actually having to recollect data. This tool also provides rapid playback and capability to jump to any point (forward and backward) of the video and subsystem/fusion data. The tool provides a video view and a top-down lane geometry view of the fusion systems inputs and outputs. Figure 8.2 -8.3 show a snapshot of the tool on some freeway driving scenarios; a top-down view of the forward road geometry estimated by different sensors (shown as right and left lane markers) is shown in the left subwindow. The corresponding video frame (as viewed by a forward-looking camera) is shown in the right top subwindow. The confidence estimates of the various subsystems are also shown by different colors in the rightmost pane. Additionally, subsystem displays can be turned on/off in the tool.

Map Geometry Visualization Tool

Additional tools were developed to assist in visualizing forward geometry from specific subsystems and to identify and understand difficult instances. A tool was developed to provide rapid playback and capability to jump to any point of the video and subsystem data. The tool provides a video view, a scrolling map view, and a lookdown lane geometry view of the fusion systems inputs and outputs. In addition, there were a number of features developed to aid in the further refinement of the GPS/Map subsystem.

Finally, tools and measures were developed for subsystem validation, for the computation of simple statistics on the performance of the fusion systems inputs and outputs, and to help identify enhanced rules for fusion. Details about this work are provided in the results section.

Ground Truth Method and Tool

Accurate knowledge of the forward road geometry is necessary to develop, evaluate, and validate the vision, scene tracker, GPS/Map, and data fusion subsystems. The goal is to develop ground truth for the forward road geometry out to ~ 100 m. For development, a ground truth accuracy of ~ 20 cm was desirable. To evaluate/validate the performance of the subsystems, an accuracy ~0.75 m – 1.0 m (lane width) is required. For forward geometry ground truthing, absolute accuracy is unimportant[1]. What is required is relative accuracy over the forward 100 m path. Additionally, we don't need ground truth 100% of the time; we do, however, need to know when we are producing accurate measurements. We reviewed the existing sources, road maps, road plans, aerial photos, etc. and determined that existing sources were not adequate for our ground truthing needs.

[1] Absolute position accuracy is required by the GPS map based geometry subsystem.

The EDV and prototype vehicles are instrumented with a fiber optic gyro yaw rate sensor, a GPS receiver, speed and odometer. Our initial approach was to use a pair of NovAtel DL GPS receivers in a *base station* and *rover* pair with post-processing of logged data for differential correction. After numerous trials, different post processing software, and working with the vendors, we were routinely finding post-processed errors of up to tens of meters. Cycle-slip errors were the dominant problem. The cycle-slip errors of cm class DGPS do not occur in meter class DGPS. We changed to a Trimble AgGPS 132 real-time DGPS receiver using OmniStar L1-based correction. This receiver is specified with an accuracy of ~1 m and a 10 Hz measurement rate. In Southern California we found that errors and dropouts due to poor signal conditions were common but detectable (number of satellites, and satellite signal strength). To reduce the effects of multi-path, the satellite elevation cutoff mask is set to 10°. Errors due to multi-path were still a significant problem, and could not be reliably detected from the GPS measurements.

To convert the GPS measurements to forward geometry we need to determine the vehicle heading. We found that converting the GPS measurements into the local tangent plane and regularizing with a smoothing spline supported robust heading measurements based on the arctangent.

The EDV and prototype vehicles are equipped with a KVH E-core 1000 fiber optic gyro (yaw-rate sensor). Speed is measured with a Delco Vehicle speed sensor. We convert from yaw-rate to a local tangent plane coordinate system based on integrating yaw-rate into a heading angle and incrementally computing the new position based on speed and heading. We determined that the error sources in the measured yaw rate could be ignored by limiting the yaw rate integration to a short interval of ~ 3 – 5 seconds, with vehicle speeds greater than 20 mph. We developed a least squares method to estimate the yaw-rate sensor bias and to measure the errors between the GPS path and integrated yaw-rate path. Based on the error, instantaneous fusion was used to provide a fused estimate.

The vehicle's host state information (lane heading, lane offset, and lane width) can be used to provide a correction to the measurements of the vehicle's path to provide a better estimate of the lane geometry. A method was developed to apply the host state measurements as corrections to the lane geometry estimate.

Intermediate and Final Results

Final Results

The real-time DF software has been completed and successfully ported into the prototype vehicle. All interfaces (inputs and outputs) have been thoroughly tested and validated. The software has been fully integrated within the overall ACC/FCW system and is fully functional. Real data has been collected from the prototype vehicle and analyzed using ground-truth tools developed at HRL. It has been verified that data fusion is providing all the expected output estimates (see *Goals and Purposes*) and operating at the expected 10Hz rate. Details of performance analysis are presented in the verification section.

Intermediate Results

Following are brief summaries of the two intermediate DF algorithms, highlighting one selected example from real data. In Figure 8.2 below, the forward lane geometry estimated by different subsystems at a curve transition (straight to upcoming left curve as seen in video window) is indicated by left and right lane markers in corresponding colors. Note the significant differences in the subsystem estimates. The fused estimate obtained by using the COF algorithm is also shown (red) below. In this case, DF correctly estimates the upcoming curvature mostly because the Map subsystem is in high confidence mode and affects the far range estimate more than other subsystems.

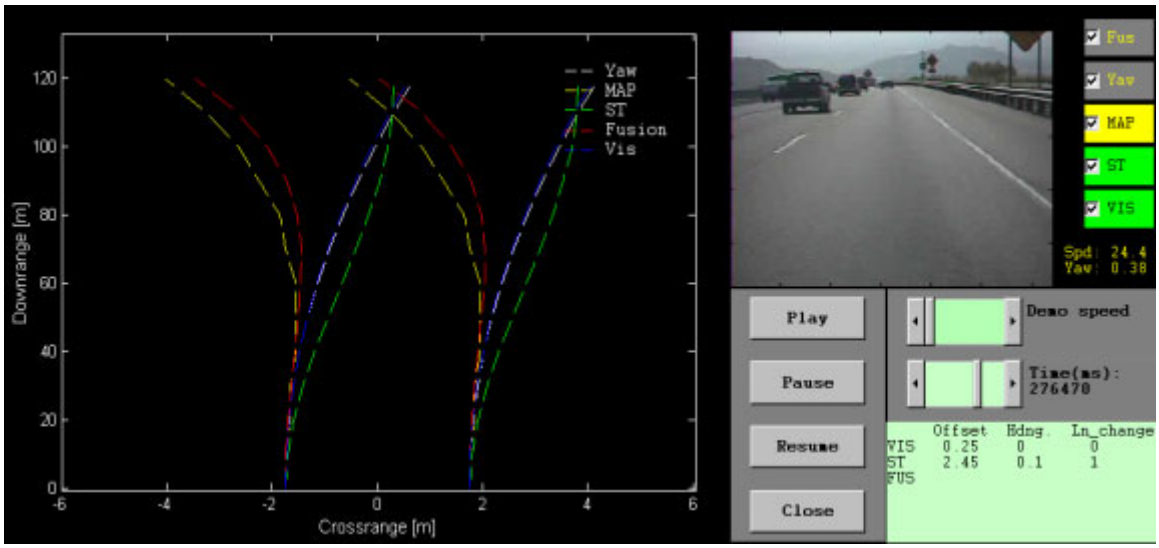

Figure 8.2 COF Algorithm Performance During Straightaway to Curve Transition

For the same driving scenario, the fused estimates obtained by using the CNF algorithm are shown in Figure 8.3. In this case, since Map was the only subsystem correctly indicating the curve transition, it was incorrectly identified as "wrong" sensor within the consensus framework and was not fused. In the current algorithm, heuristic rules have been added to identify special conditions to circumvent this type of problem.

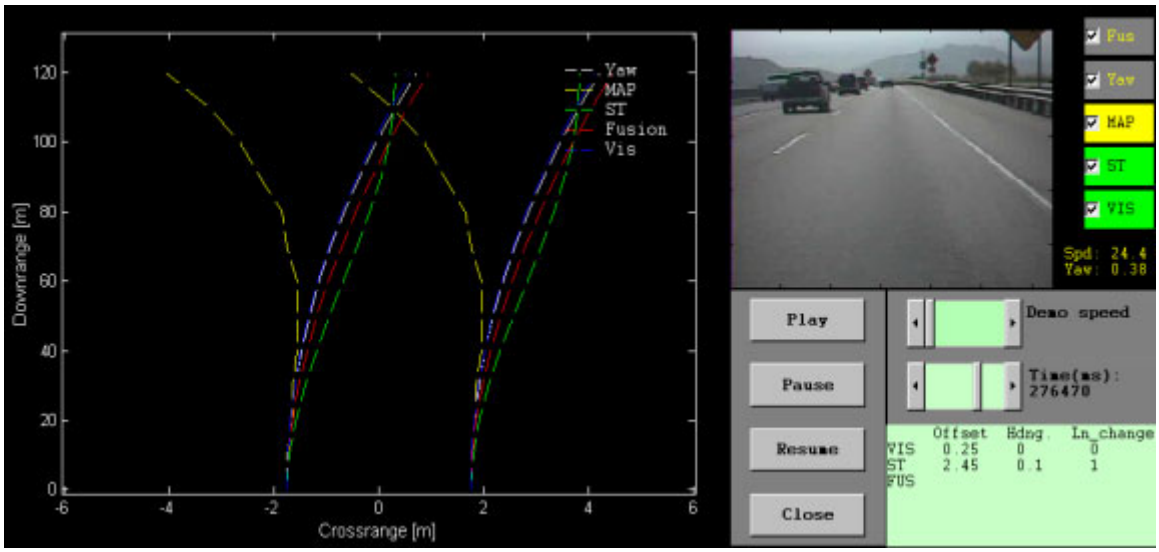

Figure 8.3 CNF Algorithm Performance During Straightaway-to-Curve Transition

We have similarly analyzed lane change scenarios and found differences in performance of the fusion algorithms. The CNF algorithm correctly estimates forward road geometry by using in-consensus sensors (vision and scene-tracker) when they provide correct estimates at this time. We have completed development and implementation of the novel road model, incorporated it into the DF software, and evaluated its performance. Results show that this model is superior to a conventional "single clothoid" road model as it has smaller road geometry estimation errors, especially during sharp transitions in road curvature.

Verification Testing

The goal of verification testing is to ensure that DF (1) has all the correct interfaces to the various input-output subsystems, (2) functions in real-time, and (3) provides outputs that are expected based on the specific inputs and the algorithm and statistical error analysis. Verification of (1) and (2) was relatively straightforward and carried out by collecting and analyzing many hours of driving data using some of the tools described earlier. Verification of (3) required more effort and the development of error metrics in conjunction with the use of the ground-truth tool. Details are provided below.

Statistical Error Analysis

To validate the behavior of the fusion subsystem, we analyzed its inputs and outputs. We collected data from all the subsystems via the CAN bus logger and used the integrated yaw-rate method to generate *ground truth* files. Ground truth was generated for all data instances for which the following conditions were true for 98% of the measurements along the forward path out to 120 m beyond the current point.

1. vehicle speed ≥ 20 MPH
2. vehicle lane offset < 0.5 m
3. lane offset confidence is high (≥ 2)

Note: this ground truth method *does not* handle the cases of : 1) changing lanes, 2) lane merges, or 3) lane separations.

The outputs of the yaw-rate, vision, scene tracker, GPS/Map, and fusion subsystems were then compared to the ground truth. Normalized histograms (pseudo-pdf[2]) were generated for the error at 60 m. Additionally, for each of the subsystems, maximum and RMS errors for the entire 120 m forward path were determined which were combined into a single score to allow simple comparison of subsystem estimates for the data set(s). We also analyzed the histogram distributions of error for different situations, such as speed categories, shape of the road, etc.. We have been able to identify a number of potential future fusion rule enhancements.

We present one typical result here. Figure 8.4 shows the histogram (pseudo-pdf) of forward geometry errors of one data-set for the road shape category of *straight transition to a gentle curve*. These histograms suggest a rule that when GPS map classifies the road shape as a straight transition to a gentle curve, that: 1) scene tracker should have an increased fusion weight for medium to high confidence and a decreased fusion weight for low to no confidence, 2) vision should have a decreased weight, 3) GPS map fusion weight should be unchanged, and 4) yaw-rate fusion weight should be increased.

[2] Pseudo-pdf: histogram bins sum to one. This is a discrete sampled approximation of the Probability Density Function.

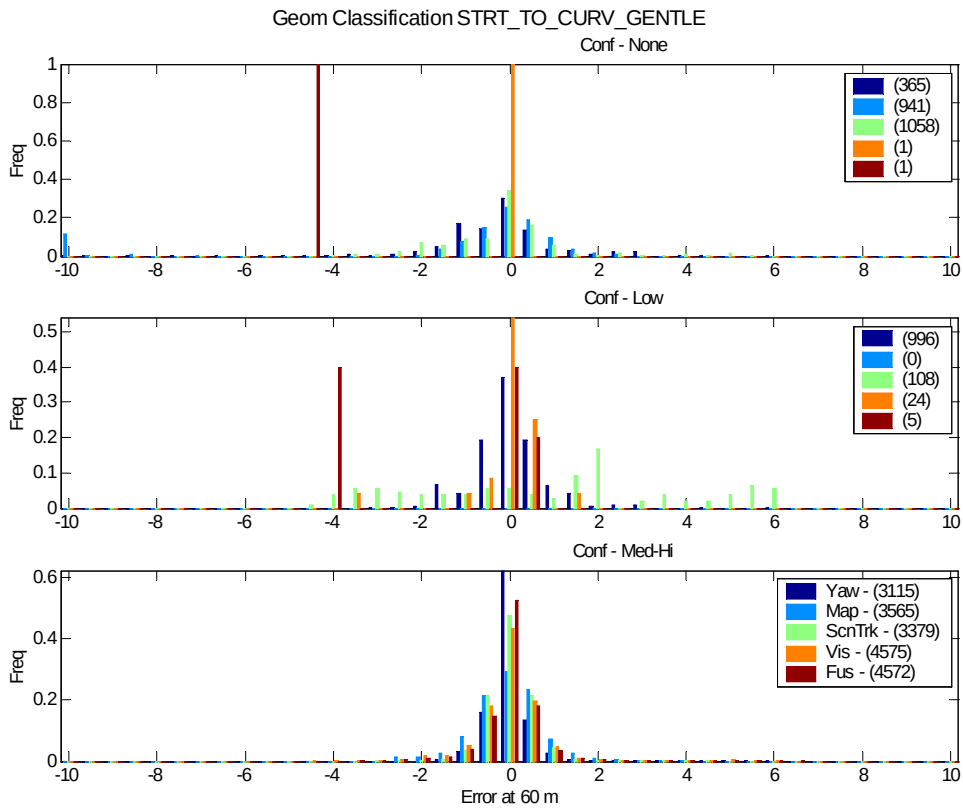

Figure 8.4 Histogram (pseudo-pdf) Distributions of Forward Geometry Errors. Road shape classified as *straight to gentle curve*. [Note: the number beside each legend is the number of sample measurements, per subsystem, per confidence class.]

Technical Problems

In the course of DF algorithm development and subsequent performance analysis on real data, several technical difficulties and challenges arose and had to be overcome. The initial fusion architecture was developed under the premise that the subsystems would provide reliable confidence estimates. In other words, if a subsystem was operating under conditions where it was unable to provide good estimates, it would associate the estimate with a zero or low confidence so that DF would ignore or give very low weighting to this subsystem. Since subsystems were not able to accurately assess the "goodness" of their estimates (we had to wait for real data in order to perform this analysis), we had to make some minor modifications to the fusion approach late in the program.

Fortunately, the initial architecture had envisioned this as a potential issue and we had made provisions for modifying subsystem confidences at the fusion end prior to fusing. As discussed in the technical approach section, this led to the consensus-based fusion (CNF) algorithm. While this approach works better than the confidence-based fusion (COF) algorithm, it is still limited in that (1) it needs at least two sensors to agree and (2) it will perform poorly when there is only one good sensor that does not agree with any other sensor. Thus, a hybrid approach based on combination of the two ideas is a better

solution. One of the major issues for the hybrid method is in developing a reliable approach to determine the "goodness" of subsystem estimates and confidences. We attempted to solve this problem by developing and incorporating some initial heuristics and rules that modify fusion under special conditions. More effort is needed in this direction to ensure that the rules are correct and applied under suitable conditions. Besides, since the number of rules is expected to increase exponentially with the number of conditions considered (and as more data is analyzed), advanced methods, such as machine learning, may be needed to automatically identify and extract these rules.

Another technical difficulty that we had to overcome was the lack of good tools available for data playback, ground-truth, and statistical analysis. We had not anticipated the need for such advanced tools at the start of the program. But in the very early stages of data analysis, we discovered the need for such tools and developed them quickly. These tools have served us very well by drastically reducing the manual effort needed to analyze data and tune the DF algorithms.

Significant Research Findings and Results

The main research finding of this task is that the DF subsystem must be robust and able to detect and handle situations when there is missing or invalid data.

1. The "new" road model is superior to a conventional single-clothoid road model as it produces smaller road geometry estimation errors, especially during sharp transitions in road curvature. In some of the simulation studies, during a transition from a straightaway to a 300m curvature segment, the single-clothoid road model had errors of about one-half lane width, while the new model had maximum errors on the order of less than one-quarter of a lane width. Better road geometry estimation should translate into lower errors in identifying in-path targets vs. out-of-path targets.
2. The Kalman filter fusion framework is robust and suitable for the forward geometry estimation problem. It allows a natural way to register subsystem outputs (geometry, confidences) in different coordinate systems and bring all measurements into a common framework. The noise-lag tradeoff is obtained by adjusting filter parameters.
3. The confidence outputs from the various subsystems cannot be directly used by the fusion system. Additional methods and heuristic rules are needed to effectively fuse the correct estimates and ignore the incorrect ones. Based on the analysis of limited driving data under different scenarios, it appears that consensus-based fusion approach can be further improved by identifying/developing special rules and heuristics that can be applied under special conditions. Some examples of such rules are those based on speed, detection of 90-degree turns, specific road types, etc. Since the number of such rules can potentially be very large and interact with each other, use of automated machine learning type methods is desirable.

Current Schedule and Progress for Task C1

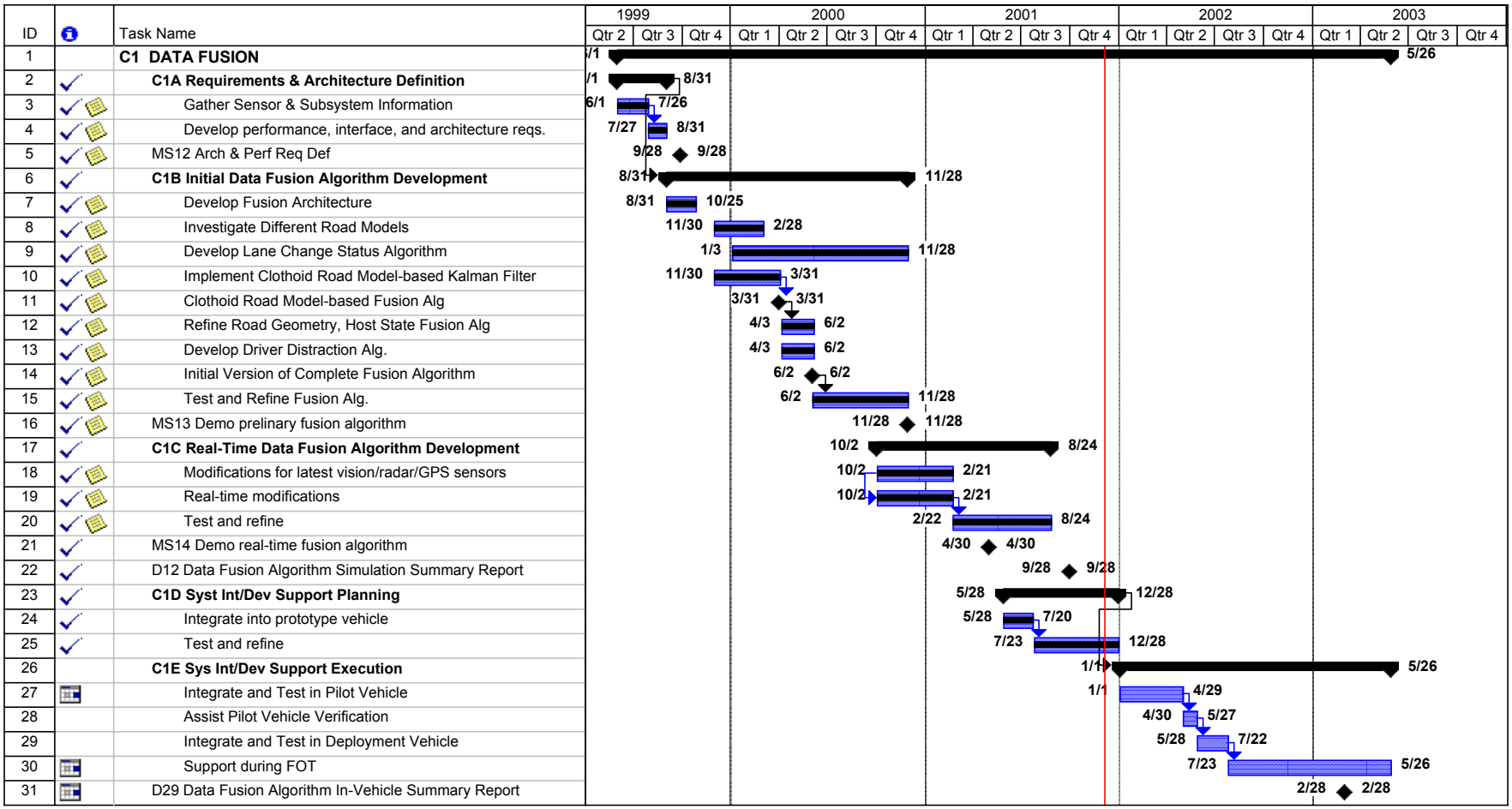

Figure 8.5 Task C1 Schedule

9 Tracking and Identification (Task C2)

The objectives of the Tracking and Identification task are to refine the Path Estimation and Target Identification algorithms, to incorporate Vision and Global Positioning System (GPS) derived information, to integrate these components into the FOT vehicle system, and to support Field Operational Test (FOT) deployment.

Significant progress has been made during the first phase of the Automotive Collision Avoidance System (ACAS) FOT program under Task C2. Delphi has been responsible for the Conventional Target Path Estimation (Task C2A) and radar-based Scene Tracking activities (Task C2B) associated with the Tracking and Identification Task. General Motors has been responsible for the Enhanced GPS approach (Task C2C). This section provides a summary of the major activities that were initiated and the achievements that were accomplished under these tasks.

9.1 Conventional Approach Development (Task C2A)

The performance of Delphi's conventional yaw rate based path estimation and target selection algorithms showed steady and continuous improvement during the first year of the ACAS/FOT program. These algorithms use the instantaneous roadway curvature at the host vehicle to predict the roadway characteristics in the region ahead of the host vehicle. The number of false target selections (incorrectly selected non-in path targets, such as adjacent lane or roadside objects), and missed detections (non-selected valid in-path targets) have been substantially reduced. However, the problem of estimating the correct host and target vehicle path has proven to be very complex. Consequently, during the second year of the ACAS/FOT program, modifications were made to the conventional path estimation algorithms to incorporate a fusion-based parametric representation of the host and road state.

Goals, Purpose and Background

Adaptive Cruise Control (ACC) and Collision Warning (CW) systems require an ability to robustly resolve and identify the existence of both stationary and moving 'target' vehicles that are in the motion path of the host vehicle. The performance of these systems is affected by their ability (1) to estimate the relative inter-vehicular path motion (range, relative speed, radius of curvature, etc.) between the host vehicle, the roadway ahead of the host, and all of the appropriate targets (roadside objects, in-lane, adjacent lane, and crossing vehicles, etc.); and (2) to predict the mutual intersection of these motion paths. In addition, these systems must be robust in the presence of various types of driving behavior (in-lane weaving/drift, lane change maneuvers, etc.) and roadway conditions (straight roads, curved roads, curve entry/exit transitions, intersections, etc.) that are encountered in the real-world environment.

The goal of Conventional Target Selection is to correctly identify all of the targets that are within the Host vehicle's path, and to select the primary in-path moveable and

stationary targets. Two primary approaches are used to estimate the forward host state and forward road state. The baseline target selection approach uses yaw rate and host vehicle speed to estimate the road curvature ahead of the host. State-based target selection uses a parametric representation of the host and road state to estimate the road geometry ahead of the host. Both approaches use radar derived target data to monitor the position and kinematic behavior of forward roadway and roadside objects. In order to identify the primary targets that are in the path of the host vehicle, the target selection algorithms must differentiate between in-lane and adjacent lane targets. They must also be robust enough to handle host and target vehicle lane changes, close range target cut-ins, driver variability due to host vehicle lane hunting and in-lane weaving, and changes in forward road curvature (i.e., curve entry and curve exit transitions).

Background

During the previous ACAS TRP Program (1994-1996), significant activities were undertaken to improve Delphi's first generation yaw rate-based path estimation and in-path target selection algorithms. The first generation path estimation algorithms used a single active forward looking radar sensor augmented with an inexpensive analog yaw rate sensor. The forward-looking radar sensor provided target range, range rate, and angular position information. The yaw rate sensor was used to estimate the roadway curvature ahead of the host vehicle. Delphi's first generation target discrimination algorithms were used to identify overhead bridge objects and to discriminate between moving cars and trucks. The target and host kinematics were evaluated to determine target motion status (oncoming, stopped, moving, cut-in and cut-out, etc.), and geometric relationships were employed to determine which of the valid roadway objects fell within the host vehicle's forward projected path. The improved algorithms yielded very good results, but they were prone to false alarms during curve entry/exit scenarios, during left and right turns, and during host lane changes.

Technical Approach

The Delphi radar sensor provides target position information relative to the host frame of reference. To be useful, the target position is transformed into a frame of reference that is relative to the host path and the road. This reference frame uses the *host's predicted lane center* to describe the path of the host vehicle, on both straight and curved roads. The determination of when a target vehicle is in the path of the host vehicle can be visualized as a *target selection zone*. The zone is defined by the left and right edges of the host vehicle's lane, the host's predicted position at some future time, the target's current longitudinal position and kinematics, and the length of time that the target has previously been in the zone.

During the first year of the ACAS/FOT program, the baseline Path Estimation algorithms used host speed, yaw rate, and a vision-based host state to estimate the *host's predicted lane center*. The low cost analog yaw rate sensor in the Delphi radar unit was replaced with a highly accurate and robust KVH digital yaw rate sensor. Additional rules and heuristics were added to reduce stationary object false alarms during periods of rapid curvature change, to improve moving target detection performance.

During the second year of the ACAS/FOT program, the path estimation algorithms were extended to use a fusion-based host and road state to approximate the *host's predicted lane center*. This fused state information was derived from the following four complementary approaches:

1. vision-based road prediction and host state estimation (Task B2)
2. GPS-based road prediction (Task C2C)
3. radar-based scene tracking (Task C2B)
4. yaw rate-based road and host state estimation (Task C2A)

These four approaches to road and host state estimation were then fused by the Data Fusion function (Task C1). The fused road and host state information was used to provide an improved estimate of the roadway shape/geometry in the region ahead of the Host vehicle, and an improved estimate of the host vehicle's lateral position and heading within its own lane. This fused information has been incorporated into the Tracking and Identification function (Task C2A) in order to provide more robust roadside object discrimination, and improve performance at long range, during lane change maneuvers, and during road transitions.

Both the baseline yaw rate and state-based path estimation algorithms have been fully tested and integrated into the ACAS/FOT Prototype vehicle. The target selection process selects between these two approaches based on the host and road state confidences and on the selected road geometry source(s) (e.g. vision, yaw, map, scene tracking, or prediction) that were used to update the fused host and road state measurements.

Relevant Activities

During the first phase of the ACAS/FOT program, significant progress has been made in enhancement and refinement of the path estimation and target selection algorithms, and in the integration, validation, and testing of the Target Selection subsystem within the ACC/FCW Prototype vehicle.

Algorithm Development

During the first year of the ACAS/FOT program, enhancements were made to the baseline path estimation and target selection algorithms to improve performance during curve transitions and host lane changes. The low cost analog yaw rate sensor in the Delphi radar unit was replaced with a highly accurate and robust KVH digital yaw rate sensor. Stationary Object false alarms were reduced by (1) refining target selection heuristics and persistency requirements, (2) optimizing target lane position estimation during severe right and left-hand turns, and (3) and rejecting bridge objects. The moving target cut in/cut-out response was improved by dynamically altering the shape of the target selection zone based on target lateral rate, acceleration, and proximity to the host

vehicle. An additional analysis and development effort was also undertaken to improve target selection performance at low speeds. The development effort utilized FOT steering sensor data together with a bore-sight based path estimation approach to estimate the host's predicted path at low vehicle speeds.

During the second year of the ACAS/FOT program, path estimation and target selection algorithms were modified to incorporate fusion-derived parametric estimates of the host and road state. The target selection algorithms were tuned to switch between the conventional yaw rate-based approach and the state-based fusion approach based on the data fusion confidence measures, the source and continuity of the fused road, and host state. In addition, improvements were made to shift the target selection zone to the adjacent lane during host lane changes, and to alter the zone's characteristics while the host was settling into the new lane.

We evaluated the accuracy and timeliness of the GPS landmark information (e.g. distance to intersection, fork, tunnel, T-junction, and intersection), road type (e.g., limited access road, surface street, paved road) , and road category (e.g., straight, straight to curve, s-curve, etc.). An analysis effort is currently underway to incorporate some of the road category information into the target selection process.

Figure 9.1 depicts a short road segment that contains a curve to straight to curve road segment. The different colored signals that are plotted depict the predicted road offset at a range of 60 meters ahead of the host vehicle. The horizontal blue and cyan lines that are labeled with text represent the road category information provided by the GPS/Map system. The legend on the lower right hand side of the figure maps the color of each road offset signal to its road geometry source. For example, the cyan signal indicates the road offset from an integrated ground truth. The dark blue signal indicates the road offset from data fusion's road state estimate, and the yellow signal indicates the road offset from data fusion's combined road and host state estimates. The green signal indicates the road offset from scene tracking, and the red signal indicates the road offset from GPS/Map. Finally, the black signal indicates the road offset from raw yaw rate and speed. The plot is illustrative of the type of signals that are correlated and fused to provide a parametric estimate of the road state.

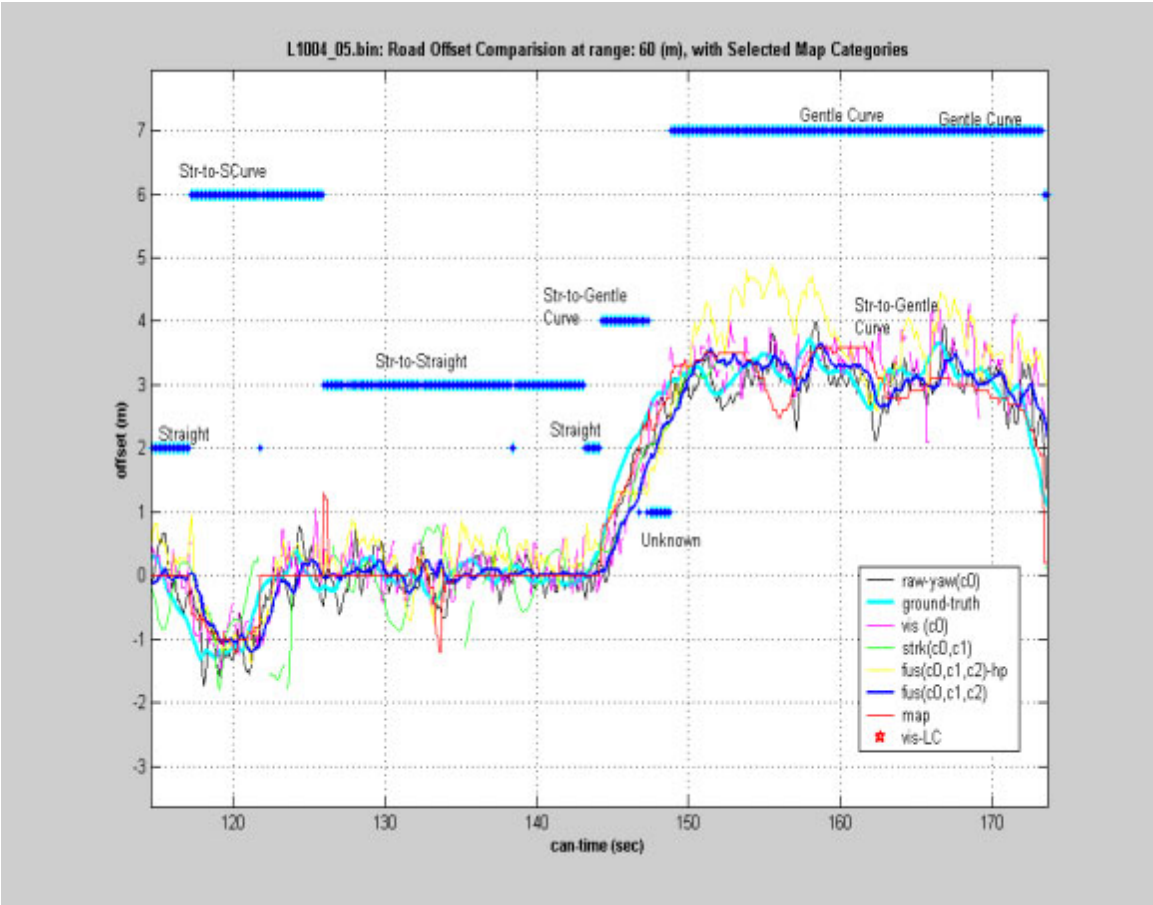

Figure 9.1 Road Offsets and Road Categories

Subsystem Integration

The target path estimation and target selection algorithms were integrated into a custom Delphi Radar Collision Avoidance Processor (RCAP) depicted in Figure 9.2 below. The RCAP unit has a Motorola 68332 processor and various on-board serial, A/D, and CAN interfaces.

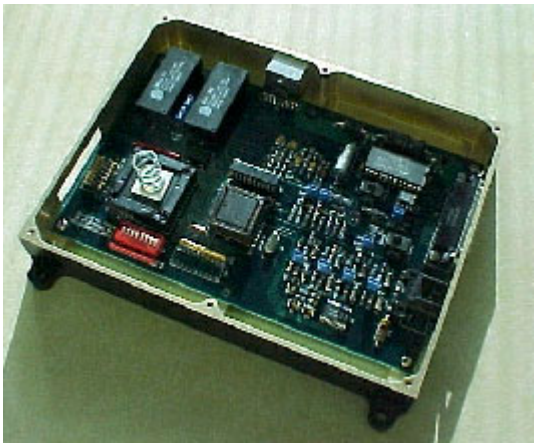

Figure 9.2 Target Selection Radar Collision Avoidance Processor

The Target Selection RCAP was interfaced to the following subsystems via a 500K CAN bus interface:

1. Delphi ACC/A Forward Looking Radar
2. GM Data Fusion subsystem
3. GM Sensor Processor
4. Delphi Driver-Vehicle Interface (DVI) subsystem
5. GM Threat Assessment subsystem

The timing and correct message content of the Target Selection subsystem has also been verified for all of the internal and external Target Selection interfaces.

During the first phase of the ACAS/FOT program, the Target Selection interface to the Delphi ACC-Alert (ACC/A) Radar Sensor and Vehicle Controller was modified to perform the following tasks:

1. Set up and initiate the radar instrumentation CAN bus output message
2. Override the internal ACC/A Radar yaw rate sensor with the more accurate external (KVH) digital yaw rate signal
3. Replace the primary in-path target selected internally by the ACC/A controller with the Closest In-Path Moveable Target (CIPV) identified by Target Selection
4. Direct the ACC/A radar controller to operate in either Conventional Cruise Control Mode (CCC) or Adaptive Cruise Control Mode (ACC) mode
5. Insert the user selected ACC/FCW gap setting into the ACC/A Controller

In addition, the Target Selection Processor was modified to provide the following primary in-path target information to Threat Assessment at all times:

1. a <u>yaw rate-based CIPV</u> target to both the ACC/A controller and Threat Assessment during ACC
2. a <u>fusion-based CIPV</u> target to the Threat Assessment subsystem, when ACC is off or CCC is on
3. a <u>fusion-based CIPS</u> (Closest In-Path Stopped Target).

Subsystem and System Testing and Validation

Figure 9.3 depicts the collaborative multi-stage integration, testing and validation efforts that occurred during the past year. The activities that were the focus of Target Selection testing and validation efforts are highlighted in orange. The test and validation activities shown in the figure were performed both on the Prototype vehicle, and in the laboratory. Extensive open road and track tests were performed on freeways, city streets, and rural areas of Southern California and Detroit to collect a robust suite of test data. Individual subsystem performance and overall ACC and FCW system performance were evaluated. Key areas of improvement and problematic scenarios were identified, corrected, and flowed down to the lower level subsystems. A real-time vehicle simulation bench was set up in Malibu, California to further test and validate all of the ACAS/FOT subsystems. Subsystem algorithms and interfaces have subsequently been improved, and the collected data has been re-run on the real-time bench to verify the improvements. Specialized tools were developed to perform a real-time playback of data collected on the Prototype vehicle, and to verify performance improvements.

<table>
<tr><th>STAGE 0</th><th>STAGE I</th><th>STAGE II</th><th>STAGE III</th><th>STAGE IV</th><th>STAGE V</th></tr>
<tr><td rowspan="2">Veh Interf Proc
External Yaw, Speed, ..</td><td>GPS/Map</td><td rowspan="3">Data Fusion
ST, LT, GPS, External Yaw</td><td rowspan="4">Tgt Selection
ACCA Tracker
Data Fusion
ST, LT, GPS, external Yaw</td><td rowspan="3">Threat Assess
Tgt Selection
ACCA Tracker
Data Fusion
ST, LT, GPS, external Yaw</td><td rowspan="6">Threat Assess.
ACCA Control
Tgt Selection
ACCA Tracker
Data Fusion
ST, LT, GPS, external yaw, DVI</td></tr>
<tr><td>Lane Tracking</td></tr>
<tr><td rowspan="3">ACCA Tracker (internal Yaw Rate Sensor)</td><td>Scene Tracking
(ACCA Tracker)</td></tr>
<tr><td>Tgt Selection
ACCA Tracker
(intern. yaw rate)</td><td>Tgt Selection
ACCA Tracker
(extern yaw rate)
Threat Assess.</td><td rowspan="3">ACCA Control
Brakes, Throttle
external yaw
ACCA Tracker
Tgt Selection</td></tr>
<tr><td>Brakes</td><td rowspan="2">ACCA Controller
Brakes, Throttle,
ACCA Tracker</td><td colspan="3" rowspan="2">ACCA Controller
Brakes, Throttle,
External Yaw Rate
ACCA Tracker</td></tr>
<tr><td>Throttle</td></tr>
</table>

Figure 9.3 Collaborative Multi-Stage Prototype Integration, Testing and Validation

The yaw rate-based Target Selection subsystem was first integrated with the ACC/A radar sensor during stage I of the integration effort. During this stage, Target Selection utilized the yaw rate signal that was internal to the radar sensor. At the same time, the GPS/Map, Lane Tracking (LT), and Scene Tracking (ST) subsystems were being individually tuned in the lab, in simulation, and on the Prototype vehicle. The ACC/A controller was also being integrated and tuned with the Prototype vehicle's brakes and throttle.

During Stage II, Target Selection was integrated with the external digital yaw rate sensor, and the Threat Assessment subsystem. Target Selection was also modified to insert the more accurate digital yaw rate signal directly into the ACC/A radar, in order to improve the performance of the ACC/A tracker. At the same time, the Data Fusion subsystem was integrated with the external yaw rate and vehicle speed provided by the sensor processor, and with the road and host state estimates from the Scene Tracking, Lane Tracking, and GPS/Map subsystems.

During Stage III, the state-based version of Target Selection was integrated with Data Fusion. At the same time, the tuning continued on the closed loop ACC/A controller, using the Prototype brakes, throttle, speed, and external yaw rate sensor.

During stage IV, the state-based Target Selection subsystem was integrated with both Data Fusion and Threat Assessment. At the same time, the yaw-based module was integrated with the ACC/A radar and controller. The closed loop control of the system was then evaluated using the CIPV that was selected by the yaw-based target selection module. During this stage, the performances of the conventional yaw rate-based and fusion state-based target selection approaches were compared and evaluated with real-time data collected with the Prototype vehicle. Performance was evaluated in terms of road type, host dynamics, and accuracy of the fusion road and host state versus confidence. Key areas of improvement and problematic scenarios were identified, and corrected.

During stage V, the Target Selection subsystem was evaluated within the context of the overall Prototype ACC/FCW system. Both the yaw rate-based and state-based target

selection approaches were integrated with the ACC Controller and Threat Assessment subsystems. Target Selection was modified to provide the following:

1. a yaw rate-based CIPV target to Threat Assessment and the ACC Controller during ACC
2. a state-based CIPV target to Threat Assessment when ACC was off, or CCC was on
3. a state-based CIPS to Threat Assessment at all times

Testing during this stage was carried out both in California and in Michigan.

Diagnostic Tools

Delphi has developed a suite of data collection and analysis tools to:

1. observe near real-time and real-time system behavior while performing system integration on laboratory bench hardware
2. evaluate real-time system performance while performing on-road vehicle testing
3. perform in-depth ACC/FCW system data analysis and quantify ACC/FCW system performance
4. iterate, refine, and validate key algorithm improvements with collected road test data, both in simulation and on the lab bench

Figure 9.4 summarizes Delphi's validation and refinement process and the suite of tools that are used. The data collection and validation process can be performed in real-time on a vehicle or on lab bench hardware. A PC-type laptop computer is used to interface to the CAN bus and to host the various data collection tools. The tools consist of various graphically oriented Delphi data collection and playback utilities, and a video system (camera, 8mm video recorder, and mixer) which is used to mix time-stamped video with the graphical output from the Delphi diagnostic tools. A commercial Canalyzer™ CAN bus utility, by Vector CANtech, is also used to generate test vectors and to gather CAN bus timing measurements.

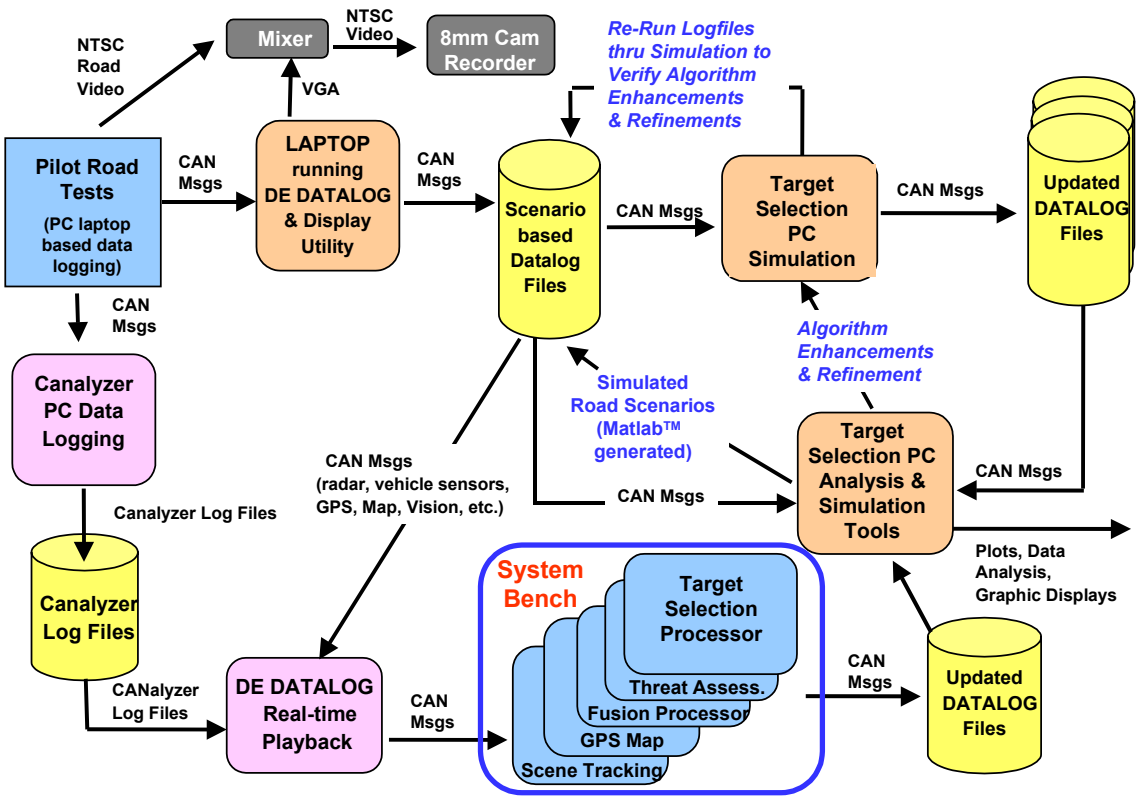

Figure 9.4 Subsystem Test, Validation, and Refinement Process

Delphi's custom utilities and tools are used to dynamically record performance results and interfaces for various key ACC/FCW subsystems, and to graphically depict the target environment and road geometry in front of the ACC/FCW vehicle. Delphi's CAN bus recording utility records, collects, time stamps, and displays all of the system's CAN bus messages and events, in real-time. The data recorded by these utilities, as well as by Delphi's Matlab™ based road scenario generator are used to build up a scenario database. The database can then be played back, in real-time, through the system bench hardware. This playback capability provides a mechanism to refine and iterate the various subsystems, and verify key algorithm improvements.

In addition, custom Matlab™ tools have been developed to decode the CAN bus data collected on the test vehicles. The data is categorized by subsystem (Radar, Threat Assessment, Fusion, Vision, Scene tracking, GPS/Map, Target Selection, ACC, Brakes, Sensor Processor, etc.). Performance statistics are accumulated, and road and host state information is extracted, correlated, and compared with computed ground truth data.

Figure 9.5 depicts one of Delphi's graphical target displays in a split screen video format.

Figure 9.5 Delphi Diagnostic Tracking and Identification Display

The middle portion of the display contains text describing the Target Selection, Lane Tracking, Scene Tracking, Data Fusion, and Radar subsystems. The radar trackfile data is displayed on the lower portion of the screen. The radar track features of the CIPV target are highlighted in blue in both the lower and upper left portions of the screen.

The upper portion of the screen depicts a real-time graphical representation of the detected radar scene targets. The exterior color of the rectangles is based on relative target speed. For example, green rectangles denote targets "moving away" from the host vehicle, red rectangles denote targets that the host vehicle is "closing on." Magenta rectangles denote "oncoming" targets (targets traveling in the opposite direction). Yellow rectangles denote targets that are "matched in speed" to the host, and white rectangles depict "stationary" targets. The relative size of the rectangular-shaped "targets" is based on the target range and in-path target status. The "narrow" rectangle boxes denote "non-primary in-path" target. The large rectangle with the dark blue center denotes the CIPV target , and a large white rectangle with an oval green center (not shown), denotes the CIPS target.

The colored lines and curves on the upper portion of the screen graphically depict the estimated forward road offsets and lane boundaries from the various FOT subsystems. The green lane boundaries represent the road offsets from Scene Tracking, the red lane boundaries represent the lane boundaries from Lane Tracking, and the blue lane boundaries represent the road offsets from Data Fusion. Yellow lane boundaries represent the road offsets from raw yaw rate and speed, and the gray lane boundaries represent the road offsets from filtered yaw rate and speed.

The upper left portion of the screen describes the target attributes of CIPV and CIPS Targets. In addition, the target ID and level of the threat identified by Threat Assessment is displayed under the CIPV and CIPS information. Below the threat assessment information, road categories from the GPS/Map subsystem are displayed. In this example, the road categories of paved road (PAV), and surface street (SST) are displayed.

The upper right portion of the display depicts the host vehicle speed, host yaw rate, radar scan index and radar software version. Below the radar data, GPS/Map road structure information is displayed. This information describes structures such as the location of T-junctions, intersections, forks, tunnels, etc.

The lower right portion of the screen is used to display real-time video imagery of the roadway environment ahead of the host vehicle. This video-based diagnostic system is an extremely useful tool. It provides a mechanism to review lengthy time segments of "on-road" data, and to isolate time segments with marginal or questionable performance. Once identified, voluminous files of more detailed sensor and system data, recorded together with the video, can be more carefully investigated, to determine the precise cause of any observed anomalies or unusual results.

Intermediate and Final Results

This section will discuss the overall Target Selection task accomplishments and performance. A summary of Target Selection's performance on the verification tests will also be provided.

The baseline path estimation and target selection uses a yaw rate-based path for moving and stationary targets. Overall yaw rate-based Target Selection performance on freeways is excellent due to the improvements made to bridge discrimination. In addition, enhanced target selection persistency heuristics have helped to significantly reduce the number of stationary false target selections (targets that have been incorrectly identified as in-path targets) during lane changes and curve entry / exit scenarios.

The use of the fusion-based host state has eliminated many of the stationary false target selections that were caused by host lane changes, and curve entries and exits. In addition, the overall performance of the individual Vision, GPS/Map, and Scene Tracking subsystems, which are used to derive the fused road state, have improved significantly during the first phase of the program. However, some form of long-range vision is still needed to further reduce the rate of curve entry / exit false target selections on winding rural roads with tight curvature. Moreover, some additional work is still needed to further minimize false alarms during host left and right turns through intersections, and during approaches to road forks.

A series of verification tests were performed on the Prototype vehicle, both on the open road and at the General Motors Milford Proving Grounds, in Michigan. A representative sample of the open road and Milford track tests will be discussed in the next section.

Milford Straight Road Verification Tests

Figure 9.6 depicts the video scene from a Straight Road Stationary Object Collision Alert test that was run at the Milford test track. In this particular scenario, the host approached a stopped car on the left lane of a straight two-lane highway, at a speed of approximately 61mph. At the end of the test run, the host vehicle swerved to avoid a collision with the parked vehicle.

Figure 9.6 Video Frame from a Straight Road Stationary Object Collision Alert Test

Figure 9.7 summarizes the performance of the Target Selection subsystem on a representative Straight Road Stationary Object Collision Alert test run at Milford. The figure is divided into three distinct sub-plots. The x-axes of each of the three plots correspond to the radar scan index of the active radar scan. The scan index measurements are updated ten times per second.

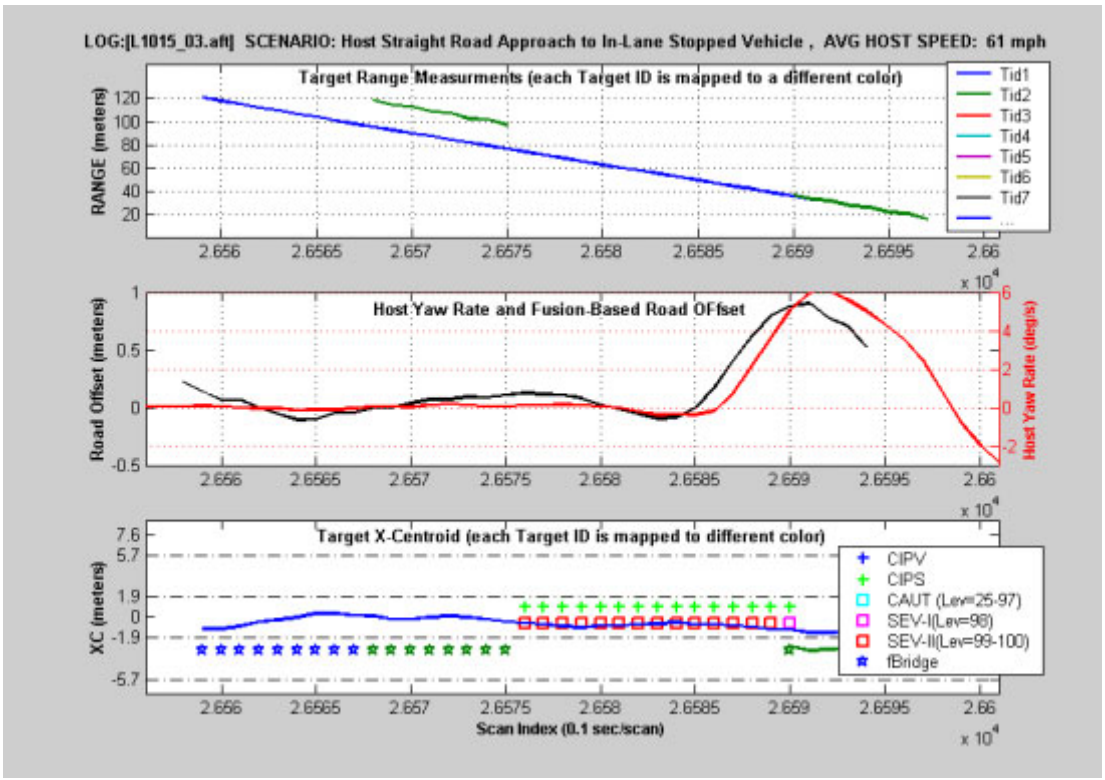

Figure 9.7 Straight Road Stationary Object Collision Alert Test Result

The upper plot depicts the closing ranges of all of the valid radar scene targets. The range measurements for each target are represented by a different color. For example, target ID 1 is blue, target ID 2 is green, etc. The range plot shows that target ID 1, the primary track on the in-lane stopped object, was detected from 120 meters to 36 meters. Target ID 2 is a second track that corresponds to a road-side object which appears briefly from 120 to 100 meters. The stopped in-lane vehicle breaks into two tracks (target ID 1 and target ID 2) at a range of approximately 38m, when the host vehicle begins to swerve to avoid a collision with the stopped car.

The middle plot depicts the host vehicle yaw rate, and the road offset from data fusion at the range of the in-lane CIPS target. The host yaw rate signal is colored red and its y-axis is on the right hand side of the plot. The road offset from data fusion is depicted in black, and its y-axis is on the left-hand side of the middle plot.

The plot in the bottom section of the figure depicts the cross-range position of the in-lane target during the host vehicle's approach. The stars on the lower plot indicate that a given target has an "off-road bridge" designation. As in the upper plot, the cross range measurements and bridge designations for each target are drawn in a different color. The green 'plus' marks denote the target ID of CIPS target identified by Target Selection. Similarly, the colored squares drawn on the lower plot indicate threat level of the CIPS target, as determined by the Threat Assessment subsystem. It should be noted that while Target Selection processes stopped targets with an "active bridge" designation, bridge targets cannot be selected as the CIPS target. Thus, target ID 1 was identified as the CIPS target at 76 meters, the scan after it lost its bridge designation. During this time, the target was also flagged as a severe threat. Target ID 1 was killed at 36 meters as the host began to swerve to avoid the stopped car. Target ID 1 was eventually replaced by target ID 2. However, since the host had swerved to the right, the position of target ID 2 was no longer within the host vehicle's forward path, and the target was not selected as the CIPS target.

Figure 9.8 summarizes Target Selection performance on a representative Straight Road Moving Vehicle Collision Alert test. During the course of the test, the host vehicle approached a slow moving vehicle at 50 mph, on the right lane of a two-lane divided highway. The host vehicle began to swerve to avoid a collision vehicle at about 45 meters from the lead vehicle.

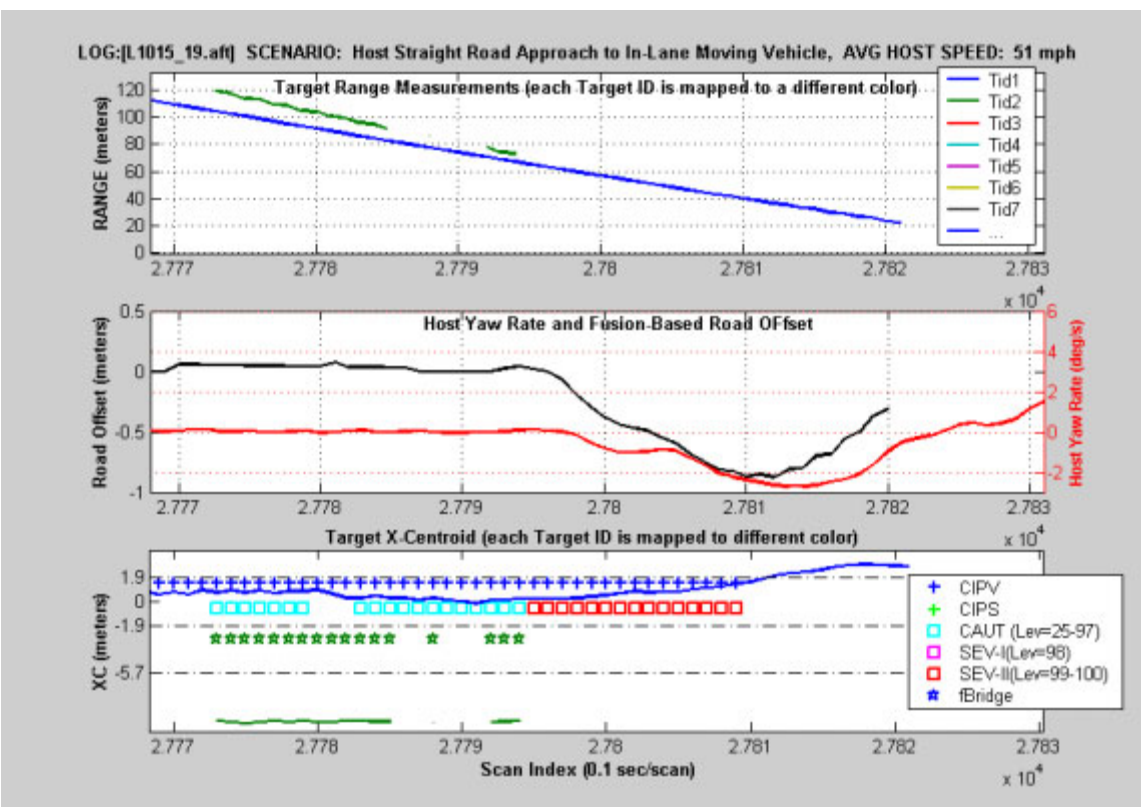

Figure 9.8 Straight Road Moving Vehicle Collision Alert Test Result

Figure 9.8 is divided into three distinct sections similar to those in Figure 9.7. The top sub-plot of the figure depicts the closing range to the lead moving vehicle. The vehicle is represented by target ID 1, and it is plotted in blue. This target was first detected at a range of 130m. The green range plot shown for target ID 2, corresponds to a roadside stopped object that is passed by the host vehicle. The middle section of the figure depicts the host vehicle yaw rate and estimated road offset from Data Fusion. The lower plot depicts each target's cross range position and bridge designation. The green target position signal represents target ID 2, and it is to the left of the host vehicle. The blue signal represents target ID 1, and it is close the host vehicle's bore-sight. The dark blue 'plus' marks on the lower plot denote the target ID of the CIPV target that was identified by the Target Selection subsystem. Similarly, the colored squares drawn on the lower plot indicate threat level of the CIPV target, as determined by Threat Assessment.

In this test run, the in-lane moving target was flagged as the CIPV by target selection at 124 meters. The target remained the CIPV until 42 meters, at which time the host began to swerve, and the target fell outside the host vehicle's predicted path. Similarly, Threat Assessment flagged the CIPV target as a severe threat from 65 meters to 43 meters.

Milford Curved Road Verification Tests

Figure 9.9 depicts the video scene from a Curved Road Stationary Object Collision Alert test that was run at the Milford test track. In this particular scenario, the host approached a stopped car on an approximately 500 meter curve, at a speed of 50 mph. The stopped vehicle was parked on the right lane of a two-lane divided road. At the end of the test run, the host vehicle swerved to avoid a collision with the parked vehicle.

Figure 9.9 Video from a 500m Curved Road Stationary Object Collision Alert Test

Figure 9.10 summarizes Target Selection performance on the Curved Road Stationary Object Collision Alert test. The figure is divided into three distinct sub-plots, similar to those discussed previously. The top plot depicts range to the stopped target. In this case, the middle plot depicts the host yaw rate and estimated roadway radius of curvature from the Data Fusion subsystem, rather than the road offset. The bottom plot depicts each target's cross-range lane position (XOLC), bridge status, and the overall system CIPS and threat status.

The top plot shows that the stopped in-lane vehicle was not tracked as a single continuous track. The object was first detected at 120 meters as track ID 1. This track subsequently died at 100 meters and was replaced with track ID 2. Track ID 2 then coasted out and died at 80 meters, and was replaced by the new track with ID 1. Track ID 1 remained active from 80 meters to 20 meters. This 'breaking up behavior' was observed on numerous high speed test runs with stationary objects in curves. Data analysis later determined that there was a software bug in the ACC/A radar tracker's angle rate estimation process. The bug was found to cause targets with high range rates and high lateral angle rates to move out of their angle gates, and be coasted and killed. This tracker problem has subsequently been fixed, and these curved road tests will be re-run at the start of the next phase of the program.

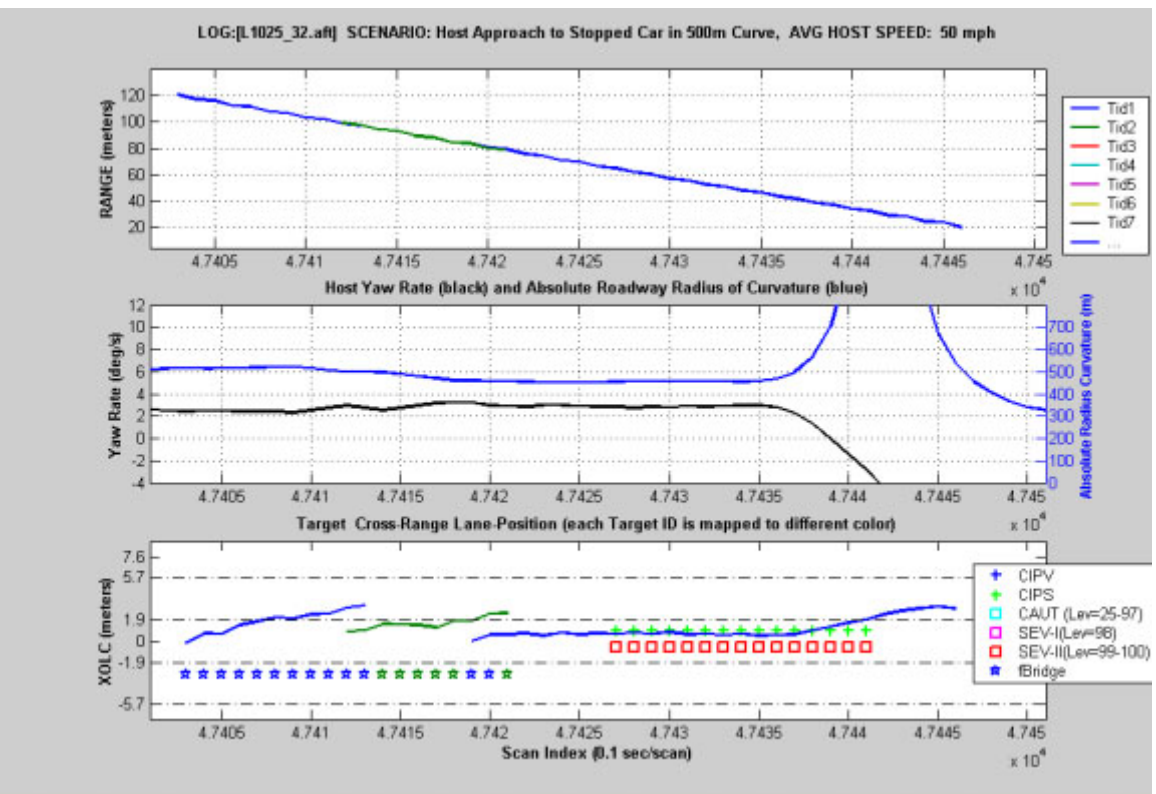

Figure 9.10 500m Curved Road Stationary Target Collision Alert Test Results
The lower sub-plot of Figure 9.10 depicts each target's cross-range lane position (XOLC) and bridge designation (star symbols). The target XOLC measurement indicates the target positions relative to the estimated host lane center provided by Data Fusion.

The green 'plus' marks denote the target ID of the CIPS target that was identified by Target Selection. Similarly, the red colored squares drawn on the lower plot indicate the level of the CIPS target threat. In this case, target ID 1 was identified as the CIPS target with a severe threat level from 66 meters to 38 meters. This XOLC plot also reflects the 'target break-up' behavior observed in the upper range plot. The consequence of the non-continuous tracking of this stopped object is that the Target Selection subsystem was only able to obtain a mature valid track on the stopped object at approximately 78 meters, rather than at the 120 meter range at which the object was first detected. This range reduction subsequently reduced the overall CIPS detection range and threat warning range. It should be noted that Target Selection treats stationary and moveable targets differently in terms of the following:

1. the criteria for determining target validity
2. size and characteristics of the target selection zone used to make in-path target decisions
3. type of filtering applied to target position measurements
4. the amount of persistency required for a target to be confirmed as the CIPS or CIPV target

One of the critical issues for Target Selection is to balance the responsiveness of the system with the need to minimize false alarms. Thus, there is a trade off between added persistency to reduce false alarms and the need for a rapid detection response. In this example, several additional cycles of persistency were required to confirm the in-lane stopped target as the CIPS target once it became a valid mature track.

Figure 9.11 depicts the video scene from a Curved Road Moving Vehicle Collision Alert test that was run at the Milford test track during a rain storm. In this particular scenario, the host followed a moving vehicle from a straight road on to an approximately 300 meter curve, at a speed of 48 to 50 mph. The moving vehicle was approximately 60 meters from the host during the first part of the test run. Toward the end of the test run the lead vehicle began to decelerate. The host closed on the lead car and eventually made a severe lane change to avoid a collision with the lead car.

Figure 9.11 Video from a 300m Curved Road Moving Vehicle Collision Alert Test

Figure 9.12 summarizes Target Selection performance on one of the Curved Road Moving Vehicle Collision Alert tests. The top plot depicts the range to the lead moving vehicle. The middle plot depicts the lead vehicle's range rate (colored in blue) and host yaw rate (colored in red). The range rate y-axis scale is on the left of the middle sub-plot, and the yaw rate y-axis scale is on the right of the middle sub-plot. The bottom sub-plot depicts each target's cross-range lane position (XOLC), bridge status, and the overall system CIPV status and threat status. The host and lead targets were matched in speed for most of the test run. Near radar scan index 50890, the lead vehicle began to decelerate and the target closing range rate became increasingly more negative.

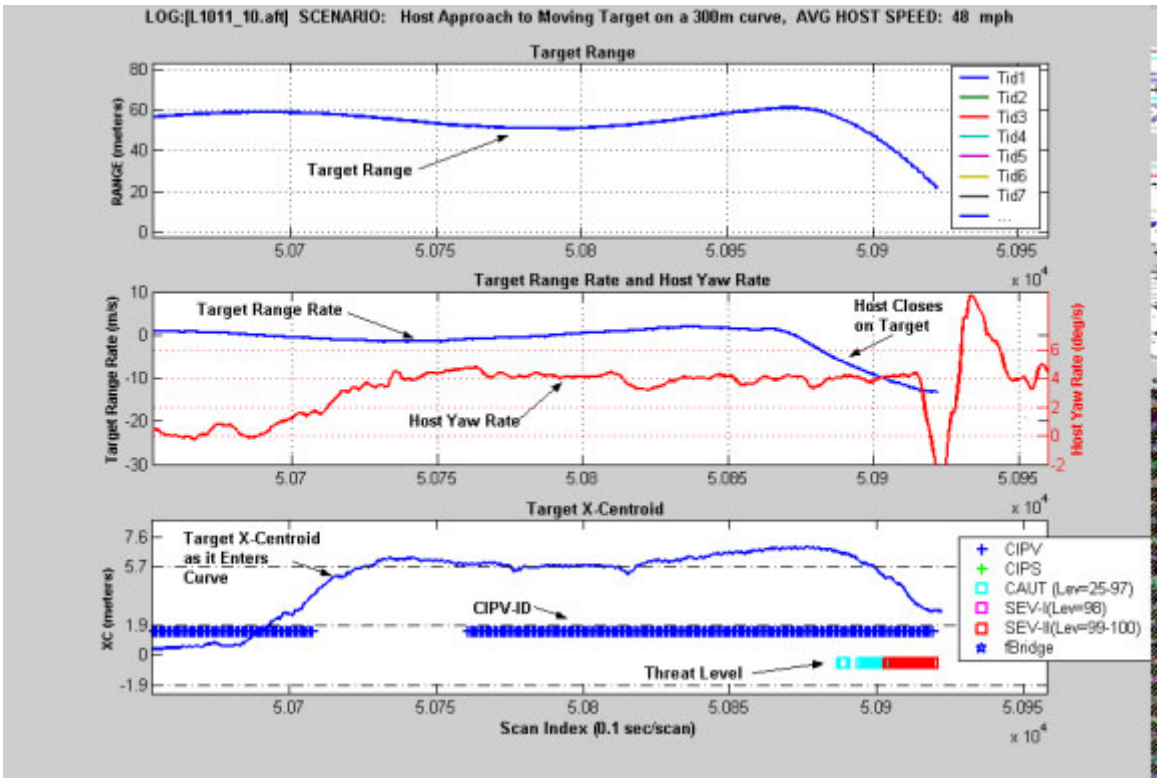

Figure 9.12 300m Curved Road Moving Target Collision Alert Test Results

The lower sub-plot depicts the lead vehicle's target position during the test run. The blue 'pluses' on the plot indicate that the lead vehicle with target ID 1, was chosen as the CIPV target by the Target Selection subsystem. The lead vehicle was dropped as the CIPV when the target entered the 300 meter curve from the previously straight road segment. The lead vehicle was then reacquired as the CIPV target when the host vehicle entered the curve. Near the end of the test run when the lead vehicle began to slow down, its closing range rate increased. Consequently, the Threat Assessment subsystem designated the CIPV target as a caution threat (cyan square). Then, as the target's closing rate increased, the CIPV target was designated as a severe threat (red square symbol). The lead vehicle was finally dropped as the CIPV and as a threat when the host vehicle made a lane change out of the lead vehicle's path. It should be noted that during this test run, the computed road and host state estimates from Data Fusion were only derived from yaw rate and speed. This was due to the following factors: (1) the vision-based Lane Tracking subsystem had low confidence due to the rain, (2) no GPS/map data was available for the test track, and (3) the Scene Tracker's confidence was low due to lack of moving roadway vehicles. The consequence of only operating with yaw-rate based road state estimate was that there was little preview of the curve entrance during the test. This was illustrated as the CIPV target was dropped during the curve entrance.

Open Road Sub-System Verification Tests

Various open road sub-system verification tests were performed in the Detroit and Los Angeles areas. The open test sub-system verification tests covered freeways, one and two lane highways, straight and winding rural roads, congested city streets, and intersections. The road surfaces were both paved and unpaved. Some of the roads had well defined lane markers, and others did not. Tests were performed both during the day and at night. Moreover, the traffic density varied from heavy to non-existent.

An open road sub-system verification test was held on 10-04-01, in the Detroit area (shown in Figure 9.13). The test route was based on the CAMP program's Night Route. The route covered a distance of 90 miles, and took approximately 2.2 hours to complete. An overview of the route is depicted in the map below.

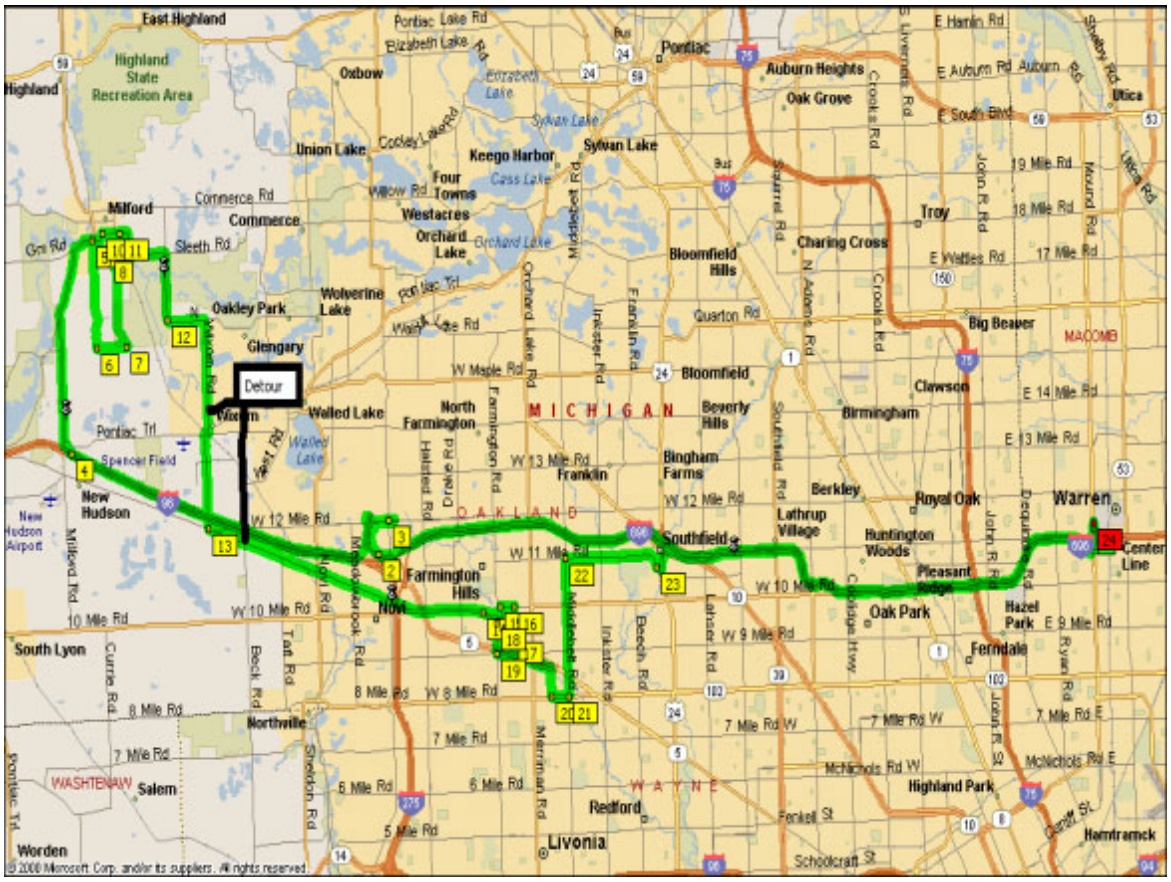

Figure 9.13 10-04-01 Sub-System Verification Short Test Route, held in the Detroit Area

Tables 9.1 and 9.2 summarize the Target Selection sub-system's performance on the 90 mile Short Route sub-system verification test held on 10-04-01. Table 9.1 breaks the detected Closest In-Path Stationary Target (CIPS) events into the three road classes: (a) freeways, (b) well marked limited access highways and city streets, and (c) poorly marked rural roads and winding roads.

Table 9.1 Summary of the Short Route 10-04-01 Sub-System Tests vs. Road Type

	False CIPS Events per hour (15 mph to 68 mph)	False CIPS Audible Alerts per hour (15 mph to 68 mph)
Freeways	0	0
Well Marked Limited Access Highways and City Streets	8	2
Poorly Marked and Winding Rural Roads	16	5

Table 9.1 shows that no false CIPS targets or audible alerts were generated on any of the multi-lane freeways in the Detroit area. On well-marked city streets and limited access highways, an average of eight false CIPS targets were observed per hour of driving, over speed ranges of 15 mph to 68 mph. Approximately two audible false alerts per hour were generated from the CIPS target data. On poorly marked paved and unpaved winding rural roads an average of 16 false CIPS targets were observed per hour of driving, over speed ranges of 15 mph to 60 mph. However, in this case, only five audible false alerts were observed per hour of driving.

The majority of the false CIPS targets were detected during curve entry and exit scenarios on winding rural roads, or during left and right turns through intersections. Most of these false CIPS detections did not trigger audible alerts for the following reasons: (a) the host speed was below the FCW operating range, (b) the host was braking, or (c) the CIPS event did not persist for a significant amount of time.

Table 9.2 breaks the detected Closest In-Path Stationary Target (CIPS) events into eight distinct road categories. The road categories are defined as follows:

1. Left and Right Hand Turns through Intersections
2. T-junctions and Road Forks
3. Curve Entries and Exits
4. Overhead Signs and Bridges
5. S-Curves
6. Road Jogs (road transitions in which the host lane jogs to the right or left
7. Host Lane Changes
8. Host State Errors on Straight Roads

Table 9.2 shows that overall, 17.7 false CIPS events and 2.7 valid CIPS events were observed per each hour of driving. Moreover, approximately 4.5 audible false CIPS alerts were observed per each hour of driving, and one valid audible CIPS alert was observed during the entire test 2.2 hour run. The valid CIPS events were typically due to host approaches and lane changes toward stopped cars at intersections, on both straight and curved roads. The majority of the false CIPS targets were detected during curve entry and exit scenarios on winding rural roads, or during left and right turns through intersections.

Table 9.2 Summary of 10-04-01 Open Road Sub-System Tests vs. Road Category

Test Log File	Test Run Time (min)	Left Turns & Right Turns	T-Junct and Forks	Curv Entry & Exit	Over-head Signs & Bridge	S-Curve	Road Jog	Host Lane Change	Straight Roads (due to Host State Errors)	Total FA CIPS or FA Audio Alerts	Valid CIPS Events
00 -- CIPS	35 min									0	2
01 -- CIPS	23.4 min		3	9		2	2		2	18	
02 -- CIPS	21 min	3		2			3			8	
03 -- CIPS	11.2 min	1	1	2			1			6	1
04 --CIPS	30.4 min	1	1	4				2	1	7	2
05 -- CIPS	11.5 min									1	1
TOTALS CIPS-EVENTS	132.5 min (2.2hrs)	**5**	**5**	**17**	**0**	**2**	**5**	**2**	**3**	**39 (17.7 CIPS per hour)**	**6**
TOTALS CIPS AUDIBLE ALERTS	132.5 min (2.2 hrs)	**0**	**0**	**4**	**0**	**1**	**2**	**1**	**2**	**10 (4.5 audio alerts per hour)**	**1**

Test segment 1 had the most false CIPS events and false audible alerts. Much of this test segment contained numerous winding rural roads, few roadway vehicles, irregular or missing lane markers, and uneven pavement. Two of the false CIPS events on this test segment were caused by heading errors in the vision-based host state. The heading errors were attributed to severe vertical curvature and a roadway exit. The majority of the freeway driving occurred during test segment 0. This segment had no false CIPS events, and two valid CIPS events. No audible alerts were observed during this test segment.

Figures 9.14 through 9.17 contain video snapshots of various freeway scenarios and valid CIPS scenarios from test segment 0. The white circles drawn on the video segments illustrate the location of valid CIPS events (host approach to an in-lane stopped car, etc.).

Figure 9.14 Typical Freeway Segment with Overhead Bridges (No false CIPS targets)

Figure 9.15 Typical Freeway Roadway Segment, Numerous Trucks and Cars (No false CIPS targets)

Figure 9.16 Valid CIPS Event on Host Lane Change Left into Adjacent Lane Stopped Vehicle
(Host Speed: 35 – 15 mph,
CIPS Range: 46 -12 meters)

Figure 9.17 Valid CIPS Event on Intersection Approach
(Host Speed: 45 – 10 mph,
CIPS Range: 49 -15 meters)

Figures 9.18 – 9.26 contain video snapshots indicative of the roadway scenarios that caused false CIPS events during the November 4th validation test run. The white circles drawn on the video segments illustrate the location of the false CIPS events.

Figure 9.18 Straight Road False CIPS Event and Audible Alert Caused by Effect of Divergent Right Lane Marker on the Vision-Based Host Heading
(Host Speed: 37 mph, CIPS Range: 42 meters)

Figure 9.19 Straight Road False CIPS Event and Audible Alert Caused by Effect of Vertical Road Curvature on the Vision-Based Host Heading
(Host Speed: 39 mph, CIPS Range: 50 meters)

Figure 9.20 False CIPS Event Due to a Road Fork, No Audible Alert
(Host Speed: 22 - 14 mph, CIPS Range: 76 to 24 meters)

Figure 9.21 False CIPS Event Due to a T-Junction, No Audible Alert
(Host Speed: 27 - 16 mph, CIPS Range: 67 to 53 meters)

Figure 9.22 False CIPS Event Due to a Right Turn Followed by a Left Turn, No Audible Alert (Host Speed: 15 mph, CIPS Range: 28 to 30 meters)

Figure 9.23 False CIPS Event Due to a Right Turn, No Audible Alert (Host Speed: 21 mph, CIPS Range: 53 to 48 meters)

Figure 9.24 False CIPS Event and Audible Alert Due to an S-Curve
(Host Speed: 32 mph, CIPS Range 54-33 meters)

Figure 9.25 False CIPS Event and Audible Alert Due to a Curve Entry (Host Speed: 35-38 mph, CIPS Range 71- 54 meters)

Figure 9.26 False CIPS Event and Audible Alert due to Triple Host Lane Change Right (Host Speed: 47 mph, CIPS Range: 34 to 20 meters

The Scene Tracking, Lane Tracking, and GPS/Map subsystems were operational during most of the open road validation testing. A consensus version of Data Fusion was used to estimate the host and road state from these subsystems. The fused host and road state helped to improve the overall FCW system performance, especially during host lane changes, during road jogs, and during gentle curve transitions. However, three of the observed false CIPS events were caused by errors in the host state. These errors have been attributed to severe vertical curvature and divergent lane markers. In the validation tests, the curve entry exit road category had the largest number of false CIPS events. During many of these events, there were not enough moving cars on the road for the Scene Tracking subsystem to provide a confident estimate of the forward road geometry. Moreover, the short range vision system used on the host vehicle was only able to provide host state and near range road curvature. In addition, when map information was available, the GPS/Map subsystem was able to provide some curve entry and exit preview. However, the GPS/Map road state information was infrequently incorporated into the consensus form of Data Fusion due to the low map confidence and disparity with regards to the other subsystems.

Figure 9.27 depicts valid road offsets from various FOT subsystems at a range of 60 meters from the host vehicle. The plot shows a straight road segment that transitions into a right curve, and then into a left curve. The road offsets from Scene Tracker are depicted in green, the road offsets from GPS/Map are depicted in red, the road offsets from Vision-based Lane Tracking are depicted in magenta, and the road offsets from Data Fusion are depicted in dark blue. As a baseline, the road offsets from raw yaw rate and speed are depicted in black, and the road offsets from an integrated non-causal

ground truth are depicted in cyan. The figure shows that GPS/Map provides a slight preview to raw yaw rate, followed by Vision, Scene Tracker, and finally Data Fusion. The vision-based Lane Tracking offsets are fairly noisy, and the Scene Tracker offsets appear to be noisy during the straight road and curve exit segments, but accurate during the curve segments. The Data Fusion road offsets are comparable to a nicely smoothed composite of all of the signals, with a lag of about 2 seconds from the ground truth during the curve entry transition and about a second during the curve exit transition. During the curve the Data Fusion road offsets appear fairly well matched to the ground truth.

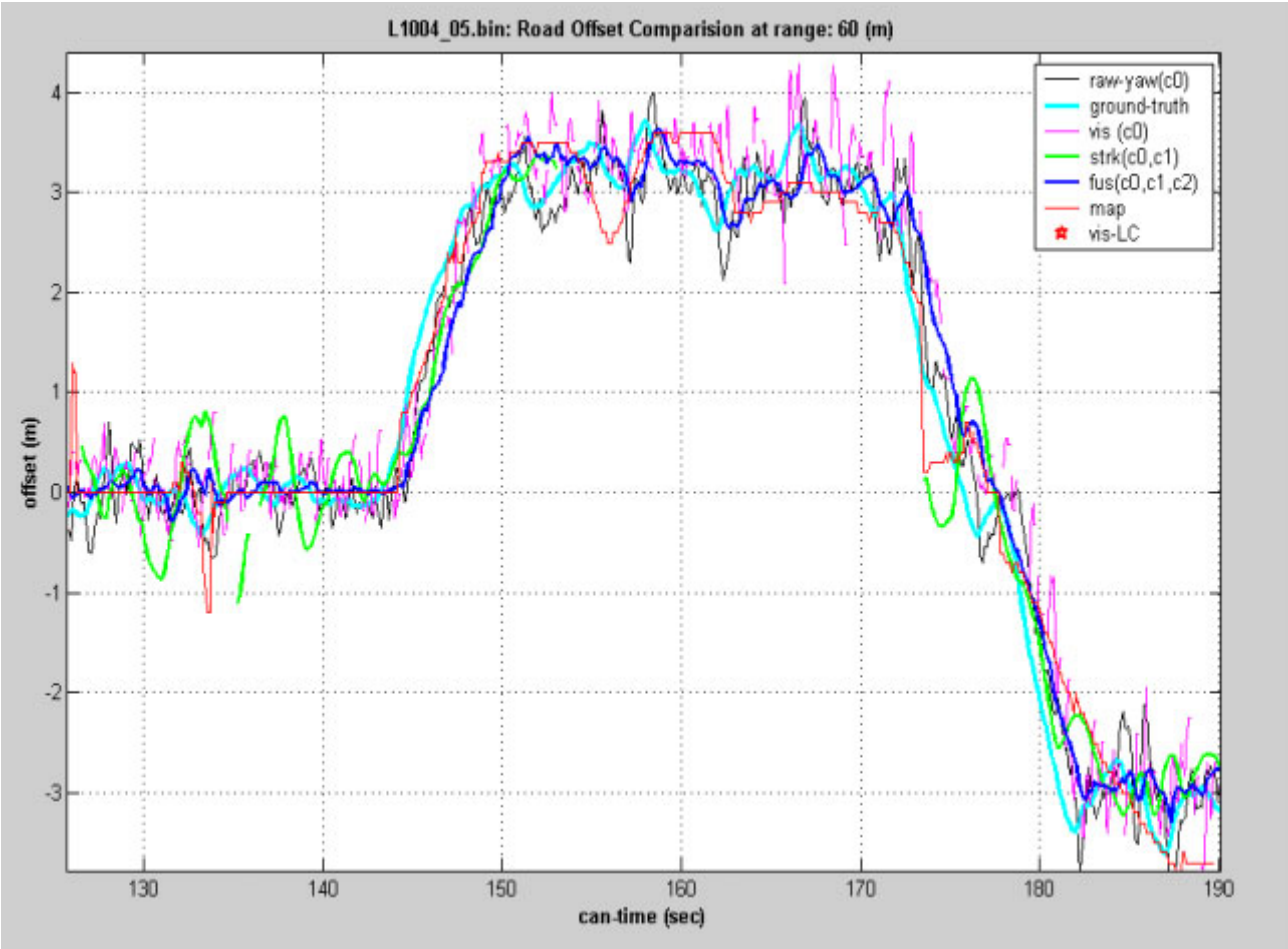

Figure 9.27 Road Offsets from Various Prototype Subsystems, Test Segment 5 of the Open Road Validation Tests

During the next phase of the ACAS/FOT program, the following efforts will be undertaken to improve the Data Fusion road and host state estimates and the overall Target Selection performance:

1. incorporation of long-range vision into the FOT system
2. additional tuning of the GPS/Map, Scene Tracker, and Vision confidence measures

3. incorporation of additional fusion rules and heuristics to better correlate and fuse the GPS/Map, Vision, Scene Tracker, and yaw rate-based road and host estimation inputs
4. incorporation of the GPS/Map categories into the target selection process
5. tuning of the target selection heuristics and persistence to maximize stationary object detection, and minimize stationary object false alarms.

9.2 Scene Tracking Approach Development (Task C2B)

Goals, Purpose and Background

Scene tracking is an enhancement to the conventional path prediction process in which preceding vehicles are classified as being in-lane or not in-lane. The conventional yaw rate-based road estimation approach cannot reliably predict changes in road curvature ahead of the host, since the road curvature is assumed to be constant. Moreover, the conventional yaw rate-based approach also assumes that the host is not weaving in-lane or changing lanes. In the scene tracking approach, the paths of the preceding vehicles are observed in order to estimate the upcoming forward road curvature. This approach assumes that most of the preceding vehicles are staying in their lanes, and that there are reasonable constraints on the rate at which the road curvature can change. In addition to estimating the upcoming road shape, the scene tracking approach also estimates the angular orientation of the host vehicle in its lane, thereby accounting for in-lane weaving or lane changing by the host.

Scene Tracker is charged with providing estimates of the road curvature parameters c0 and c1, which describe the shape of the upcoming road segment, and an estimate of the host's heading angle in the lane. A confidence indication is also provided.

At the start of this program, a scene tracking algorithm existed which will be referred to here as the 'original' version. During this program, several other approaches to scene tracking were developed. In all, the various versions can be summarized as:

1. the 'original' version, in which target tracking filters estimate target heading angles and target trajectory curvatures at range, allowing estimation of road curvature and host heading angle
2. the 'unified' approach, in which a single variable-dimension Kalman filter estimates c0, c1, host heading angle, and target lateral positions
3. the 'parallel' approach, in which each target has its own Kalman scene tracking filter, the outputs of which are combined
4. the 'snail tracking flow field' approach, in which stored target position data is used to calculate a flow field that is analyzed
5. the 'snail tracking unified' approach, in which stored target position data is directly analyzed to form estimates of the desired quantities

Each version in the sequence was intended to improve performance in some area(s) deemed deficient in earlier versions.

Early on, scene tracking algorithm performance was judged primarily in the simulation domain. The use of simulated radar data to drive the algorithm, compared to using data collected on a real vehicle, has the advantages of easy scenario scripting, control over all

aspects of data corruption, repeatability, and the availability of ground truth. Clearly, the advantages of using real data include the presence of unmodeled errors in the data and unanticipated target and host maneuvers which can expose unexpected algorithm performance characteristics. These early simulations were conducted entirely in the MathWorks Matlab environment.

A significant accomplishment in the scene tracking algorithm development was its migration to a real-time C-language implementation on a PC in a real vehicle. The more recent versions of the scene tracking algorithm exist only in C. The software is set up to run either in a real-time mode, exchanging CAN messages with other processors in the vehicle, or in a desk-top mode, processing previously logged radar messages or simulated data generated by the Matlab traffic/radar simulation.

Performance evaluation of the scene tracking algorithm consists primarily of measuring errors in the estimates of c0, c1 and host heading angle, and summarizing statistically. The relationship between the confidence indication and the performance is also studied. Additionally, it is interesting to observe the algorithm behavior under a variety of conditions which are anticipated to affect it, for example road curvature transitions, host or target lane changes, type of road, host speed and number of targets.

In the simulation environment, errors in the estimates provided by the scene tracking algorithm are directly measurable by comparing the estimates to the known true values. When running the algorithm using data from a real vehicle scenario, performance evaluation is hampered by the lack of truth data. In this case, a reasonably locally-accurate estimate of the host vehicle's actual path can be constructed after the fact using the recorded histories of the host's speed and yaw rate. This estimated path can be viewed as 'truth' and analyzed to yield estimates of true c0 and c1 for the entire run, by making certain assumptions on allowable road shape (for example, to eliminate effects of host 'weaving'). It seems possible also to estimate true host heading angle using this procedure. However, the approach actually taken has primarily been to use the scene tracking estimates of c0, c1 and heading angle to predict the road location at a certain distance downrange (e.g., 80 meters). This predicted position is compared to the host's path derived using integrated yaw rate, and a prediction error is calculated. Clearly, this error will include non-error effects due to host maneuvers over the road surface which don't reflect the road shape (e.g., weaving and lane changes). For example, application of this approach to a scenario involving a quick host lane change and a properly functioning scene tracking system could result in a false error indication of up to one lane width for a transitory period. In some cases, manual inspection of the accompanying video record is used to determine when the host changed lanes, and this is accounted for in the data analysis. In other cases, it is simply acknowledged that the error is somewhat overestimated using this procedure.

One consequence of evaluating the algorithm performance using this prediction-error-at-range technique is that the errors in the individual quantities (c0, c1 and heading angle) are not available. The prediction of downrange position depends on all three quantities and the overall error is some function of the individual errors. This effect, where the overall error results from varying amounts of error in the individual quantities, has been referred to as 'sloshing'.

Intermediate and Final Results

The primary accomplishment of this task is the fully functional real-time scene tracking software which resides in the scene tracking PC, receives CAN messages from the radar, and transmits to the fusion processor CAN messages containing the scene tracker's estimates of host heading angle in lane, the road curvature parameters c0 and c1, and an indication of the confidence in the accuracy of those estimates. Although there is still room for improvement in the performance of the scene tracking algorithm, the subsystem as it currently exists will work for this program.

As previously mentioned, a number of different approaches were investigated, each one intended to be an improvement in areas where earlier approaches were weak. These problem areas included such things as:
(1) fundamental radar phenomena (occlusion of targets, multipath, multiple returns from a single target, etc.) and their consequent effects on the radar tracker;
(2) insufficient target data in the current field-of-view (FOV);
(3) unattainable transient response characteristics of individual target scene tracking filters;
(4) detection and rejection of outlier targets (e.g., lane changers);
(5) targets disappearing from the FOV during a host lane change;
(6) accounting for differences in transient response to host yaw motions between the yaw rate sensor and the radar tracker;
(7) operation at low speeds in urban environments; and
(8) dealing with problematic but common road geometries such as onramps, offramps, and merging lanes of traffic.

To some extent, the transition to 'snail tracking' approaches alleviated problems associated with the radar phenomena and insufficient data in the FOV. The improper coasting problem has been handled by using only 'updated' detections (not 'coasted'). Heavy filtering of the sensed yaw rate, and appropriate adjustment of the associated time constant, has largely solved the problem due to the discrepancy in transient responses to yaw motions. Rejection of outlier target data, which is important because it falsely reports on the road shape, remains an important area of work. The parallel approaches (#3 and #4 in the list of approaches near the beginning of Section 9.2) are naturally better at this than the unified approaches (#2 and #5 in the list). The issues of urban environments and problematic road geometries remain. The snail tracking approach seems to be the best way to attack these problems.

The impact of these problems on the scene tracking performance is primarily a reduction in the fraction of the time that the scene tracker reports a high confidence. The algorithm usually can detect that things don't make sense, and lower the reported confidence. Therefore, it is unlikely that these problems will dramatically reduce overall system performance, as might happen if bad estimates were reported with high confidence.

As mentioned earlier, the performance of the scene tracking algorithm will be evaluated in the context of downrange prediction of the lateral position of the road, not in the context of errors in individual estimates of c0, c1 and heading angle. This prediction 'error' is determined using the calculated actual path of the host, so some careful interpretation is necessary. For example, in a host lane change scenario, some error will be attributed to a properly operating scene tracker just prior to and during the lane change, due to the fact that the host's actual path doesn't represent the true road shape. In other words, even if the scene tracking prediction of the road shape is perfect, an "error" will occur because the host vehicle did not follow the road shape when it changed lanes. See Figure 9.28 for a depiction of this error measurement scheme.

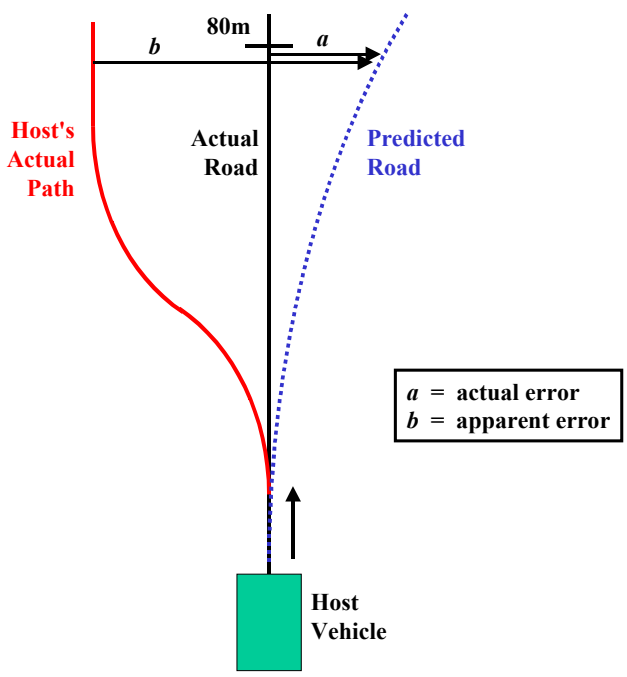

Figure 9.28 Depiction of Error Measurement Scheme

In the following paragraphs, the current performance level of the scene tracking algorithm will be shown for a typical highway scenario and for a typical surface street scenario, using data collected on the engineering vehicle. It will be seen that Scene Tracker performs better on the highway than on surface streets. It will also be seen that it has high confidence more frequently on the highway than in the urban environment. The benefits of scene tracking relative to the conventional yaw rate based path prediction is mainly expected to be apparent during host lane changes and during curve entry or exit. For this reason, some details of a host lane change and curve entry will be shown, both taken from a highway scenario, in order to demonstrate that Scene Tracker performs well under these conditions. It will also be seen that the confidence indication is a reliable

measure of performance. The results which are shown are those for the 'snail tracking flow field' approach which is currently running in an engineering development vehicle.

A histogram of the prediction error at 80 meters downrange is shown in Figure 9.29 for a typical highway scenario. This figure shows results only for times when the scene tracker indicated a confidence level of MEDIUM or HIGH. This run was approximately 17 minutes in duration, was primarily in a highway environment with many target vehicles, and contained numerous host and target lane changes.

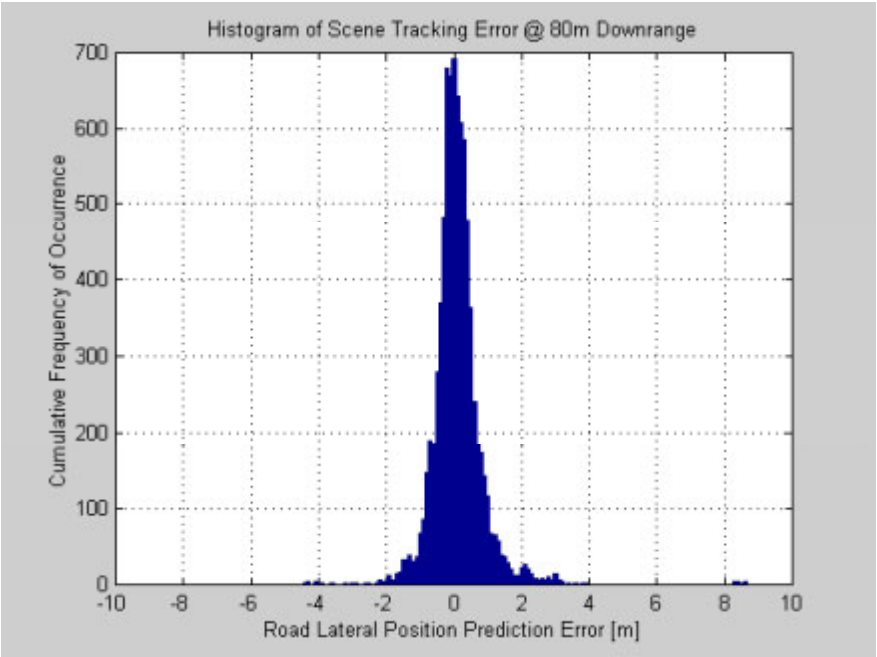

A2L0827.003 SNTRK3

Figure 9.29 Prediction Error at 80m for a Highway Scenario
MEDIUM or HIGH Confidence

Clearly, the lateral error is almost always less than half a lane width (1.8m). As explained earlier, there are several non-error phenomena which contribute to this error, such as weaving host and host lane changes, in addition to the scene tracking errors.

The MEDIUM or HIGH confidence results for a surface street scenario are shown in Figure 9.30. This run was approximately 28 minutes in duration. Data was taken predominantly on a multilane surface street with varying numbers of targets in stop and go traffic. Turns at intersections were also present in this run.

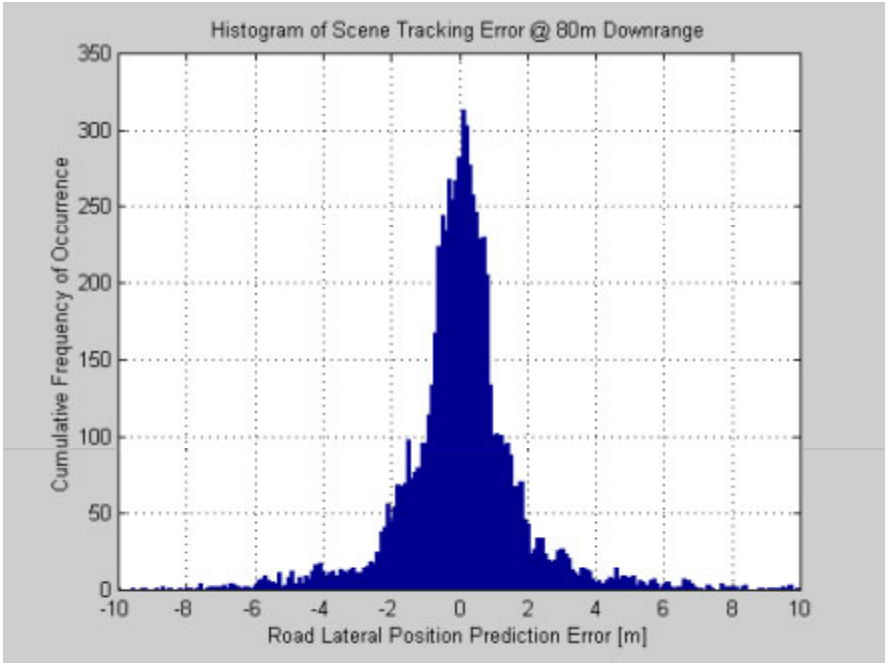

A2L0827.007 SNTRK3

Figure 9.30 Prediction Error at 80m For a Surface Street Scenario
MEDIUM or HIGH Confidence

Comparison of Figures 9.29 and 9.30 reveals that Scene Tracker works better on the highway than in an urban environment. Another revealing indication of this is contained in the following table, which shows the fraction of time spent in each confidence level in the two different environments. On the highway, MEDIUM or HIGH confidence is indicated 80% of the time, compared to only 43% on surface streets.

Confidence Level	Highway	Surface Street
NONE	.18	.55
LOW	.01	.01
MEDIUM	.17	.29
HIGH	.63	.14

The main situations in which the scene tracking algorithm is expected to provide valuable information are during host lane changes and curve entry/exit scenarios, which are not available using the conventional yaw rate-based path prediction approach. Therefore, some details will now be shown to demonstrate proper operation of Scene Tracker during these situations. Both the host lane change and the curve entry discussed below were taken from the highway scenario mentioned above.

Figure 9.31 shows a 'hair plot' of a host lane change. In this plot, a red trace shows the post-calculated trajectory of the host vehicle over the Earth's surface, determined using the method discussed earlier based on recorded host yaw rate and speed. On either side of this red trajectory line is drawn a black line at a distance of one-half of a lane width, for reference. These black lines are just for perspective, and are clearly not an indication

of where there were actual lane markings (because the host is changing lanes in this diagram). Every 10 meters or so along the red trajectory, a blue trace is drawn indicating the scene tracker's estimate of where the road is for the next 80 meters.

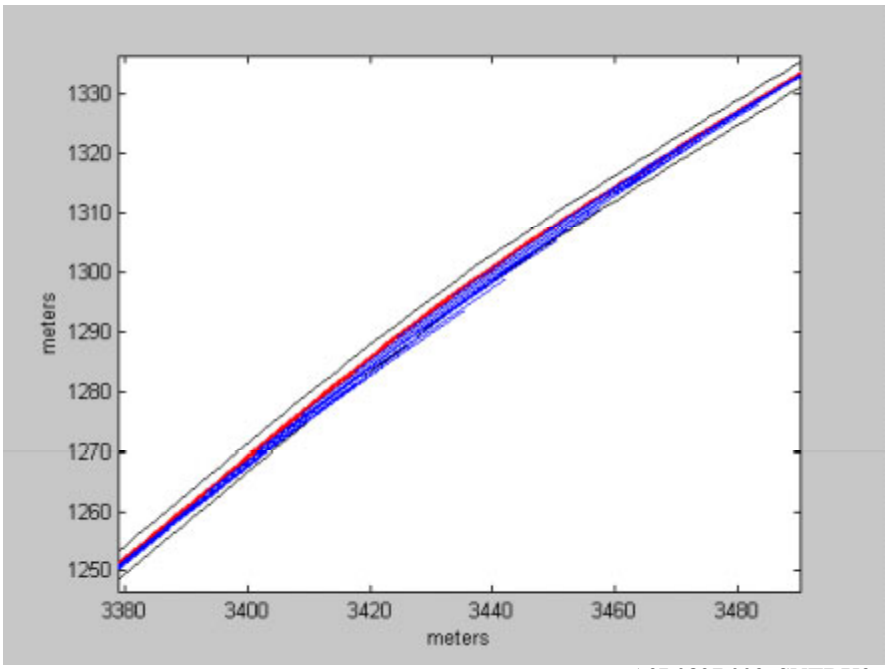

A2L0827.003 SNTRK3

Figure 9.31 Host's Post-Calculated Trajectory (Red) **and Scene Tracker's Estimates of Upcoming Road** (Blue)

In this figure, the host moved from the lower left to the upper right, and made a left lane change part way through. It should be noted that this lane change occurred in a 1000m radius right turn (the dominant feature evident in the figure). The blue lines indicate Scene Tracker's estimate of where the road diverges from the red path, and there appears to be nearly one lane width of 'error' between the two near the center of the figure. This indicates proper operation. As was discussed with Figure 9.28, Scene Tracker is designed to show the direction of the true road, rather than the path taken by the host vehicle, starting at the host's current location. After the completion of the lane change, the blue lines again lie approximately on top of the host's trajectory (upper right corner).

Figure 9.32 shows the estimated host's heading angle for a 60 second window surrounding the lane change. As expected with a left lane change, the heading angle goes substantially negative, peaking at approximately -2.5 degrees, then returns to zero.

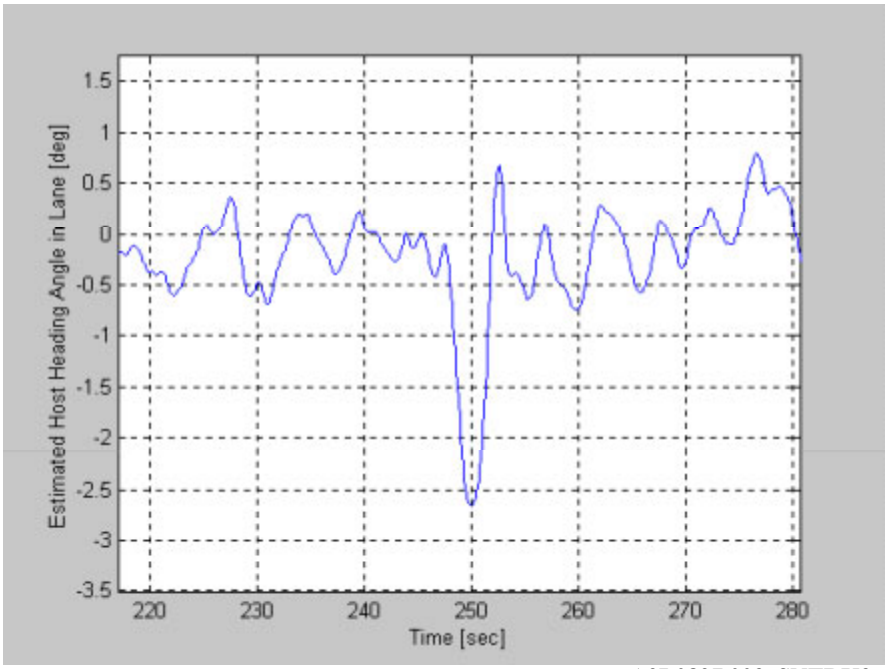

A2L0827.003 SNTRK3

Figure 9.32 Estimated Host Heading Angle in Lane in the Vicinity of a Host Lane Change

In Figure 9.33, the prediction error at 80 meters is shown as a function of time in this same window surrounding the host lane change. The prediction error during the host lane change rises to approximately 3 meters. As explained earlier, this 'error' shows that the scene tracking algorithm is working properly during the host lane change.

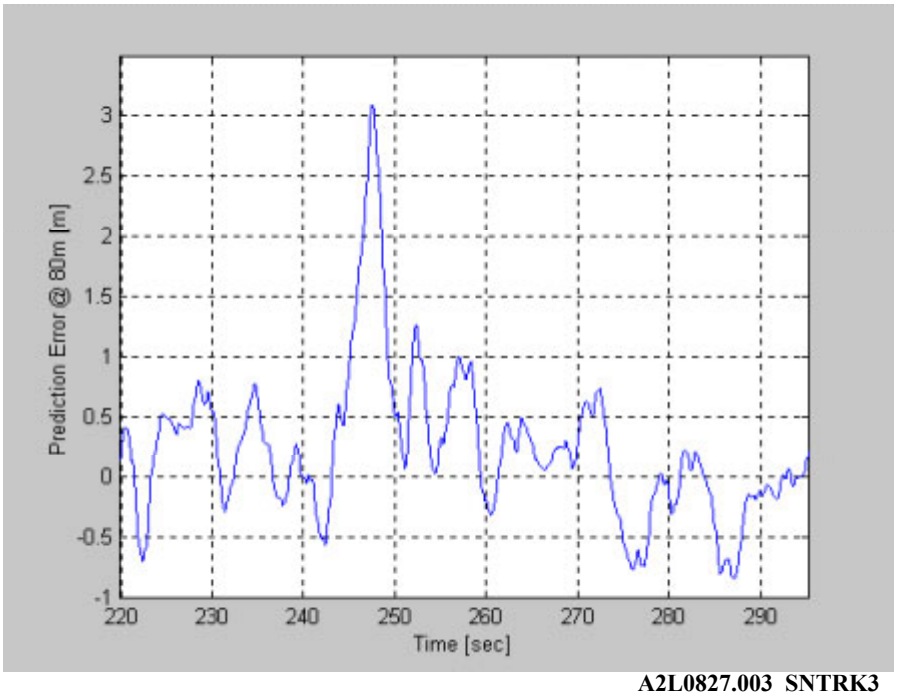

A2L0827.003 SNTRK3

Figure 9.33 Prediction Error at 80m in the Vicinity of a Host Lane Change

A curve entry scenario is considered next. In this highway scenario, the host is on a straight section of road and a distant target is part way through a 1000 meter right turn. Figure 9.34 shows an overhead snapshot of an instant of time prior to the host's curve entry. Numerous 'snail tracks' are shown, which are points on the Earth's surface where a target has been observed by the radar at some point in time. The red trace shows the post-calculated trajectory of the host. The black parallel lines show where the scene tracker thinks the lane boundaries are, given that the host is currently in the center of its lane, and under an assumption of known lane width. Clearly, Scene Tracker is aware of the upcoming curve and has a good idea of the shape of the road.

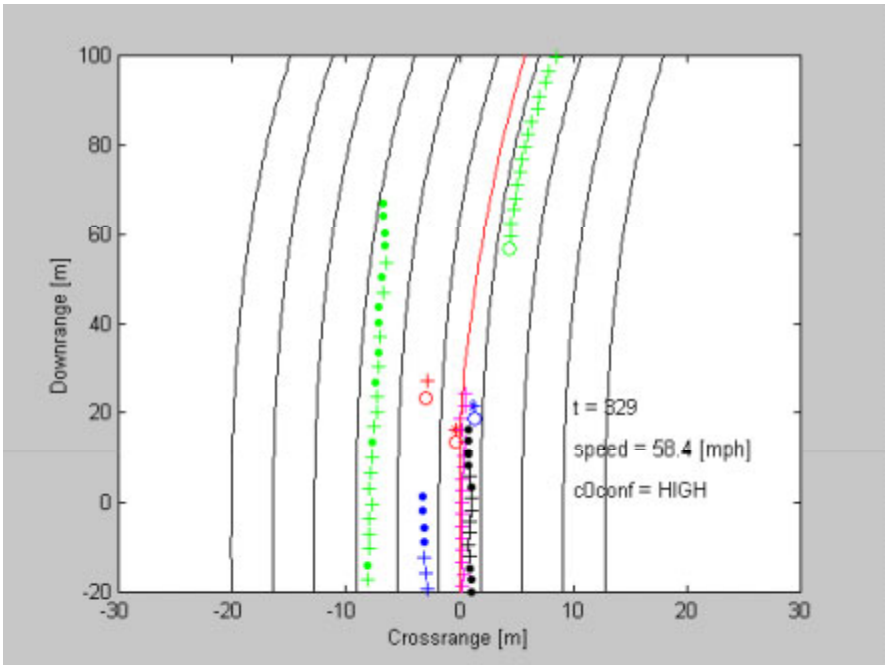

Figure 9.34 Overhead Snapshot Prior to Host Curve Entry
Shows target snail tracks, postcalculated host trajectory, and estimated lane markers

An important characteristic of each subsystem contributing information to the Data Fusion processor must be that it gives a reliable indication of the quality of the estimates being transmitted. The data summarized in Figure 9.35 show that the accuracy of the estimates coming out of the scene-tracking algorithm is reliably indicated by the confidence signal. Using data from the aforementioned highway scenario, that figure shows a histogram for each of the four confidence levels (NONE, LOW, MEDIUM, and HIGH). It is clear that the accuracy correlates well with the indicated confidence.

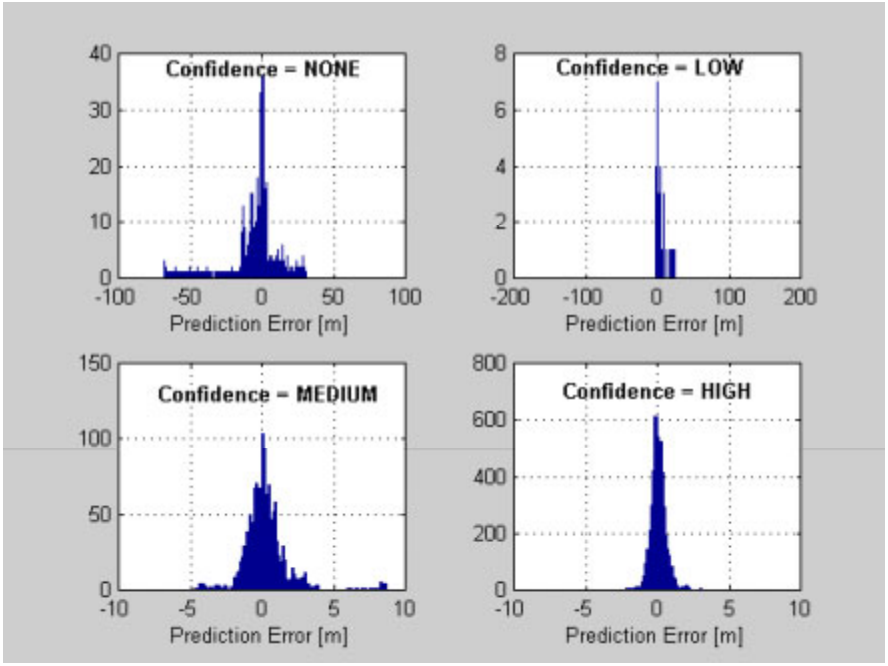

A2L0827.003 SNTRK3

Figure 9.35 Prediction Error at 80m for Four Confidence Levels in a Highway Scenario

In summary, the scene tracking algorithm provides estimates whose accuracy is reliably indicated by the accompanying confidence signal. Scene Tracker provides useful estimates under conditions where the conventional yaw rate based path prediction can not, particularly during host lane changes and curve entry/exit situations. The scene tracking algorithm works well enough in its current form to be of benefit to this program, though some additional refinement may increase the fraction of the time during which it provides estimates with relatively high confidence.

9.3 Enhanced GPS Approach Development (Task C2C)

Goals, Purpose and Background

Radar systems identify potential collision targets, but forward path prediction is essential to allow the system to eliminate irrelevant targets – those not actually in the forward path of the vehicle. The problem of estimating the correct host vehicle path is a very complex and challenging one. The purpose of this subtask is to investigate the applicability of advances in Global Positioning System (GPS) and dead reckoning sensors in conjunction with roadway map databases, to develop a method that can predict the upcoming forward geometry of the host vehicle. In particular, the objective is to examine the suitability of the road maps as a preview sensor to develop a robust path prediction method during lane changes and curve transitions, and to provide other map-derived information (for example, road geometry classification, and presence of forks, ramps, intersections, T-junctions, start and end of curves and distances to them) that is potentially useful in enhancing the performance of other subsystems.

Development of a GPS/Map-based host path prediction algorithm began in 1997-98 under the auspices of a GM R&D Forward Collision Warning (FCW) system development project. This initial attempt yielded satisfactory results for certain road classifications in controlled testing environments. However, it revealed several shortcomings of the approach that was being developed. The subsystem data output rate (1 Hz) was not sufficient to keep up with the requirements of an FCW application. This was mainly because of the data output rate of the GPS receiver that was used, and the latencies involved in the map retrieval and computation process. The method used to extract forward road geometry yielded inaccuracies, especially during transitions from one road section to another. In addition, its precision was insufficient relative to the radar resolution. Finally, the technique lacked the ability to estimate its confidence in the results it generated and to obtain other information present in the map to aid in the potential performance enhancements of other subsystems.

The focus of the current effort has been to address the above issues and develop methods to provide sufficient accuracy and timelines. The current system is designed to provide smoother road geometry transitions, confidence estimation, road geometry classification, and auxiliary map derived information

Technical Approach

In this approach, path prediction is achieved by continuously estimating the location of the vehicle on the road, searching a stored road database for road segments in the vicinity of the vehicle's location, matching the vehicle location to a point on a road in the stored roadway map, tracking the path traversed by the vehicle, and extracting the upcoming road geometry from the map. The objectives of this task are met using several sensors such as DGPS, dead reckoning, and a digitized road map. The overall functional block diagram of this subsystem is shown in Figure 9.36.

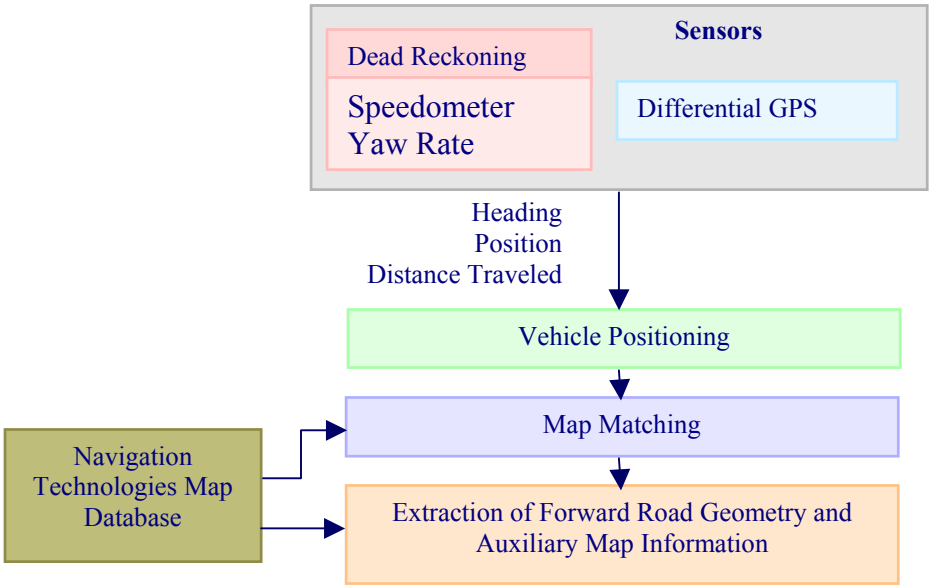

Figure 9.36 Overall Block Diagram of the GPS/Map Subsystem

A Differential Global Positioning System (DGPS) is used to compute the heading and distance traversed by the vehicle. The accuracy of determining the heading and distance is further enhanced by computing the heading angle and distance relative to the previous position of the host vehicle. Apart from the benefits that DGPS-based systems offer, they are hindered by outages in GPS signals that occur in the presence of, among other things, tunnels and tall buildings. To overcome this shortcoming, the current approach is augmented with dead reckoning sensors, where a vehicle speed sensor is used for distance measurement and a yaw rate sensor is used for relative heading measurement.

The combination of dead reckoning and DGPS with the map database has been explored to obtain a map-based path prediction system. DGPS, in conjunction with the map database, can provide fairly accurate path prediction except during GPS signal outages. At such times, the dead reckoning is expected to carry forward the task of path prediction.

Subsystem Input-Output Description

This subsystem receives inputs, at the rate of 10 Hz, describing absolute vehicle position in terms of latitude and longitude information from a GPS receiver, heading information from a yaw rate sensor (relative heading) and GPS (absolute heading), and host vehicle distance traveled information from vehicle speed.

This subsystem has been designed to output the following information at the rate of 10 Hz:

1. Forward road geometry 120m ahead of the host vehicle spaced 10 meters apart (along the vehicle path) in terms of 12 offsets to the direction of the host vehicle heading.
2. Provide an estimate of possible error in conjunction with every offset in the forward geometry specification.

3. Classify the upcoming 120 m forward geometry to flag a continuing straight or curved road that could be a gentle, sharp or S-shaped curve, or a curve transition to or from straight to a curved road (gentle curve/sharp curve/S-shaped curve).
4. Additional map derived information related to upcoming forward geometry such as:
   - Presence of and distances to forks, ramps, intersections, T-junctions and tunnels.
   - Presence of curves and distances to start and end of curve from current host vehicle position, with curvature estimation.
   - Information related to road class (freeway, ramp, arterial, local) along with its surface type (paved/unpaved)

Relevant Activities

Subsystem Architecture

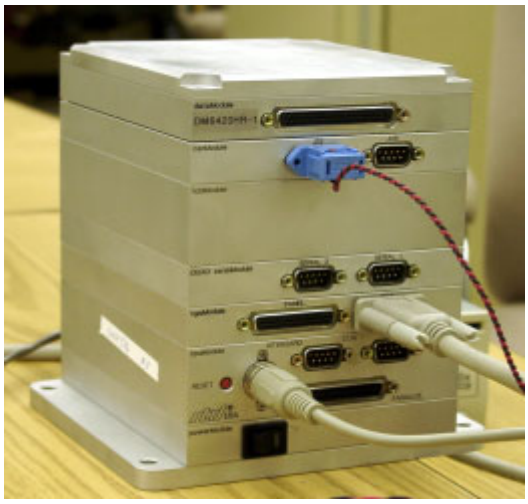

Figure 9.37 GPS/Map Processor

The GPS/Map subsystem is housed in a PC104-based computer shown in Figure 9.37. This subsystem communicates with other subsystems via a CAN bus interface. It is designed in a modular fashion, i.e., it is internally self-sufficient, and can be housed either in its own processor or in a processor that runs other subsystems. This subsystem uses the commercially available digital road map database provided by Navigation Technologies. The timing, message content, and format of its input and output have been verified for all the subsystem interfaces.

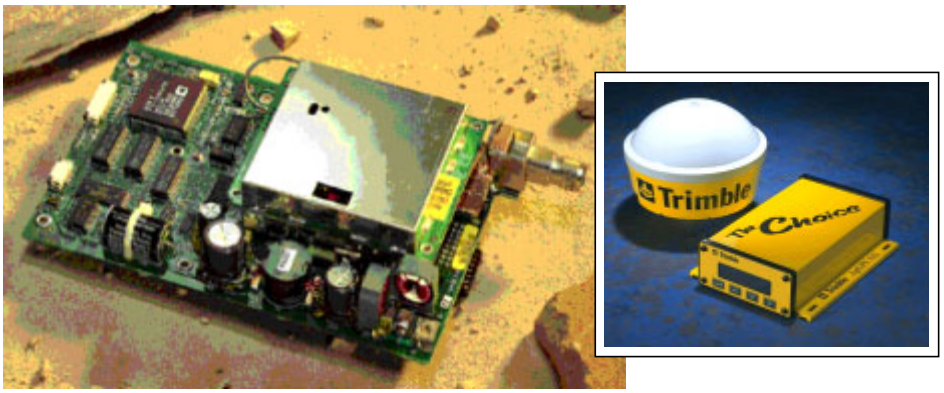

Figure 9.38 Trimble AB132 Receiver and Antenna

The DGPS receiver Trimble AG132 (Figure 9.38) was chosen because it operates at the rate of 10 Hz, thereby meeting the overall ACAS-FOT system specifications. In addition, it supports the national area of coverage for differential corrections that proved to be an attractive feature during algorithm development and testing, in both the Detroit and Malibu areas. This feature also offers the flexibility to FOT participants to travel outside their immediate local areas.

Algorithm Development

The process of predicting the forward road geometry of the host vehicle using a digital roadmap database consists of the following steps:

1. Estimate vehicle position in terms of longitude and latitude
2. Perform map matching, which involves matching the vehicle position and heading to a road in the map database
3. Determine likely successors to the current road
4. Retrieve the forward path of the host vehicle from the map database

Map Matching using GPS and Dead Reckoning

The sensors used in matching the GPS position of the vehicle to a road in the map database are a DGPS receiver, a yaw rate sensor, and the vehicle speed sensor. In addition, this process uses a digital roadmap database and data access functions from Navigation Technologies.

The accuracy of map matching and subsequent geometry retrieval is guaranteed as long as (a) the received GPS position is accurate and timely, and (b) the road segments stored in the map database are described with sufficient accuracy and resolution, both relative to each other and absolutely, so they can be correlated with the GPS position. However, in many instances either or both the conditions are not met for one or more of the following reasons:

1. A GPS update is not received due to either insufficient data transfer bandwidth, or excessive dilution of precision, or blockage due to roadway/roadside structures such as tunnels, bridges, buildings, hillsides or leafy trees.
2. Inaccurately stored data in the map database, especially in curved sections.
3. Missing data in the database, due to newly constructed roads and detours.

In such cases, the process of map matching would yield a failure to map match or an incorrect map match. In order to overcome the shortcoming due to GPS outages further refinements of the subsystem have been undertaken.

When the GPS/Map subsystem determines that the unmodified GPS position and map data are providing inaccurate results, it employs dead reckoning to obtain modified host vehicle position using inertial navigation software functions. This feature is designed to fill during the GPS outage. Additionally, dead reckoning aids in determining how closely the path of the vehicle is conforming the map database. This functionality relies on the yaw rate sensor and vehicle speed, as well as periodic crosschecks with the GPS and map data.

Forward Road Geometry Extraction

The function that performs the extraction of forward geometry is invoked following every successful map matching process, i.e., each time the vehicle is determined to be on a mapped road. This function uses the map-matched vehicle position that is presented to it and obtains a set of plausible road segments ahead of the host vehicle position using the roadmap database and the travel direction of the vehicle. Forward road geometry is estimated by examining the plausible road segments, and applying heuristics to choose a set that most likely defines the forward path of the vehicle. Forward geometry several hundred meters of road ahead is retrieved in order to determine road classification, an important attribute of the forward geometry, with sufficient context. Curve fitting is applied selectively to the upcoming road based on heuristics. Twelve interpolated points along the presumed vehicle path are computed at 10-meter intervals starting at the host vehicle position, to yield 120m of forward geometry. The upcoming path of the host vehicle is finally defined in terms of offset distances from each of the 12 points along the road to the vehicle direction.

The described process of defining host vehicle forward geometry works well when the following two conditions are met:

1. The map-matched position is accurate and timely, especially regarding the exact location of the vehicle in the vicinity of road geometry transitions, such as upcoming curves.
2. The shape points representing curves identify the exact location of the start and end of the curve, and represent the curve smoothly.

Unfortunately, neither of these conditions is met with a great degree of accuracy or consistency. Therefore many heuristic rules have been implemented in order to express high confidence when the conditions are met, and low confidence otherwise. At this time, a very conservative approach to the expressing confidence has been adopted. Further refinement of this method is underway.

Map-Derived Auxiliary Information Extraction

The attributes and the geometries of all the segments that connect to the determined forward path of the vehicle are examined to determine if they hold additional information regarding road features of interest, such as:

1. Presence of and distances to forks, ramps, intersections, T-junctions and tunnels.
2. Presence of curves, and distances to start and end of curve from current host vehicle position with its curvature estimation.
3. Information related to road class (freeway, ramp, arterial, local) along with its surface type (paved/unpaved).

Development of Confidence Estimates

The confidence estimate for the predicted path is defined as the radius of a circle of uncertainty around each of the points defining the expected road geometry. It is derived from a statistical analysis of recorded trip data, and is based on the distribution of errors for a specific road classification. This value is further adjusted to indicate improved confidence if there is a close conformance between vehicle position and GPS heading with the map, if the distance over which the host vehicle has been on the current map segment is above a threshold and improves further the longer it stays on the same segment, and if the current segment is a legitimate successor road segment of a previously map matched segment. The confidence measure is adjusted to flag reduced confidence if the vehicle is performing a turning maneuver or if it is determined to be on a S-shaped or a sharp curve.

Subsystem Testing and Validation

Testing was performed on open roads because the variety of road types and conditions that are encountered make the tests more realistic and applicable to real driving as compared to any predefined course. This type of testing is especially important for this subsystem because its performance is mainly dependent on maps and GPS signal reception, and open test road test sites are the only way to get map data (of varying quality – superior, adequate, poor and non-existent), and GPS measurements over a variety of locations (normal and challenging, namely urban canyons, and under bridges, tunnels, and leafy trees) and times (night, day).

The test and validation activities have been performed using the GM Engineering Development Vehicle (EDV), the Prototype vehicle, and in the laboratory. Since program inception, the algorithm development, analysis of results and subsequent improvements to the subsystem has been carried out using our bench setup, which is essentially a real-time vehicle simulation using diagnostic tools developed by GM R&D. Algorithm improvements are verified by exercising the subsystem on the bench, using on-road data collected using the ACAS vehicles (GM EDV and Prototype Vehicle). This has proved to be a valuable tool for testing, debugging and validation and has significantly reduced the overall subsystem development time.

This subsystem has been exercised using a rich suite of scenarios captured on open roads in the Detroit and Southern California areas. This scenario suite comprises a variety of road types (freeways, surface streets, rural roads, paved and unpaved roads) and road geometries (straight, curved, S-shaped, and curve transitions), time of day, different weather conditions and GPS outages caused by satellite obscurations due to bridges, tunnels and urban canyons.

Diagnostic Tools

GM R&D has developed a data logger (a video and CAN data logging tool) to perform in-vehicle and on-bench data logging, and a special visualization tool nicknamed "vtool" to perform a real-time playback and visualization of data collected using the GM EDV, the ACAS Prototype vehicle and the relogged data from the bench setup. These tools have been extensively employed to verify real-time system behavior on the bench setup as well as in-vehicle operation.

GM Data Logger

Figure 9.39 shows a general block diagram of the in-vehicle data logging and data display tool. This tool has the ability to log selected subsets of vehicle CAN messages and replay them (or a subset of them) in real time over the CAN bus in the vehicle or on the bench setup. It also serves as an in-vehicle diagnostic tool to display CAN bus data textually, graphically, and overlaid on video data. It has the ability to collect compressed digital sequences, time-aligned with radar and other vehicle sensor data, thus has the capability of recreating the entire driving experience on the bench setup.

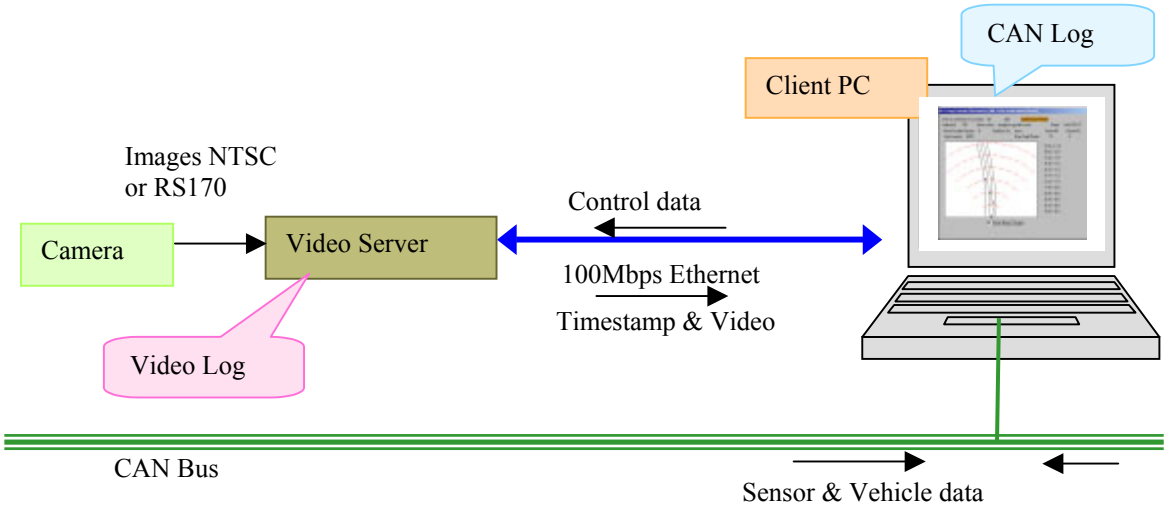

Figure 9.39 In-Vehicle Data Logging Mechanism With Real-Time Data Display

GM Visualization Tool

A separate tool (vtool), shown in Figure 9.40, has been developed for off-line visualization and examination of logged data. This tool uses the video logs and the raw CAN logs collected from logging sessions. The advantage of the vtool over the real-time displays is that the logged data can be replayed any number of times at any desired speed including single step and backward.

Figure 9.40 is displayed in greater detail in Figures 9.41 through 9.44. These figures show the graphical and textual screens of interest in the GPS/Map based path prediction development process. Figure 9.41 shows the radar targets (with their target Ids), detailed in the screen shown in Figure 9.43, overlaid on the logged video image, where targets displayed in red are slowing targets while those displayed in blue are moving away from the host vehicle. Figure 9.44 shows a textual display of various sensor data including those used by this subsystem, namely GPS information, yaw rate sensor data, vehicle speed, and odometer readings (used for distance measurements). Figure 9.42 shows a graphical top-down view of the upcoming road geometry as computed by the GPS/Map subsystem, with superimposed radar targets. This screen, when observed in conjunction with the video/radar overlaid screen, provides an immediate visual indication of algorithm performance. In addition, this screen also provides a textual display of all other information output by this subsystem.

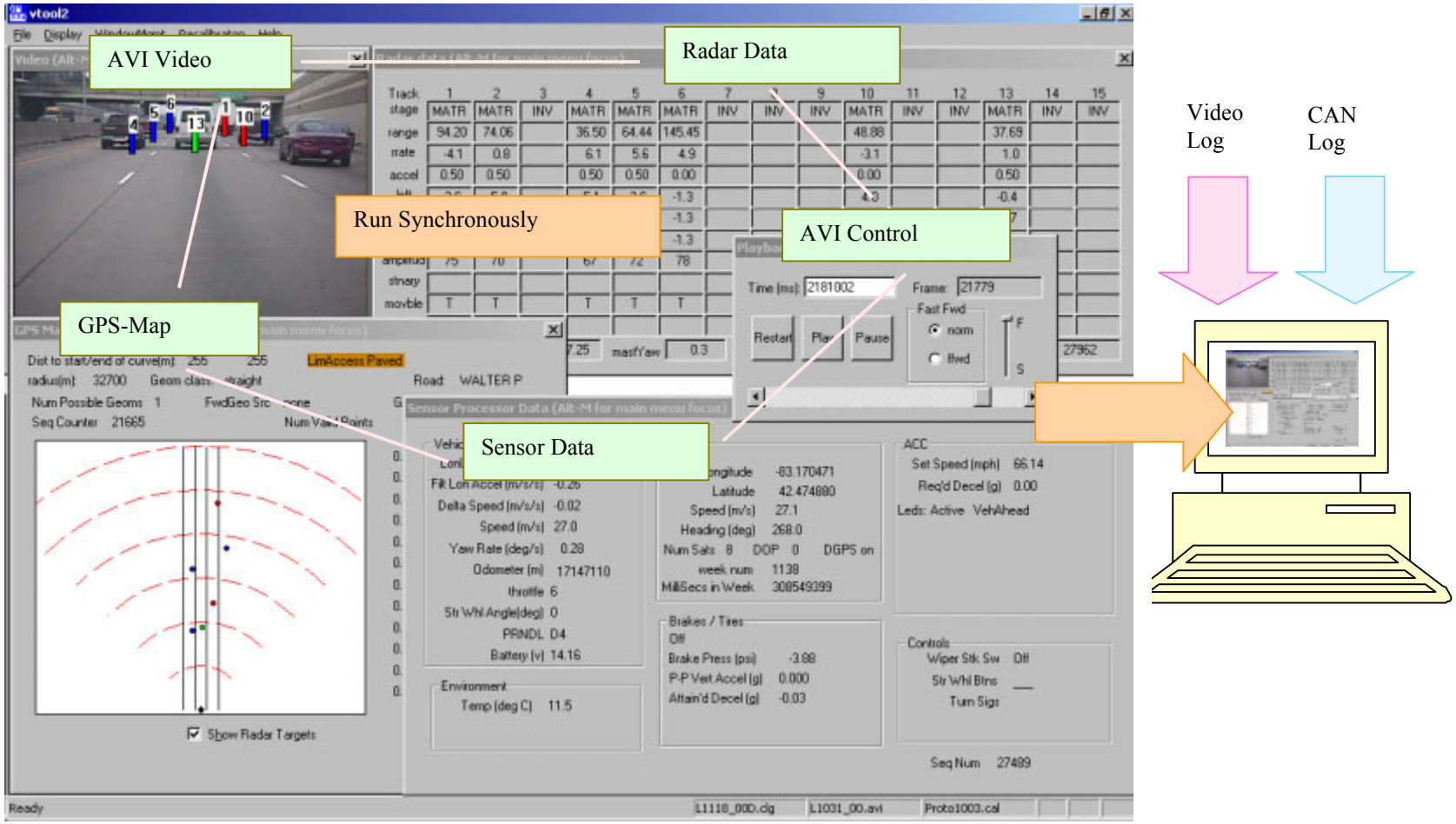

Figure 9.40 Vtool for Evaluation and Analysis of Logged Data

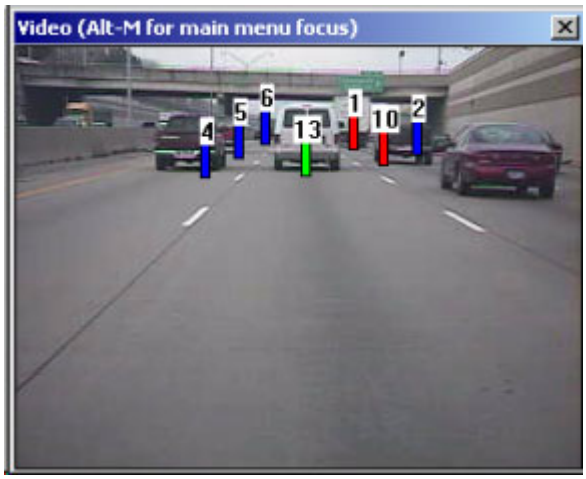

Figure 9.41 Video and Radar Overlay Display

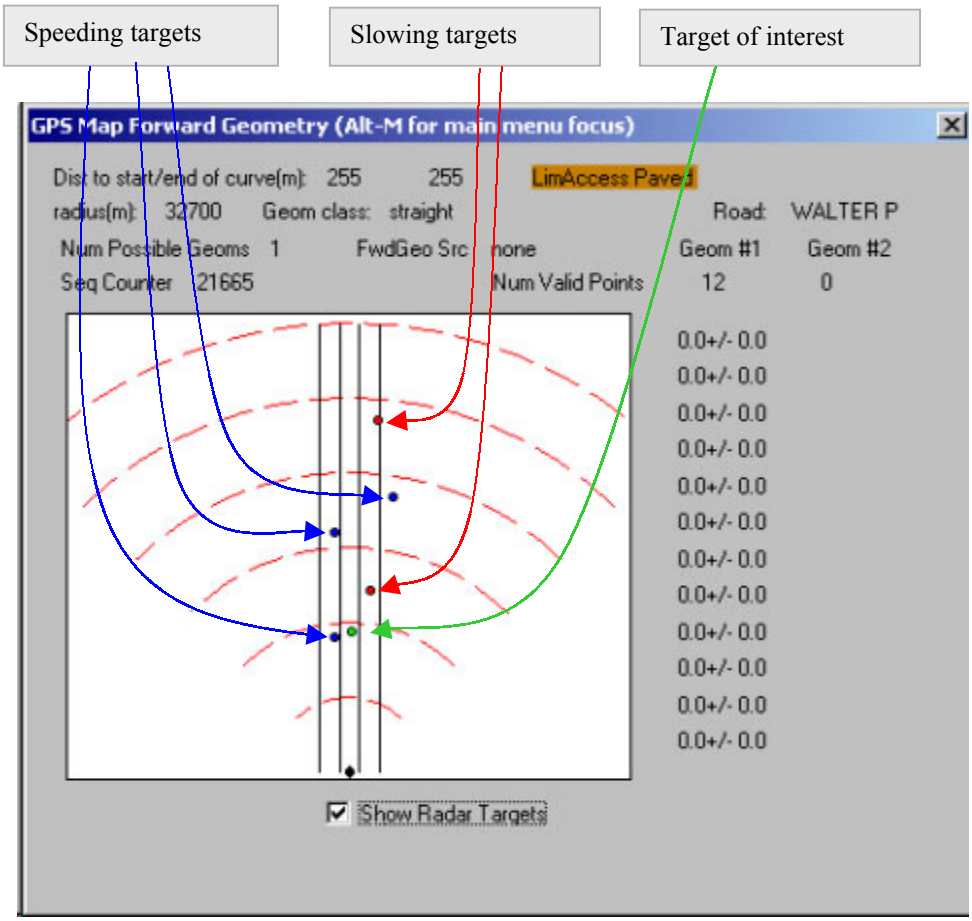

Figure 9.42 Results From the GPS/Map Processor

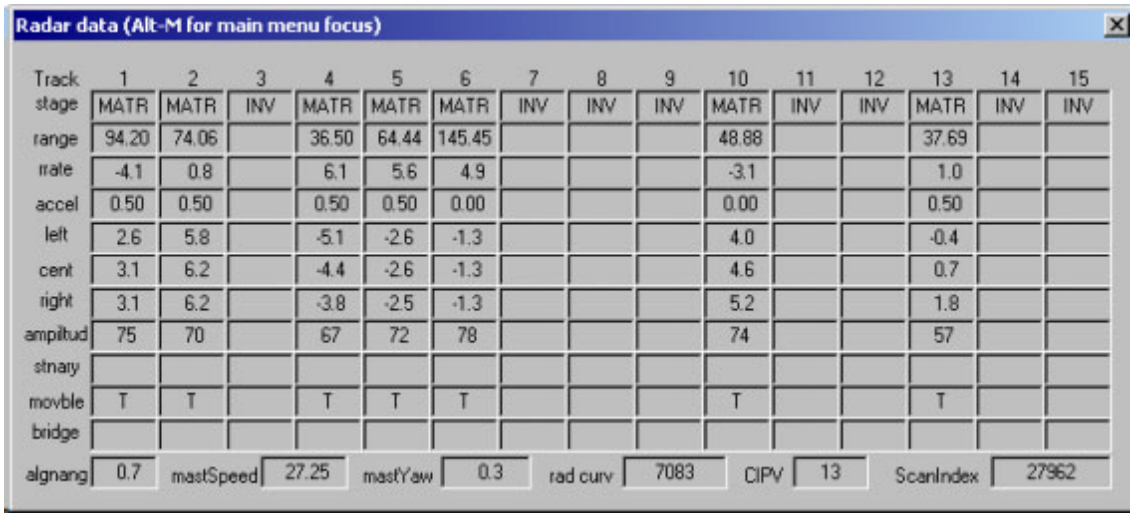

Radar data (Alt-M for main menu focus)

Track	1	2	3	4	5	6	7	8	9	10	11	12	13	14	15
stage	MATR	MATR	INV	MATR	MATR	MATR	INV	INV	INV	MATR	INV	INV	MATR	INV	INV
range	94.20	74.06		36.50	64.44	145.45				48.88			37.69		
rrate	-4.1	0.8		6.1	5.6	4.9				-3.1			1.0		
accel	0.50	0.50		0.50	0.50	0.00				0.00			0.50		
left	2.6	5.8		-5.1	-2.6	-1.3				4.0			-0.4		
cent	3.1	6.2		-4.4	-2.6	-1.3				4.6			0.7		
right	3.1	6.2		-3.8	-2.5	-1.3				5.2			1.8		
ampltud	75	70		67	72	78				74			57		
stnary															
movble	T	T		T	T	T				T			T		
bridge															

algnang 0.7 mastSpeed 27.25 mastYaw 0.3 rad curv 7083 CIPV 13 ScanIndex 27962

Figure 9.43 Radar Data Screen

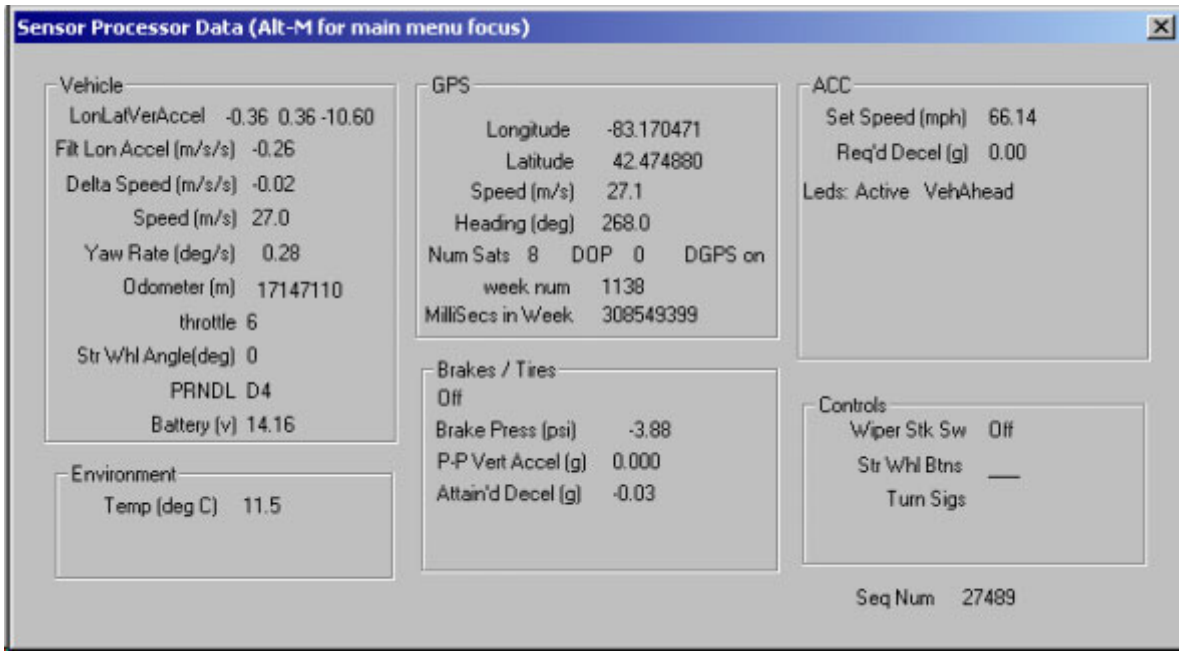

Figure 9.44 Sensor Data Display

<u>Development of a Ground Truth Method</u>

A ground truth method to determine the actual vehicle path has been developed to evaluate the performance of the predicted host path. It uses the vehicle speed and yaw rate to trace the actual vehicle path traversed by the vehicle.

A ground truth procedure was also developed independently at HRL Laboratories to determine the actual vehicle path. Both methods yield matching results, as shown by plotting offsets at 80m ahead of the vehicle in Figure 9.45 below.

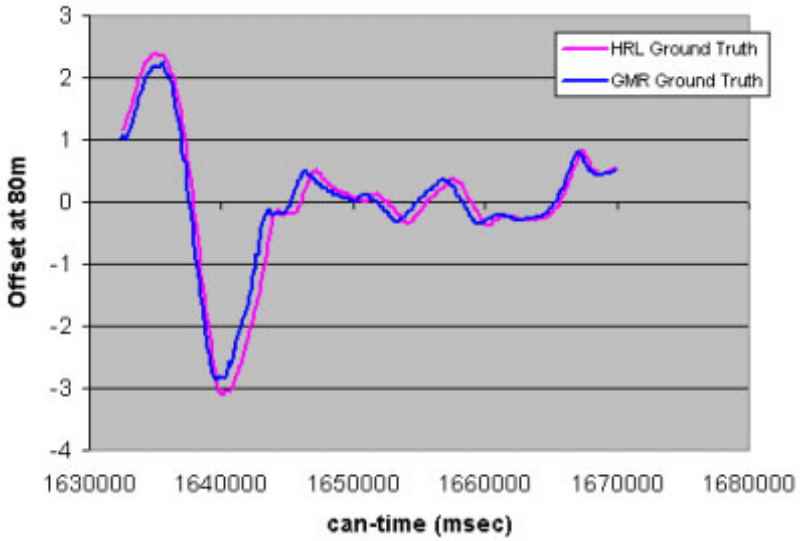

Figure 9.45 Comparison of the HRL and GMR-Developed Ground Truth

Intermediate and Final Results

This section discusses the overall GPS/Map subsystem task accomplishments and performance.

Verification Testing

A series of verification tests were performed on the Prototype vehicle on the open road in the Detroit area during the month of October 2001. All the logged data from these road trips has been examined to draw conclusions about the current state of the subsystem and to define future improvements that must be undertaken to resolve the current shortcomings. A representative sample of the open road tests performed on October 31, 2001 will be discussed in this section.

The test under consideration was performed on a 200-mile route covering a variety of road types including freeways, one and two lane highways, straight and winding rural roads, congested city streets, and intersections. The road surfaces were both paved and unpaved. Tests were performed both during the day and at night, with traffic density varying from heavy to non-existent.

To enable the presentation of results in a freeway-driving environment, a specific section of this test route comprising the I-696 freeway as it was traveled in the westbound direction has been considered. Figure 9.46 shows the results of the map-matching function overlaid in red on the chosen section of the test route. Figure 9.47 shows the result of vehicle positioning in terms of raw GPS data superimposed on the map prior to map matching. It can be observed that derived vehicle positioning does not always result

in a match on a point along the road. In this case it has resulted in a position not on the road and in worse cases it could place the vehicle completely off to the side of the road. However, applying the process of map matching to the vehicle position results in the placement of the vehicle on the road as shown in Figure 9.48.

Figure 9.49 depicts the results of forward geometry extraction (in blue) following the map-matching process. Each blue section represents 12 points (spaced 10m apart) that trace an arc from the vehicle in the direction that forward geometry has been projected by the GPS/Map processor. This plot shows the results of map matching for the entire test section, while the results of the forward geometry extraction have been sampled (based on vehicle speed) to enable the comprehension of the results. Plotting the forward geometry for all the vehicle position instances where map matching was obtained would have yielded a continuous blue line overlaid on the red line.

The GPS/Map subsystem functionality of assigning additional map-derived attributes to the computed forward road geometry is shown in the form of vtool displays in Figures 9.50 through 9.57. These figures show the results obtained upon application of the algorithms to the input scenes represented by the video inserts in each of the figures, with superimposed radar targets. Slowing target are indicated in red while speeding targets are highlighted in blue color. The video insert in Figure 9.50 shows a straight section of the Walter P. Reuther freeway (I-696). The larger white square in the display window shows the graphical representation of the forward geometry computed by this subsystem superimposed with the radar targets. The red arcs represent distances 20m apart, starting at the host vehicle position. Visual conclusions can be drawn by trying to match up the targets from the video insert to the appropriate lane in the forward geometry depiction. The same information regarding the 120m forward geometry is presented textually along with associated uncertainty measures in a column format on the right side of the display with the number of valid points in the forward geometry. The lower most set of numbers represent geometry 10m ahead of the vehicle and the top most set depicts geometry 120m ahead of the host vehicle. The uncertainty measures in this case are zero, which implies that the map process is highly confident about the forward geometry offsets that it has computed. Additionally, this display also shows that the road is paved and has a designation of limited access (freeway), its name is Walter P [Reuther] and its geometry class as determined by the GPS/Map subsystem is “straight”.

Figures 9.51 through 9.53 depict an assortment of curves (gentle, sharp and S-shaped) encountered in everyday driving. These figures display the upcoming path of the vehicle in graphical (with superimposed radar target) and textual forms along with the amount of uncertainties in accurate path prediction in meters estimated by the algorithm. In addition to the road geometry class (gentle, sharp and S-shaped in Figures 9.51 through 9.53), road type (paved limited access) and road name, these figures display the radius of the curve that is currently being negotiated. A negative radius implies a left-handed curve, while a positive value is assigned to a right-handed curve. A value of 32700m implies a straight road (infinite radius).

Figures 9.54 and 9.55 depict the forward path computed by the host vehicle when it encounters curve transitions. Figure 9.54 depicts the case when the road changes from a straight section to a gentle curve, while Figure 9.55 shows the case when the road transitions from a straight section to an S-shaped curve. In addition to providing all the information pertaining to road geometry listed in the above section, the distances to the start of curves are displayed on the first line.

Scenarios including other roadway features, namely intersections, T-junctions, and tunnels are highlighted in the video displayed in Figures 9.54 through 9.57. Figure 9.55 and Figure 9.56 flag an upcoming intersection and T-junction, respectively, by displaying the distances to them in the last row on the right side of the display. Figure 9.57 flags the presence of a tunnel via the highlighted display on the first line of the display screen.

The remainder of this section describes the performance of the subsystem over longer stretches of the road, as opposed to the sampled results presented thus far. Figure 9.58 shows a section of the map traveled by the host vehicle (A to B) on a surface street in the Detroit metropolitan area. Figure 9.59 shows the values of the offset defined 80m ahead of the host vehicle plotted against two values of ground truth obtained from the HRL (cyan line) and the GM (yellow line) developed methods. The graph also shows the classification of the road geometry as computed by the GPS/Map subsystem. The road as seen from the map appears to be fairly a straight section and the GPS/Map processor aptly defined the geometry 80m ahead of the host vehicle as having no offset from the vehicle heading (blue line) and classified the geometry as “straight” (light blue colored line). In addition, a maroon line in this figure highlights the distances (in meters scaled down by 10) to intersections as encountered by the host vehicle. The entire section was flagged as a paved surface street.

Figure 9.60 shows a section of the Walter P. Reuther freeway (I-696) that was traversed in the west bound direction. The section of this test route that will be used for the remainder of this discussion extends from the point marked “A” in the top right corner to the point “G” (bottom left corner) of Figure 9.60. This section was chosen because it represents a typical driving scenario, comprising a variety of curve transitions and a host vehicle lane change. Figure 9.61 shows the overall GPS/Map results in terms of offsets 80m ahead of the host vehicle, plotted against the ground truth generated by the HRL method, and the road classification.

The results encountering a left curve (A to B in Figure 9.60), a right curve (E to F), curve transitions in terms of exiting a curve, entering a straight section and transitioning into a right curve (B to C), and a lane change (D to E) are shown in Figures 9.62 through 9.65. These figures show the deviation of the predicted forward geometry at 80m ahead of the vehicle from the HRL-developed ground truth. They also show the road classification as predicted by this subsystem.

The overall summary of results for a 42-minute section of the October 31, 2001 run is presented in Table 9.3. The "error" is defined as the difference between the offset computed by the GPS/Map subsystem and the GM-developed ground truth at 80m ahead of the vehicle.

Table 9.3 Summary of Errors versus Road Classification

Road Classification	% Test Instances			% Test Instances
	Error < 2m	2m ≤ Error < 5m	5m ≤ Error	
Straight	42.5	1.8	0.1	44.4
Gentle Curve	6.2	0.8	0.1	7.1
Curve Transitions	26.6	4.3	0.4	31.3
Acute Curves (Sharp and S-shaped)	4.8	2.2	2.3	9.3
% Test Instances	80.1	9.1	2.9	92.1

The cells in this table indicate the percentage of total test instances when a specific case was encountered. For example, the first cell in this table indicates that for 42.5% of the entire trip the vehicle traversed straight roads and the difference between the offset computed by the GPS/Map subsystem and the GM developed ground truth at 80m ahead of the vehicle was less than 2m. The table also captures the fact that 44.4% of the trip comprised straight roads as classified by this subsystem. Also, the error was observed to be less than 2m for 80.1% of the trip consisting of different road classifications. It must be noted that the subsystem was able to classify 92.1% of the trip into different road geometry classes, while 5.2% was categorized as "unknown" because the system was not able to classify those road types into the defined classification reliably. "No map matching" was experienced in 2.7% of the trip, which could have resulted when the vehicle made a turn to traverse from one road to another, or when a map match resulted on a segment that was not a logical successor to a previously well matched road segment due to an erroneous GPS position or map errors.

Although, the performance in terms of accuracy of predicting forward road geometry and associated geometry attributes is satisfactory, the development of appropriate confidence measures deserves further refinement. Figure 9.66 shows the evaluation of the current confidence assignment technique to different road classifications. As seen from the figure the current scheme assigns conservative confidence values to the predicted road offsets and many instances of proper prediction by the GPS/Map system are being ignored by the data fusion subsystem. Those instances need to be captured.

Figure 9.46 Map Matching Over a Stretch of Freeway

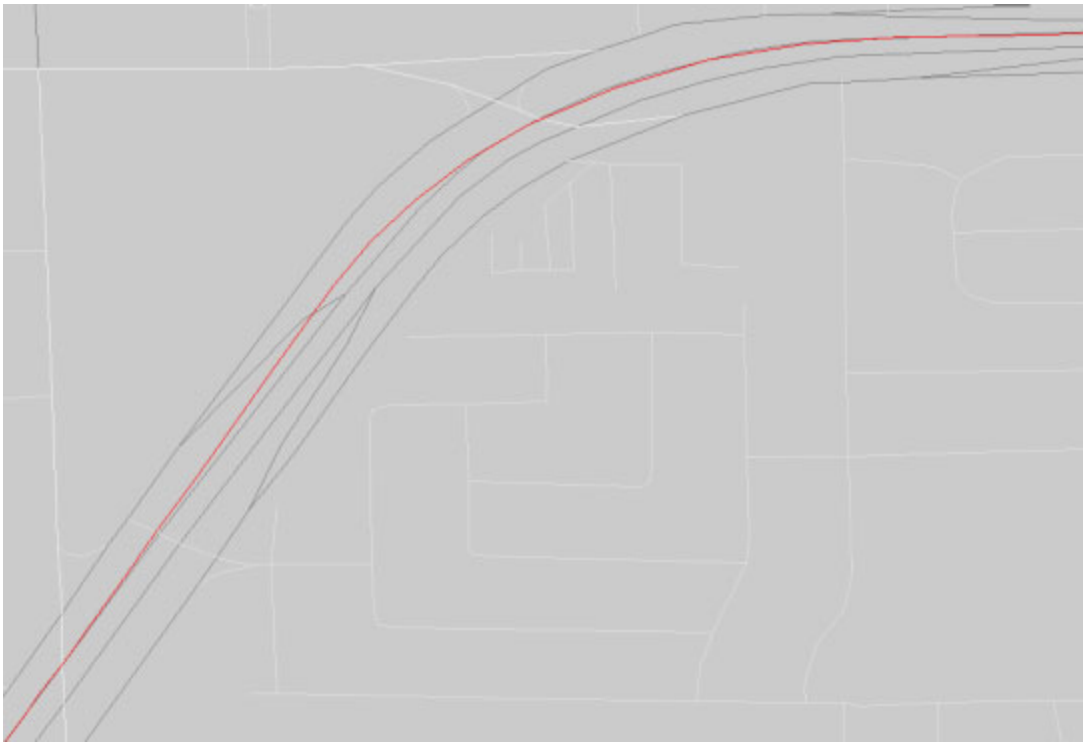

Figure 9.47 Raw GPS Data Superimposed on a Section of Map

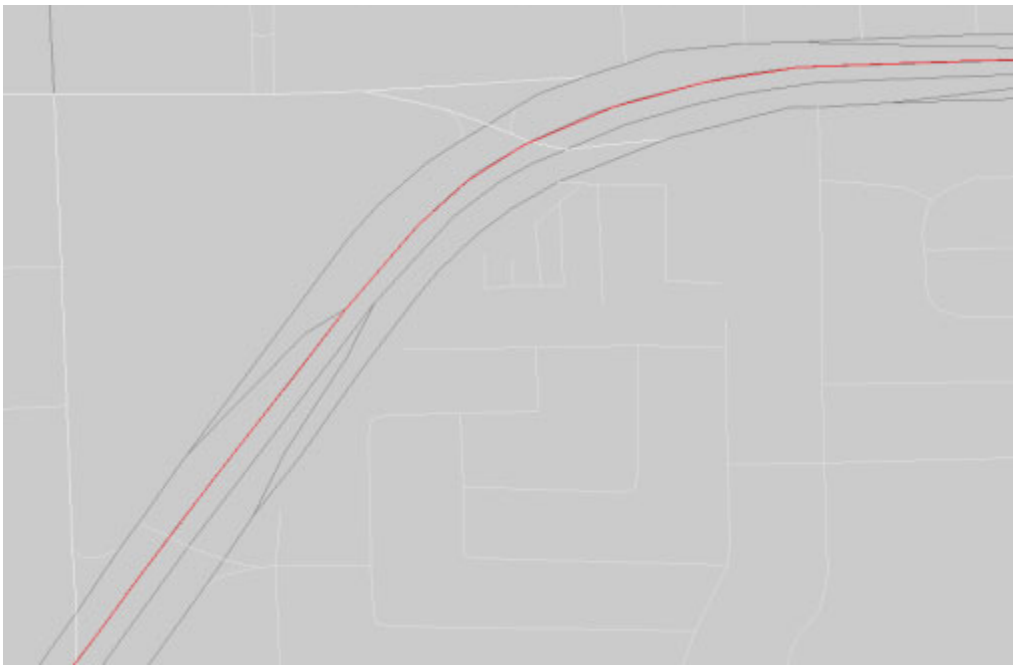

Figure 9.48 Map Matching Using GPS Data From Figure 9.46

Figure 9.49 Predicted Forward Geometry Superimposed on Map

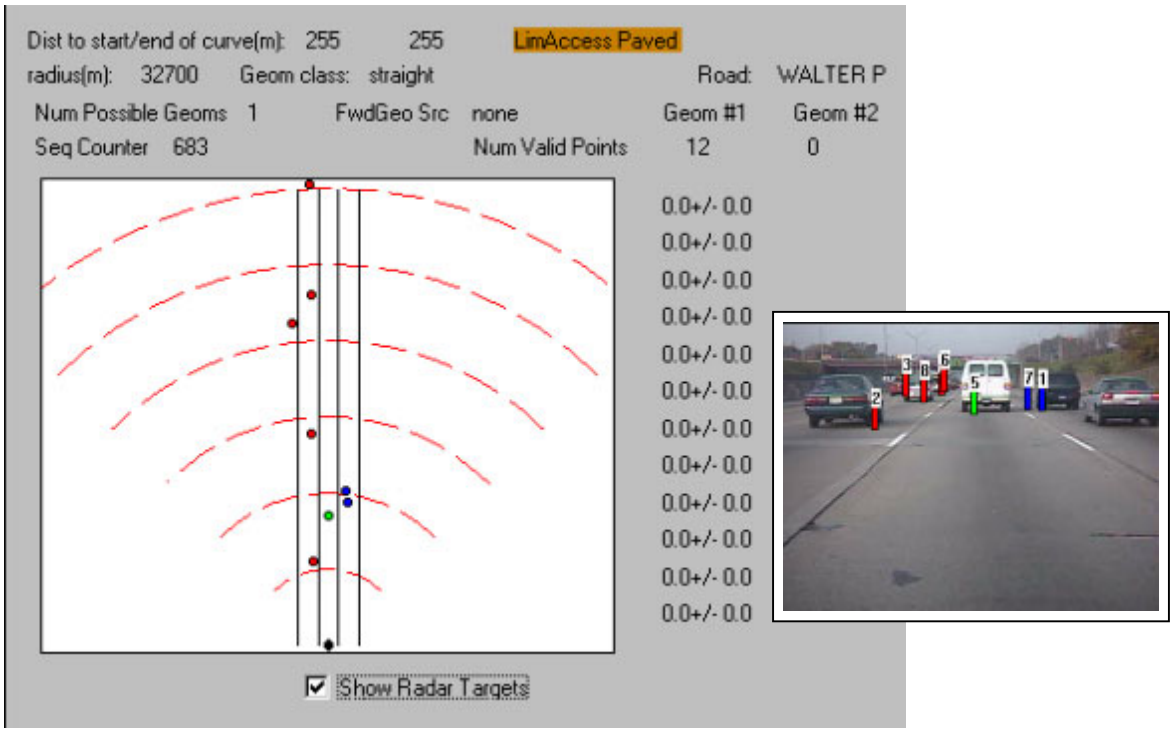

Figure 9.50 Forward Geometry Prediction on a Straight Road

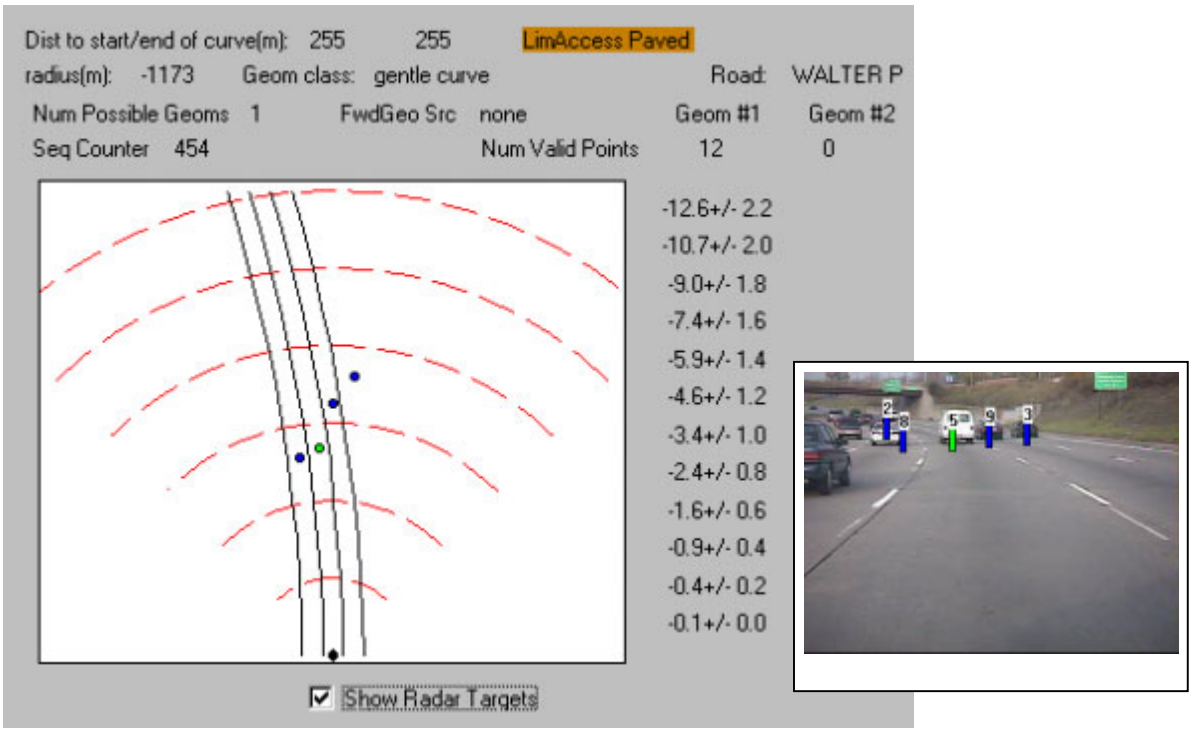

Figure 9.51 Forward Geometry Prediction on a Gently Curved Road

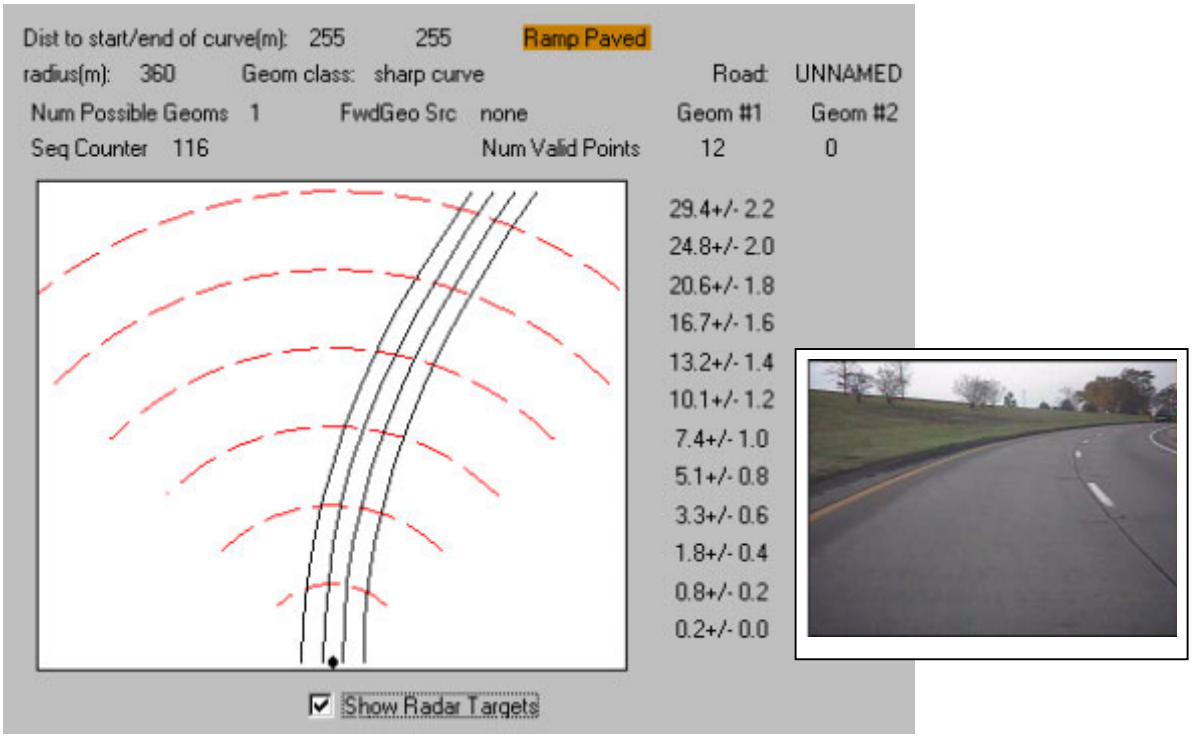

Figure 9.52 Forward Geometry Prediction on a Sharply Curved Road

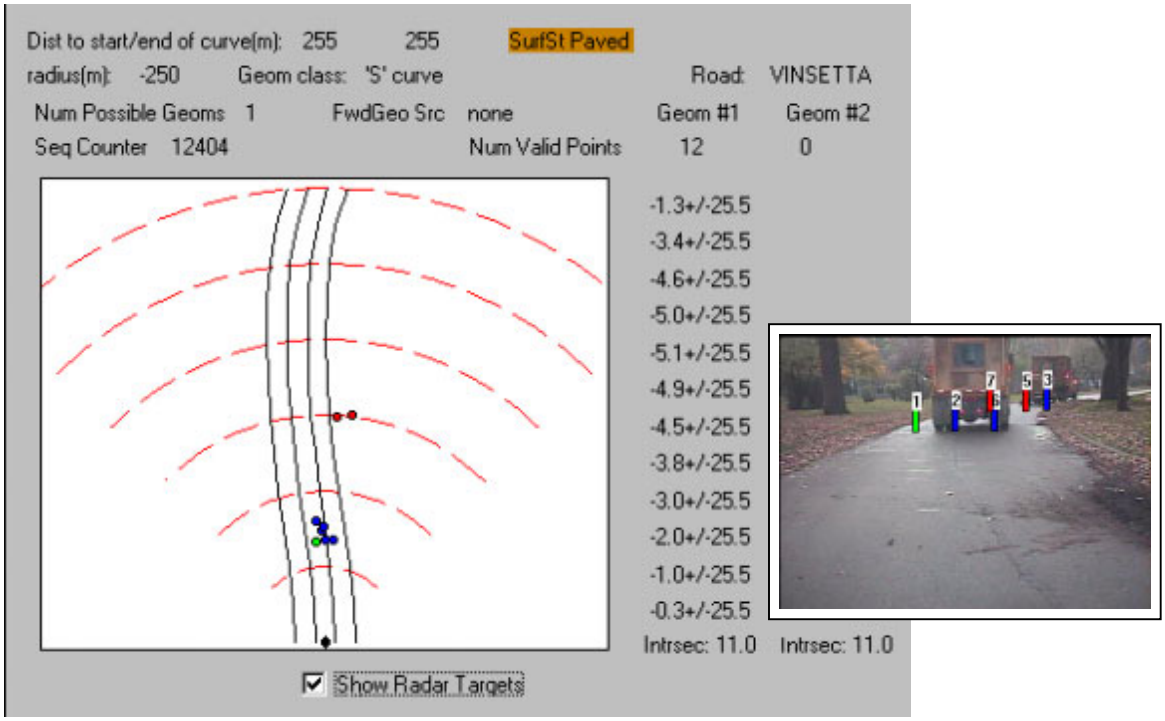

Figure 9.53 Forward Geometry Prediction on a S-shaped Road

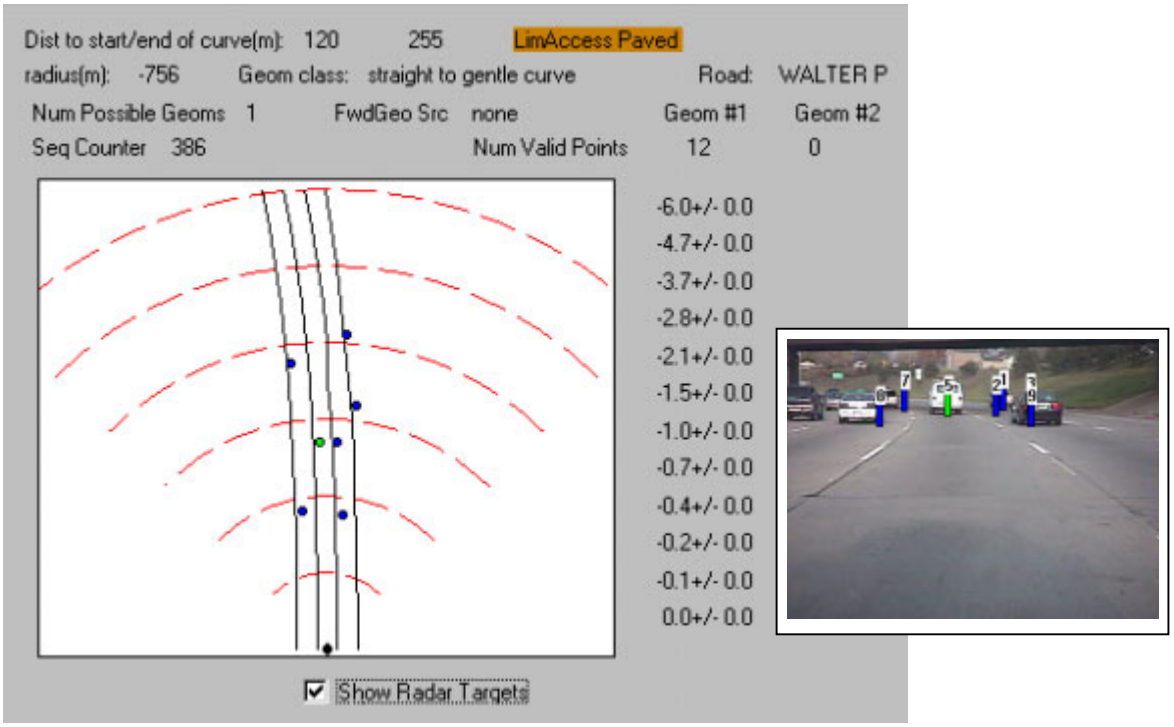

Figure 9.54 Forward Geometry on a Transition from Straight to a Gentle Curve

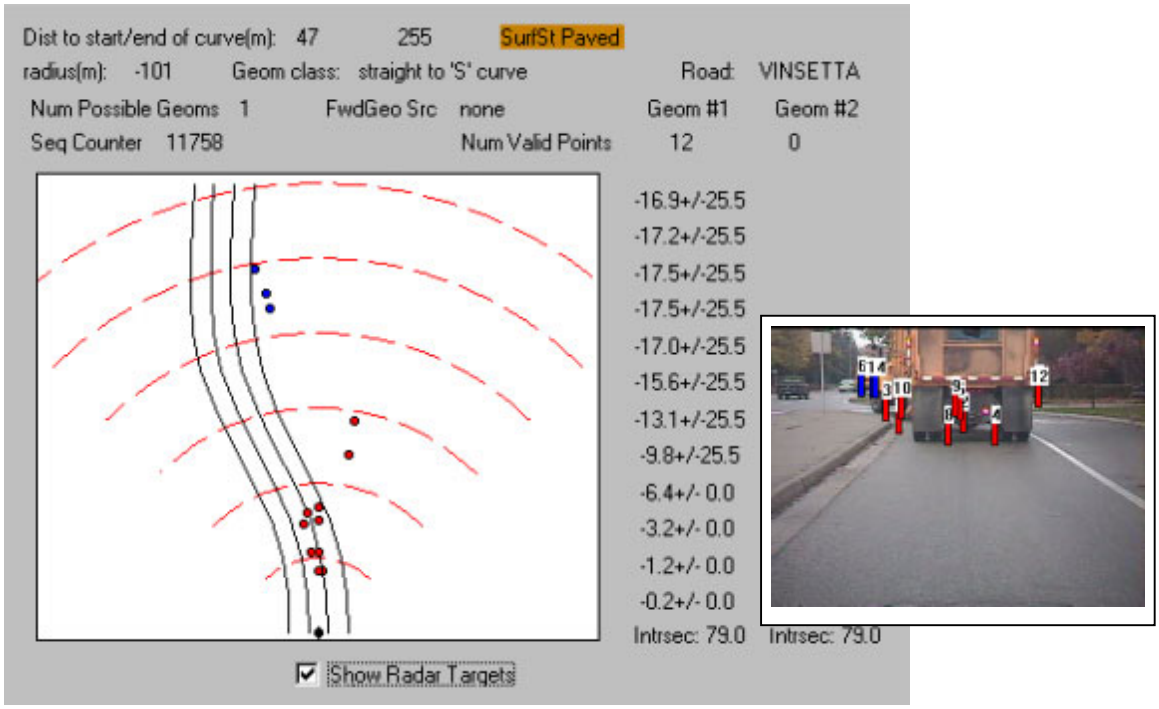

Figure 9.55 Forward Geometry on a Transition from Straight to an S-Shaped Curve

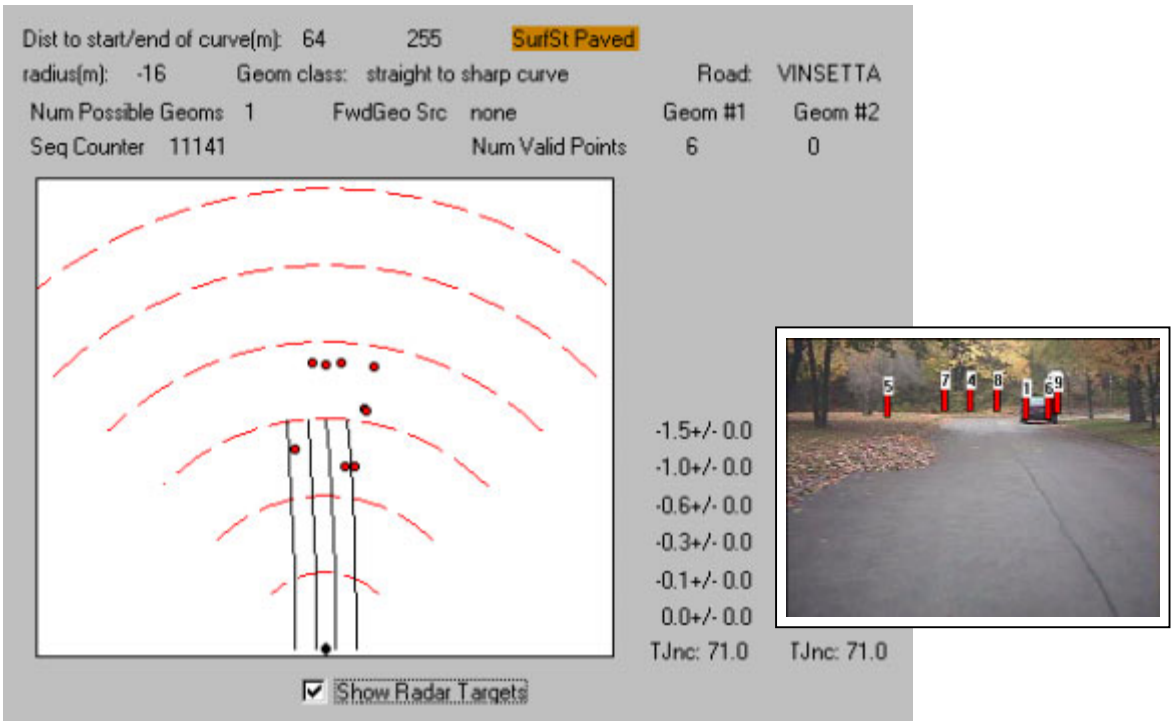

Figure 9.56 Upcoming T-Junction with Forward Geometry

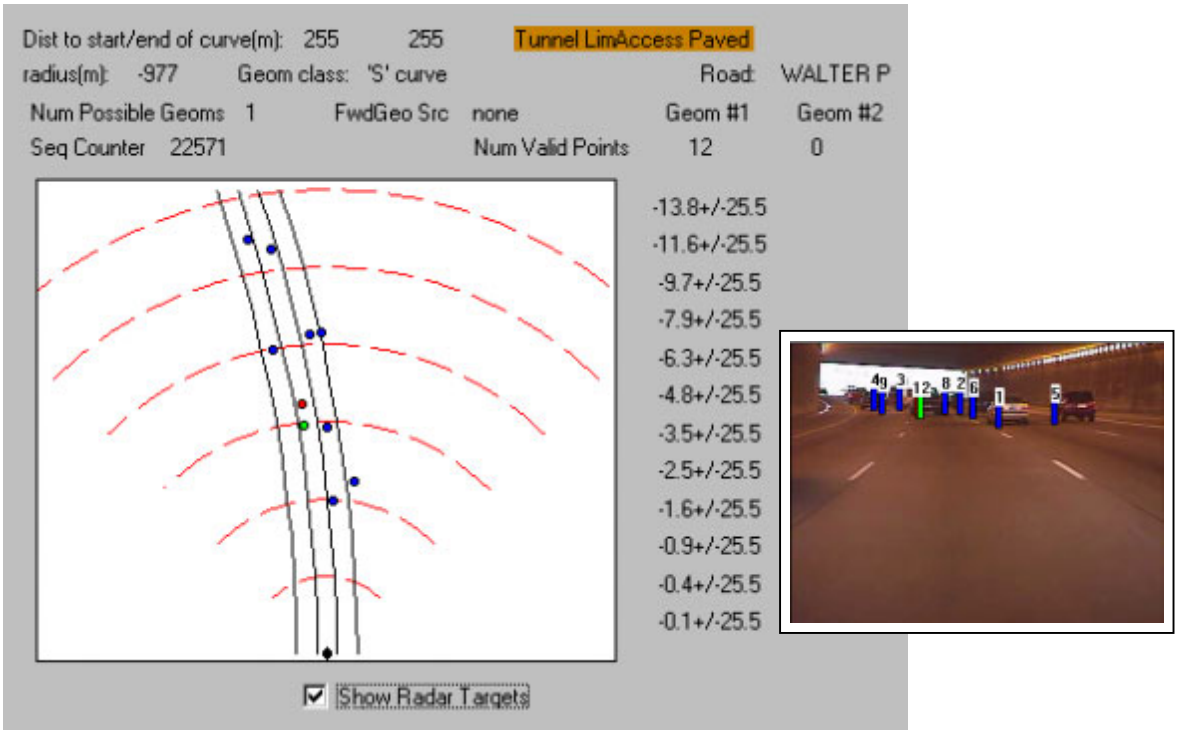

Figure 9.57 Presence of Tunnel with Forward Geometry

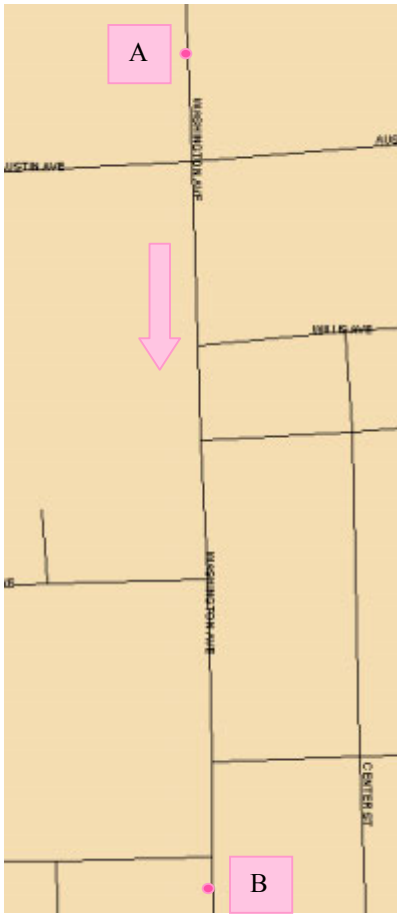

Figure 9.58 Map with Intersections

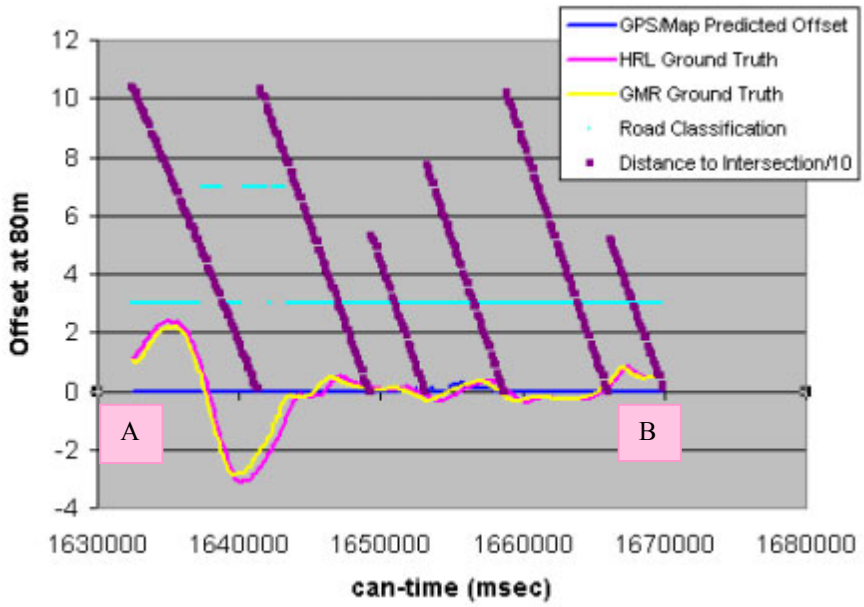

Figure 9.59 Forward Road Preview for Map Section of Figure 9.58

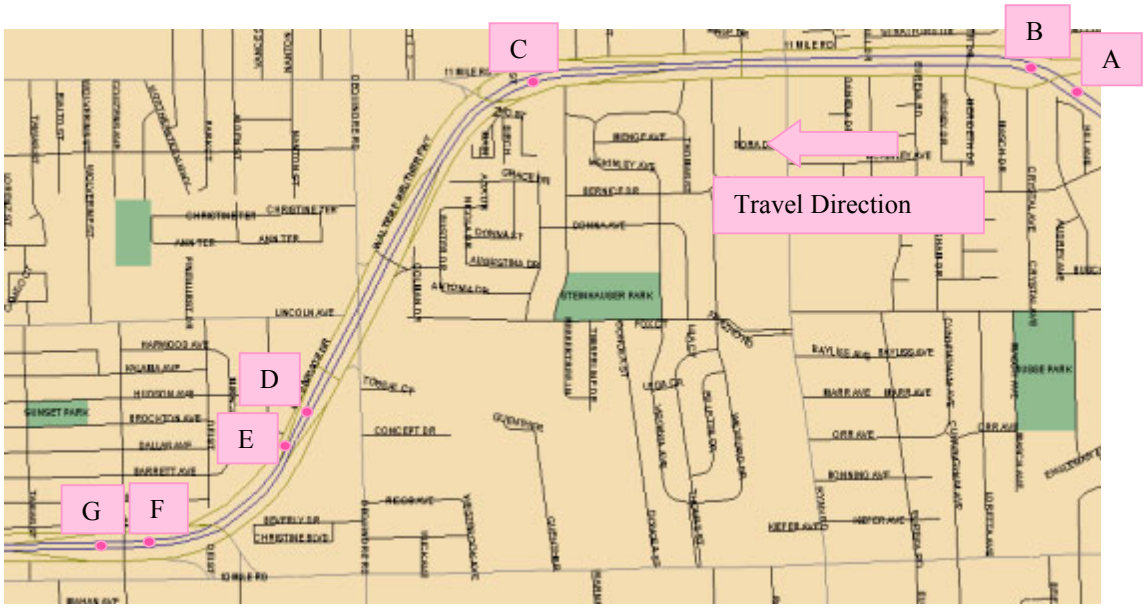

Figure 9.60 Map Depiction of the Test Freeway Road Section

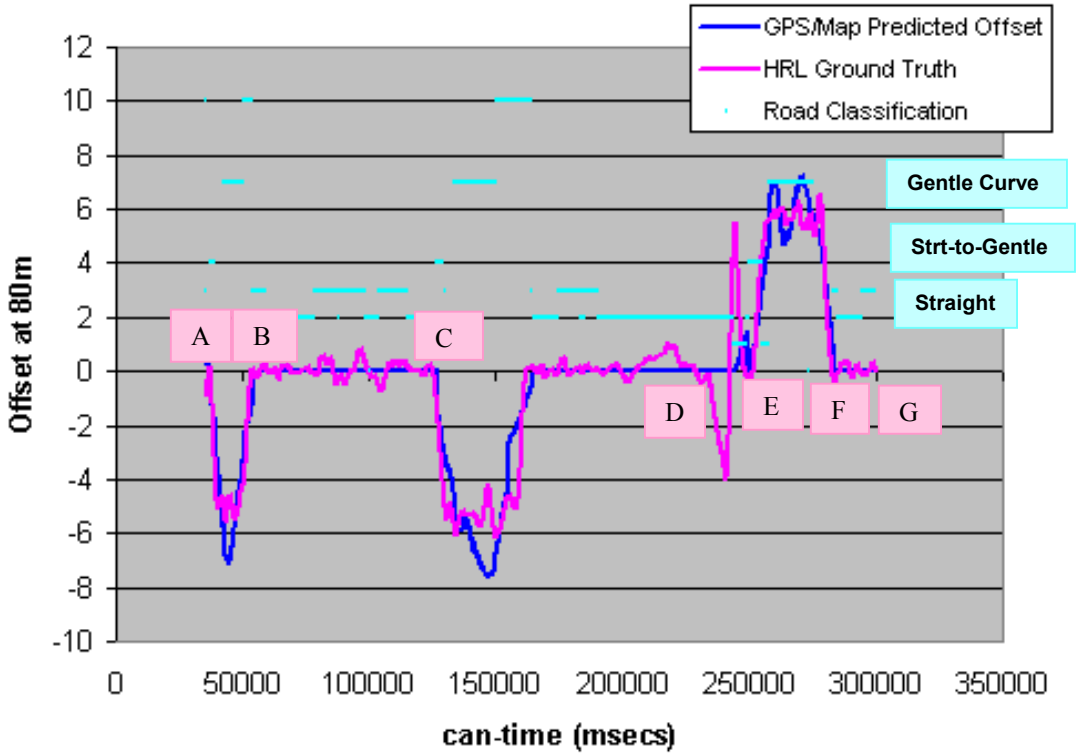

Figure 9.61 Road Offset at 80m with Road Classification

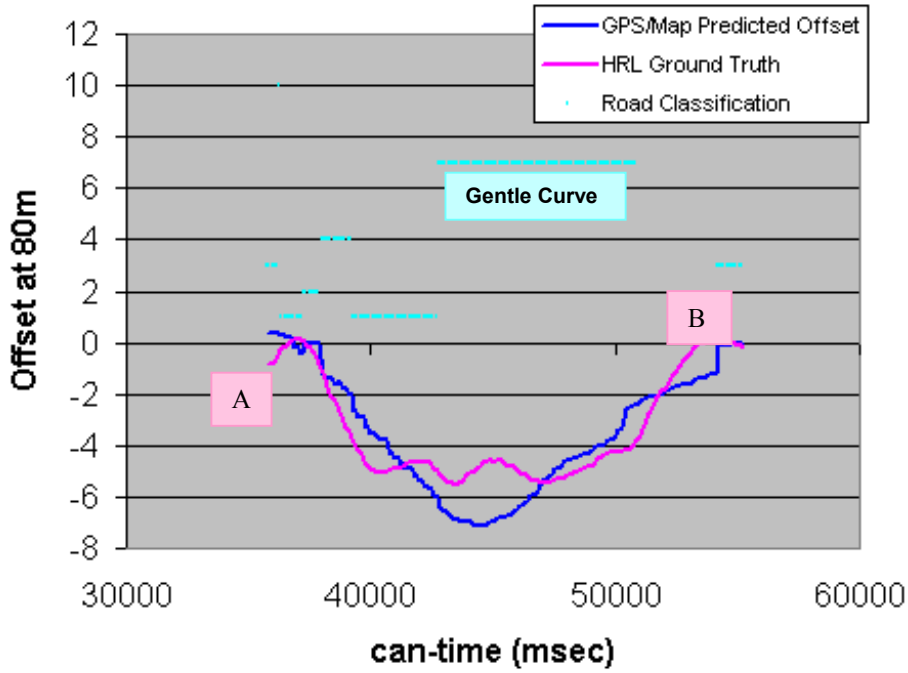

Figure 9.62 Road Offset at 80m for a Left-Hand Turn with Road Classification

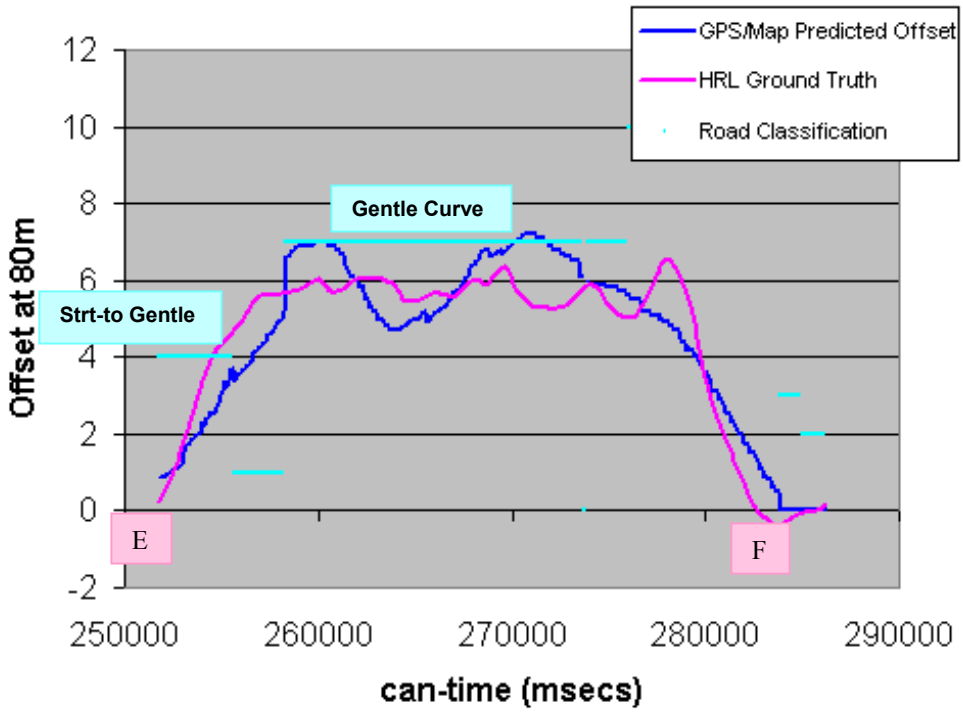

Figure 9.63 Road Offset at 80m for a Right-Hand Turn with Road Classification

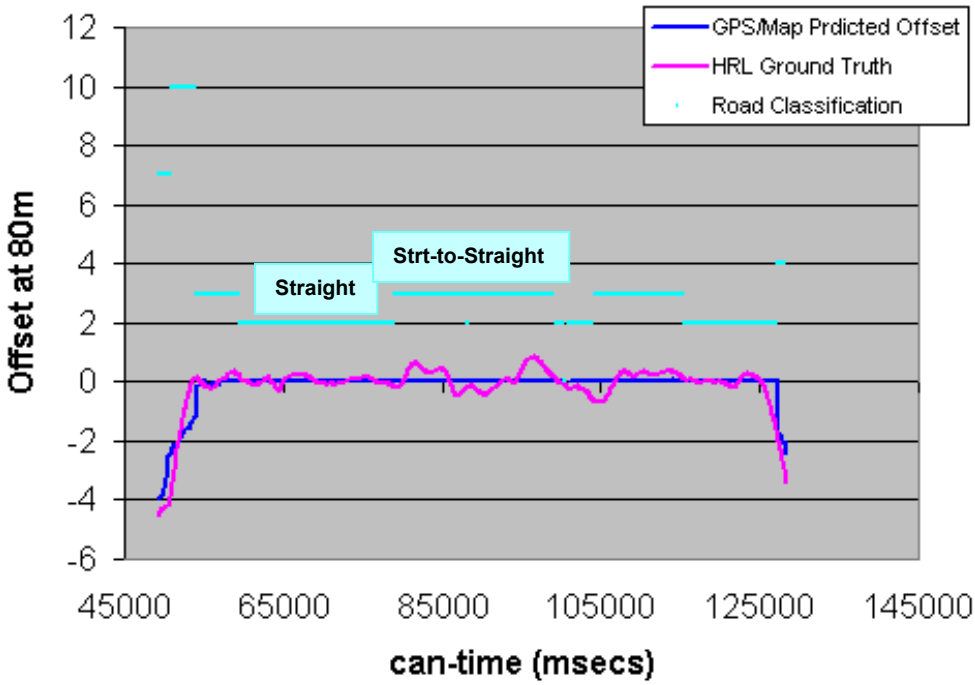

Figure 9.64 Road Offset at 80m in Curve Transitions with Road Classification

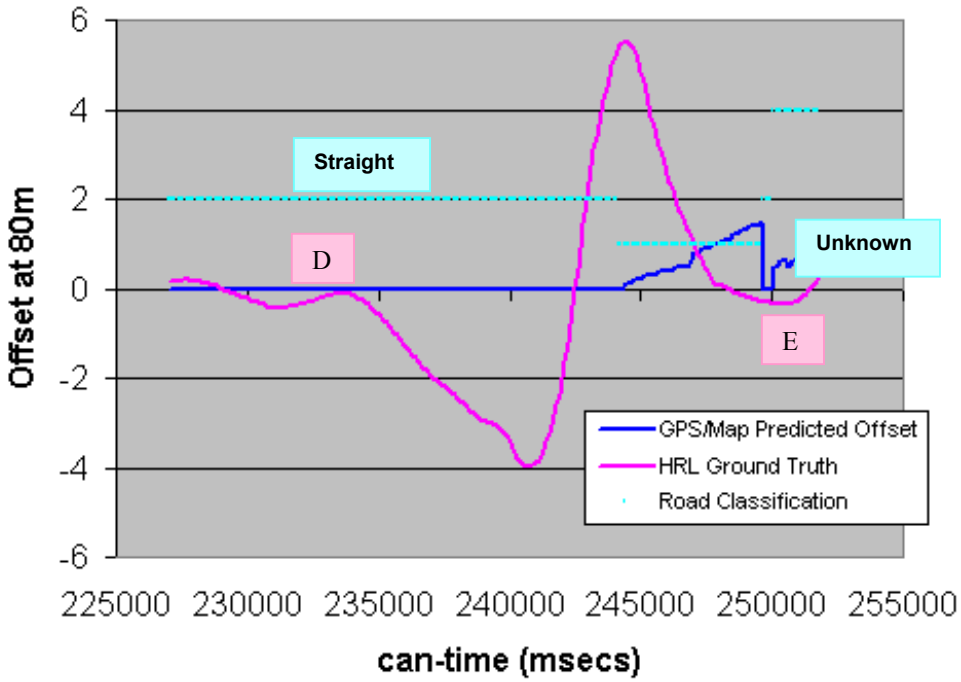

Figure 9.65 Road Offset at 80m During Lane Change with Road Classification

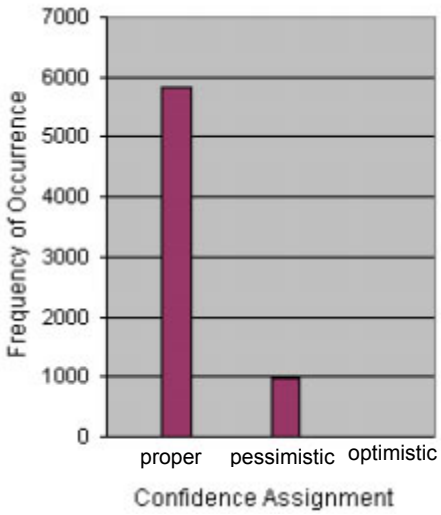

(a) Straight Roads

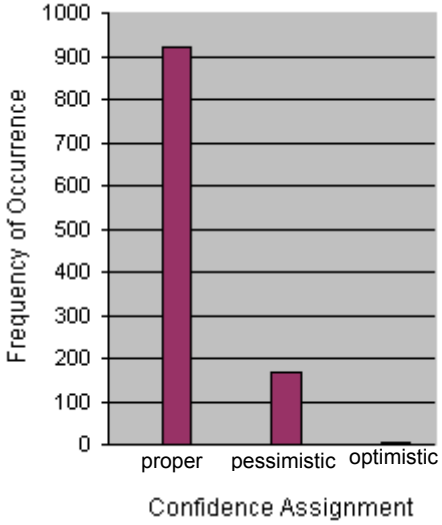

(b) Gently Curved Roads

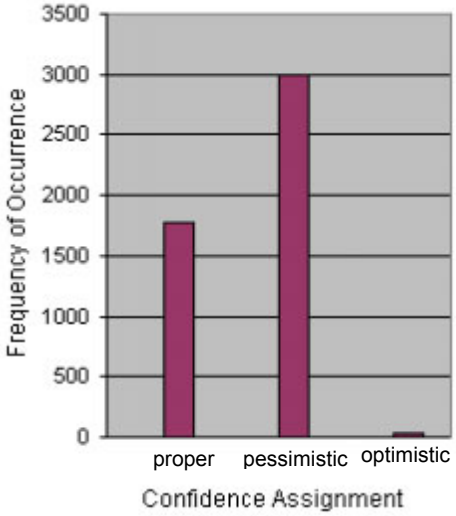

(c) During Curve Transitions

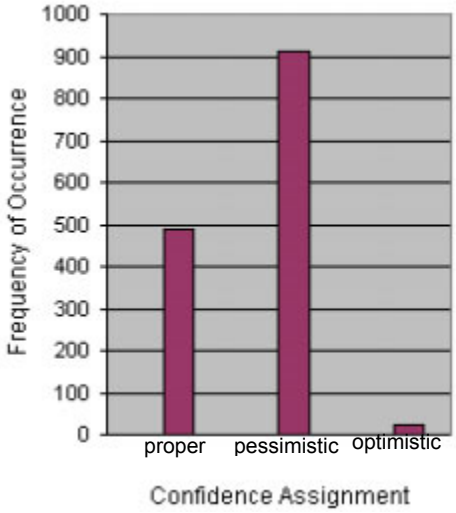

(d) Sharp and S-shape Curves

Figure 9.66 Evaluation of Confidence Assignment

Technical Problems

1. The current representation of the map database does not lend itself to the accurate geometry representation required to employ map for path prediction in a forward collision application. Accuracy in existing maps continues to be a problem for map matching as well for forward geometry prediction especially at curve transitions.
2. Quality of maps is not uniform and varies from place to place. Based on this fact, accessing quality of results is non-trivial

Current Schedule and Progress for Task C2C

Refinement of confidence measures	03/01/02
Detailed Validation of the GPS/Map subsystem	04/01/02

Current Schedule and Progress for Task C2

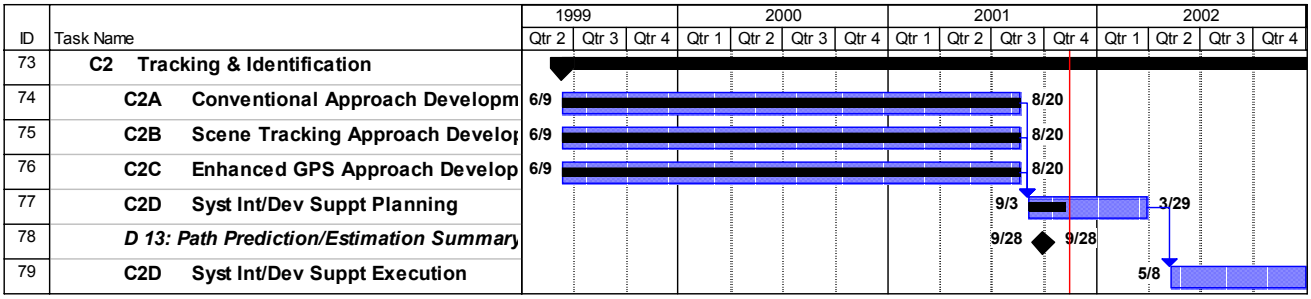

Figure 9.67 Task C2 Schedule

10 Collision Warning Function (Tasks C3 and C5)

10.1 Threat Assessment Simulation Development (Task C3A-5A)

Goals, Purpose and Background

The Threat Assessment Simulation tool, TASIM, was developed to simulate the performance of forward collision warning systems (FCWS). TASIM incorporates detailed mathematical models of sensors and algorithms that are part of the FCWS, and provided a realistic simulation environment for evaluating the performance of various threat assessment algorithms considered in the Automotive Collision Avoidance System Field Operational Test (ACAS/FOT) program. In this section we present a summary of results on threat assessment simulation that have been conducted as part of the ACAS/FOT program. We used TASIM to evaluate the performance of four different threat assessment algorithms under consideration in the ACAS/FOT program. Algorithms 1 and 2 were developed by General Motors Research and Development Center (GMR), algorithm 3 was developed by the Crash Avoidance Metrics Partnership (CAMP), and algorithm 4 was developed by the National Highway Traffic Safety Administration (NHTSA).

We first introduce the TASIM tool and describe the error models and system delays that have been incorporated in TASIM.

The TASIM Tool

TASIM enables quick evaluation of threat assessment for multiple scenarios (algorithms, sensors, vehicles, roadway conditions) and consists of the following tools:

- TASIMSHIFT – the core simulation.
- Hwyc - the highway compiler
- TAVIS – the GUI and 2D visualization tool
- VENTURI - the 3D visualization tool

VENTURI uses recorded simulation data from TAVIS for playback and provides realistic animation of the FCWS simulation. TASIM was developed by California PATH, University of California, Berkeley, using system model descriptions and algorithms provided by the ACAS/FOT team members. A graphical sketch of the TASIM tool is shown in Figure 10.1.

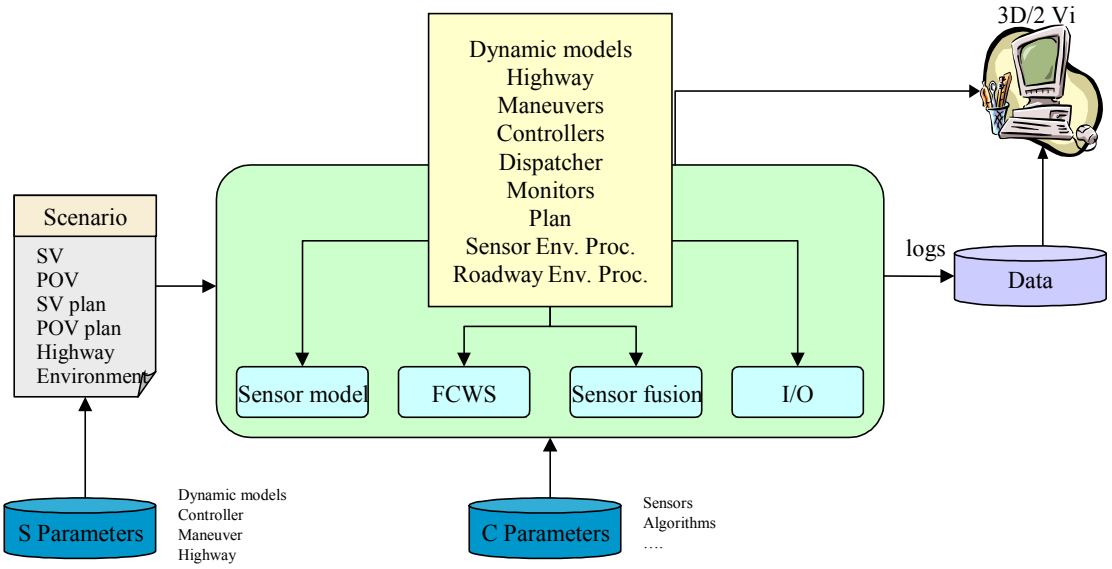

Figure 10.1 The TASIM Tool

The functional block diagram of the FCWS that is implemented in TASIMSHIFT is shown in Figure 10.2.

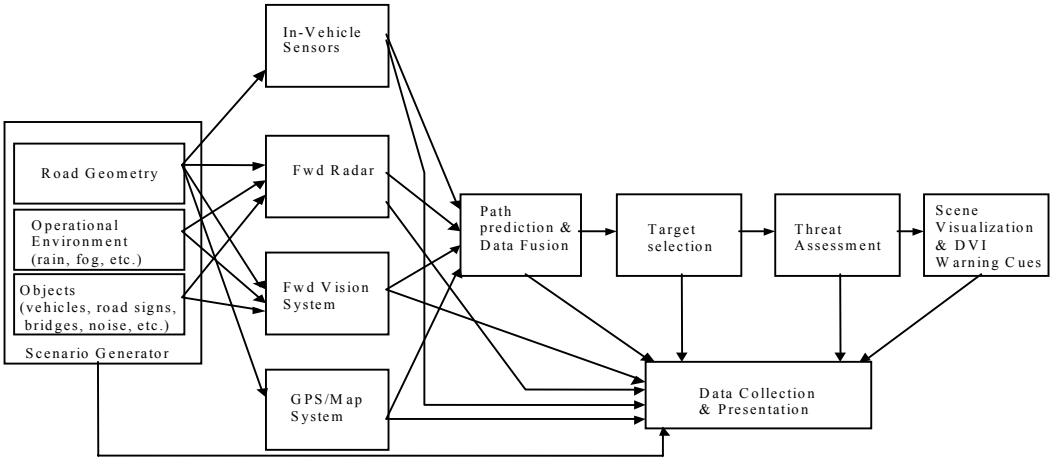

Figure 10.2 FCWS Functional Block Diagram

Error Models in TASIM

TASIM models need to be of appropriate fidelity in order to accurately gauge the effectiveness of unique user-defined ACAS threat assessment algorithms. TASIM incorporates realistic math models (including errors) of all sensors used in the FCWS. This makes the analysis results closer to what would occur with an actual experimental scenario. Within TASIM, all but the vehicle kinematic and dynamic models were created by GMR or HRL. California PATH created vehicle models based on relatively simple equations of motion. Using all these models, TASIM integrates a sequence of sensor, fusion, vehicle, and roadway models into a useable and reasonable FCWS simulation.

Radar Sensor Model

Detailed model of a frequency modulated continuous wave (FMCW) radar that is used in automotive collision avoidance applications is incorporated in TASIM. Here we briefly provide a description of the errors that are introduced for the range, range-rate, azimuth, and relative acceleration in this radar model.

The radar model in TASIM first determines if the target of interest is in the radar field of view. The radar field of view parameters are given in Table 10.1. Target range R is the slant range between the subject vehicle (SV) and the target. Target range rate, RR, (i.e. relative range rate) is the radial component of the difference between the SV and target velocity vectors, and target acceleration, a, (i.e. relative acceleration) is the radial component of the difference between the SV and target acceleration vectors. Finally θ is the azimuth angle between the SV and the target. Target relative acceleration is estimated by (10-1) as

$$a = \frac{RR(t) - RR(t - \delta T)}{\delta T} \tag{10-1}$$

where

$RR(t)$ = relative range rate measured at time t
$RR(t-\delta T)$ = relative range rate measured at time $t-\delta T$
δT = radar data rate = 0.1 sec

Table 10.1 Radar Field of View Parameters

	Parameter	Value
Minimum instrumented range	R_{min}	2 m
Maximum instrumented range	R_{max}	150 m
Minimum range rate	RR_{min}	- 64 m/s^2 (closing target)
Maximum range rate	RR_{max}	+ 32 m/s^2 (opening target)
Azimuth field of view	FOV	± 7.5^o relative to the vehicle longitudinal axis
Elevation field of view	ϕ_b	4.1^o

If a target is within the radar field of view it is processed further. Otherwise it is ignored. Targets also have a radar cross section (RCS), as shown in Table 10-2, and a fluctuation characteristic (Swerling Case I or Swerling Case V) that depends on whether they are moving or stationary.

Table 10.2 RCS for Objects of Interest

Object	RCS, σ (m^2) for SW V (nonfluctuating)object	Average RCS, σ_{av} (m^2) for SW I (fluctuating) object
Truck	10	100
Automobile	0.5	20
Person	0.5	0.4
Motorcycle	0.1	2

Next, multiple targets in the radar field of view are tested for discrimination. Table 10-3 gives the radar discrimination parameters.

Table 10.3 Radar Discrimination Parameters

	Discrimination
Range	2 m
Range Rate	3 m/s
Azimuth	2°

Discrimination refers to how close two targets can be, in the respective dimension, before they merge into one report. For example, two targets separated in range by less than 2 m would be reported as one target. However if they were separated in range by 2.5 m, for example, they would be reported as two separate targets. If two or more targets are within any of the discrimination parameters above, they are combined into one target.

The next step is to see if a target is detected. If it is, it is passed on to the target tracker with the appropriate parameters. The process is as follows:

1. Calculate the target probability of detection P_d .

2. Compare P_d to r_1 which is a uniform random number in the interval 0 to 1.

3. If $r_1 < P_d$ declare the target detected, otherwise ignore the target from further processing.

4. Output the target to the target tracker with the following random errors ε_i as follows:

   Range = $R + \varepsilon_r$
   Range rate = $RR + \varepsilon_{rr}$
   Azimuth = $\theta + \varepsilon_\theta$
   Acceleration = $a + \varepsilon_a$

where the errors are zero-mean normal distributions given by

$\varepsilon_r \sim N(0,\sigma_r)$
$\varepsilon_{rr} \sim N(0,\sigma_{rr})$
$\varepsilon_\theta \sim N(0,\sigma_\theta)$
$\varepsilon_a = [(\varepsilon_{rr})_i - (\varepsilon_{rr})_{i-\delta T}]/\ \delta T$ for scan i

The expressions for the rms measurement errors for range, range rate, azimuth and acceleration are estimated as follows:

$$\sigma_r = k_r\ \delta R/(2S)^{1/2} \qquad (10\text{-}2)$$

$$\sigma_{rr} = k_{rr}\ \delta RR/(2S)^{1/2} \qquad (10\text{-}3)$$

$$\sigma_\theta = k_\theta\ \theta_b/(2S)^{1/2} \qquad (10\text{-}4)$$

where

σ_r = rms range measurement error
σ_{rr} = rms range rate measurement error
σ_θ = rms azimuth measurement error
$\delta R = 1$ m
$\delta RR = 1.5$ m/s
$\theta_b = 3\ \delta B$ azimuth beam width = 1.7^{o}
S = signal-to-clutter plus noise ratio
k_r, k_{rr}, k_θ are constants = 1

<u>Accelerometer Sensor Model</u>
A detailed model of an accelerometer that is used for measuring the longitudinal acceleration of the SV is incorporated in TASIM and is shown in Figure 10.3. Here we briefly provide a description of the errors that are introduced for the longitudinal acceleration in this model.

The true longitudinal acceleration of the SV from the longitudinal dynamics is used as the input and the output represents the unfiltered accelerometer output that is used as input to threat assessment. Three errors representing shot noise, bias drift and scale factor drift are modeled while temperature effects are neglected. Descriptions of the Low Pass Filter (LPF) block, the Noise block and the Limiter block are given in Figure 10.6 at the end of this section.

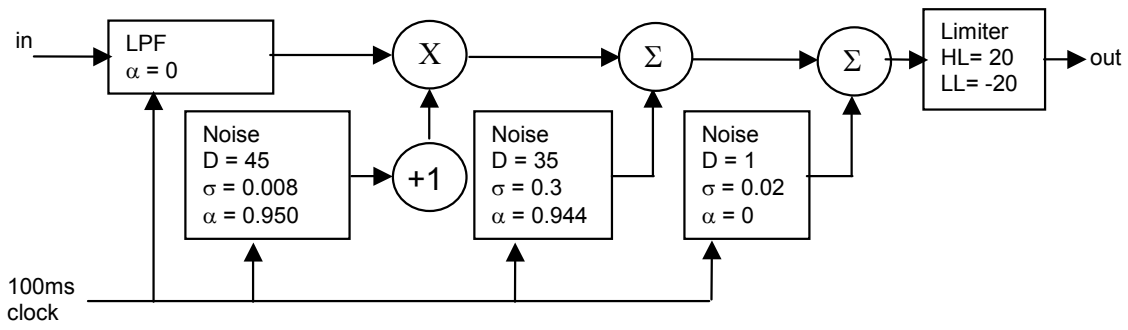

Figure 10.3 Accelerometer Model

<u>Speed Sensor Model</u>
A detailed model of a speed sensor that is used for measuring the longitudinal speed of the SV is incorporated in TASIM and is shown in Figure 10.4. Here we briefly provide a description of the errors that are introduced for the longitudinal speed in this model.

The true longitudinal speed of the SV from the longitudinal dynamics is used as the input; the output represents the internally filtered output that is used as input to threat assessment. The error represents mechanical variations in sensor teeth and variations in tire diameter.

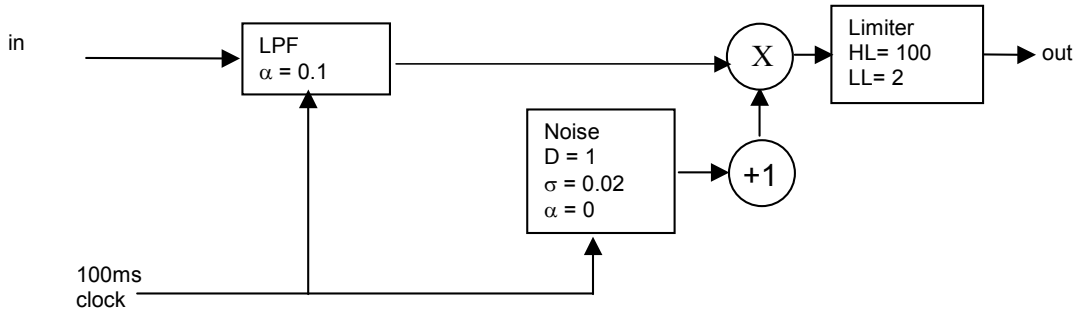

Figure 10.4 Speed Sensor Model

GPS/Map Sensor Model

The output of this model consists of 12 lateral offsets of the center of the lane from points that are 10 m apart along the lane tangent drawn forward from the vehicle position represented on the map. TASIM computes these lateral offsets, which are then used as inputs for data fusion in order to obtain the forward road geometry. Moreover, confidence measures that represent error tolerance are also expressed for each of the 12 lateral offsets.

Two sources of errors are modeled here – error in vehicle position sensing, and map database error. We model both these errors in TASIM as follows. First, we disturb the ideal SV position with map error that has been statistically obtained based on experimental data collection. Then we further disturb this position by vehicle position sensing errors due to Global Positioning System (GPS) and Differential Global Positioning System (DGPS) sensors (each with probability of 0.5). These errors have also been statistically obtained based on data collection from experiments. We next find the point on the road closest to the new (disturbed) position at the center of the lane. The 12 lateral offsets that are outputs of this model are computed with respect to this position.

In the ideal case, these errors would be zero and therefore the 12 lateral offsets could be used to accurately represent the forward road geometry up to a range of 120 m. But in practice, the vehicle position sensing errors (due to GPS or DGPS errors) and the map database errors are very significant, which may affect the forward road geometry estimation.

Vision Sensor Model

The lane sensing system consists of a forward-looking camera located behind the vehicle windshield together with associated frame-grabber hardware and video analysis software. The main inputs to the model are the true coordinates of the right and left lane markers. The main outputs are vehicle position and orientation in the lane, and the forward geometry of the lane. The forward road geometry is represented by a third order curve ($y = y_0 + ax + bx^2 + cx^3$) representing the lane centerline in a coordinate system aligned with the vehicle (camera) axes. The X coordinate corresponds to the longitudinal distance from the camera. The Y coordinate is orthogonal to this and positive to the right of the camera (vehicle) centerline.

A detailed model of a vision sensor that is used in automotive collision avoidance applications is incorporated in TASIM. Here we briefly describe the errors that are introduced in this model.

A medium-range lane sensing vision model with nominal values for system inputs as shown in Table 10.4 is incorporated in TASIM.

Table 10.4 Vision Model Parameters

Horizontal angle of view (AOV)	24 deg
Pixel width (p)	1×10^{-6} m
Focal length (f)	0.015 m
Nominal lane marker distance (d)	15, 22, 29, 36, 43, 50 m

The first module in this model determines the contrast ratio between lane marker and background pixels. The first source of error is a random zero-mean Gaussian noise with a standard deviation of 0.2 (dimensionless) that affects the contrast ratio output of this module. This error affects the lane marker detection accuracy. The second module determines whether a lane marker is detected and, if so, the position accuracy of detection. The process is as follows:

1. Calculate the lane marker probability of detection P_d.

2. Compare P_d to r_1 which is a uniform random number, $r_1 \sim U(0,1)$.

3. If $r_1 < P_d$ declare the lane marker detected, otherwise ignore the lane marker from further processing.

4. If the lane marker is detected, the lane marker position accuracy is a function of the traffic density in the vicinity and is defined by a positive value indicating the standard deviation (σ) in lateral position accuracy of an incorrect lane marker detection (*e.g.* due to detecting vehicle edge as lane marker).

The third module determines whether detected lane markers lie within the camera field of view. In addition it calculates data errors due to camera movements and incorrect lane marker detection. Suppose the true lane marker distance and lateral offset are given by (x_T, y_T). The output of this module is (x_{out}, y_{out}), the reported distance and lateral offset of the lane marker where

$$x_{out} = x_T$$
$$y_{out} = y_T + N(0,\sigma)$$

and $N(0,\sigma)$ represents a zero-mean Gaussian random variable with standard deviation σ.

The final module performs a third order polynomial curve fit of the targets corresponding to the right and left lane markers respectively, and calculates the final outputs of the vision model that are mentioned earlier.

In the ideal case, all errors would be zero and therefore the vision model output would accurately represent the forward road geometry up to a range of 50 m. But in practice these errors are very significant, which may affect the forward road geometry estimation.

System Delays

The sampling delay for FCWS sensors in TASIM is at most 100 ms. Computations within the modules that run at 100 ms are done sequentially. In a real system, computations take time and therefore this feature is modeled in TASIM by introducing time offsets between two consecutive computations. The user can specify the time offsets for all these components. In our simulations we use offsets that amount to a total delay of 40 ms between the time data is sampled by the various FCWS sensors and the time at which threat assessment issues an alert based on the current sampled data.

Brake actuation delay may be defined as the time interval between the moment the brake pedal is actuated and the moment the vehicle deceleration (or brake pressure) reaches the desired set point. We model the brake actuation delay as a first order dynamical system with a time constant of 50 ms. With this time constant, the total time interval needed to reach a desired deceleration level is about 200 ms which is close to experimentally measured values for passenger cars (see D.V.A.H.G. Swaroop, 1994).

Intermediate and Final Results

TASIM incorporates the following threat assessment algorithms:

Algorithm 1 – developed by GMR
Algorithm 2 – developed by GMR
Algorithm 3 – developed by CAMP
Algorithm 4 – developed by NHTSA

TASIM uses the actual C codes for these threat assessment algorithms as provided by the algorithm developers, and the versions are the same as in the experimental development vehicle. TASIM incorporates version 4 of the C code dated 05/30/01 for algorithms 1, 2 and 3, while the C code for algorithm 4 is version 1.3 dated 05/16/01. This was done to avoid any error in the implementation of these algorithms.

We restricted our current simulations to reflect dry weather and road conditions. The input variables provided by TASIM to the threat assessment algorithms are the following:

1. longitudinal speed of subject vehicle (SV), V_f,
2. longitudinal acceleration of SV, a_f,
3. range, R, range-rate, Rdot, of closest in-path moving (CIPV) / closest in-path stationary (CIPS) targets
4. relative acceleration , a_r, of CIPV / CIPS targets

Computation of other variables required by the threat assessment algorithms are done as follows:

1. longitudinal speed of CIPV / CIPS target, $V_l = Rdot + V_f$
2. longitudinal acceleration of CIPV / CIPS target, $a_l = a_r + a_f$

The performance of the threat assessment algorithms is evaluated using sixteen straight, scenario-specific tests. These tests are used to determine if the range of imminent alerts issued by the various algorithms in the TASIM simulator is consistent with that of

nominal values for these tests. Furthermore, these tests are used to evaluate the risk of crash posed by the timing of imminent alerts for an alert test driver braking at the onset of an imminent alert in order to avoid a crash while conducting the tests. A time series analysis based on Monte-Carlo simulation is presented for computing the probabilities of late alerts and early alerts issued by the various threat assessment algorithms on four major pre-crash scenarios that have been identified in the literature. These tests determine if the timing of an imminent alert issued by the threat assessment algorithms is late or early. An instantaneous analysis of four major pre-crash scenarios is based on a Monte-Carlo simulation for computing the probabilities of false alarms and misses due to the various threat assessment algorithms. These tests determine if the threat assessment algorithms' decision to issue an imminent alert or not is correct.

Evaluation of Threat Assessment Algorithms Using Scenario-Specific Tests
Using TASIM, we evaluated the performance of each of the threat assessment algorithms using sixteen scenario-specific tests. For each algorithm and scenario, we recorded the range at which an imminent alert is issued and determined whether the imminent alert occurred at a range that is consistent with the nominal values for that algorithm. This was done as a means of validating the performance of the threat assessment simulation in TASIM that includes various algorithms and error models of FCWS modules, including system delays.

Furthermore, once an imminent alert was issued by the selected algorithm, the SV braked at –0.6g after an assumed 1.0 s delay time made up of 0.8 s driver response time plus a 0.2 s brake actuation delay. This was an assumed response characteristic of an alert test driver to a warning stimulus that was used to determine the amount of risk in the timing of the imminent alert for an alert test driver while running the test in an experiment.

The following definitions are used here:
Nominal Range of Imminent Alert: Ideal range at which threat assessment algorithm would issue an imminent alert for the particular test if there were no sensor errors, no system delays, and if the SV and Principal Other Vehicle (POV) were traveling on the same lane and in a straight road.

TASIM Range of Imminent Alert: Actual range at which threat assessment algorithm issues an imminent alert for the particular test in TASIM simulation that includes all the sensor error models, system delays and other FCWS modules as described.

TASIM Minimum Range if No Crash: Minimum range between SV and POV in the TASIM simulation if there is no crash.

TASIM Crash DeltaV if Crash: Relative speed of impact if there is a crash in TASIM simulation.

Algorithms 1, 2 and 3 were simulated with sensitivity setting equal to 4, while algorithm 4 was simulated with sensitivity setting equal to 1.

Test 1 – SV 60 mph to POV Stopped

In this test the SV travels at a constant 60 mph (26.82 m/s) on a straight, flat road. Ahead of the SV, in the same lane, is a single stopped POV. The initial headway is 5.6 s, which corresponds to an initial range of 150 m. Table 10.5 provides the alert ranges of imminent alerts for the various threat assessment algorithms and may be used to evaluate the risk for an alert test driver in Test 1.

Table 10.5 Results of Test 1

Algorithm No.	Nominal Range of Imminent Alert (m)	TASIM Range of Imminent Alert (m)	TASIM Minimum Range if No Crash (m)	TASIM Crash DeltaV if Crash (m/s)
1	48.3	48.6	-	20.4
2	93.9	92.9	9.0	
3	118.0	116.5	32.6	
4	104.6	98.8	14.9	

We note that, for algorithms 1, 2 and 3, the range of imminent alerts in the TASIM simulation are consistent with the nominal values despite the sensor errors and system delays modeled in TASIM. The difference in the range and timing of imminent alert of algorithm 4 in TASIM from the nominal values is due to additional delays introduced by filters used for longitudinal acceleration and relative acceleration measurements in the TASIM implementation of algorithm 4. Algorithm 1 issues the imminent alert too late for the test driver. This is due to the 50 m range clip used in algorithm 1 for issuing alerts due to stationary targets.

Test 2 – SV 50 mph to POV 10 mph

In this test the SV travels at a constant 50 mph (22.35 m/s) on a straight, flat road. Ahead of the SV, in the same lane, is a single POV traveling at a much slower speed of 10 mph (4.47 m/s). The initial headway of 6.7 s corresponds to an initial range of 150 m. Table 10.6 provides the alert ranges of imminent alerts for the various threat assessment algorithms and may be used to evaluate the risk for an alert test driver in Test 2.

Table 10.6 Results of Test 2

Algorithm No.	Nominal Range of Imminent Alert (m)	TASIM Range of Imminent Alert (m)	TASIM Minimum Range if No Crash (m)	TASIM Crash DeltaV if Crash (m/s)
1	87.4	86.4	44.0	
2	87.4	86.4	44.0	
3	85.6	84.4	42.0	
4	57.0	58.8	16.5	

We note that, for all algorithms, the range of imminent alerts in the TASIM simulation are consistent with the nominal values despite the sensor errors and system delays modeled in TASIM.

Test 3 – SV 60 mph to POV Braking Moderately Hard from 60 mph
In this test the SV travels at a constant 60 mph (26.82 m/s) on a straight, flat road. Ahead of the SV, in the same lane, is a single POV initially traveling at the same speed as the SV. The initial headway is 2 s, which corresponds to an initial range of 53.6 m. The POV then brakes moderately at –0.3g. Table 10.7 provides the alert ranges of imminent alerts for the various threat assessment algorithms and may be used to evaluate the risk for an alert test driver in Test 3.

Table 10.7 Results of Test 3

Algorithm No.	Nominal Range of Imminent Alert (m)	TASIM Range of Imminent Alert (m)	TASIM Minimum Range if No Crash (m)	TASIM Crash DeltaV if Crash (m/s)
1	43.7	45.9	24.4	
2	37.6	37.7	3.2	
3	49.9	49.1	33.7	
4	43.7	44.3	20.2	

We note that, for all algorithms, the range of imminent alerts in the TASIM simulation are consistent with the nominal values, despite the sensor errors and system delays modeled in TASIM. The timing of the imminent alert of Algorithm 2 is such that the test driver is just able to avoid the crash.

Test 4 – SV 50 mph to POV Stopped in Transition to Curve
In this test the SV begins by traveling at a constant 50 mph (22.35 m/s) on a straight section of a flat road. Ahead of the SV, after the beginning of the curve, is a single POV stopped in the lane of travel. The initial headway is 6.7 s, which corresponds to an initial range of 150 m. The POV is stationary at a distance of 83 m from the beginning of the curve. The radius of curvature of the center of the travel lane is 752 m. Table 10.8 provides the alert ranges of imminent alerts for the various threat assessment algorithms and may be used to evaluate the risk for an alert test driver in Test 4.

Table 10.8 Results of Test 4

Algorithm No.	Nominal Range of Imminent Alert (m)	TASIM Range of Imminent Alert (m)	TASIM Minimum Range if No Crash (m)	TASIM Crash DeltaV if Crash (m/s)
1	49.4	48.4	-	12.4
2	80.7	80.3	19.0	
3	100.8	100.0	38.6	
4	78.4	77.9	16.5	

We note that, for all algorithms, the range of imminent alerts in the TASIM simulation is consistent with the nominal values despite the curved roadway geometry, and sensor errors and system delays modeled in TASIM. TASIM predicts the roadway geometry well in advance as is observed from the alert range of algorithm 3. Algorithm 1 issues the imminent alert too late for the test driver. This is due to the 50 m range clip used in algorithm 1 for issuing alerts due to stationary targets.

Test 5 – SV 50 mph to POV 25 mph in a Tight Curve
In this test the SV begins by traveling at a constant 50 mph (22.35 m/s) on a curved, flat road. Ahead of the SV, in the same lane on the curve, is a single POV traveling at a lower constant speed of 25 mph (11.175 m/s). The initial headway is 2.42 s, which corresponds to an initial range of 54 m. The radius of curvature of the center of the travel lane is 208.7 m. Table 10.9 provides the alert ranges of imminent alerts for the various threat assessment algorithms and may be used to evaluate the risk for an alert test driver in Test 5.

Table 10.9 Results of Test 5

Algorithm No.	Nominal Range of Imminent Alert (m)	TASIM Range of Imminent Alert (m)	TASIM Minimum Range if No Crash (m)	TASIM Crash DeltaV if Crash (m/s)
1	47.4	46.2	26.1	
2	47.4	46.2	26.1	
3	54.1	46.2	26.1	
4	30.6	30.3	10.1	

We note that, for algorithms 1,2 and 4, the range of imminent alerts in the TASIM simulation are consistent with the nominal values despite the curved roadway geometry, and sensor errors and system delays modeled in TASIM. For algorithm 3, the initialization time needed for the TASIM simulation delayed the imminent alert.

Test 6 – SV 60 mph Cut-off by POV 40 mph
In this test the SV travels at a constant 60 mph (26.82 m/s) on a straight, flat road. Ahead of the SV, in an adjacent lane, is a single POV traveling at a slower speed of 40 mph

(17.88 m/s). The initial headway is 3 s, which corresponds to an initial range of 80.5 m when the slower POV changes lanes in front of the SV. Table 10.10 provides the alert ranges of imminent alerts for the various threat assessment algorithms and may be used to evaluate the risk for an alert test driver in Test 6.

Table 10.10 Results of Test 6

Algorithm No.	Nominal Range of Imminent Alert (m)	TASIM Range of Imminent Alert (m)	TASIM Minimum Range if No Crash (m)	TASIM Crash DeltaV if Crash (m/s)
1	35.8	35.7	21.3	
2	35.8	35.7	21.3	
3	51.9	50.5	36.1	
4	24.1	23.9	9.5	

We note that, for all algorithms, the range and of imminent alerts in the TASIM simulation are consistent with the nominal values despite the sensor errors and system delays modeled in TASIM.

Test 7 – SV 45 mph Changes Lanes and Encounters POV Stopped

In this test the SV travels at a constant 45 mph (20.1 m/s) on a straight, flat road. Ahead of the SV, in an adjacent lane, is a single stopped POV. The initial headway is 7.46 s, which corresponds to an initial range of 150 m when the SV begins to change lanes and encounters the stopped POV directly ahead. Table 10.11 provides the alert ranges of imminent alerts for the various threat assessment algorithms and may be used to evaluate the risk for an alert test driver in Test 7.

Table 10.11 Results of Test 7

Algorithm No.	Nominal Range of Imminent Alert (m)	TASIM Range of Imminent Alert (m)	TASIM Minimum Range if No Crash (m)	TASIM Crash DeltaV if Crash (m/s)
1	49.5	47.6	-	6.8
2	69.6	60.8	9.4	
3	89.7	65.3	13.8	
4	67.6	60.8	9.4	

We note that, for all algorithms, the timing of imminent alerts in the TASIM simulation occurs later than the nominal values. This is because the SV changes lanes and encounters the POV only at a range of 66.5 m, so a CIPS target is not reported by target selection until the range is about 66.5 m. Algorithm 1 issues the imminent alert late for the test driver and the SV crashes into the POV. This is due to the 50 m range clip used in algorithm 1 for issuing alerts due to stationary targets.

Test 8 – SV 60 mph Tailgating POV Braking from 60 mph

In this test the SV travels at a constant 60 mph (26.82 m/s) on a straight, flat road. Ahead of the SV, in the same lane, is a single POV initially traveling at the same speed as the SV. The initial headway is 0.6 s, which corresponds to an initial range of 16.1 m. The POV then brakes at –0.2g. Table 10.12 provides the alert ranges of imminent alerts for the various threat assessment algorithms and may be used to evaluate the risk for an alert test driver in Test 8.

Table 10.12 Results of Test 8

Algorithm No.	Nominal Range of Imminent Alert (m)	TASIM Range of Imminent Alert (m)	TASIM Minimum Range if No Crash (m)	TASIM Crash DeltaV if Crash (m/s)
1	13.6	14.4	9.2	
2	13.6	13.5	7.0	
3	16.1	16.1	14.5	
4	14.4	14.1	8.5	

We note that, for all algorithms the range of imminent alerts in the TASIM simulation are consistent with the nominal values despite the sensor errors and system delays modeled in TASIM.

Test 9 – SV 60 mph Approaches Motorcycle and Truck POVs 20 mph

In this test the SV travels at a constant 60 mph (26.82 m/s) on a straight, flat road. Ahead of the SV, in each adjacent lane, is a large truck POV traveling at a slower speed of 20 mph (8.94 m/s). Between the trucks, in the same lane as the SV, is a motorcycle POV traveling at the same speed as the trucks The initial headway is 5.6 s, which corresponds to an initial range of 150 m. In TASIM, motorcycles and trucks are simulated by using appropriate values for their radar cross sections as shown in Table 10.2. A moving truck has a radar cross section that is 5 times that of a moving passenger car. Likewise, a moving motorcycle has a radar cross section that is 0.1 times that of a passenger car. Table 10.13 provides the alert ranges of imminent alerts for the various threat assessment algorithms and may be used to evaluate the risk for an alert test driver in Test 9.

Table 10.13 Results of Test 9

Algorithm No.	Nominal Range of Imminent Alert (m)	TASIM Range of Imminent Alert (m)	TASIM Minimum Range if No Crash (m)	TASIM Crash DeltaV if Crash (m/s)
1	103.4	96.2	53.8	
2	103.4	96.2	53.8	
3	92.7	96.2	53.8	
4	57.0	56.9	14.5	

We note that, for algorithms 1 and 2, the range of imminent alerts in the TASIM simulation are not consistent with the nominal values. In algorithms 1 and 2, a DeltaV threshold of 40 mph makes the algorithm switch between two different formulas for the assumed SV braking capability. Hence, the range rate error could cause chattering in the timing of the imminent alert when DeltaV is around 40 mph. This phenomenon is clear in this simulation.

Test 10 – SV 60 mph Approaches Motorcycle behind Truck POVs 20 mph
In this test the SV travels at a constant 60 mph (26.82 m/s) on a straight, flat road. Ahead of the SV, in the same lane, is a motorcycle POV behind a large truck POV traveling at a slower speed of 20 mph (8.94 m/s). The initial headway between the SV and motorcycle POV is 5.6 s, which corresponds to an initial range of 150 m. The initial distance between the motorcycle POV and the truck POV is 10 m. In TASIM, motorcycles and trucks are simulated by using appropriate values for their radar cross sections as shown in Table 10.2. A moving truck has a radar cross section that is 5 times that of a moving passenger car. Likewise, a moving motorcycle has a radar cross section that is 0.1 times that of a passenger car. Table 10.14 provides the alert ranges of imminent alerts for the various threat assessment algorithms and may be used to evaluate the risk for an alert test driver in Test 10.

Table 10.14 Results of Test 10

Algorithm No.	Nominal Range of Imminent Alert (m)	TASIM Range of Imminent Alert (m)	TASIM Minimum Range if No Crash (m)	TASIM Crash DeltaV if Crash (m/s)
1	103.4	104.1	61.7	
2	103.4	104.1	61.7	
3	92.7	96.2	53.8	
4	57.0	60.8	18.4	

We note that, for all algorithms, the range of imminent alerts in the TASIM simulation is consistent with the nominal values

Test 11 – SV 50 mph to POV Stopped in Transition to Curve with Poor Lane Markings
The scenario description for this test is the same as in Test 4. The poor lane markings are simulated in TASIM by setting the vision health flag to zero. Table 10.15 provides the alert ranges of imminent alerts for the various threat assessment algorithms and may be used to evaluate the risk for an alert test driver in Test 11.

Table 10.15 Results of Test 11

Algorithm No.	Nominal Range of Imminent Alert (m)	TASIM Range of Imminent Alert (m)	TASIM Minimum Range if No Crash (m)	TASIM Crash DeltaV if Crash (m/s)
1	49.4	48.4	-	12.35
2	80.7	80.33	19.0	
3	100.8	100.0	38.6	
4	78.4	77.9	16.5	

We note that, for all algorithms, the range of imminent alerts in the TASIM simulation is consistent with the nominal values despite the curved roadway geometry, absence of vision sensor output, and sensor errors and system delays modeled in TASIM. TASIM predicts the roadway geometry well in advance as is observed from the alert range of algorithm 3, and in this case with just the GPS/Map sensor. Algorithm 1 issues the imminent alert too late for the test driver. This is due to the 50 m range clip used in algorithm 1 for issuing alerts due to stationary targets

Test 12 – SV 50 mph on Curve to POV Braking Moderately Hard from 50 mph on Curve
In this test the SV begins by traveling at a constant 50 mph (22.35 m/s) on a curved, flat road. Ahead of the SV, in the same lane on the curve, is a single POV traveling the same speed. The initial headway for the simulation is 2 s, which amounts to an initial range of 44.7 m. The POV begins braking at –0.3g, so that the SV begins closing on the POV. The radius of curvature of the center of the travel lane is 502 m. Table 10.16 provides the alert ranges of imminent alerts for the various threat assessment algorithms and may be used to evaluate the risk for an alert test driver in Test 12.

Table 10.16 Results of Test 12

Algorithm No.	Nominal Range of Imminent Alert (m)	TASIM Range of Imminent Alert (m)	TASIM Minimum Range if No Crash (m)	TASIM Crash DeltaV if Crash (m/s)
1	38.2	40.2	24.8	
2	33.2	32.7	4.4	
3	41.8	42.2	31.0	
4	36.9	37.6	17.5	

We note that, for all algorithms, the range and timing of imminent alerts in the TASIM simulation are consistent with the nominal values despite the curved roadway geometry, and sensor errors and system delays modeled in TASIM.

Test 13 – SV 61 mph Tailgating POV 60 mph
In this test the SV travels at a constant 61 mph (27.27 m/s) on a straight, flat road. Ahead of the SV, in the same lane, is a single POV traveling at a speed of 60 mph (26.82 m/s). The initial headway for the simulation is 0.37 s, which corresponds to an initial range of

10 m. Table 10.17 provides the alert ranges of imminent alerts for the various threat assessment algorithms and may be used to evaluate the risk for an alert test driver in Test 13.

Table 10.17 Results of Test 13

Algorithm No.	Nominal Range of Imminent Alert (m)	TASIM Range of Imminent Alert (m)	TASIM Minimum Range if No Crash (m)	TASIM Crash DeltaV if Crash (m/s)
1	5.4	5.5	5.1	
2	5.4	5.5	5.1	
3	2.6	2.7	2.3	
4	5.4	5.3	4.9	

We note that, for all algorithms, the range of imminent alerts in the TASIM simulation is consistent with the nominal values despite the sensor errors and system delays modeled in TASIM. Algorithm 3 allows the SV to tailgate the POV very closely and does not have a special tailgating mode for providing imminent alerts.

Test 14 – SV 50 mph to POV Braking Unusually Hard from 50 mph
In this test the SV travels at a constant 50 mph (22.35 m/s) on a straight, flat road. Ahead of the SV, in the same lane, is a single POV initially traveling at the same speed as the SV. The initial headway for the simulation is 2 s, which corresponds to an initial range of 44.7 m. The POV then brakes hard at –0.6 g. Table 10.18 provides the alert ranges of imminent alerts for the various threat assessment algorithms and may be used to evaluate the risk for an alert test driver in Test 14.

Table 10.18 Results of Test 14

Algorithm No.	Nominal Range of Imminent Alert (m)	TASIM Range of Imminent Alert (m)	TASIM Minimum Range if No Crash (m)	TASIM Crash DeltaV if Crash (m/s)
1	44.7	44.6	20.7	
2	44.7	44.6	20.7	
3	44.6	44.6	20.7	
4	44.2	44.4	18.2	

We note that, for all algorithms the range of imminent alerts in the TASIM simulation is consistent with the nominal values despite the sensor errors and system delays modeled in TASIM.

Test 15 – SV 45 mph to POV Stopping from 45 mph
In this test the SV travels at a constant 45 mph (20.1 m/s) on a straight, flat road. Ahead of the SV, in the same lane, is a single POV initially traveling at the same speed as the SV. The initial headway for the simulation is 6 s, which corresponds to an initial range of

120.7 m. The POV then brakes hard at –0.5 g. Table 10.19 provides the alert ranges of imminent alerts for the various threat assessment algorithm and may be used to evaluate the risk for an alert test driver in Test 15.

Table 10.19 Results of Test 15

Algorithm No.	Nominal Range of Imminent Alert (m)	TASIM Range of Imminent Alert (m)	TASIM Minimum Range if No Crash (m)	TASIM Crash DeltaV if Crash (m/s)
1	73.5	71.4	18.8	
2	73.5	71.4	18.8	
3	92.4	88.6	36.7	
4	67.4	66.9	14.3	

We note that, for all algorithms the range of imminent alerts in the TASIM simulation is consistent with the nominal values despite the sensor errors and system delays modeled in TASIM.

Test 16 – SV 45 mph behind 45 mph POV Changing Lanes to Reveal Stopped POV
In this test the SV travels at a constant 45 mph (20.1 m/s) on a straight, flat road. Ahead of the SV, in the same lane, is a single POV traveling at the same speed as the SV. The SV follows the POV at an initial headway of 1 s, which amounts to an initial range of 20.1 m. Far ahead of the SV is another POV stopped in the same lane. The initial range between the SV and the stopped POV is 163.4 m. The POV changes lanes to avoid the stopped POV thus revealing the stopped POV to the SV in its lane of travel. Table 10.20 provides the alert ranges of imminent alerts for the various threat assessment algorithms and may be used to evaluate the risk for an alert test driver in Test 16.

Table 10.20 Results of Test 16

Algorithm No.	Nominal Range of Imminent Alert (m)	TASIM Range of Imminent Alert (m)	TASIM Minimum Range if No Crash (m)	TASIM Crash DeltaV if Crash (m/s)
1	48.7	47.6	-	6.8
2	68.9	67.5	16.0	
3	89.0	85.2	33.7	
4	66.8	63.0	11.6	

We note that, for all algorithms, the range of imminent alerts in the TASIM simulation is consistent with the nominal values despite the sensor errors and system delays modeled in TASIM. Algorithm 1 issues the imminent alert late for the test driver and SV crashes into the stopped POV. This is due to the 50 m range clip used in algorithm 1 for issuing alerts due to stationary targets.

Evaluation of Threat Assessment Algorithms Using Analysis of Early and Late Alerts

Using TASIM, we determine if the timing of the imminent alert is early or late for each of the threat assessment algorithms. We consider four major rear-end crash scenarios that accounts for 84.3 % of all rear-end pre-crash scenarios (see W.G. Najm, C.J. Wiacek, and A.L. Burgett, 1998) as shown in Table 10.21.

Table 10.21 Four Major Rear-End Pre-Crash Scenarios

No.	Scenario Definition	Relative Frequency, %
1	SV is traveling at constant speed on a straight road and encounters stopped POV in traffic lane ahead	30.2
2	SV is traveling at constant speed on a straight road and encounters POV traveling at a constant, lower speed in traffic lane ahead	14.1
3	SV and POV are traveling at constant and similar speed on a straight road in same lane; POV then decelerates	37.0
4	SV is traveling at constant speed and encounters stopped POV on a curved road in traffic lane ahead	3.0
	Total	84.3

For each scenario and selected threat assessment algorithm, we conduct a Monte-Carlo, time series analysis, based on 2000 runs of the simulation, in order to compute the number of early and late alerts respectively. Certain variables that define the scenarios are assumed to be random distributions. The initial conditions for the simulation are such that there is no imminent alert at time t = 0. When the selected threat assessment algorithm issues an imminent alert, it is assumed that the driver of the SV brakes to achieve a certain constant random deceleration after a certain random driver response time. If a crash occurs, then the imminent alert is late; otherwise the imminent alert is early. If the imminent alert is late, we determine the crash DeltaV; otherwise we determine the final range between the vehicles. A record of the results for the tests is used to determine the probabilities of early and late alerts for each threat assessment algorithm, and to determine how early (or late) the imminent warning is issued.

The following definitions are used in this section:

p(early):	probability that the imminent alert is issued early.
p(late):	probability that the imminent alert is issued late.
p(early and final range > 5 m):	probability that the imminent alert is issued early and the final range between the SV and POV is greater that 5 m (approximately 1 car length).
p(early and final range > 10 m):	probability that the imminent alert is issued early and the final range between the SV and POV is greater that 10 m

	(approximately 2 car lengths).
p(late and crash DeltaV > 3 m/s):	probability that the imminent alert is issued late and the relative speed at impact is greater than 3 m/s.
p(late and crash DeltaV > 13.4 m/s):	probability that the imminent alert is issued late and the relative speed at impact is greater than 13.4 m/s or 30 mph.
final range:	range between SV and POV when simulation ends if the alert is early.
crash DeltaV:	relative speed of impact if alert is late.

A good threat assessment algorithm must aim to achieve the following:

p(late) must be close to zero
p(late and crash DeltaV > 3 m/s) must be very small and close to zero
p(late and crash DeltaV > 13.4 m/s) equal to zero
p(early) must be close to one
p(early and final range > 5 m) must be small
p(early and final range > 10 m) must be very small and close to zero

Test 1 – SV Traveling at Constant Speed on a Straight Road Encounters Stopped POV

In this test the SV travels at a constant speed on a straight, flat road. Ahead of the SV, in the same lane, is a single POV stopped in the lane of travel. The initial range between the SV and POV is 150 m. The speed distribution of the SV for this test is approximated from the posted speed limits for this pre-crash scenario [2]. Table 10.22 provides the speed distribution of the SV used for this test.

Table 10.22 Speed Distribution of SV for Test 1

Speed (mph)	20	25	30	35	40	45	50	55	60
Percentage	1.2	10.2	7.8	24.9	13.7	20.2	4.1	12.5	5.4

When an imminent alert is issued, we assume that the driver of the SV brakes after a random driver response time of T_R (in sec) until the SV comes to a stop. The random desired braking rate is assumed to be A_F (in g) that is reached after an additional 0.2 s brake actuation delay from the moment of brake actuation. This is an assumed response characteristic of drivers to a warning stimulus in this crash scenario, and we use this to determine if the timing of an imminent alert is early or late. The random distributions for driver response time and SV braking rate are given in Table 10.23. The distribution for the driver response time is chosen as the surprised response time distribution from P.L. Olsen, and M. Savak, 1986. Surprised response time corresponds to that of a driver in a neutral driving state who is responding with some degree of urgency to a surprising stimulus. The distribution for the SV braking rate is chosen as the truncated normal distribution in (see N. Phamdo, 2001).

Table 10.23 Random Distributions T_R and A_F

Variable	Distribution Type	Mean	Standard Deviation	Minimum	Maximum
T_R	Normal	1.1 s	0.305 s	0 s	2 s
A_F	Normal	-0.6 g	0.1 g	-0.8 g	-0.3 g

Table 10-24 provides a summary of the probabilities of early and late alerts for Test 1.

Table 10.24 Probability of Early and Late Alerts for Test 1

Algorithm No.	p(early)	p(early and final range > 5 m)	p(early and final range > 10 m)	p(late)	p(late and crash DeltaV > 3 m/s)	p(late and crash DeltaV > 13.4 m/s)
1	0.692	0.527	0.278	0.308	0.287	0.071
2	0.835	0.572	0.265	0.165	0.142	0
3	0.999	0.994	0.970	0.002	0.002	0
4	0.798	0.523	0.210	0.202	0.171	0.003

By examining the results in Tables 10.24, we find that algorithm 1 results in a higher number of late alerts. This is due to the 50 m range clip used in algorithm 1 for issuing alerts due to stationary targets. Algorithms 2, 3, and 4 virtually prevent severe injury-causing crashes. Algorithm 3 issues alerts too early that are likely to be considered nuisance alerts by the driver. Algorithms 2 and 4 are similar in performance and balance the probabilities of late and early alerts well.

<u>Test 2 – SV Traveling at Constant Speed on a Straight Road Encounters POV Traveling at a Constant, Lower Speed Ahead</u>

In this test the SV travels at a constant speed on a straight, flat road. Ahead of the SV, in the same lane, is a single POV traveling at a much slower speed of 10 mph (4.47 m/s). The initial headway between the SV and POV is 6.7 s. The speed distribution of the SV for this test is approximated from the posted speed limits for this pre-crash scenario that is presented in [2]. Table 10.25 provides the speed distribution of the SV used for this test.

Table 10.25 Speed Distribution of SV for Test 2

Speed (mph)	20	25	30	35	40	45	50	55	60
Percentage	2.0	9.5	10.3	24.1	12.0	15.8	2.9	17.2	6.1

When an imminent alert is issued, we assume that the driver of the SV brakes after a random driver response time of T_R (in sec) until the speed of the SV equals the speed of

the POV. The random desired braking rate is assumed to be A_F (in g) that is reached after an additional 0.2 s brake actuation delay from the moment of brake actuation. This is an assumed response characteristic of drivers to a warning stimulus in this crash scenario, and we use this to determine if the timing of an imminent alert is early or late. The random distributions for driver response time and SV braking rate are the same as in Test 1. Table 10.26 provides a summary of the probabilities of early and late alerts for Test 2.

Table 10.26 Probability of Early and Late Alerts for Test 2

Algorithm No.	p(early)	p(early and final range > 5 m)	p(early and final range > 10 m)	p(late)	p(late and crash DeltaV > 3 m/s)	p(late and crash DeltaV > 13.4 m/s)
1	0.998	0.993	0.953	0.002	0.001	0
2	0.998	0.993	0.953	0.002	0.001	0
3	1	1	1	0	0	0
4	0.937	0.607	0.180	0.064	0.046	0

By examining the results in Tables 10.26, we find that algorithms 1 and 2 perform identically. All algorithms virtually prevent severe injury-causing crashes. Algorithms 1,2, and 3 issue alerts too early that are likely to be considered nuisance alerts by the driver. Algorithm 4 has a good balance of probabilities of late and early alerts. The imminent alert from algorithm 4 appear to be timed appropriately.

<u>Test 3 – SV and POV are Traveling at Constant and Similar Speed on a Straight Road; POV Decelerates</u>

In this test the SV travels at a constant speed on a straight, flat road. Ahead of the SV, in the same lane, is a single POV initially traveling at the same speed as the SV. The initial headway between the SV and POV is 2 s. The speed distribution for this test is approximated from the posted speed limits for this pre-crash scenario that is presented in [2]. Table 10.27 provides the speed distribution of the SV and POV used for this test.

Table 10.27 Speed Distribution of SV for Test 3

Speed (mph)	20	25	30	35	40	45	50	55	60
Percentage	0.9	10.3	10.6	25.1	15.0	19.9	4.6	9.9	3.5

The POV then brakes moderately. The random moderate braking rate of the POV is assumed to be A_L (in g) that is reached after an additional 0.2 s brake actuation delay from the moment of brake actuation. When an imminent alert is issued, we assume that the driver of the SV brakes after a random driver response time of T_R (in sec) until the SV comes to a stop. The random desired braking rate is assumed to be A_F (in g) that is reached after an additional 0.2 s brake actuation delay from the moment of brake actuation. This is an assumed response characteristic of drivers to a warning stimulus in this crash scenario, and we use this to determine if the timing of an imminent alert is

early or late. The random distributions for driver response time and SV braking rate are the same as in Test 1. The random distribution for POV braking rate is given in Table 10.28.

Table 10.28 Random Distribution A_L

Variable	Distribution Type	Mean	Standard Deviation	Minimum	Maximum
A_L	Normal	-0.3 g	0.1 g	-0.5 g	-0.1 g

Table 10.29 provides a summary of the probabilities of early and late alerts for Test 3.

Table 10.29 Probability of Early and Late Alerts for Test 3

Algorithm No.	p(early)	p(early and final range > 5 m)	p(early and final range > 10 m)	p(late)	p(late and crash DeltaV > 3 m/s)	p(late and crash DeltaV > 13.4 m/s)
1	0.987	0.944	0.812	0.013	0.006	0
2	0.878	0.738	0.517	0.122	0.101	0
3	0.996	0.975	0.903	0.004	0.003	0
4	0.882	0.644	0.310	0.119	0.090	0

By examining the results in Tables 10.29, we find that algorithms 2 and 4 perform similarly and better than algorithms 1 and 3. All algorithms virtually prevent severe injury-causing crashes. Algorithms 1 and 3 issue alerts too early that are likely to produce more nuisance alerts to the driver. The imminent alerts from algorithms 2 and 4 appear to be timed appropriately with algorithm 4 having a better balance of probabilities of late and early alerts.

<u>Test 4 – SV Traveling at Constant Speed Encounters Stopped POV on a Curved Road</u>
The roadway geometry for Test 4 consists of a straight section followed by a curved section. The radius of curvature of the center of travel lane of the curved section is 752 m. In this test the SV begins by traveling at a constant speed on the straight section. Ahead of the SV, in the same lane after the beginning of the curve, is a single POV stopped in the lane of travel. The initial range is 150 m. The POV is stationary at a distance of 83 m from the beginning of the curve. The speed distribution of the SV for this test is approximated from the posted speed limits for this pre-crash scenario that is presented in [2]. Table 10.30 provides the speed distribution of the SV used for this test.

Table 10.30 Speed Distribution of SV for Test 4

Speed (mph)	20	25	30	35	40	45	50	55	60
Percentage	1.2	12.7	7.1	28.7	7.1	21.6	3.9	13.6	3.9

When an imminent alert is issued, we assume that the driver of the SV brakes after a random driver response time of T_R (in sec) until the SV comes to a stop. The random desired braking rate is assumed to be A_F (in g) that is reached after an additional 0.2 s brake actuation delay from the moment of brake actuation. This is an assumed response characteristic of drivers to a warning stimulus in this crash scenario, and we use this to determine if the timing of an imminent alert is early or late. The random distributions for driver response time and SV braking rate are the same as in Test 1. Table 10.31 provides a summary of the probabilities of early and late alerts for Test 4.

Table 10.31 Probability of Early and Late Alerts for Test 4

Algorithm No.	p(early)	p(early and final range > 5 m)	p(early and final range > 10 m)	p(late)	p(late and crash DeltaV > 3 m/s)	p(late and crash DeltaV > 13.4 m/s)
1	0.735	0.581	0.321	0.265	0.247	0.060
2	0.842	0.580	0.280	0.158	0.129	0
3	0.999	0.993	0.973	0.001	0.001	0
4	0.801	0.533	0.220	0.199	0.163	0.003

By examining the results Tables 10.31, we find that algorithm 1 results in higher number of late alerts. This is due to the 50 m range clip used in algorithm 1 for issuing alerts due to stationary targets. Algorithms 2,3, and 4 virtually prevent severe injury-causing crashes. Algorithm 3 issues alerts too early that are likely to be considered nuisance by the driver. Algorithms 2 and 4 are similar in performance and try the balance the probabilities of late and early alerts.

Evaluation of Threat Assessment Algorithms Using Analysis of False Alarms and Misses

Using TASIM, we determine if the decision to issue an imminent alert or not is correct for each of the threat assessment algorithms. We consider the four major rear-end crash scenarios described earlier, which account for 84.3 % of all rear-end pre-crash scenarios. For each scenario and selected threat assessment algorithm, we conduct a Monte-Carlo, instantaneous analysis, based on 2000 runs of the simulation, in order to compute the number of false alarms and misses respectively.

We consider an arbitrary instance of time, say t_0, and we define the speed of the SV, speed of the POV, the range, the acceleration of the SV, and the acceleration of the POV at that particular instance of time. These are the initial conditions for the Monte-Carlo simulations corresponding to the scenarios and they are assumed to be random distributions. It is assumed that, instantaneously, the driver of the SV brakes to achieve a certain constant random deceleration after a certain random driver response time. If an imminent alert is not given by the threat assessment at t_0 and a crash occurs, then it is a MISS. On the other hand, if an imminent alert is given by the threat assessment at t_0 and there is no crash, then it is a FALSE ALARM. If the case of a MISS, we determine the

crash DeltaV. In the case of a FALSE ALARM, we determine the final range between the vehicles. A record of the results for the tests is used to determine the probabilities of MISSES and FALSE ALARMS for each threat assessment algorithm corresponding to each scenario, and to determine other important statistics regarding the MISSES and FALSE ALARMS.

The following definitions are used in this section:

p(false alarm):	probability that an imminent alert is issued and there is no crash
p(miss):	probability that an imminent alert is not issued and there is a crash
p(false alarm | alert):	probability of false alarm given an imminent alert
p(miss | no alert):	probability of miss given no imminent alert
final range:	range between SV and POV when simulation ends in case of false alarm
crash DeltaV:	relative speed of impact in case of miss

<u>Test 1 – SV Traveling at Constant Speed on a Straight Road Encounters Stopped POV</u>
In this test the SV travels at a constant speed on a straight, flat road. Ahead of the SV, in the same lane, is a single POV stopped in the lane of travel. The speed distribution of the SV for this test is the same as in Table 10.22. At an arbitrary instant of time, say t_0, the range, R_0, between the SV and POV is assumed to be a random distribution as given in Table 10.32. At that instant t_0, we assume that the driver of the SV brakes after a random driver response time of T_R (in sec) until the SV comes to a stop. The random desired braking rate is assumed to be A_F (in g) that is reached after an additional 0.2 s brake actuation delay from the moment of brake actuation. This is an assumed response characteristic of drivers in this crash scenario (i.e. without any warning stimulus), and we use this to determine the false alarms and misses respectively. The random distributions for driver response time and SV braking rate are given in Table 10.32. The distribution for the driver response time is chosen as the un-alerted response time distribution in (see M.S. Chang, C.J. Messer, and A.J. Santiago, 1985). Un-alerted response time corresponds to that of a driver in a neutral driving state and is responding to an unsurprising stimulus. The distribution for the SV braking rate is chosen as the truncated normal distribution in [4].

Table 10.32 Random Distributions R_0, T_R and A_F

Variable	Distribution Type	Mean	Standard Deviation	Min	Max	Median	Dispersion Parameter
R_0	Uniform	-	-	2 m	120 m	-	-
T_R	Lognormal	1.27 s	0.72 s	-	-	1.1 s	0.53 s
A_F	Normal	-0.6 g	0.1 g	-0.8 g	-0.3 g	-	-

Table 10.33 summarizes the probabilities of false alarms and misses for Test 1.

Table 10.33 Probability of False Alarms and Misses for Test 1

Algorithm No.	p(false alarm)	p(miss)	p(false alarm | alert)	p(miss | no alert)
1	0.053	0.051	0.145	0.079
2	0.063	0.031	0.161	0.05
3	0.175	0.013	0.335	0.026
4	0.057	0.033	0.147	0.053

By examining the results in Tables 10.33, we find that algorithm 1 results in higher number of misses relative to the other algorithms. The false alarm rate is significantly higher in algorithm 3 relative to the rest. Algorithms 2 and 4 are similar in performance and try to balance the probabilities of false alarms and misses.

Test 2 – SV Traveling at Constant Speed on a Straight Road Encounters POV Traveling at a Constant, Lower Speed Ahead

In this test the SV travels at a constant speed on a straight, flat road. Ahead of the SV, in the same lane, is a single POV traveling at a much slower speed of 10 mph (4.47 m/s). The speed distribution of the SV for this test is the same as in Table 10.25. At an arbitrary instant of time, say t_0, the range, R_0, between the SV and POV is assumed to be a uniform random distribution, U(20 m, 80 m). At that instant t_0, we assume that the driver of the SV brakes after a random driver response time of T_R (in sec) until the speed of the SV equals the speed of the POV. The random desired braking rate is assumed to be A_F (in g) that is reached after an additional 0.2 s brake actuation delay from the moment of brake actuation. This is an assumed response characteristic of drivers in this crash scenario (i.e. without any warning stimulus), and we use this to determine the false alarms and misses respectively. The random distributions for driver response time and SV braking rate are the same as given in Table 10.32. Table 10.34 provides a summary of the probabilities of false alarms and misses for Test 2.

Table 10.34 Probability of False Alarms and Misses for Test 2

Algorithm No.	p(false alarm)	p(miss)	p(false alarm | alert)	p(miss | no alert)
1	0.223	0.011	0.613	0.017
2	0.223	0.011	0.613	0.017
3	0.343	0.002	0.695	0.003
4	0.090	0.034	0.431	0.043

By examining the results in Tables 10.34, we find that algorithms 1 and 2 perform identically. Algorithms 1,2, and 3 have high rate of false alarms. Algorithm 4 has low probabilities of misses and false alarms and its performance is better than the rest for this scenario.

Test 3 – SV and POV are Traveling at Constant and Similar Speeds on a Straight Road; POV Decelerates

In this test the SV travels at a constant speed on a straight, flat road. Ahead of the SV, in the same lane, is a single POV initially traveling at the same speed as the SV. The speed distribution of the SV and POV for this test is the same as in Table 10.27. The POV brakes moderately and the random moderate braking rate of the POV is assumed to be A_L (in g) which is given in Table 10.28. At an arbitrary instant of time, say t_0, the range, R_0, between the SV and POV is assumed to be a uniform random distribution, U(10 m, 50 m). At that instant t_0, we assume that the driver of the SV brakes after a random driver response time of T_R (in sec) until the SV comes to a stop. The random desired braking rate is assumed to be A_F (in g) that is reached after an additional 0.2 s brake actuation delay from the moment of brake actuation. This is an assumed response characteristic of drivers in this crash scenario (i.e. without any warning stimulus), and we use this to determine the false alarms and misses respectively. The random distributions for driver response time and SV braking rate are the same as given in Table 10.32. Table 10.35 provides a summary of the probabilities of false alarms and misses for Test 3.

Table 10.35 Probability of False Alarms and Misses for Test 3

Algorithm No.	p(false alarm)	p(miss)	p(false alarm | alert)	p(miss | no alert)
1	0.179	0.023	0.712	0.031
2	0.099	0.046	0.666	0.054
3	0.227	0.018	0.746	0.026
4	0.042	0.051	0.483	0.056

By examining the results in Tables 10.35, we find that algorithms 2 and 4 perform better than algorithms 1 and 3. Algorithms 1 and 3 have higher rates of false alarms in comparison to algorithms 2 and 4. Algorithm 4 has a better balance of probabilities of false alarms and misses for this scenario.

Test 4 – SV Traveling at Constant Speed Encounters Stopped POV on a Curved Road

The roadway geometry for Test 4 consists of a straight section followed by a curved section. The radius of curvature of the center of travel lane of the curved section is 752 m. In this test the SV begins by traveling at a constant speed. Ahead of the SV, in the same lane after the beginning of the curve, is a single POV stopped in the lane of travel. The POV is stationary at a distance of 83 m from the beginning of the curve. The speed distribution of the SV for this test is the same as in Table 10.30. At an arbitrary instant of time, say t_0, the range, R_0, between the SV and POV is assumed to be a uniform random distribution, U(2 m, 80 m). At that instant t_0, we assume that the driver of the SV brakes after a random driver response time of T_R (in sec) until the SV comes to a stop. The random desired braking rate is assumed to be A_F (in g) that is reached after an additional 0.2 s brake actuation delay from the moment of brake actuation. This is an assumed response characteristic of drivers in this crash scenario (i.e. without any warning

stimulus), and we use this to determine the false alarms and misses respectively. The random distributions for driver response time and SV braking rate are the same as given in Table 10.32. Table 10.36 provides a summary of the probabilities of false alarms and misses for Test 4.

Table 10.36 Probability of False Alarms and Misses for Test 4

Algorithm No.	p(false alarm)	p(miss)	p(false alarm | alert)	p(miss | no alert)
1	0.081	0.062	0.149	0.134
2	0.084	0.048	0.150	0.107
3	0.258	0.009	0.335	0.037
4	0.077	0.05	0.141	0.111

By examining the results in Tables 10.36, we find that algorithm 1 results in slightly higher number of misses relative to algorithms 2 and 4. The false alarm rate is significantly higher in algorithm 3 relative to the rest. Algorithms 2 and 4 are similar in performance and try the balance the probabilities of false alarms and misses well.

The results of this analysis may only be used for relative comparison of threat assessment algorithms. This is due to the fact that absolute numbers computed for false alarm rate and rate of misses are very sensitive to the distribution of R_0 that is chosen for the test. While relative comparisons between algorithms can be made using an assumed distribution for R_0 as we have done in this test, absolute calculations of false alarms and misses rely very much on the accurate prediction of distribution of R_0 which is very difficult to obtain in practice.

Summary of Results

A summary of the results of threat assessment simulation conducted as part of the Automotive Collision Avoidance System Field Operational Test (ACAS/FOT) program has been presented. We have used TASIM to evaluate the performance of four different threat assessment algorithms under consideration in the ACAS/FOT program: algorithms 1 and 2 developed by GMR, algorithm 3 developed by CAMP, and algorithm 4 developed by NHTSA.

We have evaluated the performance of the threat assessment algorithms using the following tests:

1. Sixteen straight-road test scenarios.

2. Time series analysis using Monte-Carlo simulation of four major pre-crash scenarios for computation of probabilities of late alerts and early alerts issued by the various threat assessment algorithms.

- When POV is stopped (tests 1,4)
  - algorithm 1 issues more late alerts
  - algorithms 2 and 4 are similar and good
  - algorithm 3 issues alerts too early
- When following a POV of lower speed (test 2)
  - algorithms 1, 2 and 3 issue alerts too early
  - algorithm 4 is good
- When following a POV braking from similar speed (test 3)
  - algorithms 1 and 3 issue alerts too early
  - algorithms 2 and 4 are good

3. Instantaneous analysis using Monte-Carlo simulation of four major pre-crash scenarios for computation of probabilities of false alarms and misses due to the various threat assessment algorithms.
   - When POV is stopped (tests 1,4)
     - algorithms 1, 2 and 4 are similar and good
     - algorithm 3 issues too many false alarms
   - When following a POV of lower speed (test 2)
     - algorithms 1, 2 and 3 issue too many false alarms
     - algorithm 4 is good
   - When following a POV braking from similar speed (test 3)
     - algorithms 1 and 3 issue too many false alarms
     - algorithms 2 and 4 are good

The following general conclusions are based on the results of this study:

1. Algorithms 2 and 4 perform better than algorithm 1 and 3 in a majority of the tests.

2. The performance of algorithms 1 and 2 is similar in several tests. However the range clip of 50 m used in algorithm 1 for issuing alerts on stationary targets poses a serious limitation, resulting in its inability to prevent a larger number of crashes. With the prediction of forward road geometry that is made using the GPS/Map and vision sensors in the ACAS/FOT project, it would be best to increase the range clip of 50 m used in algorithm 1 for issuing alerts on stationary targets.

3. Algorithm 3 issues alerts too early, and has a higher probability of false alarms in a majority of tests. Further tuning of this algorithm may be necessary to reduce the number of false alarms and too early alerts. In our tests we used a sensitivity level of 4 for this algorithm. It remains to be seen if using a lower value of the sensitivity level for this algorithm would reduce the number of too early alerts and false alarms.

4. The performance of algorithms 2 and 4 are quite similar in a majority of tests and they perform as expected.

Work during Phase II will involve the following developments:

- Further analysis for selecting optimal parameters for algorithm 2 that optimizes the measures of effectiveness.

- Interfacing TASIM to actual field data from CAN BUS as shown in Figure 10.5.

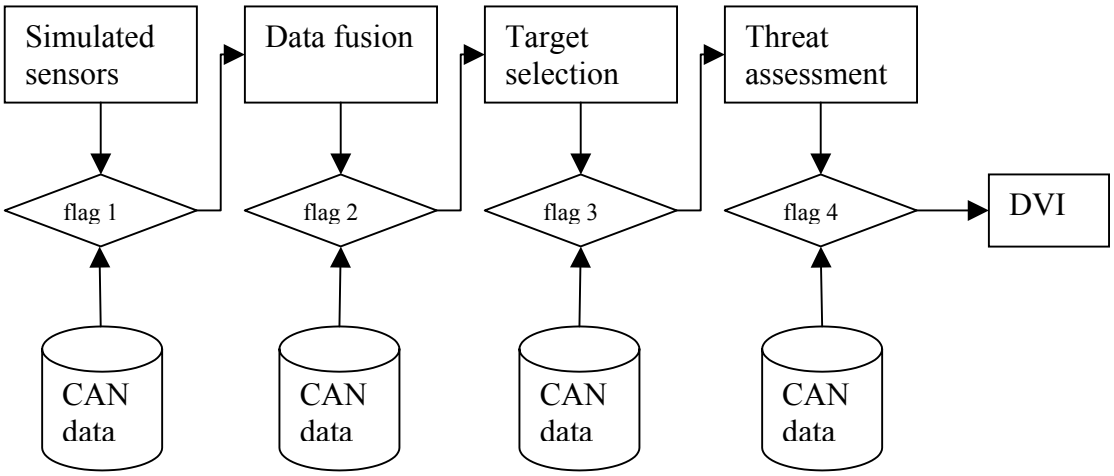

Figure 10.5 Interfacing TASIM to CAN BUS Field Data

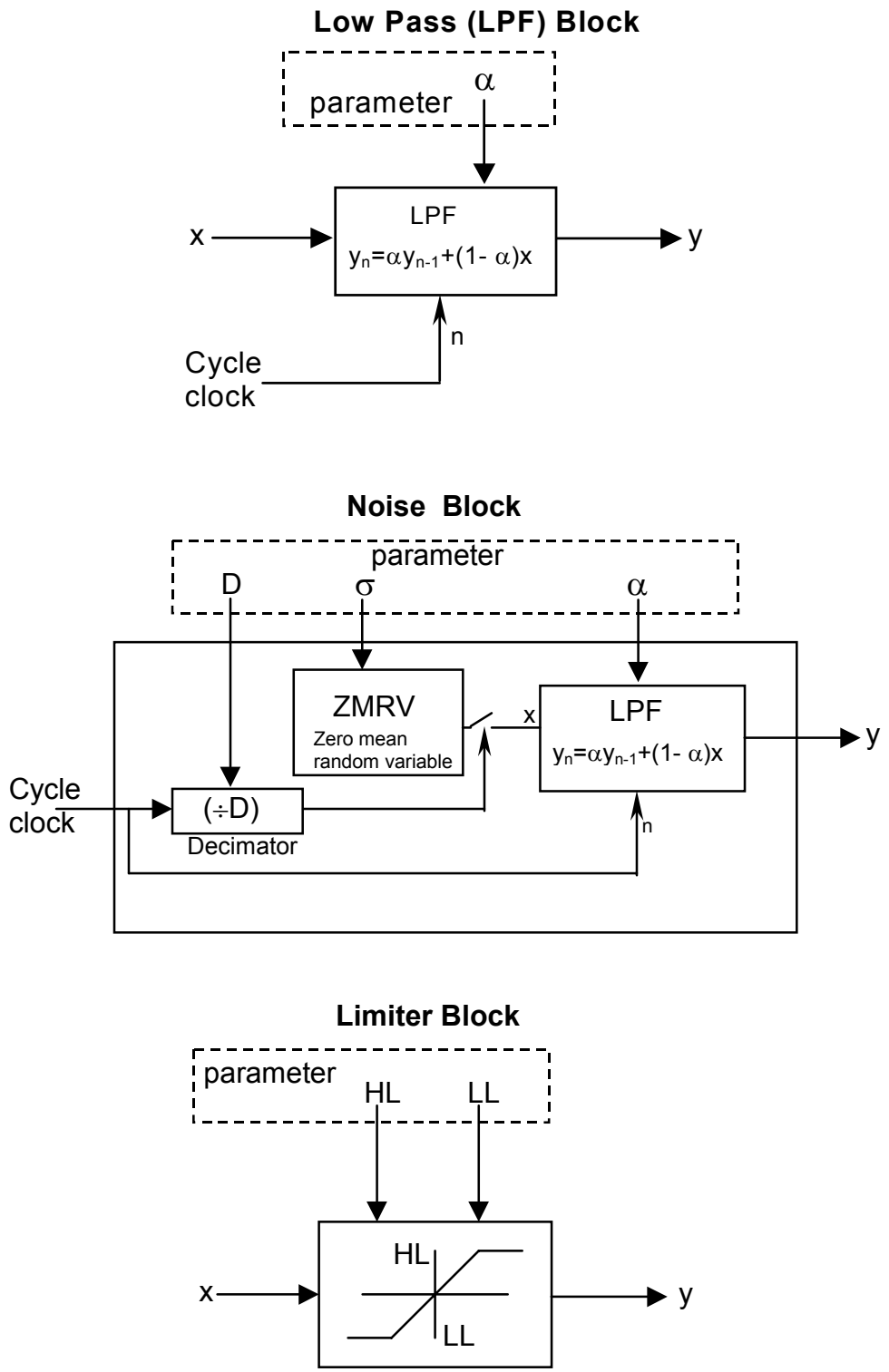

Figure 10.6 Descriptions of Low Pass, Noise, and Limiter Blocks

10.2 Threat Assessment In-Vehicle Development (Task C3B and C5)

Goals, Purpose and Background

Goals and Purpose

The purpose of this task was to develop a threat assessment algorithm through analysis and simulation, and to test the algorithm in instrumented vehicles on test tracks and in real traffic. In addition, the program team supported the development of the "NHTSA Algorithm" by implementing it on the GM EDV and Prototype vehicles.

The Treat Assessment Algorithm uses data supplied by the Threat Assessment function, radar and vehicle sensors to produce an alert to the driver that an imminent collision will occur if he or she does not take action to brake and/or steer the vehicle. It was expected that this could be implemented, but the question was, could it be done with a false alarm rate low enough for driver tolerance. This was thought possible by adding additional sensors and algorithms to what is in currently in use. The additional sensors and algorithms are vision, scene tracking, GPS/data map and data fusion (these technologies are fully described in other parts of this report). These additional technologies make it possible to discern the closest in-path object when operating on transition curves.

Background

The usefulness of the driver alert warning depends on the robustness of the threat assessment algorithm. The threat assessment algorithm must determine the probability of a collision with a vehicular target that is in the forward path of motion of the Host Vehicle. This estimation is determined from the Host Vehicle's and target's velocity and deceleration, the distance between the vehicle and object, and the driver's reaction time. The time of collision could be determined from these parameters if they were deterministic. However, in real-world traffic scenarios, multiple traffic lanes, roadway curvature, multiple vehicles, roadside obstacles, and driver attentiveness and reaction times confound these parameters. Because of these non-deterministic occurrences, modeling techniques were developed (see Section 10.1) to assist in the selection of the algorithm or algorithms with the highest chance of success. Several iterations of algorithm candidates were simulated, analyzed and tested on instrumented vehicles.

The threat assessment algorithms were integrated into project vehicles for real-time evaluation and assessment. These project vehicles were driven in various traffic conditions and on test track situations, which simulate potential crash situations, to determine alert range rate and false-alarm-rate for the various combinations of threat and path prediction algorithms. Seven threat algorithms were evaluated by simulation. Five algorithms were evaluated in the GM Engineering Development Vehicle (EDV). Only two algorithms were implemented in the Prototype vehicle. In the Prototype vehicle, the algorithms were evaluated with all of the path prediction algorithms (e.g., conventional approach, scene tracking approach, vision sensor, and enhanced GPS approach).

Technical Approach

Seven Threat Assessment Algorithms were initially evaluated for the program. They are referred to as:

1. GMR1 (General Motors Research 1)
2. GMR2 (General Motors Research 2)
3. CAMP1 (Single stage alert described in the 1st CAMP Final Report)
4. CAMP2 (Two stage alert similar to CAMP1)
5. HW (An algorithm derived from the Host vehicle headway to the Lead Vehicle)
6. TTC (An algorithm derived from the Host vehicle time-to-collision to the Lead Vehicle)
7. NHTSA (An algorithm developed by NHTSA and implemented by APL)

The above algorithms were initially analyzed with desktop simulations. The alert range determined by Algorithms 5 and 6 often differed considerably from the others because they did not utilize actual or estimated Following or Lead Vehicle acceleration. That is, for Algorithms 4 and 5,

$$Rca = f(V_f, V_l, T)$$

Where

Rca = collision avoidance range
V_f = Following Vehicle speed
V_l = Lead Vehicle speed
T = delay time before the Following Vehicle decelerates after the Lead Vehicle starts to decelerate

It was concluded that not taking vehicle accelerations into account resulted in a probability of miss, Pm, that was too high in a number of operational scenarios. For that reason Algorithms 5 and 6 were dropped from further consideration.

The remaining algorithms used a_f and a_l to determine Rca. That is,

$$Rca = f(V_f, V_l, a_f, a_l, T)$$

Where

a_f = Following Vehicle acceleration
a_l = Lead Vehicle acceleration

Algorithms 1 and 2 were designed to drive a graded display. They use the same equations to determine the alert onset range, Ro. The equations for Ro are,

$$Ro = Rca + (V_f - V_l)\tau_i \qquad (1)$$

or

$$Ro = V_f T_i \qquad (2)$$

Where τ_i and T_i are constants in units of time, and i = 1 though 6 corresponding to the driver selectable sensitivity levels.

In GMR1, Equation 1 was used to determine Ro if $V_f - V_l > 1.12$ m/s. Equation 2 was used to determine Ro if $V_f = V_l \leq 1.12$ m/s. In GMR2 Ro is determined by

$$Ro = \max[Rca + (V_f - V_l)\tau_i, V_f T_i]$$

In GMR1, the transition between using Equation 1 vs. Equation 2 for Ro turned out to be a problem. It was observed that Ro was not always monotonically increasing (other parameters remaining equal) as range between the Lead and Following vehicles decreased. Also in the test vehicles, the graded display seemed often to have an annoying flicker. For these reasons, the original GMR1 was eliminated from further consideration. However the GMR1 designation was used in the later part of Phase I as a sub-algorithm to test heuristics.

Algorithms CAMP1 and CAMP2 were replaced by what was called the inverse time-to collision algorithm. This algorithm was conceived in the 2nd CAMP program. However there were insufficient program resources to optimize parameters within the algorithm. Therefore it was also dropped from consideration.

GMR2 and the NHTSA algorithms were implemented and tested in the Prototype vehicle. The NHTSA algorithm was provided to GM by APL as a callable subroutine. No further discussion of the NHTSA algorithm is covered in this section of report. However the NHTSA algorithm is present on the vehicle and runs in the background. That is, it does not drive the Driver Vehicle Interface (DVI), but its performance can be determined by reducing the data collected during vehicle operation.

The rest of this report discusses the GMR2 algorithm. Most of the work done to develop GMR2 was in the areas of selecting and optimizing internal parameters and heuristics. These parts of the algorithm are proprietary and will only be discussed in general. An additional requirement of development of the Forward Collision Warning (FCW) algorithm was to make it compatible with Adaptive Cruise Control (ACC) operation.

The ACC/FCW alert scheme is shown in Table 10.37 below.

Table 10.37 ACC/FCW Alert Scheme

Alerts Generated	ACC Off	ACC On
Moving Vehicles (CIPV) ACC follows the CIPV	X	
Stationary Objects (CIPS)	X	X
Maximum Deceleration Requested (from ACC Controller)		X

In Table 10.37, CIPV stands for the Closest In-Path Movable Vehicle and CIPS stands for Closest In-Path Stationary object. Movable means an object (presumably a vehicle) that is currently moving or was once observed to be moving. It should be pointed out that the system does not automatically brake on stationary objects (unless they were previously observed to be moving), but it does alert the driver if an in-path stationary object is detected. So a vehicle that is in track as a moving object then stops will cause automatic braking if ACC is engaged. Also, the system alerts the driver if the maximum ACC acceleration of –0.3 g or less is being requested by the ACC Controller.

The ACC maximum deceleration alert and the FCW Imminent alert are presented to the driver identically. The action for the driver, whether the alert means maximum deceleration requested in ACC or imminent alert in FCW, is the same. That is, the driver should take control of the vehicle and brake and/or steer the vehicle so as not to collide with the vehicle in front.

The I/O data to/from the Threat Assessment Algorithms are taken off, and put onto the CAN bus by the various system modules. The Threat Assessment process is as follows:

1. The Target Selection function inputs, to the FCW Processor (via the CAN bus), the Radar Track ID for the closest in-path moving vehicle (CIPV) and the closest in-path stationary object (CIPS).
2. The FCW Processor collects (for the Threat Assessment Algorithms) the required Radar Track Data (see Table 10.38) off the CAN bus.The FCW Processor also collects other required Threat Assessment Input Data (see Table 10.39) from other modules, off the CAN bus.Threat Assessment then calculates an Alert Level and determines other messages (see Table 10.40). The FCW Processor outputs this data to the CAN bus.

Table 10.38 Target Selection and Radar Input Data

Alert Parameter	Source
Closest in-path movable vehicle (CIPV) Track ID	Target Selection
Closest in-path stationary object (CIPS) Track ID	Target Selection
Track Stage, Range, Relative Range Rate and Relative Acceleration of the closest in-path movable vehicle (CIPV)	Radar
Track Stage, Range, Relative Range Rate and Relative Acceleration of the closest in-path stationary object (CIPS)	Radar

Table 10.39 Other Threat Assessment Input Data

Alert Parameter	**Source**
Following (host) vehicle velocity	Vehicle Sensors
Following (host) vehicle acceleration	Vehicle Sensors
Wiper Speed	Vehicle Sensors
Outside Temperature	Vehicle Sensors
Brake Applied	Vehicle Sensors
ACC Engaged	ACC Controller
Vehicle Ahead	ACC Controller
Max Deceleration Requested	ACC Controller
Driver Distraction	Data Fusion
ACC On/Off	DVI
FCW Sensitivity/ACC Headway	DVI
System Fault	FCW Processor

Table 10.40 FCW Processor Output Data

FCW Output	
Alert Level	Alert level : a number between 0 and 100 which results in an indicator to the driver of the potential for a rear-end collision with the most threatening (CIPV or CIPS) object
FCW Inactive	Indicates that the alert is being inhibited (vehicle speed criteria, brake applied, system fault)

Following is a discussion of GMR2. Figure 10.7 below defines the terms in the discussions to follow.

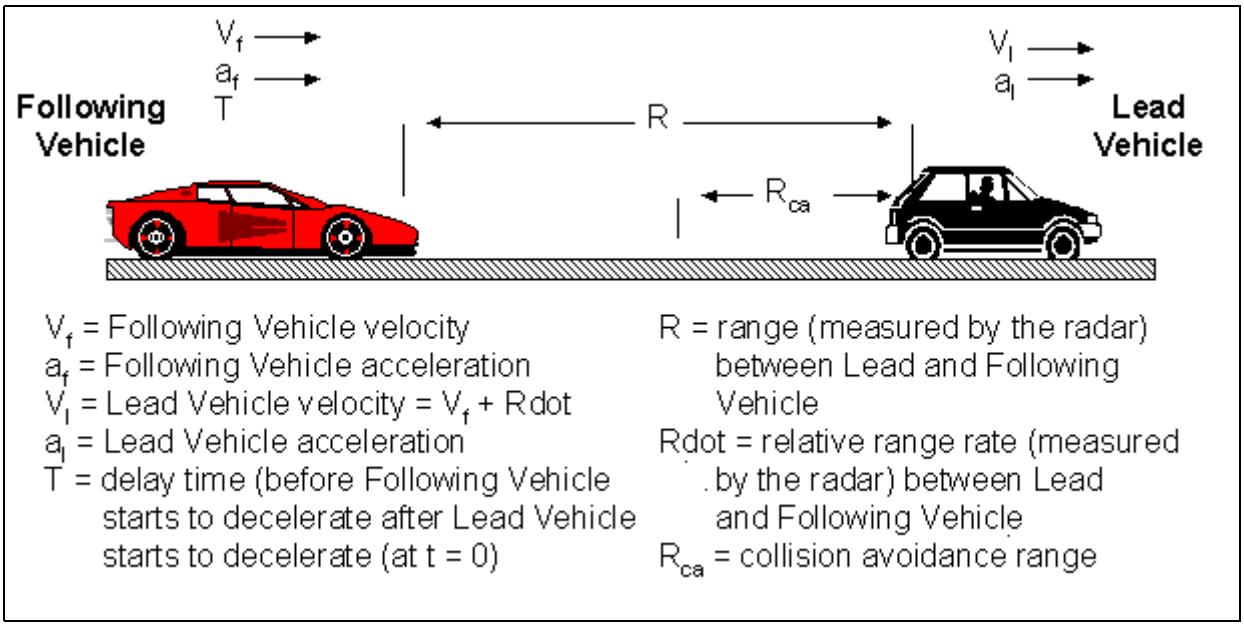

Figure 10.7 Definition of Threat Assessment Algorithm Terms

The collision avoidance range, R_{ca} is the closest possible range that the driver can make the decision to stop (or steer), using the normal equations of motion, and still avoid a collision for parameters V_f, V_l, a_l, a_f, T. These parameters may be measured, assumed or a combination of measured or assumed values $R_{ca} = f(V_f, V_l, a_l, a_f, T)$

Where

V_f is a measurement from vehicle sensors
$V_l = V_f$ + Rdot
$a_f = f(V_l, V_f$, wiper speed, outside temperature)
$a_l = f(a_f, a_{rdr})$
a_{rdr} = Relative acceleration between Lead and Following Vehicles measure by the radarT = T_o + f(driver distraction)
T_o = f(human reaction time, brake pressure buildup time, system latency)

The calculation of Ro was discussed earlier. The first expression for R_o is used for the case when the following vehicle is closing on the lead vehicle (Equation 1). The second expression for R_o is used for the case when the following vehicle is "tail-gating" the lead vehicle at the same speed (Equation 2). The Alert Level, AL is calculated using Rca and Ro from Equation 1 and Equation 2. The reason for using two expressions for Ro can be seen by examining Equation 1. In Equation 1, if $V_f - V_l$ is small or zero (the tail-gating situation), the Following Vehicle can be very close to the Lead Vehicle without issuing a cautionary alert. If the Lead Vehicle were to suddenly decelerate at a high rate, the alert

could be too late. So using Ro from Equation 2 ensures a minimum prudent range between the two vehicles based on V_f. On the other hand, if only Equation 2 were used to determine Ro, there would be instances when Ro would be too small (e.g., when $V_f - V_l$ is large) to issue an alert in time.

The Alert Level, AL, is a number between 0 and 100 that is output to the Driver-Vehicle Interface. AL is an indicator to the driver of the potential for a rear-end collision, and is intended to drive a gradient display.

AL = 0, for (R > Ro

AL = 25, for R between Ro and (Ro + Rca)/2

AL = 75, for R between Rca and (Ro + Rca)/2

AL= 100, for R ≤ Rca

The alert level is calculated for both the CIPV and CIPS (AL_CIPV and AL_CIPS) if both types of targets are present, and the maximum of the two is output as the alert level.

AL output = max[AL_CIPV, AL_CIPS]

Figure 10.8 below shows an overall flow chart of how the Output AL is determined.

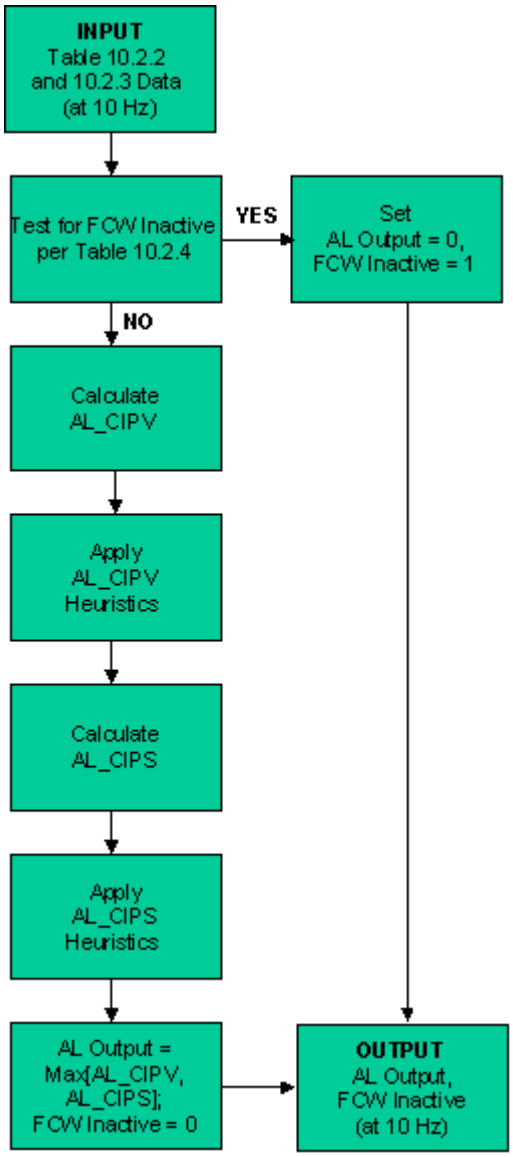

Figure 10.8 Determination of Output AL

Relevant Activities

The Threat Assessment Algorithm for the FCW function was developed in four distinct stages. The first stage was to determine mathematically what all the candidate threat assessment algorithms would be. As stated earlier, there were seven to start with. All but one came from various internal programs. One algorithm was furnished to GM by NHTSA.

In the next stage, two algorithms were eliminated after numerous desktop simulations were run. TASIM, described in Section 10.1, was used to analyze the four leading

algorithms (GMR1, GMR2, CAMP and NHTSA) from the desktop simulation. The results of those simulations are documented in Deliverables 14 and 15, Threat Assessment Simulation Summary report, July 31, 2001.

In the third stage, the four above algorithms were implemented in the GM EDV. An initial verification plan was prepared and submitted to NHTSA for testing the CW system. During this phase, the major GM attention was given to GMR2. Data supporting the NHTSA algorithm was given to APL for review by them and NHTSA.

In stage four, GMR2 and the NHTSA algorithms were implemented in the Prototype vehicle. The Verification Plan was revised to the final deliverable (refer to Deliverable 3, ACAS/FOT System Verification Plan, Revision A, Sept. 21, 2001). Verification was performed on the Prototype vehicle using the procedures in the Verification Plan from October 6 to October 30, 2001. The data collected during the tests were provided to The Volpe Center throughout the verification period. All verification tests were observed by a NHTSA designated witness. At the conclusion of the tests, Deliverable 16, Prototype Vehicle Verification Test Data and Report, November 15, 2001 was submitted to NHTSA. Summaries of the verification test results are covered in the next subsection.

In addition to verifying the proper operation of the FCW function, the Verification Plan also included tests for the ACC function. Table 10.41 shows the thirty tests covered by the Verification Plan by test type.

Table 10.41 Vehicle Verification Test Types

Test Number	Quantitative Collision Alert Test	Qualitative Nuisance Alert Test	Qualitative ACC Test
1	X		X
2	X		X
3	X		X
4	X		X
5	X		X
6	X		X
7	X		X
8	X		X
9	X		
10	X		X
11	X		X
12	X		X
13	X		
14	X		X
15	X		X
16	X		X
17		X	X
18		X	X
19		X	X
20		X	X
21		X	X
22		X	
23			X
24			X
25			X
26			X
27			X
28			X
29			X
30			X

Intermediate and Final Results
This subsection summarizes the vehicle verification tests that were performed on the ACAS FOT Prototype Vehicle between October 8 and 31, 2001. All tests except Test 22 were conducted on GM's Milford Proving Grounds. Test 22 was conducted on a variety of road types in South East Michigan. This report contains only the test results along with a summary. The detailed test procedures are contained in Program Deliverable 3 – ACAS/FOT System Verification Plan, Revision A, September 21, 2001.

Table 10.42 shows a summary of what kind of a facility was used for each test.

Table 10.42 Tests Grouped by Test Facility

Straight, 2 Lane, 2 Vehicle Track Tests
Test 1 – SV 60 mph to POV Stopped, FCW
Test 1 – SV 60 mph to POV Stopped, ACC
Test 2 – SV 50 mph to POV 10 mph, FCW
Test 2 – SV 50 mph to POV 10 mph, ACC
Test 3 – SV 60 mph to POV Braking Unusually Hard from 60 mph, FCW
Test 3 – SV 60 mph to POV Braking Unusually Hard from 60 mph, ACC
Test 4 – SV 60 mph to Motorcycle POV Braking Moderately Hard from 60 mph, FCW
Test 4 – SV 60 mph to Motorcycle POV Braking Moderately Hard from 60 mph, ACC
Test 8 – SV 45 mph Changes Lanes and Encounters POV Stopped, FCW
Test 8 – SV 45 mph Changes Lanes and Encounters POV Stopped, ACC
Test 9 – SV 60 mph Tailgating POV Braking from 60 mph, FCW
Test 14 – SV 50 mph to POV Braking Unusually Hard from 50 mph, FCW
Test 14 – SV 50 mph to POV Braking Unusually Hard from 50 mph, ACC
Test 15 – SV 40 mph to POV Stopping from 40 mph, FCW
Curve Tests
Test 5 – SV 50 mph to POV Stopped on Curve, FCW
Test 5 – SV 50 mph to POV Stopped on Curve, ACC
Test 6 – SV 50 mph to POV 25 mph in a Curve, FCW
Test 6 – SV 50 mph to POV 25 mph in a Curve, ACC
Test 12 – SV 50 mph on Curve to POV Braking Moderately Hard from 50 mph, FCW
Test 12 – SV 50 mph on Curve to POV Braking Moderately Hard from 50 mph, ACC
Multiple Lead Vehicle Tests
Test 10 – SV 60 mph Approaches Motorcycle and Truck POVs 20 mph, FCW
Test 10 – SV 60 mph Approaches Motorcycle and Truck POVs 20 mph, ACC
Test 11 – SV 60 mph Approaches Motorcycle and Truck POV 20 mph, FCW
Test 11 – SV 60 mph Approaches Motorcycle and Truck POV 20 mph, ACC
Test 18 – SV 60 mph Passing Truck POVs 20 mph in Adjacent Lanes, FCW
Test 18 – SV 60 mph Passing Truck POVs 20 mph in Adjacent Lanes, ACC
Test 16 – SV 45 mph behind 45 mph POV Changing Lanes to Reveal Stopped POV, FCW
Test 16 – SV 45 mph behind 45 mph POV Changing Lanes to Reveal Stopped PO, ACC
Test 17 – SV 50 mph Passing POVs 25 mph Around Curve, FCW
Test 17 – SV 50 mph Passing POVs 25 mph Around Curve, ACC
Circular Track and VDTA
Test 7 – SV 60 mph Cut-off by POV 40 mph, FCW
Test 7 – SV 60 mph Cut-off by POV 40 mph, ACC
Test 13 – SV 65 mph Following POV 60 mph, FCW
On-track Nuisance Tests
Test 19 – SV 60 mph following POV 60 mph
Test 20 – SV 50 mph POV 60 mph Cuts in Ahead of SV, FCW
Test 20 – SV 50 mph POV 60 mph Cuts in Ahead of SV, ACC
Test 21 – SV on Simulated Open Road No Other Traffic, FCW
Test 21 – SV on Simulated Open Road No Other Traffic, ACC

Table 10.42 Test Grouped by Test Facility (continued)

ACC Tests
Test 23 – SV following POV on Simulated Open Road
Test 24 – SV 45 mph POV 45 mph Changes Lanes in front of Accelerating SV
Test 25 – SV 60 mph changing ACC Headway following POV 60 mph
Test 26 – SV 50 mph following POV Accelerating from 50 mph
Test 27 – SV 50 mph following POV 50 mph Changes Lanes to reveal POV 50 mph
Test 28 – SV 40 mph passes POV 40 mph
Test 29 – SV 50 mph Throttle Override during Automatic Braking
Test 30 – SV 50 mph ACC Test with Anti-lock Braking Activated
Public Road Nuisance Alert Tests
Test 22 – SV Daytime Public Road Test, 188 mi

Verification Testing
Tables 10.43 through 10.45 show an assessment of how the system performed. The test were for the total CW function that including the radar, path prediction, target selection and threat assessment. Refer to Deliverable 16, Prototype Vehicle Verification Test Data and Report, November 15, 2001 for test result details.

The tables show the number of trials conducted and how many trials passed the Pass/Fail Criteria. The Status Column indicates:

G - Clear pass
Y - Marginal pass or extenuating circumstances
R - Modify system and retest in Phase II

Bracketed numbers in the Status column correspond to the explanations in the Technical Problems subsection.

Table 10.43 Quantitative Collision Alert and Qualitative ACC Test

Quantitative Collision Alert and Qualitative ACC Test	Trials Run	Trials Passed	Status
Test 1 – SV 60 mph to POV Stopped, FCW	5	5	**G**
Test 1 – SV 60 mph to POV Stopped, ACC	5	5	**G**
Test 2 – SV 50 mph to POV 10 mph, FCW	5	5	**G**
Test 2 – SV 50 mph to POV 10 mph, ACC	5	5	**G**
Test 3 – SV 60 mph to POV Braking Unusually Hard from 60 mph, FCW	6	5	**G**
Test 3 – SV 60 mph to POV Braking Unusually Hard from 60 mph, ACC	5	5	**G**
Test 4 – SV 60 mph to Motorcycle POV Braking Moderately Hard from 60 mph, FCW	7	7	**G**
Test 4 – SV 60 mph to Motorcycle POV Braking Moderately Hard from 60 mph, ACC	5	5	**G**
Test 5 – SV 50 mph to POV Stopped on Curve, FCW	7	5	**R [1]**
Test 5 – SV 50 mph to POV Stopped on Curve, ACC	5	5	**G**
Test 6 – SV 50 mph to POV 25 mph in a Curve, FCW	7	7	**G**
Test 6 – SV 50 mph to POV 25 mph in a Curve, ACC	5	5	**G**
Test 7 – SV 60 mph Cut-off by POV 40 mph, FCW	6	4	**Y [2]**
Test 7 – SV 60 mph Cut-off by POV 40 mph, ACC	5	5	**G**
Test 8 – SV 45 mph Changes Lanes and Encounters POV Stopped, FCW	7	5	**Y [3]**
Test 8 – SV 45 mph Changes Lanes and Encounters POV Stopped, ACC	5	5	**G**
Test 9 – SV 60 mph Tailgating POV Braking from 60 mph, FCW	5	5	**G**
Test 10 – SV 60 mph Approaches Motorcycle and Truck POVs 20 mph, FCW	8	3	**Y [4]**
Test 10 – SV 60 mph Approaches Motorcycle and Truck POVs 20 mph, ACC	5	5	**G**
Test 11 – SV 60 mph Approaches Motorcycle and Truck POV 20 mph, FCW	8	8	**G**
Test 11 – SV 60 mph Approaches Motorcycle and Truck POV 20 mph, ACC	5	5	**G**
Test 12 – SV 50 mph on Curve to POV Braking Moderately Hard from 50 mph, FCW	6	6	**Y [5]**
Test 12 – SV 50 mph on Curve to POV Braking Moderately Hard from 50 mph, ACC	5	5	**G**
Test 13 – SV 65 mph Following POV 60 mph, FCW	5	5	**G**
Test 14 – SV 50 mph to POV Braking Unusually Hard from 50 mph, FCW	7	7	**G**
Test 14 – SV 50 mph to POV Braking Unusually Hard from 50 mph, ACC	5	5	**G**
Test 15 – SV 40 mph to POV Stopping from 40 mph, FCW	7	7	**G**
Test 15 – SV 40 mph to POV Stopping from 40 mph, ACC	5	5	**G**
Test 16 – SV 45 mph behind 45 mph POV Changing Lanes to Reveal Stopped POV, FCW	7	7	**G**
Test 16 – SV 45 mph behind 45 mph POV Changing Lanes to Reveal Stopped PO, ACC	5	5	**G**

Table 10.44 Qualitative Nuisance Alert Test

Qualitative Nuisance Alert Test	Trials Run	Number of Alerts	Status
Test 17 – SV 50 mph Passing POVs 25 mph Around Curve, FCW	7	1	**G**
Test 17 – SV 50 mph Passing POVs 25 mph Around Curve, ACC	8	1	**G**
Test 18 – SV 60 mph Passing Truck POVs 20 mph in Adjacent Lanes, FCW	8	2	**Y [4]**
Test 18 – SV 60 mph Passing Truck POVs 20 mph in Adjacent Lanes, ACC	7	1	**Y [4]**
Test 19 – SV 60 mph following POV 60 mph	5	0	**G**
Test 20 – SV 50 mph POV 60 mph Cuts in Ahead of SV, FCW	5	0	**G**
Test 20 – SV 50 mph POV 60 mph Cuts in Ahead of SV, ACC	5	0	**G**
Test 21 – SV on Simulated Open Road No Other Traffic, FCW	5	4	**G**
Test 21 – SV on Simulated Open Road No Other Traffic, ACC	5	3	**G**
Test 22 – SV Daytime Public Road Test, 188 mi	1	9	**G**

Table 10.45 Qualitative ACC Test

Qualitative ACC Test	Trials Run		Status
Test 23 – SV following POV on Simulated Open Road	5		**Y [6]**
Test 24 – SV 45 mph POV 45 mph Changes Lanes in front of Accelerating SV	5		**G**
Test 25 – SV 60 mph changing ACC Headway following POV 60 mph	1		**G**
Test 26 – SV 50 mph following POV Accelerating from 50 mph	5		**G**
Test 27 – SV 50 mph following POV 50 mph Changes Lanes to reveal POV 50 mph	5		**G**
Test 28 – SV 40 mph passes POV 40 mph	5		**G**
Test 29 – SV 50 mph Throttle Override during Automatic Braking	5		**G**
Test 30 – SV 50 mph ACC Test with Anti-lock Braking Activated	5		**G**

b. Technical Problems

The comment numbers below refer to the numbers in the Status Columns of Tables 10.43 through 10.45.

[1] The radar track was observed to move away and to the right of the stationary POV until it was dropped. The radar then reacquired the POV after which the process repeated. The outcome was that the FCW alert was issued late because the initial track was dropped. Investigation showed that an overflow occurred in the tracking algorithm. This produced an incorrect sign that resulted in the track drifting away from the target. Once the problem in the tracking algorithm is fixed and validated, Test 5 will be rerun.

[2] This test turned out to be very difficult to execute. Several times, the POV cut in too late which resulted in a late alert relative to the Pass/Fail criteria. However, an alert was issued every time. This test is considered sufficient and will not be rerun.

[3] The test procedure was incorrect. Not enough distance was allowed for the SV to move into the lane. However, an alert was issued every time. This test, as written, turns out to be a good test of the target selection algorithm, so it will not be revised.

[4] Radar resolution is specified for two equal (or near equal) radar cross section (RCS) targets. In this case, the RCS difference between the large trucks and small motorcycle was too great to reliably issue an alert at the desired range. However, an alert was issued every time. Since the radar resolution cannot be changed at a reasonable cost on this program, the test will not be rerun.

[5] It was determined that the radar field-of-view (FOV) was only 80% of what it was supposed to be. This was due to an incorrect value for a constant that controls the antenna servo. The smaller FOV resulted in a later than desired alert. However, an alert was issued every time. The incorrect constant value was fixed and shown to be correct in tests 5 and 6.

[6] The numerous tight curves encountered on the Ride and Handling Loop proved to be too severe for the system to keep the POV in the FOV of the radar. Therefore, it is recommended the ACC not be used on this type of road.

Significant Research Findings

The tests described above demonstrated that the vehicle system is ready to proceed to Phase II which is the Field Operational Test. The problem described in Comment [1] above will be fixed for the Pilot vehicle. In addition, the following changes will be tried on the Pilot vehicle to further decrease some nuisance alerts.

1. For CIPV targets, there is an attempt to eliminate the alarm that is often seen when the Host vehicle is accelerating to pass a vehicle in front. There is already a countermeasure in the Threat Assessment Algorithm, but the Host vehicle acceleration test constant is apparently too high. Experiments will be conducted to see if this constant can be lowered in Phase II.
2. Some human factors experiments were conducted on another in-house GM program to see if the alert timing used in GMR2 and other algorithms was proper relative to the judgment of outside test subjects. It was concluded that the alert timing should be adjusted to give the Imminent Alert at a longer range when the Host vehicle is around 60 mph. This makes its way into GMR2 via the estimate of a_f used in the algorithm. It is planned to adjust the a_f subroutine to give the driver an Imminent Alert at a slightly longer range for high Host vehicle speeds. This change should be implemented by the time the Pilot vehicle is verified.
3. Another source of nuisance alerts happens when the Lead vehicle turns from in front of the Host vehicle. Although in some instances this is appropriate when the

Lead Vehicle is still close to the Host vehicle's path, in other instances, the Imminent Alert occurs when the Lead vehicle is relatively far from the Host vehicle's path. An attempt will be made to decrease the target selection funnel width to see if this problem can be reduced. This will also be done in Phase II.

4. The driver distraction part of the Threat Assessment Algorithm was not verified in Phase I. The Data Fusion function was programmed to output an indication of driver distraction when activity was sensed from the steering wheel buttons. However, there were problems in putting that information on the CAN bus. We believe this problem is solved, but we ran out of time to verify it. This will be done in Phase II.

References

D.V.A.H.G. Swaroop (1994). *String Stability of Interconnected Systems: An Application to Platooning in Automated Highway Systems*, Ph.D Thesis, Department of Mechanical Engineering, University of California Berkeley.

W.G. Najm, C.J. Wiacek, and A.L. Burgett (October 1998). *Identification of Precrash Scenarios for Estimating the Safety Benefits of Rear-End Collision Avoidance Systems*, Fifth World Congress on Intelligent Transport Systems, Seoul, Korea.

P.L. Olsen, and M. Sivak (1986). *Perception-Response Time to Unexpected Roadway Hazards*, Human Factors, 28, pp. 91-96.

N. Phamdo (April 2001). *Performance Assessment of the NHTSA Alert Algorithm*, Applied Physics Laboratory, The Johns Hopkins University, preprint.

M.S. Chang, C. J. Messer, and A.J. Santiago (1985). *Timing Traffic Signal Change Intervals Based on Driver Behavior*, Transportation Research Record, 1027, pp. 20-30.

Current Schedule and Progress

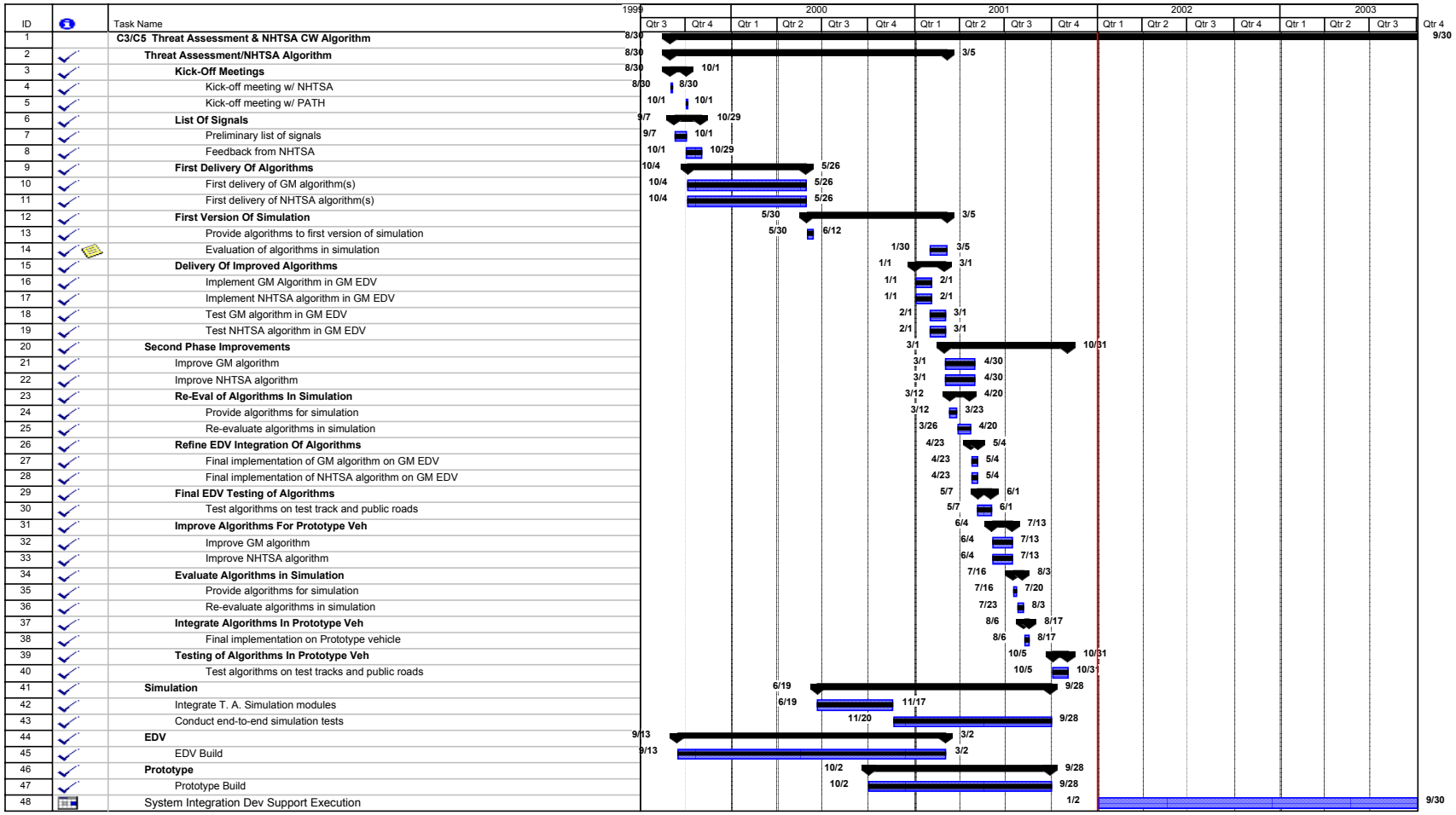

Figure 10.9 Tasks C3 and C5 Schedule

11 Adaptive Cruise Control Function (Task C4)

Goals, Purpose and Background

The purpose of this task is to add the Adaptive Cruise Control (ACC) subsystem to the vehicle, optimize system performance, and support the system during deployment. The components of this subsystem are the throttle control, the radar, and the brakes.

The subsystems of this task have been implemented on other vehicles so the technology risk was low. However, the Buick LeSabre used in this program is a new vehicle with new interfaces, so there was some communication debugging required between the subsystems as well as tuning for the platform.

Initially the brakes were making some decisions that, for this program, needed to be made by the ACC/A controller; for example the brakes would detect that the driver was exercising throttle override of the cruise system and stop applying brakes. The ACC/A controller needed to control this decision, so the protocol in the brakes was changed so that it gets the throttle override decision from the ACC/A controller. This eliminated a brake release occurring without the controller informing the driver. There was also a brake fault condition that would prevent the ACC from resuming when the resume button is pushed. A status handshake was added between the ACC controller and the brakes before engaging ACC to determine that the brakes would respond to control requests.

Initial performance on level roads was acceptable, but in downhill situations the host vehicle would get too close to the lead vehicle without applying brakes. The tuning required modifying the control loop to improve downhill performance without compromising the level road performance.

It became clear that extensive work on the ACC/A algorithm was needed to obtain the required operating characteristics. Accordingly, a simulator was developed that includes the ACC code in the loop, along with some very simplified models of vehicle longitudinal dynamics.

This simulator has been used to evaluate the effects of changes to the algorithms being made or contemplated. So far, the simulator has been used only to evaluate the ACC algorithms that respond to simple, short, longitudinal maneuvers, such as cut-ins.

While the simulator has not yet been rigorously evaluated, it is useful in making comparisons between two algorithm versions. Such a comparison is shown in Figure 11.1. Here, two algorithm versions are compared using several cut-in scenarios. Of interest was the braking level and its rate of onset. Displayed is a plot of the first three seconds of brake demand after a cut-in target is recognized. For each algorithm, there is one plot for each cut-in scenario. The scaling is the same for all plots. Each horizontal gridline represents 0.1g deceleration demand from the ACC/A controller.

It appears from the comparison plots that the newer version, v 3.13.56, produces slightly lower decelerations with slightly lower rates of onset, but with longer durations. One might conclude that the newer version gives a somewhat smoother ride than the older version, at least in certain cut-in situations. It is probable that headway excursions below the desired setting are larger, as well. Studies could also be made of the interaction between "smoothness" and magnitude of headway excursions.

The goals for this tool are to validate its accuracy, and then provide studies of the kind shown in Figure 11.1.

Intermediate and Final Results

Juries of drivers from Delphi, GM, and NHTSA have driven the prototype vehicle and experienced the ACC performance. The existing performance is acceptable and passes all testing. However, the tuning of ACC performance is a balance of several different areas of interest. These areas include (1) long-term operations such as following up hills, down hills and on level roads, and (2) short-term dynamic maneuvers, such as cut-ins and following a lead vehicle to a stop. Each of these areas requires a slightly different control approach to be most 'human-like'.

This balance is the most challenging task in the development of an ACC subsystem. More tuning will make ACC perform even better than its current level. The acquisition of the Buick LeSabre Engineering Development Vehicle (EDV), discussed in Section 12.2, will enable further refinement of the ACC subsystem.

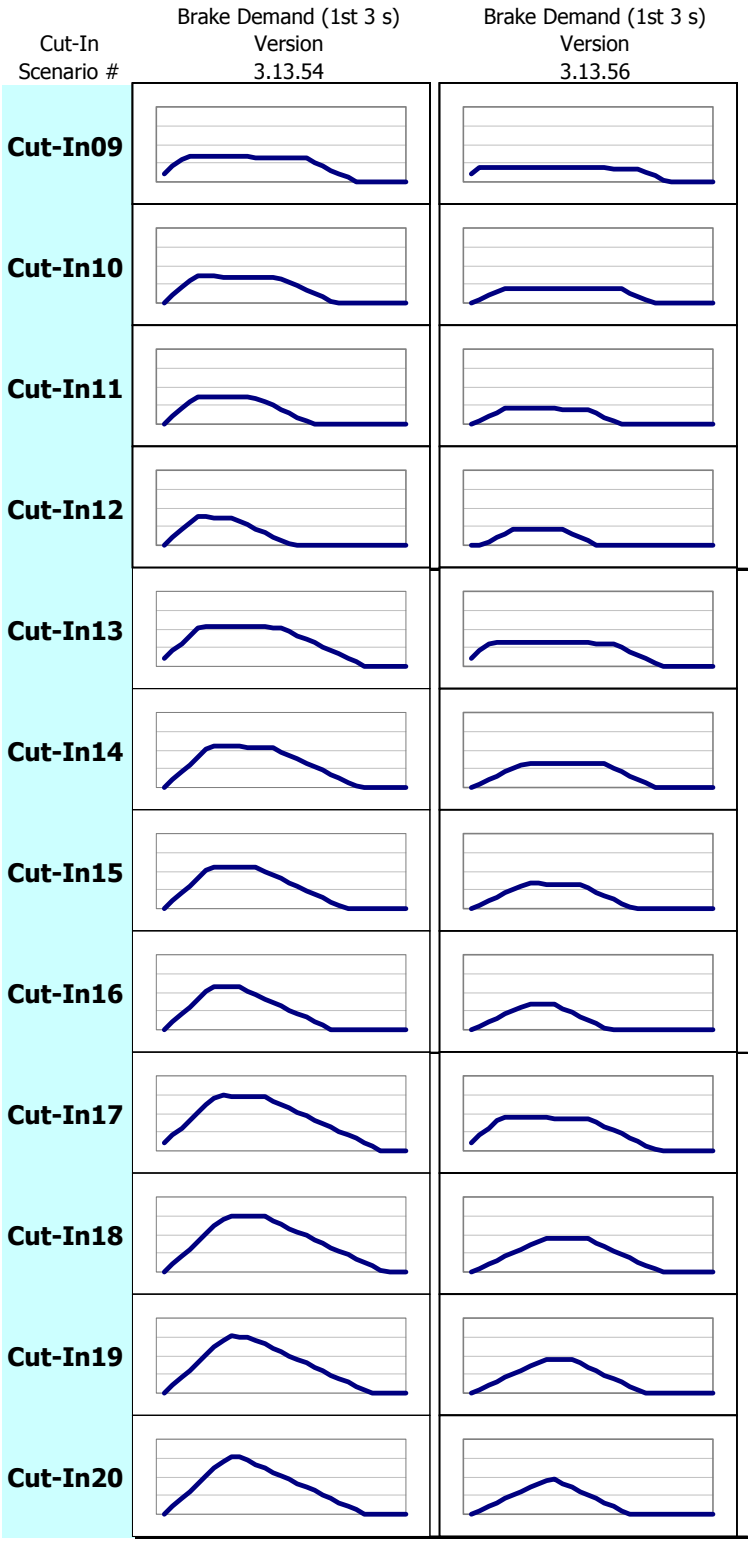

Figure 11.1 Comparison of Two ACC/A Algorithms Using the ACC Simulator

Current Schedule and Progress for Task C4

Task C4 is on schedule. Final refinement and planning for support are under way. Some problems have been identified, such as the need for a method to communicate the problems that may occur with sufficient detail to enable the responsible organization resolve the issues. In addition, a system that allows timely, in-the-field updates and repairs must be created. These issues are critical to fixing any problems that may occur. The handling of these issues, and the further refinement of the ACC performance, will be the focus of future efforts.

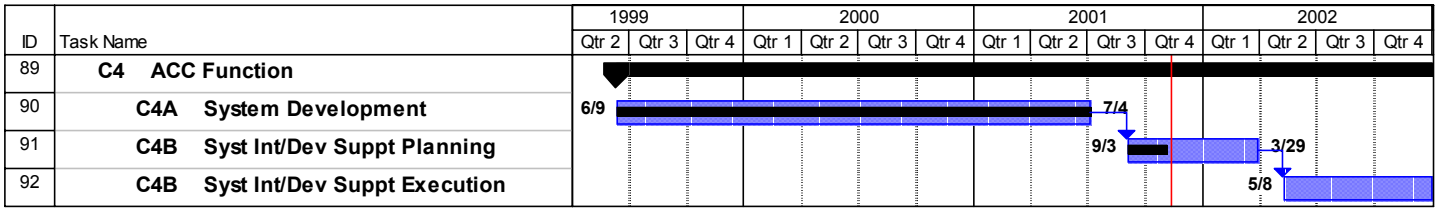

Figure 11.2 Task C4 Schedule

12 Fleet Vehicle Build (Task D)

12.1 GM Engineering Development Vehicle

Goals and Purposes

The goal and purpose of building the General Motors Engineering Development Vehicle (GM EDV) was to develop, design, implement, and investigate a subset of technologies that will potentially be available on the deployment vehicles of the ACAS/FOT Program. These technologies were evaluated on this vehicle and went through a down selection process with other technologies being investigated by partners in the program. The basic technologies focused on in this vehicle were:

1. Threat assessment
2. GPS/Map based path prediction
3. Evaluating the performance of the Assistware System
4. Human factors

These technologies are elaborated in different sections of the report and will also be summarized later in this section.

Technical Approach

The GM EDV is a 2000 model year Buick LeSabre that has been significantly modified to accommodate all the instrumentation required to investigate the intended technologies. Our approach in building this vehicle consisted of two major steps.

1. Defining the architecture. - This important step consisted of analyzing various architectures and configurations, and finally determining the best approach for this task. Important factors in this determination were:
    a. simplicity and ease of implementation
    b. compatibility with our partners' architectures
    c. ease of debugging the system
    d. ease of collecting data

2. Implementing the architecture in the laboratory. - However well a test vehicle is designed and built, it is still a very cumbersome and inconvenient environment in which to debug an electronic system. For this reason, the first step taken in this task was to implement the pertinent vehicle architecture in the laboratory. The configuration that was intended for the vehicle was implemented on a bench with exactly the same computers, same communications scheme, and same add-on sensors. However, integrating the vehicle sensors on the bench system is not possible in a laboratory environment.

Results

System Hardware

The system hardware intended for the GM EDV was integrated first, then debugged on the bench and made operational. The key to the proper operation of the system is the inter-processor communication. Initially, rudimentary software for the functions performed by each module was integrated with the communications software to make sure the communications software and processor hardware were working properly. Then, the operation of the add-on sensors was verified, although the data provided is not meaningful in this environment.

Before instrumenting the vehicle, the necessary electrical and mechanical infrastructure was built to support the system. Electrical upgrades consist of installing a high output alternator in addition to wiring, power and signal, terminals, fuses, and various relays. Mechanical upgrades consist of brackets for computers and sensors, wire and cable routing, and modifications to several parts of the vehicle to install subsystems/devices.

The instrumentation was installed in various parts of the vehicle. The grille and the engine compartment contain the radar sensor. The passenger compartment contains the yaw rate sensor, accelerometer, and compass, which are underneath the console between the driver and the passenger. A high head-down display is immediately in front of the driver embedded in the dashboard. A speaker for audio feedback is under the instrument panel and is driven by an amplifier in the trunk. Haptic feedback, which consists of a seat vibrator, is embedded into the drivers seat in the seat bottom. The engineering terminal, which consists of a liquid crystal display and a keyboard, is in the back seat immediately behind the front passenger. A single display and keyboard combination supports multiple computers in the vehicle. An electronic switch box is installed in the opening between the trunk and the passenger compartment. Pushing the selector switch on this box connects the terminal to the computers in round-robin fashion.

Most of the computers and devices are installed in the trunk. A number of computers, along with a dedicated floppy disk drive for program loading, are permanently installed. A panel with all the signals serves the purpose of a breakout box for observing the sensor signals. An Assistware system, a differential global positioning system (DGPS), a Class 2 bus to serial converter, and a sound board with amplifier, are laid out on a baseboard in the trunk. In addition, there is a data acquisition system, which resides in the trunk but will be used on demand, in conjunction with a laptop, when needed.

The exterior of the vehicle is used for antennas. The antenna for the compass is hidden in the headliner. The antenna for the DGPS of the Assistware system and the road geometry processor are mounted on the trunk lid. Another DGPS for data truthing will be used in certain tests, and then the antenna will be temporarily mounted on the trunk lid using magnets.

GM EDV Architecture

The architecture and block diagram of the GM EDV is shown in Figure 12.1.

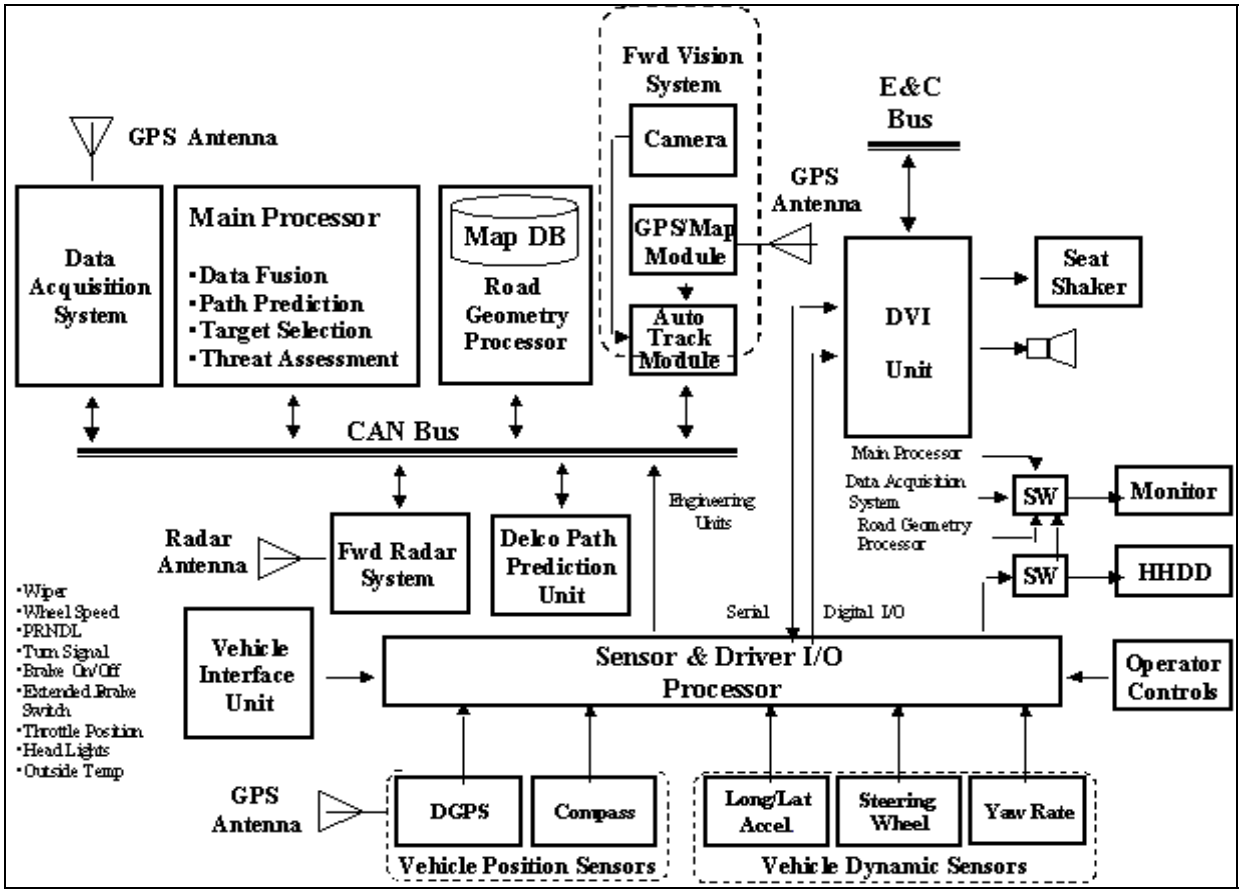

Figure 12.1 Architecture of GM Engineering Development Vehicle

The backbone of the system is a CAN bus for communicating between various subsystems in the vehicle. The bus is operating at 500 Kbaud rate and uses 11-bit identification codes for messages. One end of the bus terminates at the radar, which is at an extreme location physically. The other end terminates at the Sensor and Driver I/O Processor.

A number of processors share the tasks to be accomplished. The sensor and Driver I/O Processor is the interface between the vehicle, the driver, and the system. It is interfaced to in-vehicle production sensors and devices. This is accomplished via two separate paths. First is the Class 2 bus; any sensor information of use to the ACAS functions on this bus is monitored and captured. Then interface electronics convert Class 2 messages to RS232 format. Any sensor or device parameter not available on the Class 2 bus is directly interfaced. This information is gathered through either discrete digital inputs or an analog to digital converter. Non-production sensors are installed on the vehicle.

These are the DGPS, compass, longitudinal/lateral accelerometer, steering wheel position sensor, yaw rate sensor. Driver inputs are captured through the steering wheel buttons. The Driver Vehicle Interface (DVI) Unit consists of a High Head-Down Display (HHDD), a sound board, and a seat vibrator.

The Road Geometry Processor is used to determine the road geometry ahead of the vehicle, based on DGPS data and maps. It receives the DGPS data periodically through the Sensor Processor and the CAN bus. The maps are permanently stored in the hard disk media in this processor. It generates a data record which defines the path of the road ahead, and this information is placed on the CAN bus to be picked up by the Main Processor.

The Main Processor performs many functions: data fusion, path prediction, target selection, and threat assessment. It receives data from the radar via the CAN bus, which contains target tracks and additional pertinent information related to detected targets. It receives vehicle sensor data and road geometry processor output for data fusion to predict the vehicle path. Based on radar targets and predicted path, it selects the most threatening target. The threat assessment algorithm(s) are performed on this target based on the kinematics of the vehicle, which is monitored by the sensor processor, and the target, which is determined from radar target information.

The radar is directly interfaced to the CAN bus. At power-up it requires an initialization message that will be sent automatically by the Delphi Delco Path Prediction Unit. This initialization message configures the radar main processor to transmit the requested data periodically, at 10 Hz rate.

The Delco Path Prediction Unit, as the name implies, is a stand-alone box that predicts the vehicle path based on vehicle dynamics sensors. In addition, it initializes the radar to the proper mode.

Assistware is a forward vision system that has two functions. First, it has a forward-looking camera and a vision processor to determine the lane marker positions and the attitude of the vehicle within the lane, specifically, offset from the centerline and the heading. Second, it has a GPS/Map module that is capable of building maps as the vehicle is driven around.

The DVI unit consists of several devices that alert the driver. An HHDD is directly in front of the driver on the dashboard and, displays various graphics and icons as well as text data. The speaker generates various tones to get the attention of the driver under certain conditions. A seat shaker is the haptic output, which provides another mode for alerting the driver.

All processors are connected to a switch box, which enables them to share a common monitor and keyboard. The monitor and keyboard are mounted on the back seat where an engineer can control the overall system. Not shown in the block diagram are floppy disk drives, one for each processor. These features enable easy debugging in the field and downloading of software to the system.

The data logging / display tool set used in the GM EDV is a windows (98/NT/2000) application providing these capabilities:

- The ability to log selected subsets of vehicle CAN messages and replay them (or a subset of them) in real time over the CAN bus.
- An in-vehicle diagnostic tool to display CAN bus data textually, graphically, and overlaid on video data.
- A post-processing tool to parse and display logged CAN data graphically and overlaid on video images.
- A collection mechanism for compressed digital video sequences, time-aligned with radar and other vehicle sensor data.
- A collection mechanism for non-compressed digital video sequences, time-aligned with radar for use as data sets in vision algorithm development.
- A semi-automated procedure for camera-to-radar coordinate alignment.

The components of the data logger are shown below:

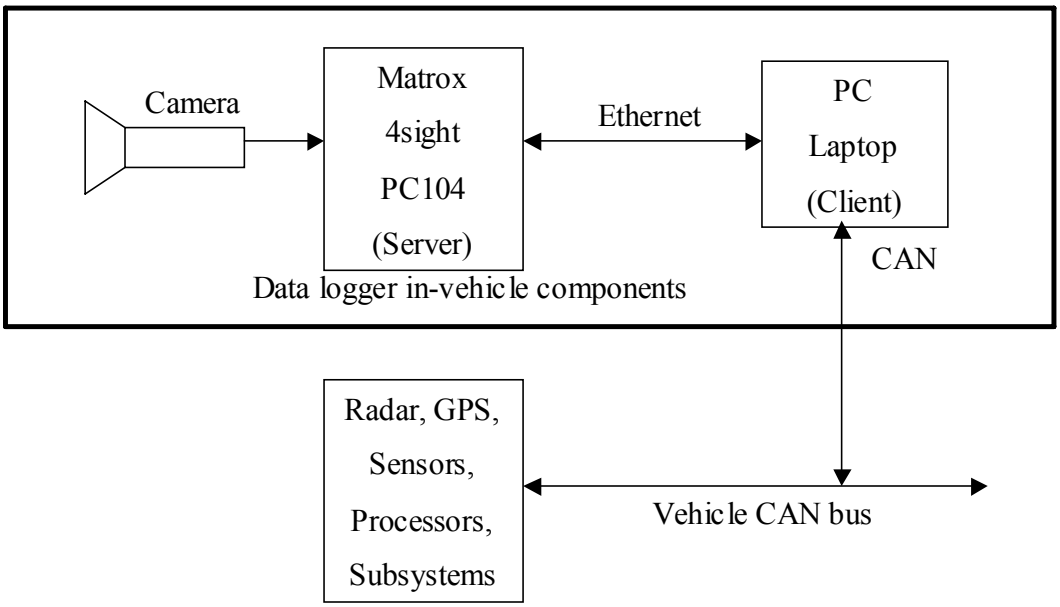

Figure 12.2 In-Vehicle Data Logger Components

An example screen from the tool is shown in Figure 12.3. The screen can be configured to show the relevant information required by a particular user. User defined windows with pertinent information are displayed for collecting and analyzing the data.

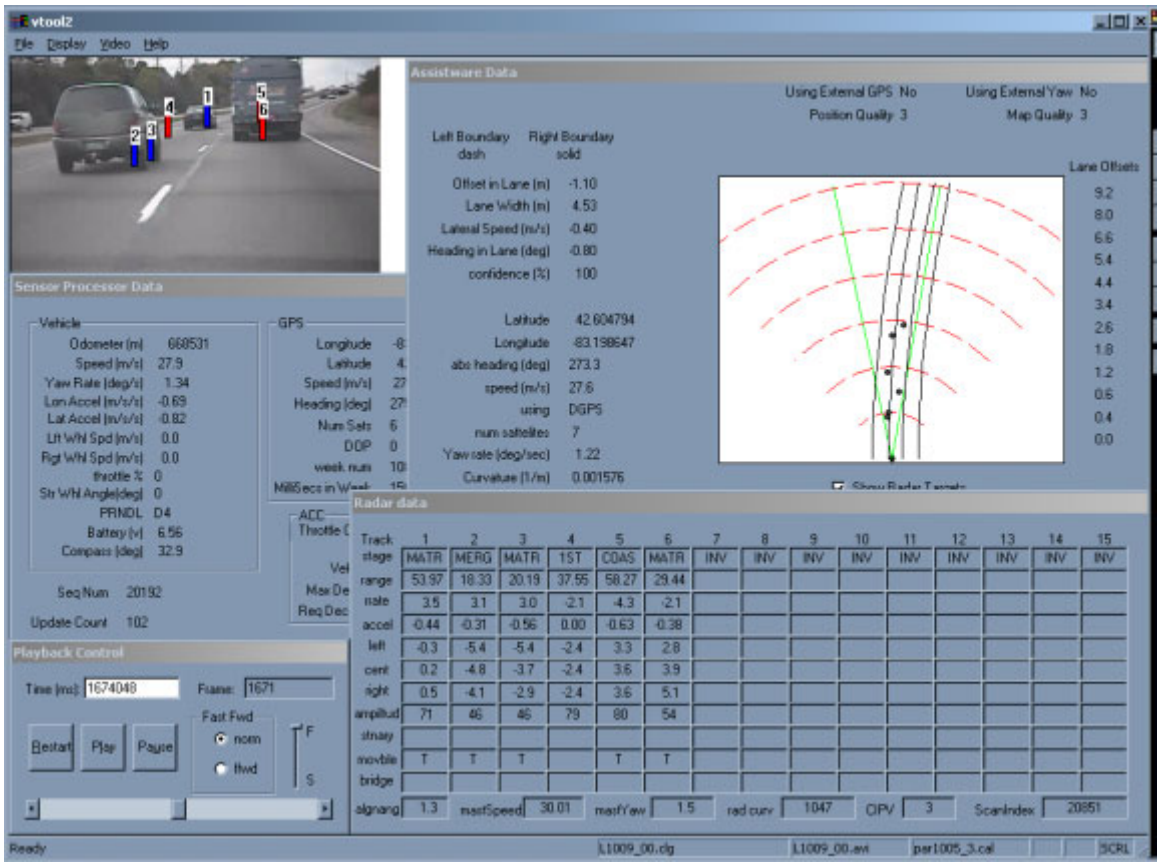

Figure 12.3 Data Logger Screen

Software Development

An initial version of all the software components of the GM EDV has been designed and coded, and tested in the lab and on the vehicle.

The software components are:

1. Program Loader - from solid state non-volatile memory
2. Real Time Multi-Threading Functions
    a. Interrupt service routines
    b. Resource locking
    c. Time slicing
    d. Pre-emption
    e. Timer services
    f. Intra processor communication functions

   g. Functions to copy data structures between program modules.
   h. CAN bus message definitions and functions
3. Asynchronous Serial Communication with External Sensors
   a. GPS
   b. Yaw rate sensor
   c. Compass
   d. Accelerometer
   e. Class 2 gateway for vehicle OEM data
   f. Audio output device
4. Map Road Geometry - Extracts forward road geometry from map database
5. Data Fusion - Combines instantaneous yaw rate with predicted Map Road Geometry
6. Target Selection - Selects a target from the radar target tracks based on host vehicle path and radar track data
7. Threat Assessment - Uses vehicle and radar data to compute alert level based on the most threatening target in the host vehicle path
8. Driver-Vehicle Interface - Presents the alert level to the driver in visual, audio and haptic form

Status

The vehicle has been designed, built, and all the electronic systems have been implemented, tested and validated. This has been accomplished systematically, using a step-by-step procedure. Data has been collected for individual components / subsystem to verify proper functioning of these system components. Algorithms have been developed for the components to perform the required tasks and have been tested individually. The software for individual components has been integrated to work in cohesion, mainly by communicating through the CAN bus. System level tests have been performed to verify the operation of the overall system by running pre-defined tests, collecting data, and analyzing and confirming that it matches the simulated data. Once the system was validated to be operating as specified, further enhancements were made to the software to enhance the functionality and improve the latency time of the algorithms.

The GM EDV is fully operational and functional, and is performing as specified.

12.2 Delphi Delco Electronics Engineering Development Vehicles

Goals, Purpose and Background

The purpose of building the Delphi Delco Electronics Engineering Development Vehicles (hereafter called the Delphi-D EDVs) is to support the development of driver-vehicle interface, data fusion, target selection, and vision technologies. These vehicles are appropriately modified, using techniques developed during the ACAS program, to support these activities. These vehicles are also used to support the vision technology

down-select activity. One of the Delphi-D EDVs that is equipped with a Vectra Collision Warning (CW)/Adaptive Cruise Control (ACC) system was provided to UMTRI for their pilot test program, in which the system was characterized.

A total of four vehicles have been used for the above purposes. Three of the Delphi-D EDV vehicles were developed on other programs and have been modified to support the ACAS/FOT. They are a Lexus, a Cadillac Seville, and an Opel Vectra, not the same type of vehicle that will be used in the FOT (the Buick LeSabre will be the FOT test vehicle). These cars have been quite useful in "roughing in" the subsystems to be provided by Delphi-D. But without a Buick LeSabre, it was very difficult to refine those subsystems to work well in the specific FOT test vehicle, especially the ACC and DVI subsystems. The fourth vehicle, purchased under the ACAS-FOT program, is a Buick LeSabre.

Results

The Lexus LS400 was Delphi's first attempt at developing a completely integrated Forward Collision Warning (FCW) system. The planning and build of this vehicle was initiated during the negotiation of the first ACAS TRP Cooperative Agreement. It was completed and demonstrated prior to the ACAS TRP contract award date of January 1995. However, while this demonstration vehicle was used extensively during the first ACAS TRP Program in order to further the understanding of the pertinent underlying issues associated with collision avoidance technologies, it was not appropriately equipped for the FOT. During the year 2000, the Lexus has been upgraded. The vehicle was rewired and the serial interfaces between the vehicle interface processor and the radar, yaw rate, and target selection processor have been converted to CAN. In addition, an HE Microwave ACC2 radar and Delphi's vision-based lane tracking processor and camera were integrated on the vehicle. This updated sensor suite was used to collect correlated radar, vision, and vehicle data to support the Data Fusion, Vision-Based Lane Tracking, and Target Selection tasks.

The Cadillac Seville was Delphi's second generation integrated FCW system. The planning and build of this vehicle was initiated during the contract negotiation phase of the first ACAS TRP Program. It was completed and demonstrated after the ACAS TRP Program contract award date of January 1995. This demonstration vehicle proved to be a useful learning tool in expanding the knowledge base of the underlying issues associated with collision avoidance technologies.

The Seville is currently equipped with two centralized processors, a Target Selection Processor (TSP) and Vehicle Interface Processor (VIP). The TSP and VIP are specialized hardware components, designed by Delphi. The VIP is the primary interface between all of the vehicle subsystems. It provides a platform to implement Delphi's FCW threat assessment algorithms and control the DVI. The DVI warning cues include: (a) customized audio system with capabilities to mute the audio system and generate various warning tones, (b) tactile response in the form of short duration brake pulse, and

(c) visual warning cues generated on an improved Delphi *Eyecue*™ color, re-configurable, Head-Up Display (HUD).
During the year 2000, the Seville has been upgraded. The vehicle was rewired and the serial interfaces between the vehicle interface processor and the radar, yaw rate, and target selection processor were converted to CAN. In addition, the following new components have been integrated on the vehicle and interfaced to the TSP: (a) an ACC/A radar, (b) Delphi's vision-based lane tracking processor, and (c) a real-time PC104 implementation of Delphi's radar-based scene tracking software (Task C2B). This vehicle has served as the primary test bed and data collection platform for Delphi's ACC/A radar, target selection, and scene tracking subsystems.

The Opel Vectra is a radar/laser based ACC vehicle that was developed internally within Delphi in 1998. In February 2001, the Vectra ACC vehicle was prepared for a May delivery to UMTRI. The Vectra was upgraded with an HE Microwave ACC1 pilot radar, and its control and target selection algorithms were refined. In addition, various CAN bus termination problems were resolved. The vehicle was used by UMTRI for various FOT-related data collection and human-use studies.

The Buick LeSabre is the newest addition to the family of Delphi-D EDVs. This vehicle has been fitted with the DVI intended for use in the FOT and is currently undergoing a retrofit that includes automatically controllable brakes and provisions for all the subsystems required for full operation of ACC and FCW. Prior to the retrofit, it was used extensively in the development of the DVI system. It has proved to be invaluable for that purpose. Only a LeSabre could be used to evaluate the on-road effectiveness of the steering wheel switches that must be manipulated by the driver, and only a LeSabre could be used to evaluate the performance of the deployment-intent head-up display, or HUD (which is specifically designed to fit in the LeSabre instrument panel). As a result of these development efforts, Delphi-D has provided to the FOT a very advanced, heavily tested, and highly effective interface that is presented to the driver.

12.3 Vehicle Brake System Mechanization (Task B3)

Goals, Purposes, and Background

The Chassis Systems Engineering Development Vehicle (EDV) is the primary resource used for brake systems development, testing, and systems support. The requirement is to perform autobraking, via new messages to the brake controller, in a smooth, quiet, and responsive fashion. The detailed specifications for the new autobraking feature are documented in Delphi Chassis System Requirements documents.

Specifications of the Chassis System EDV include:

2000 Buick LaSabre Limited Sedan
VIN Number: 1G4HR54K4YU263295
Grand Touring Package / Prestige Option Package (SE)
Software: ABS/TCS/DRP/VSE
Powertrain Software: Production ECU
Brake Modulator: Delphi / Bosch 5.3
Communications: Class 2
Sensors (Yaw Rate/Lateral Accelerometer, Variable Steering, Wheel Speed)

The initial work with the vehicle consisted of benchmarking the original equipment manufacturer's (OEM) brake control system, to determine and document functionality, performance (i.e. stopping distance and response), and mechanization. Experienced Delphi instrumentation technicians and drivers performed this work, recording vehicle base brake and ABS data.

The autobraking feature was developed, calibrated, tested, and verified as a stand-alone part of this project prior to integration at the prototype vehicle. The engineering activities required removing production hardware from the Chassis EDV and replacing it with Delphi Brake Controls 7.2 (DBC 7.2) hardware and software. A special bracket was fabricated to mount the brake actuator. The OEM wiring was modified to interface to the DBC 7.2 actuator and the brake lines were connected.

The new braking feature of ACC autobraking provides vehicle deceleration without driver input on the brake pedal. The anti-lock brake system (ABS) controller signals the motor in the modulator to pump brake fluid from the master cylinder into the wheel brake lines through hydraulic valves, which are opened by energizing their coils. Key features of this new brake technology are to match the deceleration control requirements for smooth, quiet, and uniform autobraking during ACC scenarios.

Intermediate and Final Results

Figure 12.4 shows the brake subsystem interconnections to vehicle sensors, the Class 2 communications bus, telltales, and the powertrain controller. The vehicle sensors provide information about vehicle performance for processing by the brake controls algorithm. The warning lamps provide fault information, and status of ABS, TCS, and park brake features. The wheel speed sensor components produce a sine wave that is related to the wheel speed. The Powertrain Control Module (PCM) sends a message back to the Electronic Control Unit (ECU) indicating engine torque control.

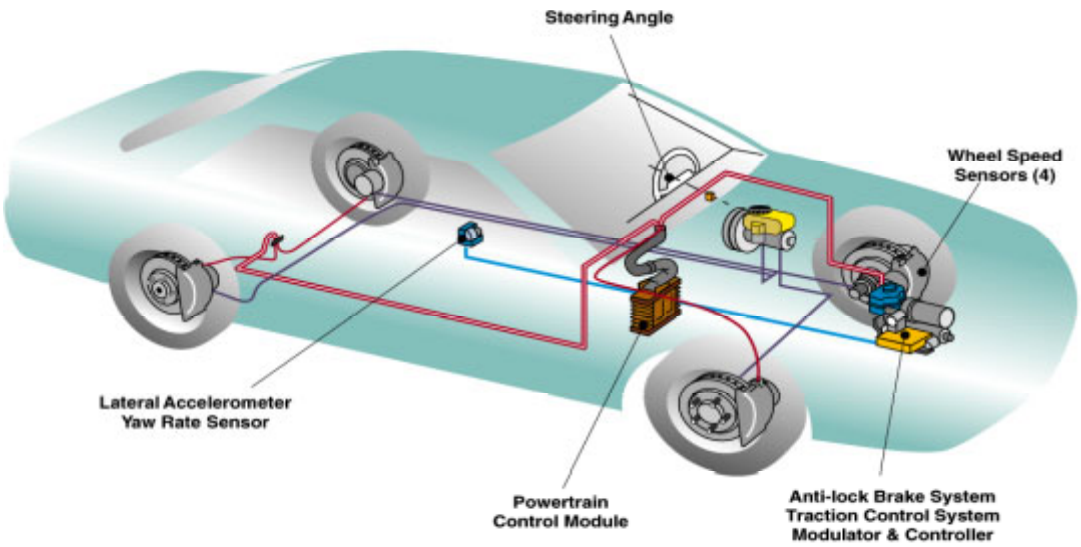

Figure 12.4 Brake Subsystem

The Chassis EDV was the test vehicle used to calibrate the brake controls software. The ABS, TCS, and VSE calibration parameters are adjusted to vehicle specific performance and handling characteristics. The calibration procedure is a formal set of work instructions that guide the engineers to perform various vehicle maneuvers and record the response data. Based upon reviews, analysis, and experience, the calibrations were fixed for the EDV and Prototype vehicles. It should be noted that the Chassis EDV and Prototype vehicles are identical in model and options.

The Chassis EDV was used to ensure that electrical requirements for intelligent braking are identical to the electrical requirements for driver-initiated braking. One of these requirements is the activation of the rear brake lamps during vehicle deceleration, which serves as a warning or indication to other drivers. During the application of intelligent braking, as in an ACC event, the driver is outside of the braking control loop and has no input to the system. Thus, the brake lamps must be activated automatically, via hardware or software, with no input from the driver. Automatic activation of the rear brake lamps was accomplished by adding a single relay to the existing hardware found on production vehicles that already have ABS. Mechanization was then carried over to the prototype vehicle and has been shown to be robust and correctly moded with the brake system.

In summary, the Chassis EDV and Prototype vehicle have identical brake control hardware and software installed. The brake system and driving performance of these vehicles are identical. Updates to the embedded software stored in the electronic ABS controller can be updated by FLASH technology. The Chassis EDV will be a resource to support the vehicle builds and FOT deployment vehicles during Phase 2.

12.4 Prototype Vehicle

Goals and Purposes

The goal and purpose of building the Prototype vehicle was to integrate all the technologies developed, evaluated, and down selected by the partners in the program into a single vehicle. The Prototype vehicle is a precursor to the Pilot vehicles. The Pilot vehicles will have the same functionality as the Prototype, however hardware partitioning of functions, hardware form factors, packaging and layout in the Pilot vehicles will be different. Functionality of the Prototype, especially with improved packaging, will carry over to the Pilot vehicles and finally to the Deployment vehicles. However, the Prototype vehicle has the full functionality as required to support ACAS/FOT.

Technical Approach

The Prototype vehicle is the last major milestone before freezing the system configuration from the functional aspect, hardware and software, and moving to the Field Operational Test phase. However, there could be some minor modifications to the system configuration during the Pilot vehicle phase. The Prototype vehicle is still a development vehicle in the sense that all the subsystems that have been verified in a number of different development vehicles are integrated into a single vehicle. This was not a straightforward task, and required significant collaborative effort among the partners to complete.

Since the build of the Prototype vehicle was a result of the effort of various ACAS/FOT partners, the task was accomplished at various sites. Delphi Chassis Systems in Brighton, MI, installed the brake system, Delphi Delco Systems in Malibu, CA installed the throttle control and ACC system, and Delphi Delco Systems in Kokomo, IN installed the Driver Vehicle Interface. GM R&D Center built the vehicle infrastructure and installed the remainder of the systems in the vehicle as well as performed the systems integrator function.

The approach was similar to that undertaken in the GM EDV. However, bench development in the laboratory was limited because this vehicle has an ACC function. The vehicle architecture was still implemented on the bench but without the ACC function. The emphasis was on integration rather than development of individual subsystems. In addition, this vehicle will contain a full-featured data acquisition system, which will be installed after the validation tests. The data acquisition system that was on the GM EDV was used throughout development and validation of the Prototype vehicle.

The software system is designed such that most of the software components of the Prototype Vehicle had been installed and tested on the GM EDV. The exceptions were:

1. Road geometry from the Vision System
2. Road geometry from Radar Scene Tracking
3. Driver-Vehicle Interface with the Head-Up Display
4. Adaptive Cruise Control

5. Throttle control for ACC
6. Brake control for ACC

Work Accomplished

The architecture and block diagram of the Prototype vehicle is shown in Figure 12.5. This is the system architecture which was designed, implemented, built and verified on the Prototype vehicle.

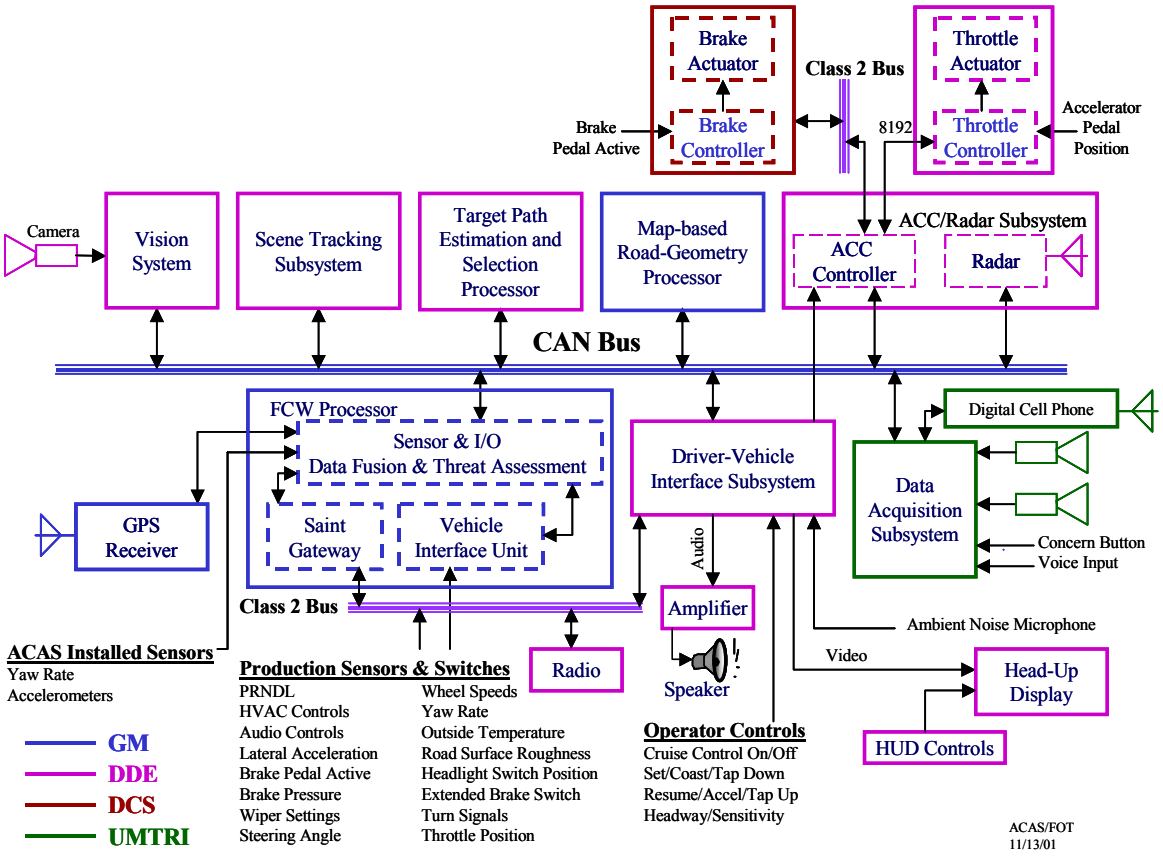

Figure 12.5 Block Diagram of Prototype Vehicle

The architecture of the Prototype vehicle is an extension of the GM EDV. The major differences are the additions of the ACC, which involves throttle and brake control, and the DVI, mainly due to the use of an HUD. The Path prediction function has been enhanced by use of vision and scene tracking, which are additional inputs to the data fusion unit. In addition, the functional mapping of tasks to hardware is unlike the GM EDV because each partner delivered one or more of the functions already implemented in various engineering development vehicles.

System Hardware

The system hardware intended for the Prototype vehicle was integrated as closely as possible to the vehicle architecture on the bench and then made operational. Again, key to the proper operation of the system is inter-processor communication. Initially, rudimentary software for the functions performed by each module was integrated with the communications software to make sure the communications software and processor hardware were working properly. Then the operation of ACAS installed sensors was verified, although the data provided was not meaningful in this environment.

Before instrumenting the vehicle, the necessary electrical and mechanical infrastructure was built to support the system. Electrical upgrades consisted of installing a high output alternator in addition to wiring, power and signal, terminals, fuses and various relays. Mechanical upgrades consisted of brackets for computers and sensors, wire and cable routing, and modifications to various parts of the vehicle to install subsystems/devices.

The instrumentation was installed in various parts of the vehicle. The grille and the engine compartment contain the radar sensor. The passenger compartment contains the yaw rate sensor and accelerometer, which are underneath the console between the driver and the passenger. A non-production HUD is installed in place of the production HUD to provide visual feedback to the driver The audio feedback is provided through an add-on amplifier and speaker combination, which is driven by the Driver Vehicle Interface Subsystem. Also, the Driver Vehicle Interface Subsystem mutes the vehicle radio by sending a command to the radio via the Class 2 bus when an alert is issued. Haptic feedback is eliminated from the Prototype vehicle. The engineering terminal, which consists of a liquid crystal display and a keyboard, is in the back seat immediately behind the front passenger. A single display and keyboard combination supports multiple computers in the vehicle. An electronic switch box is installed in the opening between the trunk and the passenger compartment. Pushing the selector switch on this box connects the terminal to the in round-robin fashion to each of the computers. Another liquid crystal terminal is installed in the front of the vehicle on the passenger side. The purpose of this display is to show exactly the same information as shown on the HUD, since only the driver can see the HUD; this display is driven directly from the Driver Vehicle Interface Subsystem.

Most of the computers and devices are installed in the trunk. A number of computers, with a dedicated floppy disk drive for program loading, are permanently installed. All the vehicle sensor signals are bundled together in a wire harness and are fed into the processor. A differential global positioning system (DGPS) and Class 2 bus to serial converter are all laid out on a baseboard in the trunk. In addition, there is a data acquisition system, which resides in the trunk but which will be replaced by an enhanced Data Acquisition System developed by UMTRI.

The exterior of the vehicle is used for antennas. The antenna for the road geometry processor is mounted on the trunk lid. Another DGPS for data truthing will be used in

certain tests, and then the antenna will be temporarily mounted on the trunk lid with magnets.

Prototype Vehicle Architecture
The architecture shown in Figure 12.5 was designed, implemented, debugged, and validated on the vehicle.

The backbone of the system is a CAN bus for communicating between various subsystems in the vehicle. The bus operates at 500 Kbaud rate and uses 11-bit identification codes for messages. One end of the bus terminates at the radar, which is at an extreme location physically. The other end terminates at the DVI Subsystem.

The Prototype vehicle architecture shown in Figure 12.5 is color-coded to identify the responsibility of partners related to vehicle functions. In addition to increasing the functionality of the Prototype with respect to the EDVs, the mapping of functions to hardware has also been changed.

A number of processors share the tasks to be accomplished. The Sensor and Driver I/O Processor is the interface between the vehicle, the driver and the system. It is interfaced to in-vehicle production sensors and devices. This is accomplished via two separate paths. First is the Class 2 bus; any sensor information of use to the ACAS functions on this bus is monitored and captured. Then interface electronics convert Class 2 messages to RS232 format. Any sensor or device parameter not available on the Class 2 bus is directly interfaced. This information is gathered through either discrete digital inputs or an analog to digital converter. Non-production sensors are installed on the vehicle. These are the DGPS, longitudinal/lateral accelerometer, steering wheel position sensor, and yaw rate sensor. Driver inputs are captured through the steering wheel buttons. The Driver Vehicle Interface Subsystem consists of a non-production HUD and an audio interface via an add-on amplifier/speaker combination.

The Road Geometry Processor is used to determine the road geometry ahead of the vehicle based on DGPS data and maps. It receives the DGPS data periodically through the Sensor Processor and the CAN bus. The maps are permanently stored in the hard disk media in this processor. It generates a data record which defines the path of the road ahead, and this information is placed on the CAN bus to be picked up by the FCW Processor.

The FCW Processor performs many functions: data fusion, path prediction, and threat assessment. It receives the data from the radar via the CAN bus, which contains target tracks and additional pertinent information related to detected targets. It receives vehicle sensor data and road geometry processor output for data fusion to predict the vehicle path. Based on radar targets and predicted path it selects the most threatening target. The threat assessment algorithm(s) are performed on this target based on the kinematics of the

vehicle, which is monitored by the sensor processor and the target, which is determined from target information.

The Sensor Processor and the FCW Processor are integrated into a single processor, however the software functions are partitioned as the original version. In this configuration, the software modules interface to each other directly rather than transferring data via the CAN bus.

The radar is directly interfaced to the CAN bus. At power up it requires an initialization message, which is sent automatically by the Delphi Delco Path Estimation Processor. This initialization message configures the radar main processor to transmit the requested data periodically, at 10 Hz rate.

The Delco Target Path Estimation and Selection Processor, as the name implies, is a stand-alone processing unit that tracks the targets and determines if they are in the host vehicle's path. This unit selects and reports the closest moving and stationary targets to the Threat Assessment unit. In addition, upon power-up, it initializes the radar to proper operating mode by sending a special message packet over the CAN bus.

The Data Fusion module, which resides in the FCW Processor combines the data from vehicle dynamics sensors, road geometry, scene tracking and vision system. It predicts the path of the vehicle by combining all this information. The Target Path Estimation and Selection Processor uses the output of this module.

The Forward Vision system has two functions. First, it uses a forward-looking camera and a vision processor to determine the lane marker positions and the attitude of the vehicle within the lane, specifically, offset from the centerline and heading. Second, it determines the geometry of the lane ahead, specifically the curvature of the lane.

The Driver Vehicle Interface Subsystem consists of visual and aural devices that alert the driver. A non-production HUD directly replaces the production HUD and displays various graphics and icons as well as text data. The audio feedback is provided through an add-on amplifier and speaker combination that generates various sound tones to get the attention of the driver under certain alert conditions. The vehicle radio is muted when an aural warning is issued to the driver.

The Prototype vehicle has computer controlled braking, which is used in ACC mode. The brake controller is interfaced to the Class 2 bus, which receives the commands from the ACC controller to activate the brake actuator. The ACC controller also controls the throttle controller, which in turn activates the throttle actuator. These functions are described in detail in earlier sections.

The Data Acquisition Subsystem (DAS) is capable of capturing all the relevant information regarding the system while operating in the field. DAS is interfaced to the

CAN communications bus to capture all the information related to the vehicle and the sensors. Also, it is interfaced to a microphone for on-demand voice input and two cameras to record the images of the forward scene and the driver when certain conditions are met. A digital cellular phone is used to transfer information between the DAS and the ground station, and also to send commands to the vehicle to modify its operating mode. DAS is described in more detail in a later section.

All processors are connected to a switch box, which enables them to share a common monitor and keyboard. The monitor and keyboard are mounted on the back seat where the engineer can control the overall system. Not shown in the block diagram are floppy disk drives, one for each processor. These features enable easy debugging in the field and downloading of software to the system. However, this is a temporary setup and will be removed when the system is fully debugged.

Software Development

An initial version of all the software components of the Prototype vehicle has been designed and coded, and tested in the lab. Currently it is being installed in the vehicle for testing and data logging.

The software components are:

1. Program Loader - from solid state non-volatile memory
2. Real Time Multi-Threading Functions
    a. Interrupt service routines
    b. Resource locking
    c. Time slicing
    d. Pre-emption
    e. Timer services
    f. Intra processor communication functions
    g. Functions to copy data structures between program modules.
    h. CAN bus message definitions and functions.
3. Asynchronous Serial Communication with External Sensors
    a. GPS
    b. Yaw rate sensor
    c. Compass
    d. Accelerometer
    e. Class 2 gateway for vehicle OEM data
    f. Audio output device
4. Map Road Geometry - Extracts forward road geometry from map database
5. Data Fusion - Combines instantaneous yaw rate with predicted Map Road Geometry
6. Scene Tracking – Predicts the path of the vehicle / road geometry based on the kinematics of other moving objects in the field of view of the radar

7. Target Path Estimation and Selection - Selects a target from the Radar target tracks based on host vehicle path and radar track data
8. Threat Assessment - Uses vehicle and radar data to compute alert level based on the most threatening target in the host vehicle path
9. Driver-Vehicle Interface - Presents the alert level to the driver in visual and aural mode
10. ACC Controller – Determines the required throttle and brake control commands
11. Brake Controller – Activates the brake actuator based on the command from the ACC controller
12. Throttle Controller– Activates the throttle actuator based on the command from the ACC controller

Current Schedule and Progress

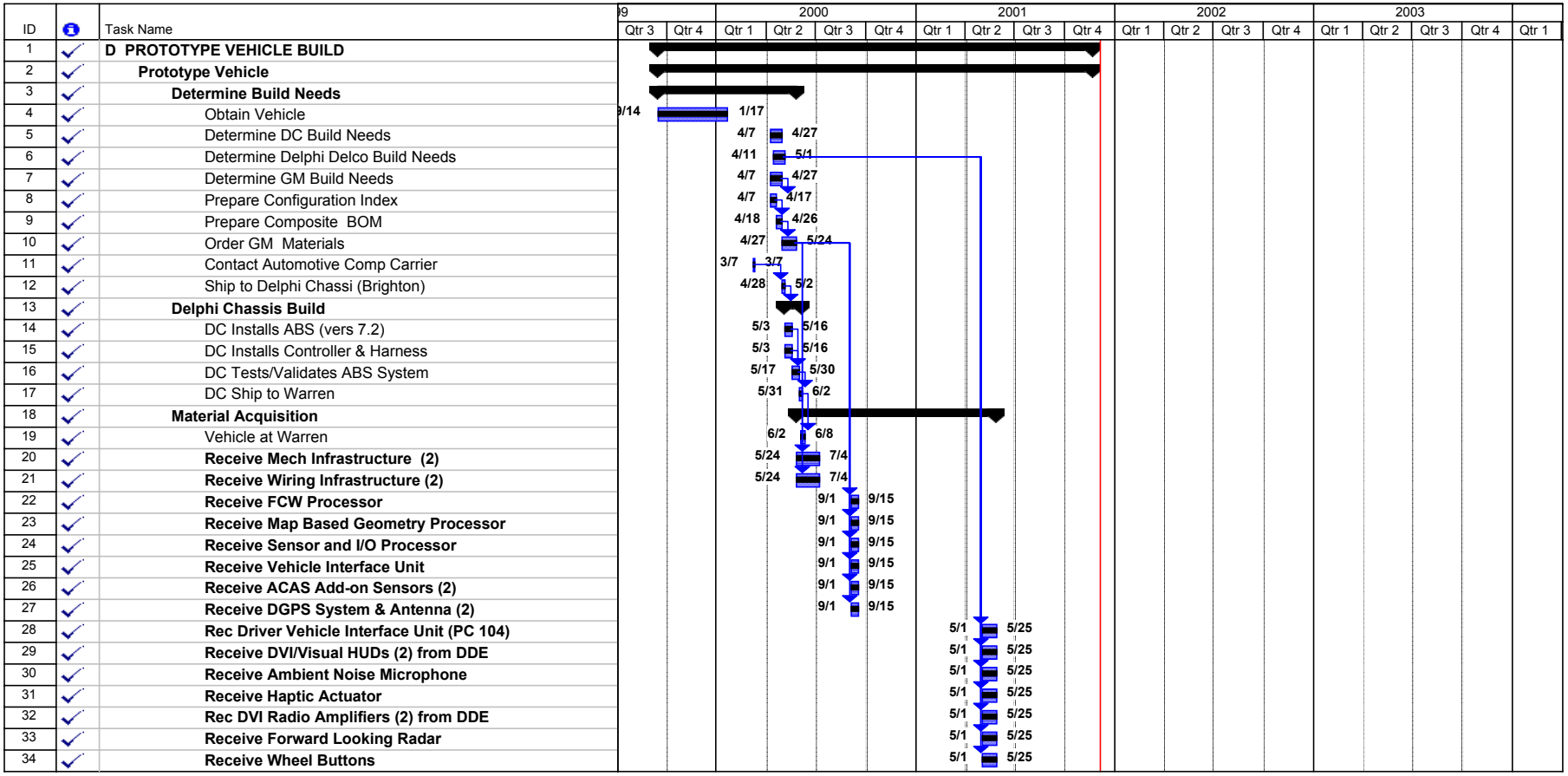

Figure 12.6 Task D Schedule, Page 1

ID	Task Name	Start	Finish
35	**Veh Subsystem & Test Groups Build (Warren)**		
36	Mechanical Modifications	6/15	9/15
37	Electrical Modification	6/15	9/15
38	**Install FCW Processor**	10/30	2/1
39	**Install Map Based Geom Processor**	10/30	2/1
40	**Install Sensor and I/O Processor**	10/30	2/1
41	**Install Vehicle Interface Unit**	10/30	2/1
42	**Install ACAS Add-On Sensors**	10/30	2/1
43	**Install GPS Receiver & Antenna**	10/30	2/1
44	**Install DVI Unit (PC 104)**	5/1	5/25
45	**Install Ambient Noise Microphone**	5/1	5/25
46	**Build Haptic Actuator/ Install in seat**	5/1	5/25
47	**Install DVI Radio Amplifiers**	5/1	5/25
48	**Install Wheel Buttons**	5/1	5/25
49	**Install Fwd Looking Radar**	5/1	5/25
50	**Install DVI/Visual HUD**	5/1	5/25
51	**Install Data Acquisition (Logger) Sys**	6/27	10/26
52	**Install Electronic Modules**	6/27	9/27
53	Contact Automotive Comp Carrier	9/8	9/8
54	Ship to Delphi Chassi (Brighton)	10/31	10/31
55	**Delphi Chassis**		
56	Hardware Upgrade	11/1	11/16
57	Software Upgrade	11/1	11/16
58	ABS System Test/Validation	11/17	11/24
59	Veh Shipped to Warren	11/27	11/27
60	**Veh Subsystem & Test Group Build (Warren)**		
61	Final Installation of Components	11/28	1/11
62	Finish Wiring & Mechanical Work	11/28	1/11
63	Test & Validate Systems	1/12	1/23
64	Contact PO Reliable Autom Carrier	1/24	1/24
65	Ship to Malibu	1/25	1/31
66	**Delphi Delco Build**		
67	**Install Scene Tracking Processor**	2/1	2/21
68	**Install Path Estimate & Tgt Selection Processors**	2/1	2/21
69	**Install Vision System With Camera**	2/1	2/21
70	**Install ACC/ Radar Subsystems**	2/1	2/21
71	**Install Throttle Controller**	2/1	2/21
72	ACC Tuning	2/22	4/4
73	Test & Validate All Systems	4/5	5/16
74	Ship to Warren	5/21	5/25

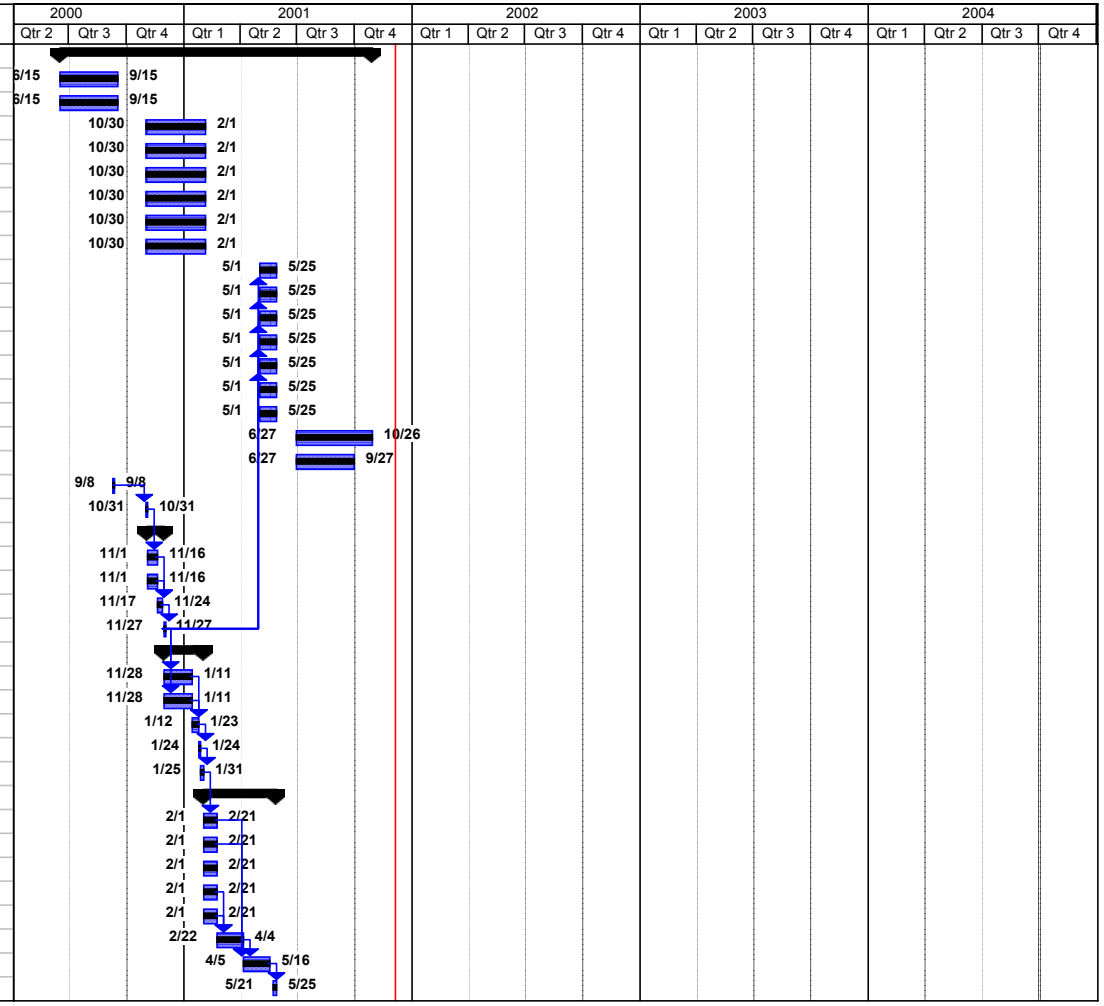

Figure 12.6 Task D Schedule, Page 2

ID		Task Name
75	✓	**Vehicle Subsystem & Test Group**
76	✓	Finishing Work on Build
77	✓	**Prototype Test &Validation**
78	✓	Install & Integrate Software
79	✓	Preliminary Validation
80	✓	**System Tested & Validated**
81	✓	Veh Sensors Tested Validated
82	✓	Vision System Tested & Validated
83	✓	DGPS Tested & Validated
84	✓	Path Prediction Tested & Validated
85	✓	Data Logger Tested & Validated
86	✓	FCW Algorithms Tested & Validated
87	✓	Test Various FCW Scenarios
88	✓	ACC Tested & Validated
89	✓	Validation Completed
90	✓	**MS 18 Prototype Vehicle Demo**
91	✓	**DEL 16 Veh Verification Test Date & Rpt**
92	✓	**UMTRI**
93	✓	Uninstall GM Data Logger System
94	✓	**Rec Data Acq Unit UMTRI (2)**
95	✓	**Rec Scene & Driver Cameras & Voice Mic**
96	✓	**Rec Dig Cell Phone & Antenna**
97	✓	**Install DAS System**
98	✓	DAS Testing
99	✓	**NHTSA Demo**
100	✓	Demo Completed
101	✓	**UMTRI Testing**
102	✓	HURP Testing

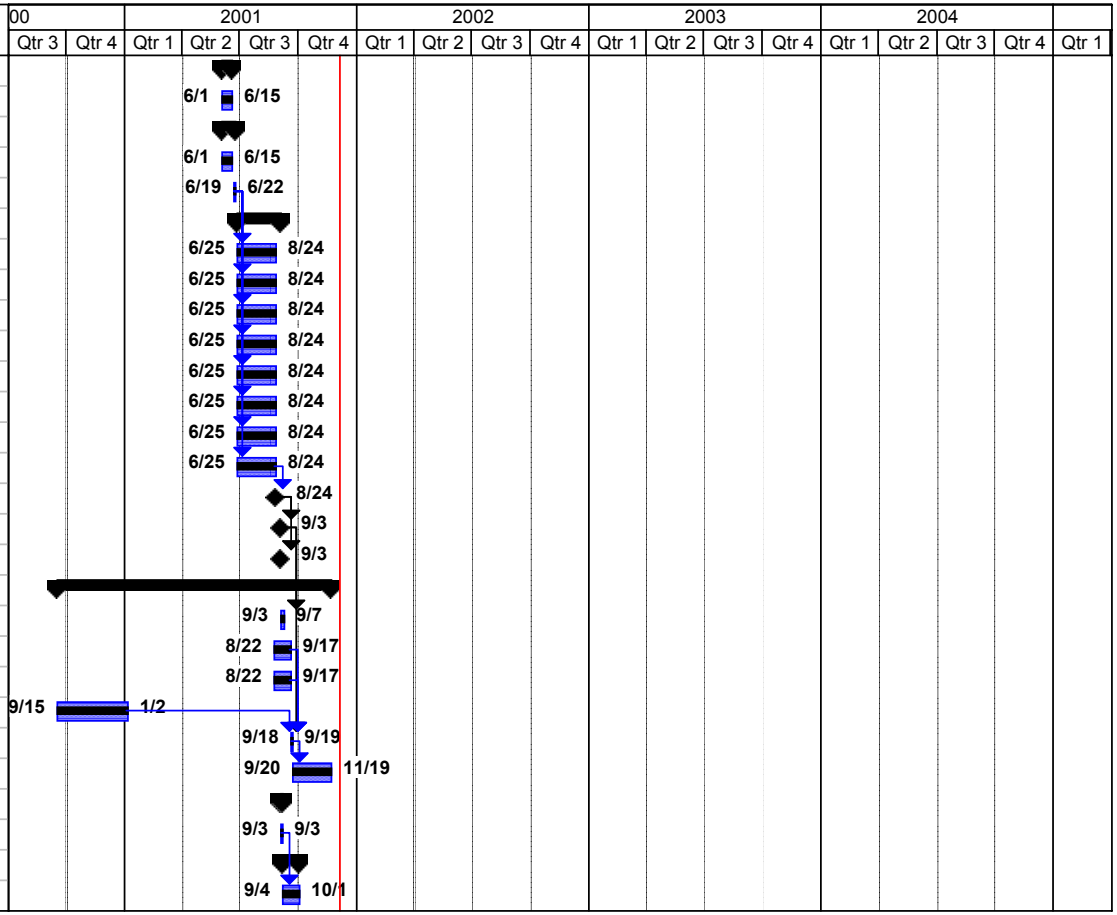

Figure 12.6 Task D Schedule, Page 3

13 Field Operational Test (Task E)

The Phase I activity for Task E is presented here in five subsections. In the first, the preliminary stages of test activity and test planning are discussed. The emphasis of this subsection is upon the empirical experience obtained by testing physical vehicles and the associated development of the Operational Test Plan for the Field Operational Test Program (FOT). The second section addresses the supportive subject of data acquisition, including the matter of selecting data variables so as to satisfy the data needs of all parties. The third subsection addresses a data processing and archiving system by which to manage and study FOT data. As the fourth item, we address the process of gaining approval for the use of laypersons as subjects in both pilot testing and the full FOT. The final subsection presents our current schedule and progress.

13.1 Test Activity and Test Planning

Goals, Purpose and Background

The goal of the Phase I effort on pilot testing and FOT planning at the University of Michigan Transportation Research Institute (UMTRI) was, of course, to prepare for a successful field test of the eventual Automotive Collision Avoidance System (ACAS) package. Since the Forward Collision Warning (FCW) function within ACAS had not been the subject of a field test before, it was intended that both "hands-on experience" and sample data be obtained through testing, both on proving grounds and in normal driving. Without such preliminary test experience, we would be going into the full-blown FOT more or less blind. Also, with regard to the ACAS ACC functionality, its relatively high level of deceleration authority compared to that examined in prior ACC field testing called for pilot-stage testing in order to anticipate the issues of layperson usage in the FOT. Together, the three separate stages of preliminary testing would support the process of developing an FOT Plan within Phase I.

The primary point of background for pilot testing and operational test planning, here, was the ICC-FOT that UMTRI performed for the National Highway Traffic Safety Administration (NHTSA) in 1996 and 1997. In that project, UMTRI established a basic form for the methodology that was proposed for the ACAS FOT. In order to apply this test method effectively to the ACAS system, a close examination was needed of the specific nature of the embedded ACAS functions and the system implementation, in light of that basic methodological framework.

A "close examination" of the ACAS function was undertaken by means of three separate stages of preliminary testing in Phase I, all involving UMTRI professional staff as drivers of the vehicle. The three activities are expanded upon, below, under the titles of "Green Opel – ACC", "Blue Opel – FCW", and "GM EDV – FCW ". Each of these separate vehicle platforms was matched with an UMTRI Data Acquisition System (DAS) and was subjected to a battery of driving test or other scripted experiments, which are described.

Testing the Green Opel – ACC
Delphi built up and provided UMTRI with an Opel Vectra passenger car, as shown below, equipped with an ACC system. Although this system could not be assured to match the eventual ACAS ACC function in its many particulars, it did have many salient features, primary among which was the 0.3 g level of deceleration authority. UMTRI tested this vehicle by means of normal driving by eight staff members over a mixed route of freeways and surface streets. The driving experience was captured by means of an extensive questionnaire and by recorded data using a DAS that was tailored for the vehicle. Because the high level of deceleration authority allowed for meaningful engagement of the system even in dense traffic, the UMTRI drivers were encouraged to sustain a high level of system utilization.

Figure 13.1 Opel Vectra Test Vehicle

Testing the Blue Opel – FCW
Delphi built and provided a second Opel that UMTRI then adapted to perform an FCW function. The high-level threat assessment algorithm was intended to approximate the structure of the ACAS algorithm that existed circa the summer of 2000. Because the parameters and formulation of this algorithm were known to UMTRI researchers, the exercise of testing was highly instructive for gaining insight into the relationship between system attribues and one's actual driving experience. Again, a mixed route was employed for normal driving by eight staff members. Another questionnaire was used to measure subjective evaluations and a method for capturing and classifying each event of FCW imminent alert was developed and employed.

Testing the GM EDV – FCW
Using virtually the identical test method, questionnaire, and data processing steps developed for testing the Blue Opel, UMTRI later tested the GM EDV. Although the GM EDV was still due for refinement and adjustment of its operative algorithms before final verification testing was done, this round of test experience provided a very useful approximation of the ACAS FCW system.

FOT Plan
A major effort in Task E, and perhaps the primary yield of Phase I in terms of a documented preparation for the field test, is the "Test Plan for the ACAS FOT". This document serves to define what is to be done in Phase II, so that we can productively and responsibly employ the fleet of ten ACAS vehicles. The vehicles are to be driven as

personal cars by a total of 78 laypersons—each for a 4-week stint—over a period totaling ten months. The plan describes the experimental design, the means for recruiting and sampling laypersons, managing their participation, and learning from their subjective experience. It describes how the ACAS system is to be characterized and then re-checked after the return of each vehicle from the field as part of the general "turnaround" procedure. It develops all the provisions for data collection and specifies the archive into which data will be loaded for computer-assisted study. It lists all the data variables and the particulars by which each signal and video clip is to be sampled and stored. It speaks to the broad program of inquiry by which UMTRI will process the data in conducting its own analysis of the results. It also indicates how data are to be transferred to The Volpe Center, in support of its assignment as the Independent Evaluator.

Intermediate and Final Results

On the strength of the three preliminary test experiences, UMTRI made many judgments and decisions on DAS design, data planning, human-use application, data processing, camera selection and sampling, subject verbal comment protocol, etc. The results of each of the testing and test-planning activities are summarized, below,

Testing the Green Opel – ACC

By driving the Opel ACC vehicle over an extensive route of mixed freeways and surface arterials, "educated guesses" were made regarding the likely utilization of such a system in normal service—for example, in the pending ACAS FOT. Figure 13.2 summarizes the startling utilization results obtained using this test vehicle. UMTRI drivers were able to reasonably keep the system engaged in the ACC mode of control over approximately 85% of all driving miles and over approximately 95% of all freeway miles. Based upon this experience, it was estimated that, after one month of using such a vehicle as a personal car, the typical layperson might be expected to utilize ACC in better than 60% of all their driving.

Assuming this projection is correct, a great deal of the FOT's total mileage exposure will occur while in the ACC mode of control. Thus, the primary experience of even the FCW function will take place while under ACC control. Noting the utilizations of conventional cruise control (CCC) that are also shown in the figure, the ACAS FOT experience of our subjects will thus differ profoundly from their normal driving by the extent of cruise usage, quite apart from the impact of the FCW function that has been the primary object of development under the ACAS project.

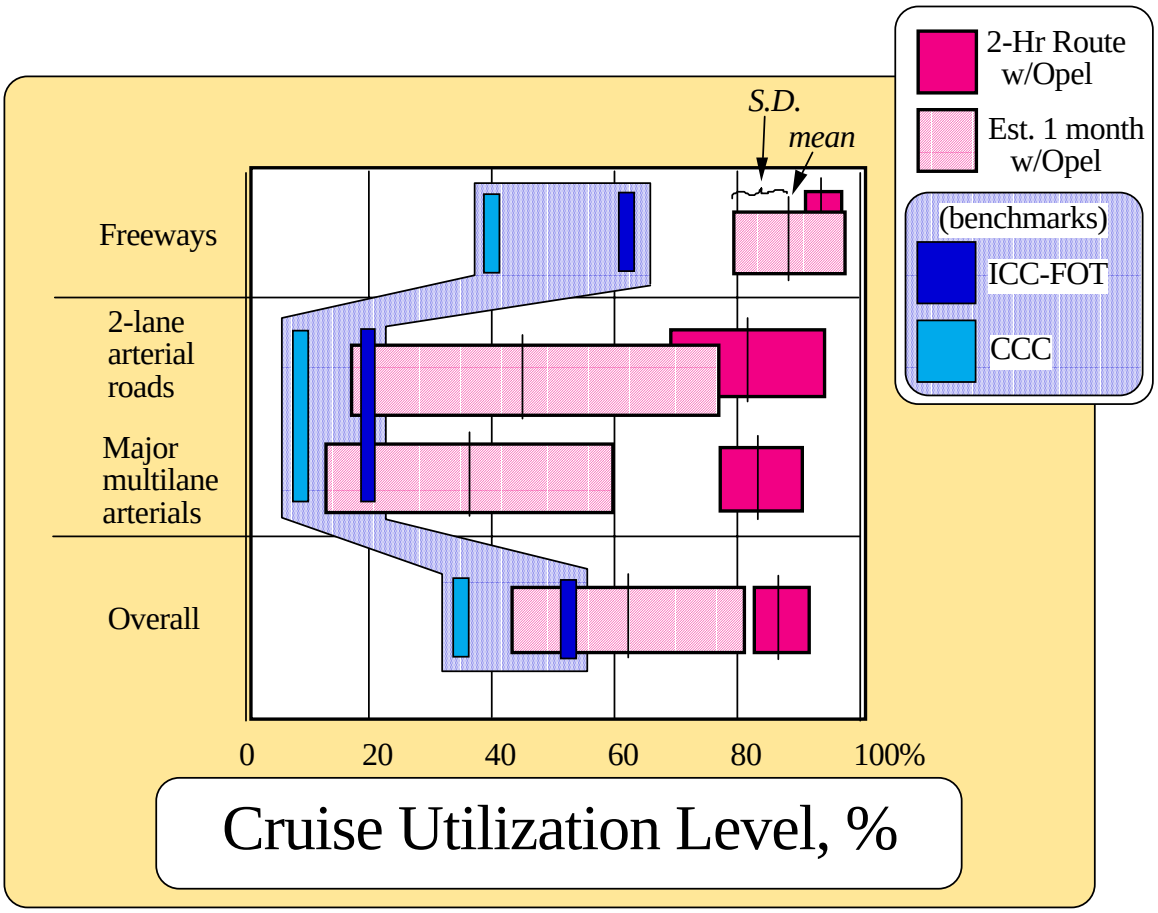

Fig. 13.2 Cruise Utilization Results, Comparing Opel ACC with Other Cases

Testing the Blue Opel – FCW

The approximated FCW function that was employed on the Blue Opel was instructive, in terms of revealing the various scenarios under which forward crash warning manifests itself. First, in Figure 13.3, an approximate ten-to-one spread is seen in the frequency with which different drivers stimulated the visual display of warning alerts. One individual experienced some visual alert only for 0.4% of driving time while another person encountered a displayed alert almost 5% of all driving time. We anticipate that, in the 78-person sample of the ACAS FOT, a considerably larger spread will exist between the most- and least-frequently alerted subjects. Clearly, the subjective reaction of the individuals at the two extremes will be entirely different. For aggressive drivers, FCW alerts will be manifest regularly—serving as a sort of persistent "critique" of the driving style, except insofar as sensitivity adjustments allow for at least subduing the visual alert display. For those with very conservative driving styles, the infrequently-manifest alerts should be something of a surprise at each encounter. To the degree that the ACAS function has some degree of spurious alert, however, even the very conservative driver will observe at least some minimum frequency of alert display, thereby suppressing the element of surprise to some degree.

The driving scenario associated with each high-level, "Imminent Alert" within the Blue Opel driving data was also examined, so as to generate a sort of classification of the conflict scenarios under which alerts occur. These results are combined from both the Blue Opel and GM EDV tests, in the next section.

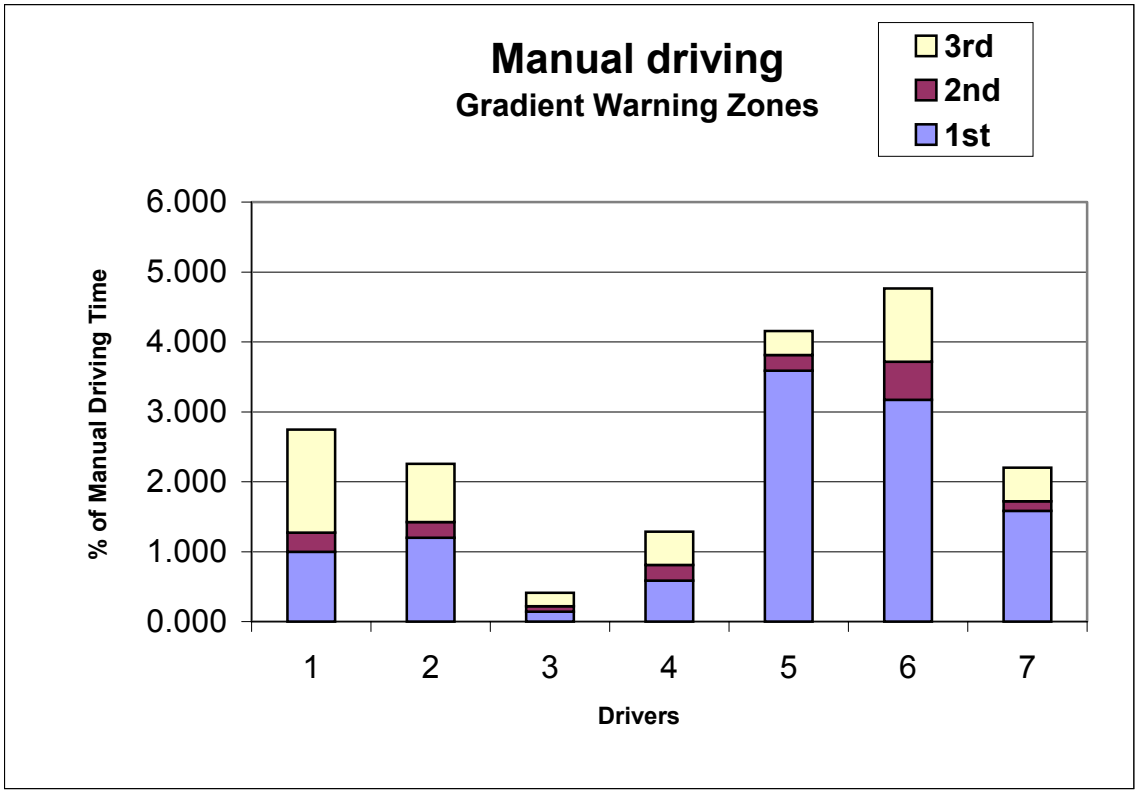

Figure 13.3 Total Occurrence of Gradient Warning Displays in Manual Driving

Testing the GM EDV – FCW

Having driven the GM EDV over essentially the same route as was used with the Blue Opel, it was possible to process the data in a way that allowed a comparison of results. While neither of the FCW systems involved had any particular significance, the comparison of data from these two cases provides a rough means of validating the data processing method. That is, it was assumed that the same drivers drove the same routes more or less equivalently in the two respective testing activities. Thus, substantial correspondence in the types of front-end conflicts might be expected, albeit with whatever distinguishing aspects of detection or threat-assessment differentiate the two systems.

In Figure 13.4, this expectation is examined by comparing the imminent alert rate per hundred miles that was obtained for each of twelve types of conflicts with another moving vehicle. Note that for the EDV only, a separate bar shows the relatively high level of fixed-object alerts that characterized this early approximation of the ACAS

system. We see that four forms of recognized conflict tend to dominate the imminent alert experience with both systems. They are:

- Lead-vehicle braking
- Approach-to-follow
- Approach-to-pass
- Approaching a turning vehicle

While lead-vehicle braking has the potential for surprising the host driver, the other three scenarios represent more or less intentional choices by the driver. The question of how drivers appraise the alert that arrives under such circumstances will, of course, await the FOT. Nevertheless, the results here reveal that it should be possible to find and differentiate the various kinds of conflicts from test data and, further, to explore the driver's reaction at this more micro-scale of classifying FCW events (in contrast, say, to simply asking drivers their overall impression of the system, at the end of the drive). To this end, we have provided an audio comment feature in the FOT data collection plan whereby the driver will be prompted, after each imminent alert, to make a comment on the usefulness of the alert.

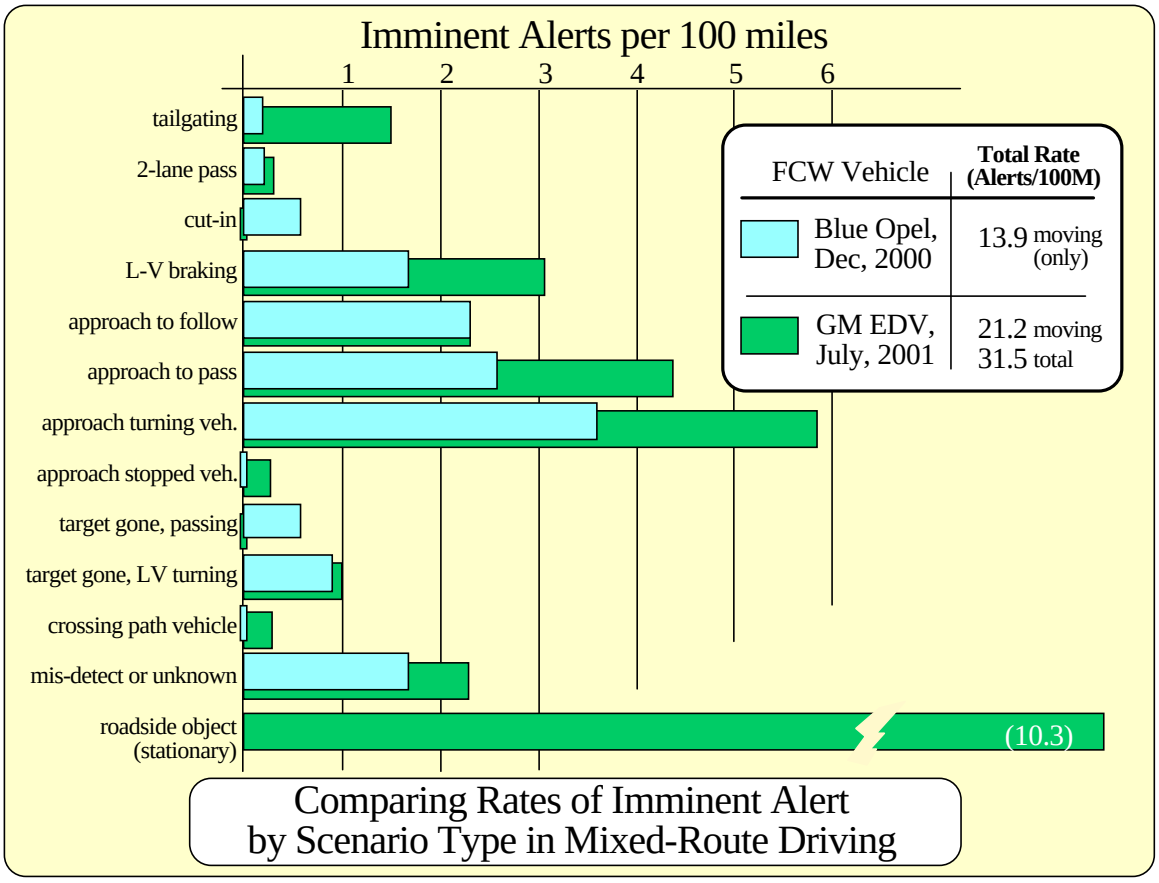

Figure 13.4 Imminent Alert Rates from driving the Blue Opel and GM EDV

Finally, note that the rates of alert shown for the EDV are at least an order of magnitude larger than were later obtained during verification testing of the more robust ACAS function in the Prototype Phase Vehicle.

FOT Plan

The Operational Test plan was submitted to NHTSA in June, 2001. Since that time, followup discussions have been held to consider various comments and concerns on the part of either The Volpe Center or NHTSA. The comments pertained largely to clarifications on points of subject sampling, data collection, and processing. Having resolved the several points of concern, the test plan has been revised in preparation for the next stage of pilot testing using the Prototype Phase Vehicle. Based upon that driving experience as well as any further changes in the physical implementation of the ACAS system, further revisions in the plan will be made. The ultimate intent is that the cumulative learning from all preliminary testing, all system development, and all collaboration between the various stakeholders will be reflected in the plan and implemented in the conduct of the FOT.

A Technical Problem

The primary technical problem that attended the conduct of the testing and the FOT planning involved manually reviewing video clips from natural driving, as a necessary means of classifying the driving conflict that was involved in each imminent alert. Currently, we know of no way to automatically process objective data measurements so as to deduce and classify the various driving conflicts, without resorting to human review of video. Nevertheless, the experience of manual review and classification has revealed so much about the nature of the conditions provoking an alert in normal driving that such review is now believed to be simply necessary for understanding the subjects' experience with all imminent alerts in the FOT. Accordingly, we have prioritized the need for much easier access to video in our data processing tools. We have also arranged that so-called "exposure video" frames will be collected throughout the FOT at one frame every 2 seconds. Thus, a useful video description of the driving scene will prevail in essentially every maneuver or conflict event of any kind, even if the circumstances were sufficiently benign that no episodic clip of video frames was triggered.

Moreover, Phase I produced several effective stages of introduction into the field testing of high-deceleration ACC and FCW functions. The aggregate learning from these experiences has been incorporated within a comprehensive FOT Plan.

13.2 Data Acquisition System and Data Planning

Goals, Purpose and Background

The goal of the data acquisition system and data planning effort has been the implementation of a series of data collection packages supporting the several stages of pilot testing and eventually the FOT itself. Since UMTRI is building DAS packages for differing versions of the GM and Delphi ACAS system, it has been necessary at each

stage to have full compatibility with each platform, complete coverage of the desired data variables, and efficient recovery of on-board data for the purposes of both test monitoring and eventual data processing and evaluation.

The background for this subtask involves the unique character of both the ACAS platform and the peculiar needs of the stakeholders for recorded data. To stay within the scope of time and money, while maximizing the utility and reliability of the DAS device, UMTRI has sought commercial off-the-shelf components and a combination of custom and tailored software. Since The Volpe Center will serve as the Independent Evaluator, it was also necessary to plan a data collection list that reflected both the practical constraints of the ACAS system and The Volpe Center's intentions for data analysis. Additional data interests trace from GM, Delphi, and UMTRI, since each party has a special perspective for valuing the alternative data products. In the end, UMTRI needed to specify various practical constraints on the size, configuration, software complexity, and need for robustness of the DAS, while maximally responding to the partners' needs. There has also been a concern to limit the scope of data collection since the total data volume eventually impacts the magnitude of the data management task. That is, all collected data must later be downloaded, backed-up, validated, converted into a relational database, managed as a whole archive for analysis, and transferred to The Volpe Center.

The technical approach toward the DAS design hinges on the collection of both quantitative and video-image data using two single-board computers, connected by an Ethernet link, as diagrammed in Figure 13.5. Since continuous computations in the quantitative- (or "objective-") data computer are needed to decide when to trigger an episodic clip of video storage, a highly integrated DAS architecture is needed. It is also necessary that a summary dataset from each trip be transmitted to UMTRI by cell modem upon occurrence of the 'ignition-off' event, thereby providing for a sustained monitoring of the data-health of all vehicles in the field. The specification for each of the several elements of this package, including GPS decoding, CAN interface, derivation of supplementary variables and histograms, and the allocation of memory for continuous (10-Hz) time histories, trip-logged variables, transition files, etc., all derive in turn from the agreed-upon list of data to be collected. Thus, the negotiation of a data-collection plan that satisfies all the stakeholders is intimately linked to the provisions for DAS design.

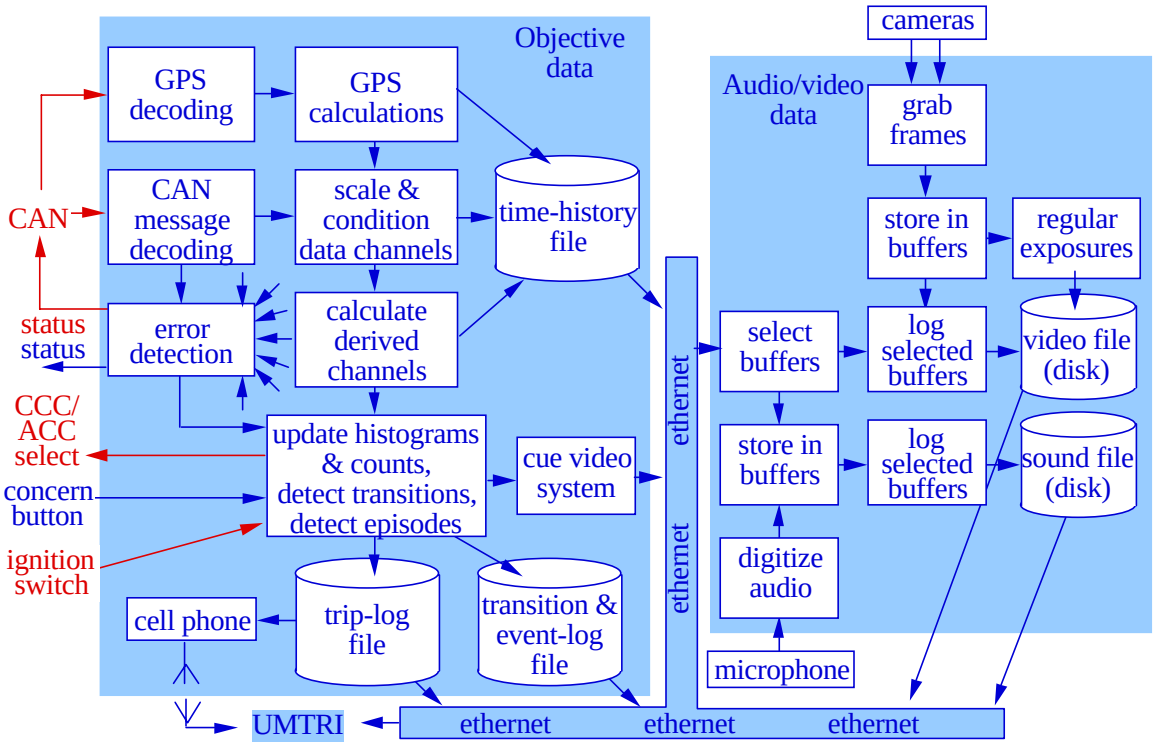

Figure 13.5 Basic Elements of the FOT Data Acquisition System

The additional product of this task is the data collection listing and specification that is incorporated within the FOT plan. The plan is now quite inclusive of all the data resources that are present on the vehicle. Up to fifteen tracks of radar are now to be recorded at 10 Hz throughout the FOT, in their original CAN message format, for later parsing and incorporation within the database. All of the The Volpe Center-requested data that was actually available on the vehicle platform will be recovered.

Intermediate and Final Results

The results of this task take two forms. First, a series of three DAS packages were implemented or otherwise adapted for operation with the two Opels and the GM EDV. In addition, a design for the final FOT-ready DAS package has been prepared and is being constructed at the conclusion of Phase I for use in layperson testing with the Prototype Phase Vehicle. This system is scaled to handle the almost 200 channels of quantitative data plus the extensive collection of scene- and face-video images. The FOT package is designed to meet the physical constraints of the Buick LeSabre installation and to withstand the large range of temperatures that must be dealt with when the vehicle is completely unattended, in normal use.

The associated product from this subtask is the data collection list that has been, essentially, negotiated to satisfy stakeholders and conform to the many practical constraints. At this point, a highly ambitious but feasible plan has emerged.

A Technical Problem
Temperature is one of the most difficult DAS specifications to satisfy with commercial off-the-shelf products. Currently, no fully satisfactory solution has been identified in the case of the low-temperature specification on either the frame-grabber cards or the militarized hard disks for the FOT. The entire commercial field has been explored and, while we can get pretty close (i.e., temperature specified down to –20C) there is still a small gap in capability to cover all conditions. Lacking the availability of suitable products covering the low-temperature extreme of a Michigan winter (down to –25 or –30C), it will be necessary to incorporate a feature into the DAS by which data collection is temporarily unavailable for perhaps the first 5 minutes following ignition on a day below –20C, until the key DAS elements have been heated into their suitable operating range. Based upon historical weather data, this should amount to no more than approximately 0.2% of the intended dataset, and this number overestimates the data loss since most people do not jump into a car and immediately drive away under frigid conditions. Instead, they often spend time either warming up the interior or scraping snow and ice off the windows, before getting underway.

Significance
The indicated plan amounts to the most comprehensive collection of driving data in any FOT and presumably in any naturalistic driving experiment ever conducted.

13.3 Test Data Processing and Analysis

Goals, Purpose and Background
The ultimate goal of UMTRI's data processing and analysis in this study is to determine the practical suitability of the ACAS function for widespread use by the driving public. Suitability for wide use will be determined by the extent to which the installed system:

- offers a marketable level of value, as perceived by its users
- yields significant safety and convenience benefits for most of them
- poses minimal added risk to almost anyone

To reach the goal of the FOT, we must learn the users' appraisal of ACAS and yet make our own objective assessment of how ACAS impacts the driving process. The unstructured character of naturalistic driving requires an investigative mentality within the team—we must acquire an extensive set of data and we must penetrate that set through creative inquiry. The future maturation of products in this class will also be aided by identifying the most significant physical and psychological phenomena which act to determine the suitability of ACAS.

Moreover, we seek to find how ACAS interacts with the driving process and why. The task of the data processing activity at UMTRI is to penetrate the vast archive of FOT data in order to address how approximately twenty issues—relating to subject driving exposure, duty cycle of the ACAS function, performance of the system itself, subject

response to ACAS events, and objective driving conditions and personal styles that serve to exercise ACAS—condition the subject's response. We also seek to explain the system's influence on the performance and opinions of each driver.

In Phase I, the technical approach toward preparing for the processing of FOT data has been the development and implementation of the "Data Model," as sketched in Figure 13.6. The sketch includes elements that provide for the creation of test data via the DAS package, investigation of data based upon browsing and analyzing the contents of the database, appending analytical results as an augmentation of the test-derived database, high-level examination of reduced or aggregated data using data mining and visualization tools, and sharing data with others via a Web server. This overall architecture provides for an integrated multi-use of software that may be downloaded onto an individual DAS package in a vehicle as well as installed as part of the archival record of FOT results within the database.

The diagram shows that data are stored in each of three forms: as metadata, the database, and a data warehouse. Metadata store objective attributes of the test design, test conditions, measured variables, real-time computations conducted on board the DAS package, etc., as well as corresponding attributes that were derived via analyses and simulations performed on test data. In general, metadata constitute instructions within the DAS package as well as a permanent bookkeeping record accompanying all measured and analyzed data elements.

The database represents one or more relational databases in which the FOT data and analytical derivations thereof are stored. Most detailed study of the FOT results will involve exercise of the indicated "Explorer" and "Cruncher" tools, shown at the upper right, as specialized utilities for accessing and operating upon the relational database.

The data warehouse provides results aggregated for high-level analysis, for convenient study by many researchers. Significant response "FACTS" are defined for aggregating the data—for example, warning events, ACC interventions, driver-cited "miss" events, etc. Each FACT has "click-able" dimensions such as driver, road, time, cruise state, etc., and each dimension has attributes such as driver age, gender, driving style, velocity range, etc. A so-called "Pivot table," then, supports a query engine that is optimized for immediate analysis of the multiple dimensions of the FACT. The practical result is that the insight process is better stimulated by richer initial displays of data whose study can be better sustained, once the researcher gets on a good discovery track, because the pursuit process has been made so efficient.

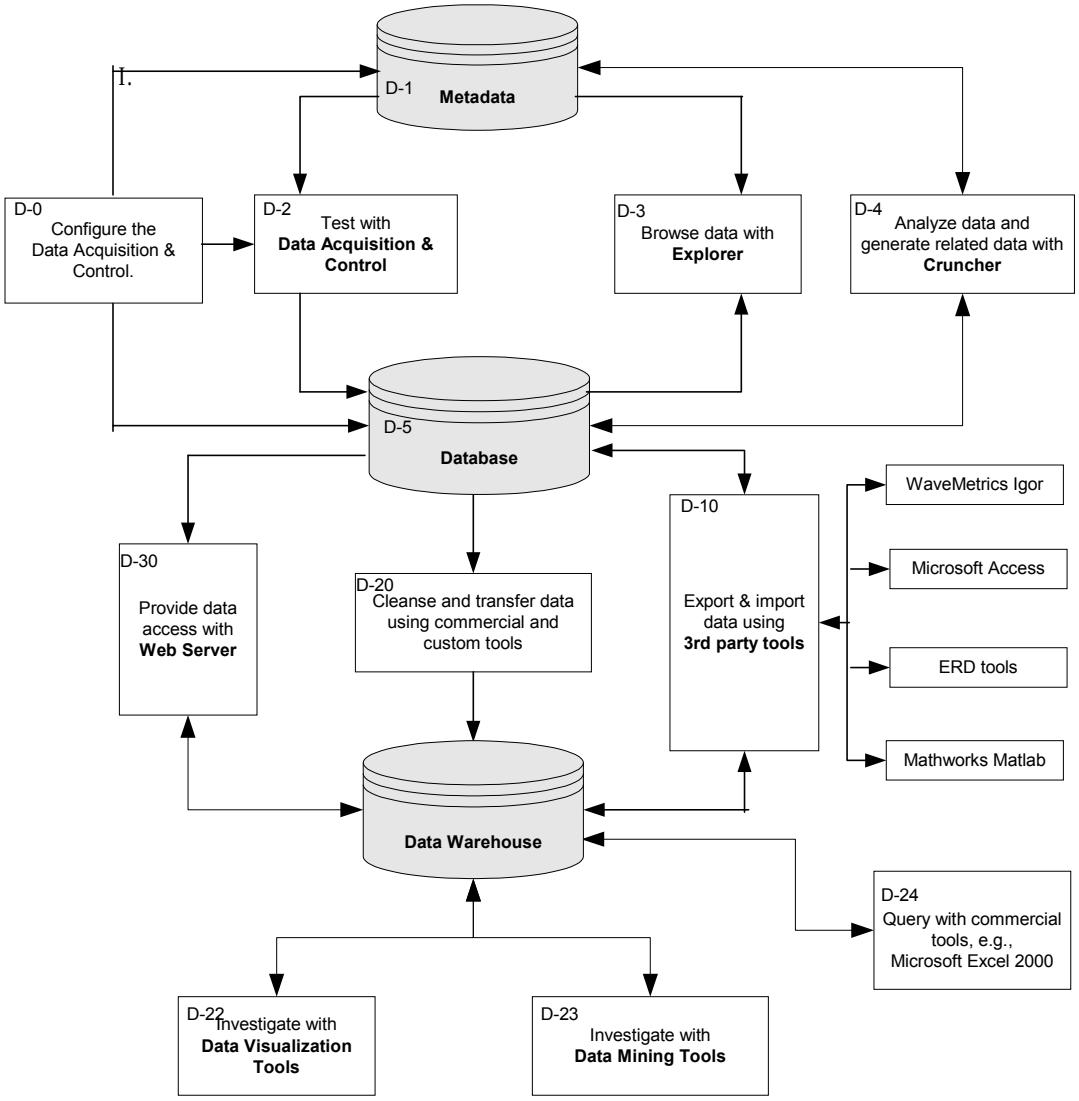

Figure 13.6 The Data Model that Supports Data Collection & Analysis

Intermediate and Final Results

The result of this subtask is contained in software that enables the many functions of the Data Model architecture as well as a physical infrastructure at UMTRI by which several desktop computers are linked to large-capacity servers. The conversion from MSAccess to MS SQL Server database software has been made successfully and each of the modest datasets from testing the Opels and the GM EDV has been suitably downloaded into the database format and used in analysis. There are no significant problems to be overcome in taking this system to the full functionality needed for the FOT.

Significance
Clearly, the ability to process test data ranks in significance with the ability to collect the data on board each test vehicle.

13.4 Human Use Approval

Goals, Purpose and Background

The conduct of a naturalistic driving experiment requires that formal approval be obtained for the use of laypersons as subjects. Thus, the goal of this subtask is to make suitable application for such approval and to successfully manage the process so that approval is received in time to support the project schedule.

The background requirement for this task involves the granting of three separate approvals. The three different boards of review that must be satisfied are as follows:

- University of Michigan Internal Review Board (IRB)
- General Motors Human Research Committee (HRC)
- NHTSA Human-Use Review Panel (HURP)

An application for approval to recruit and test subjects in the accompanied phase of pilot testing was developed by UMTRI and submitted to the UM IRB in December, 2000. Approval was received from this IRB in January, 2001, whereupon the process moved along to GM HRC. As Phase I draws to a close, there are still some issues impeding approval by the HRC, primarily involving a list of medical screening criteria requested for the recruitment of subjects. When this list was given to the UM IRB—which must also approve any changes or additions imposed by a subsequent board of approval—the UM board requested that GM HRC remove certain ambiguities from the statement of medical conditions. The resolution of these issues is still in progress.

Intermediate and Final Results

The intermediate result is a complete application for IRB, HRC, and HURP approval that defines the experiment, the risks to the subjects, the informed consent document, etc. This document will be revised as necessary throughout the approval process until all three of the cognizant bodies are satisfied, whereupon layperson testing will proceed.

A Technical Problem
Clearly, the process of human use approval is now and may continue to pose a problem for the completion of the project. Nevertheless, it is UMTRI's judgment that the ACAS system should be eminently test-able, using human subjects, once the concerns of the various organizations are fully understood and addressed. Hopefully, this process will proceed more quickly in the near future.

Significance
Human-use approval is of utmost significance since the FOT cannot proceed forward without it.

Current Schedule and Progress for Task E

All of the FOT preparatory activities are on schedule except the human-use approval process. A substantial effort continues to be devoted toward satisfying the respective requirements of the approval boards and for facilitating the communications between them. The schedule for Task E, in Figure 13.7, shows that the testing of the Prototype Phase Vehicle is the next key activity, coming early in Phase II, in which lay subjects will be accompanied by an UMTRI researcher while driving the vehicle over an extensive route of streets and freeways. With this activity scheduled to commence in January, it is necessary that IRB, HRC, and HURP approval be obtained, forthwith.

ID	Name
1	**E-Field Operational Test**
2	Collaboration/Planning/Admin
3	**Prepare and Conduct Pilot Testing**
4	Prepare FOT Pilot Test Plan
5	*D17a-Outline of FOT Pilot Test Plan*
6	*MS19-Submit FOT Pilot Test Plan*
7	*D17b-FOT Pilot Test Plan*
8	D.A.S. for Engr Phse Veh
9	**Receive Eng Phase Veh. -Green Opel**
10	Pilot Testing-Professional with Green Opel
11	**Receive Eng Phase Veh. FCW- Blue Opel**
12	Pilot Testing-Professional with Blue Opel
13	Dev. Pilot Data Proc. Software
14	Pilot Testing Data Processing-Professional
15	Pilot Testing with Blue Opel
16	*MS20-Completion Of FOT Professional Pilot, Testing & Data Processing*
17	First HURP Development
18	*D18-FOT First HURP Request*
19	*MS21-Completion Of FOT First HURP Approval Process*
20	GM EDV at UMTRI
21	**Prepare for the FOT**
22	D.A.S. for Pilot/Deplymt Veh
23	*MS35-Completion Of FOT Data Acquisition Package*
24	Dev. FOT Data Proc Software
25	Dev. Subject Mgmt. Procedures
26	Dev. Fleet and Data Mgmt. Proc.
27	Prepare Operational Test Plan
28	*D19-FOT Operational Test Plan*
29	*MS22-Submission Of FOT Operational Test Plan*

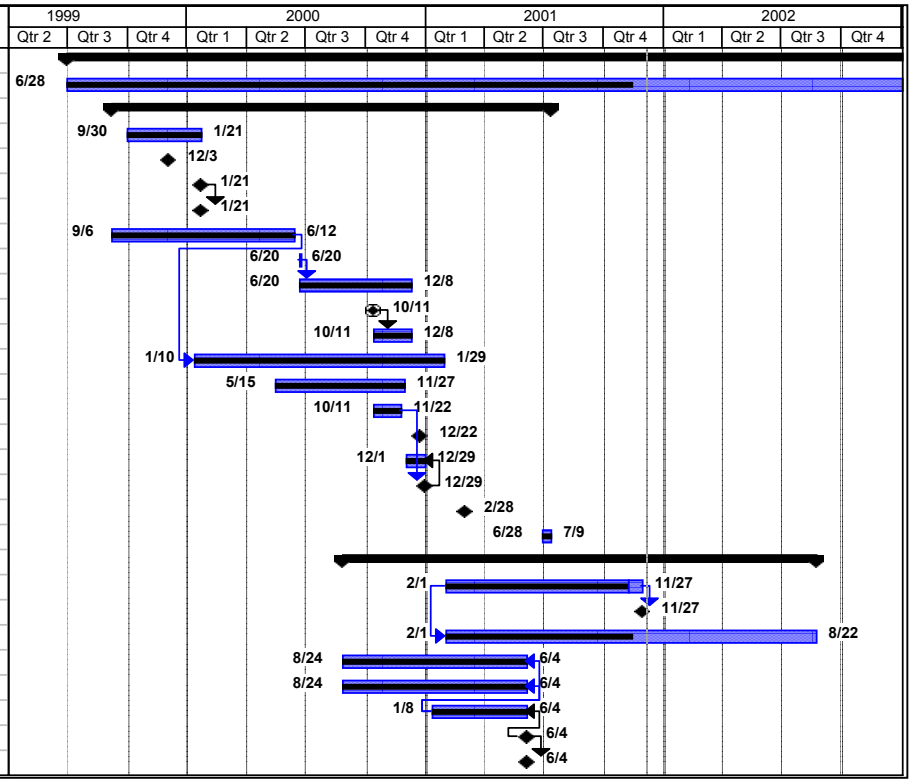

Figure 13.7 Task E Schedule

ACRONYMS

ABS	Anti-lock Brake System
ACAS	Automotive Collision Avoidance System
ACC	Adaptive Cruise Control
ANCOVA	Analysis of Covariance
AOV	Angle of View
AS	Amplitude Slope
BPM	Brake Pressure Modulator
BPMV	Brake Pressure Modulator Valve
BRT	Brake Reaction Time
CAMP	Crash Avoidance Metrics Partnership
CCC	Conventional Cruise Control
CCD	Charge-Coupled Device
CIPS	Closest In-Path Stationary target
CIPV	Closest In-Path Moving target
DAS	Data Acquisition Subsystem
DBC	Delphi Brake Controls
DCS	Delphi Chassis Systems
DDE	Delphi Delco Electronics
Delphi-D EDV	Delphi Delco Electronics Engineering Development Vehicle
DF	Data Fusion
DGPS	Differential Global Positioning System
DVI	Driver Vehicle Interface unit
DVI	Driver Vehicle Interface
DVI	Driver-Vehicle Interface
ECU	Electronic Control Unit
FACT	First Activation of controls
FCW	Forward Collision Warning
FFT	Fast Fourier Transform
FMCW	Frequency Modulated Continuous Wave
FOT	Field Operational Test program
FS	Fail Safe
GM	General Motors
GM EDV	General Motors Engineering Development Vehicle
GMR	General Motors Research and Development Center
GPS	Global Positioning System
GR	Geometric Rejection
GUI	Graphical User Interface
HHDD	High Head-Down Display
HRC	Human Research Committee (General Motors)
HUD	Head-Up Display
HURP	Human-Use Review Panel (NHTSA)
IRB	Internal Review Board (University of Michigan)
LPF	Low Pass Filter
MMIC	Microwave Monolithic Integrated Circuit

MOE	Measure of Effectiveness
MPG	Milford Proving Grounds
MTF	Modulation Transfer Function
NHTSA	National Highway Traffic Safety Administration
PCARS	Problem Corrective Action Reports
PCM	Powertrain Control Module
POV	Principal Other Vehicle
PT	Pass Through
RADS	Reconfigurable Advanced Development Sensor
RCAP	Radar Collision Avoidance Processor
RCS	Radar Cross Section
SI	Symbol for the international system of units
SLP	Short and Long Term Persistence
SMCC	Stepper Motor Cruise Control
SV	Subject Vehicle
TASIM	Threat Assessment Simulation tool
TCS	Traction Control System
THEO	Time Headway at the Event Onset
THW	Time Headway subalgorithm
TSP	Target Selection Processor
TTC	Time To Contact subalgorithm
TTL	Transistor-Transistor Logic
VCO	Voltage Controlled Oscillator
VIP	Vehicle Interface Processor
VSE	Vehicle Stability Enhancement
VSWR	Voltage Standing Wave Ratio

DOT HS 809 453
May 2002

U.S. Department
of Transportation
**National Highway
Traffic Safety
Administration**

NHTSA
People Saving People
www.nhtsa.dot.gov